Dissertation zur Erlangung des Doktorgrades
der Fakultät für Biologie
der Ludwig–Maximilians–Universität München

Quantitative proteomic analysis of early phosphorylation changes induced by 2,3,7,8-tetrachlorodibenzo-*p*-dioxin in 5L rat hepatoma cells

Melanie Schulz

München, Juni 2011

Helmholtz Zentrum München
Deutsches Forschungszentrum für Gesundheit und Umwelt
Institut für Toxikologie

Quantitative proteomic analysis of early phosphorylation changes induced by 2,3,7,8-tetrachlorodibenzo-p-*dioxin in 5L rat hepatoma cells*

vorgelegt von Melanie Schulz
geboren in Schwerin

Erstgutachter: Prof. Dr. F. Eckardt-Schupp

Zweitgutachter: Prof. Dr. B. Conradt

Sondergutachter: PD Dr. U. Andrae

Dissertation eingereicht am: 29.06.2011
Tag der mündlichen Prüfung: 19.10.2011

Ehrenwörtliche Versicherung

Ich versichere hiermit ehrenwörtlich, dass die vorgelegte Dissertation von mir selbständig und ohne unerlaubte Hilfe angefertigt ist.

Erklärung

Hiermit erkläre ich, dass die Dissertation weder als Ganzes noch in Teilen an einem anderen Ort einer Prüfungskommission vorgelegt wurde. Weiterhin habe ich weder an einem anderen Ort eine Promotion angestrebt oder angemeldet oder versucht eine Doktorprüfung abzulegen.

München, den 29.06.2011
Ort, Datum

(Melanie Schulz)

Contents

List of Figures

List of Tables

Abbreviations

2-APB	2-aminoethoxydiphenyl borate
AA	arachidonic acid
AGC	automatic gain control
AhR	aryl hydrocarbon receptor
BAPTA-AM	1,2-bis(2-aminophenoxy)ethane-N,N,N',N'-tetraacetic acid tetrakis (acetoxymethyl ester)
BLAST	Basic Local Alignment Search Tool
CID	collision-induced dissociation
CKII	casein protein kinase II
Da	Dalton
DHB	dihydroxybenzoic acid
DMSO	dimethyl sulfoxide
DRE	dioxin response element
DTT	dithiothreitol
ECL	enhanced chemiluminescence
EROD	7-ethoxyresorufin deethylase
ESI	electrospray ionization
ETD	electron transfer dissociation
FDR	false discovery rate
GAP	GTPase-activating protein
GEF	guanine nucleotide exchange factor
GO	Gene Ontology
HILIC	hydrophilic interaction liquid chromatography
HPLC	high-performance liquid chromatography
IAA	iodoacetamide
IARC	International Agency for Research on Cancer

IDA	iminodiacetic acid
IMAC	immobilized metal affinity chromatography
IPI	International protein index
KEGG	Kyoto Encyclopedia of Genes and Genomes
KN-92	2-[N-(4-methoxybenzenesulfonyl)]amino-N-(4-chlorocinnamyl)-N-methylbenzylamine phosphate
KN-93	2-[N-(2-hydroxyethyl)]-N-(4-methoxybenzenesulfonyl)]-amino-N-(4-chlorocinnamyl)- N-methylbenzylamine)
LC	liquid chromatography
LTQ	linear trap quadrupole
Lys-C	endoproteinase Lys-C
m/z	mass-to-charge ratio
MA	ratios-vs-average plot
MALDI	matrix-assisted laser desorption/ionization
MS	mass spectrometry
MS/MS	product ion scanning
MSA	multi-stage activation
MudPIT	multidimensional protein identification technology
NTA	nitrilotriacetic acid
PTM	posttranslational modification
rf	radio frequency
RP	reversed phase
SIMAC	Sequential elution from IMAC
Src	proto-oncogene tyrosine-protein kinase Src
TCDD	2,3,7,8-tetrachlorodibenzo-*p*-dioxin
TFA	trifluoroacetic acid
Tris	tris(hydroxymethyl)aminomethane
W-7	[N-(6-aminohexyl)-5-chloro-1-naphthalenesulfonamide hydrochloride]

Abstract

2,3,7,8-Tetrachlorodibenzo-p-dioxin (TCDD) is a highly toxic, ubiquitous environmental pollutant and regarded the most potent chemical carcinogen in experimental animals. Most of the biological effects of TCDD are mediated by its binding to the cytosolic Aryl hydrocarbon (Ah) receptor. The resultant alterations in gene expression have been thoroughly characterized, but for most of the multifaceted toxic actions of the dioxin the molecular mechanism is still unclear. Interestingly, there is recent evidence that TCDD also causes early changes in signal transduction unrelated to altered gene activation, but this has not been explored systematically yet. In order to address this aspect of dioxin action, a global quantitative mass spectrometric analysis of the alterations of protein phosphorylation preceding the alterations in gene expression at the protein level (at 0.5 –2 h after the start of exposure) was performed using 5L rat hepatoma cells as a model system. In order to allow a precise mass spectrometric quantitation of phosphopeptides, cells were differentially labelled using the SILAC ("stable isotope labelling by amino acids in cell culture") approach and subsequently treated with DMSO or 1 nM TCDD for 0.5, 1 and 2 h. Proteins from control and treated cells were mixed, proteolysed, and phosphorylated peptides were isolated by metal affinity chromatography using a combination of the SIMAC ("sequential elution from immobilized metal affinity chromatography (IMAC)") and the TiO_2 approach. The phosphopeptides were further fractionated by hydrophilic interaction chromatography and quantitated and identified by liquid chromatography-tandem mass spectrometry on a linear ion trap mass spectrometer (LTQ-Orbitrap XL).

In total, eight independent experiments were performed which resulted in the identification of 5648 different phosphorylated peptides comprising 6573 distinct phosphorylation sites. These peptides were derived from 2156 different phosphoproteins that were identified using the International Protein Index (IPI) database. Phosphopeptides with abundances statistically significantly "regulated" by TCDD were identified by applying an empirical Bayes moderated t-test to all peptides found at least twice for a particular exposure period

followed by the application of the "q-value method" for controlling the false discovery rate. 0, 4 and 6 peptides with a q-value <0.05 were identified for the exposure periods 0.5, 1 and 2 h, respectively. A volcano plot analysis indicated that the statistical threshold of q < 0.05 was equivalent to a biological threshold of a ± 1.5 fold-change in phosphopeptide abundance. 4, 8 and 16 phosphorylated peptides which were observed in only one of the experiments per time point and which exhibited a regulation factor >1.5 were observed for the three exposure periods. For the majority of the identified proteins wit changes on specific phosphorylation sites due to TCDD treatment, other phosphopeptides not showing any regulation were observed. This observation suggest that the phosphorylation changes were caused by the non-genomic pathway and not due to altered total levels of the respective proteins. With the exception of the up-regulation of Tyr182 phosphorylation of the MAP kinase p38alpha, none of the TCCD-induced phosphorylation changes had been described before. One of the proteins with altered phosphorylation was the transcription factor ARNT (aryl hydrocarbon receptor nuclear translocator), an obligate partner protein for gene activation by the Ah receptor. For the first time it was demonstrated that TCDD upregulates Ser77 phosphorylation of ARNT. Other proteins with altered phosphorylation included various transcriptional co-regulators previously unknown to participate in TCDD-induced gene activation, such as TIF1β, a co-repressor of the transcriptional repressor KRAB, RD RNA binding protein, a protein participating in the control of transcript elongation, and its interaction partner "Nuclear cap-binding protein subunit 1", were identified. In addition, numerous other proteins involved in functions other than transcriptional regulation were identified to carry specific TCDD-"regulated" phosphorylation sites. These proteins included, among others, six regulators of the activity of small GTPases of the Rho and Rab families, two UBX domain-containing proteins involved in different aspects of protein degradation, and AHNAK, a protein implicated in the regulation of Ca^{2+} entry and signalling. Thus, the results of the present phosphoproteomics study shed new light on proteins involved in the activation of gene expression and early changes in signal transduction by TCDD and open up new directions for future research on the molecular mechanisms of dioxin action and toxicity.

Chapter 1

Introduction

1.1 2,3,7,8-Tetrachlorodibenzo-*p*-dioxin

2,3,7,8-Tetrachlorodibenzo-*p*-dioxin (TCDD) is a ubiquitous and persistent environmental contaminant with the potential to cause a broad spectrum of adverse health effects, such as developmental defects, cardiovascular disease, diabetes, porphyria and hormonal disturbances in human [White and Birnbaum, 2009]. In 1997, TCDD was also classified as carcinogenic to humans by the International Agency for Research on Cancer (IARC) [IARC, 1997]. In spite of enormous efforts to uncover the action mechanisms underlying the various deleterious effects of TCDD and related dioxins, the precise molecular mechanisms mediating toxicity are still largely unknown for most toxic actions of TCDD.

1.1.1 The genomic actions of TCDD

TCDD is a ligand of the so-called aryl hydrocarbon receptor (AhR), a primarily cytosolic receptor which plays important roles in normal cell physiology [Barouki et al., 2007] and mediates the toxic effects of TCDD [Fernandez-Salguero et al., 1996], [Bunger et al., 2008]. Receptor binding of TCDD or a wide variety of other AhR agonists, such as the carcinogenic polycyclic aromatic hydrocarbon benzo(a)pyrene, results in the translocation of the ligand-receptor complex into the cell nucleus and dimerization with a related protein, the AhR nuclear translocator (ARNT). This heterodimer can act as a ligand-activated transcription factor by binding to specific DNA sequences known as "xenobiotic response elements" or "dioxin response elements" (DREs) [Safe, 2001], [Sogawa et al., 2004], [Boutros et al., 2004]. The binding to DREs initiates chromatin remodelling and en-

ables the transcription of a set of target genes the so-called "AhR gene battery" [Beischlag et al., 2008]. The induced gene products include the xenobiotic-metabolizing enzymes cytochrome P450 1A1 (CYP1A1), UDP-glucuronosyltransferase (UGT) 1A1 and aldehyde dehydrogenase 3A1. In addition, the ligand-receptor complex (TCDD/AhR) can directly interact with proteins of other signalling pathways, such as NF-kappa B [Tian et al., 1999], the estrogen receptor [Klinge et al., 2000] and the retinoblastoma protein [Puga et al., 2000] and induce alterations in gene expression without the dimerization with ARNT and binding to DRE. However, the relevance of these interactions for several well-known toxic responses to TCDD has been questioned recently [Bunger et al., 2008].

1.1.2 The nongenomic actions of TCDD

During the past few years, evidence has been accumulated that TCDD can also cause biochemical alterations that are detectable within a few minutes after addition of the compound to cells *in vitro*. These effects cannot be explained by the AhR-mediated gene activation, which is dependent on stimulation of *de novo* transcription and translation. This requires a minimum time of a few hours to become apparent. It has been claimed that the early responses are dependent on a functional AhR but not ARNT [Matsumura, 2009]. The effects are mainly mediated by rapid phosphorylation events and are called "protein phosphorylation pathway" or, more recently "nongenomic" pathway [Enan and Matsumura, 1995] [Li and Matsumura, 2008], [Dong and Matsumura, 2008]. These terms were coined to discriminate the "early effects" from the classical genomic pathway involving Ahr/ARNT-mediated induction of gene expression. The term "nongenomic" was adopted from the field of steroid receptor signalling which shows marked similarities with respect to the involvement of both transcription-dependent and -independent activities [Coleman and Smith, 2001], [Driggers and Segars, 2002].

The rapid increase in intracellular Ca^{2+} concentration is the most salient effect of the "nongenomic" pathway induced by TCDD and has been consistently demonstrated in organ cultures of TCDD-exposed animals [Canga et al., 1988], primary cell cultures [McConkey et al., 1988] and mammalian cell lines [Puga et al., 1992], [Monteiro et al., 2008]. The increase in intracellular calcium takes place within a few minutes after TCDD exposure and has been suggested to constitute the trigger of the nongenomic action of TCDD [Matsumura, 2009]. In certain cell lines the ubiquitous Ca^{2+}-dependent cytosolic phospholipase A2 (cPLA2) gets activated upon

the influx of Ca^{2+}, which cleaves arachidonic acid (AA) from glycerophospholipids [Dong and Matsumura, 2008], [Li and Matsumura, 2008], [Clark et al., 1991]. Furthermore, cPLA2 activation can also be effected via simultaneous phosphorylation at two serine residues (Ser505/727). In MCF10A cells [Dong and Matsumura, 2008] and the human U937 macrophage cell line [Sciullo et al., 2009], TCDD-induced cPLA2 activation was demonstrated by the stimulation of both Ser505 phosphorylation and AA release. Ser505 phosphorylation has been reported to be caused by the mitogen-activated protein kinase p38 [Börsch-Haubold et al., 1997], [Börsch-Haubold et al., 1998], [Hefner et al., 2000], but the possible involvement of p38 in cPLA2 activation in MCF10A cells or U937 cells was not investigated. The activation of the Src kinase by the formed AA is another early effect mediated by TCDD. In MCF10A cells, the activation occurs within 30 min [Mazina et al., 2004], [Dong and Matsumura, 2008]. Src activation has been tentatively explained by the observed ability of AA to cause the association of the c-Src homology 2 (SH2) domain with the EGF receptor (EGFR) at the plasma membrane. This results in an increased EGFR tyrosine phosphorylation and ERK signalling [Alexander et al., 2006]. In support of the physiological relevance of these observations, *c-src* knockout mice were reported to be less sensitive to toxic endpoints related to the classical "wasting syndrome", i.e. TCDD-induced cachexia, than their wild-type counterparts [Dunlap et al., 2002].

It has been suggested [Dong and Matsumura, 2008] that the fundamental aspects of the nongenomic pathway, i.e. the AhR (but not ARNT) –dependent initial stimulation of Ca^{2+} entry and the subsequent activation of cPLA2 and Src kinase, which occur within 15-30 min, are likely to be applicable to most cell types, although details of the phosphorylation-mediated pathways may vary between different types of cells. Moreover, evidence has been presented that several of the nongenomic actions of TCDD may be subsequently converted into genomic messages [Matsumura, 2009]. These include, for example, the activation of the inducible cyclooxygenase isoform, cyclooxygenase-2 (COX-2) [Kraemer et al., 1996], [Puga et al., 1997], [Yang and Bleich, 2004] and, in U937 macrophages [Sciullo et al., 2009], the subsequent transcriptional induction of tumor necrosis factor α and interleukin 8, cytokines involved in inflammatory responses.

Recently, a novel branch of the nongenomic pathway linking the TCDD-induced rapid elevation of intracellular Ca^{2+} concentration to the upregulation of AhR target genes, i.e. the genomic response, via phosphorylation events has been identified [Le Ferrec et al., 2002], [N'Diaye et al., 2006],[Monteiro et al., 2008]. For MCF 7 cells it was shown that the increase in intracellular Ca^{2+} concentration results in a transient activa-

tion of the ubiquitous calcium/calmodulin (CaM)-dependent protein kinase Iα (CaMKIα). CaMKIα turned out to be a prerequisite for the TCDD-triggered nuclear import of the ligand-activated AhR and promoter activation of AhR target genes. Confirmatory data were presented for primary human macrophages [Monteiro et al., 2008]. Evidence was obtained that exposure to TCDD was accompanied by an increased Thr177 phosphorylation of CaMKIα which has been associated with full CaMKIα activation [Haribabu et al., 1995]. However, a role of the Ca^{2+}/calmodulin-dependent protein kinase kinase (CaMKK) α or β in this phosphorylation could be excluded, and the protein kinase mediating CaMKIα activation remained unclear [Monteiro et al., 2008].

1.2 Phosphoproteomics

The proteome is the entire complement of proteins expressed by any given genome, cell, tissue or organism at a given time under strictly defined conditions [Wasinger et al., 1995] [Wilkins et al., 1996] and the phosphoproteome is the entirety of the phosphorylated proteins of a given proteome [Larsen et al., 2001], [Kalume et al., 2003]. The phosphorylation of proteins is a reversible post-translational modification that plays a crucial role in almost every biological process, like cellular growth, cell division, apoptosis and signalling. Protein phosphorylation can act as a switch to turn protein activity on or off [Hunter, 1995] and its dysregulation is known to result in many different human diseases including cancer, immune diseases and diabetes [Tao et al., 2005]. The process of phosphorylation and dephosphorylation is regulated by two groups of enzymes, the kinases and the phosphatases. The kinases transfer γ-phosphate from ATP to the target protein, while phosphatases remove the phosphate group from the protein. For the human proteome, approximately 100.000 phosphorylation sites have been estimated [Zhang et al., 2002], but a complete characterization of all phosphorylation sites in a proteome is still far away. Different amino acids can be phosphorylated, and the phosphorylation reactions can be divided into four different groups [Reinders and Sickmann, 2005]. The first class comprises *O*-phosphorylation which mostly occurs on serine, threonine and tyrosine residues and which plays the most important role in eukaryotes. *N*-phosphorylation, the second class, occurs on histidine and lysine residues. Cysteine phosphorylation belongs to the group of *S*-phosphorylations, the third group. The final group consists of acyl phosphorylations on aspartic and glutamic acid residues [Hohenester et al., 2010]. *N*-, *S*- and acyl phosphorylations are very labile under acidic conditions and are particularly difficult to detect [Kowalewska et al., 2010]. In the

present study, only protein phosphorylation at serine, threonine and tyrosine residues was analysed.

1.2.1 Phosphopeptide enrichment strategies

For the identification of phosphopeptides, a prior enrichment step is necessary to reduce the sample complexity by removing unphosphorylated peptides and to increase the relative concentration of the phosphopeptides in the sample. Different methods for enrichment of phosphoproteins and phosphorylated peptides have been recently developed. The majority of them are affinity-based approaches, like immobilized metal affinity chromatography (IMAC) [Neville et al., 1997] or titanium dioxide chromatography (TiO_2) [Pinkse et al., 2004]. These methods are widely used due to their high efficiency for the enrichment of phosphorylated peptides. Other techniques have been developed for the specific enrichment of phosphopeptides, such as chemical derivatisation using β-elimination [McLachlin and Chait, 2003]. This method is considered more difficult to handle and shows a reduced enrichment efficiency. An overview of the most important enrichment strategies is shown in Figure 1.1. For the present work, phosphorylated peptides were enriched using a modified IMAC strategy combined with TiO_2 chromatography. In the following, both methods will be described in more detail.

Immobilized metal affinity chromatography - IMAC

IMAC is a widely used method for the enrichment of phosphoproteins and phosphorylated peptides. The most common metal ions used for IMAC are Fe^{3+}, Ga^{3+}, Al^{3+} or Zr^{4+} which are bound to a stationary phase with the help of chelating complexes with nitrilotriacetic acid (NTA) or iminodiacetic acid (IDA) [Andersson et al., 1987], [Posewitz and Tempst, 1999]. Phosphopeptides bind to the metal ions with their negatively charged phosphoryl group through electrostatic interactions [Tsai et al., 2008]. The phosphopeptides can be eluted from the resin by an increasing pH gradient. A drawback of IMAC is the tendency of very acidic peptides to also bind the IMAC resin [Stensballe et al., 2001]. Peptides containing several aspartic acid or glutamic acid residues co-purify with the phosphopeptides due to the negatively charged carboxyl groups. This reduces the specificity and efficiency of IMAC and interferes with the subsequent MS analysis because of the better ionization of non-phosphorylated in comparison to phosphorylated peptides [Rogers and Foster, 2009]. An esterification of the acidic side chains of aspartate

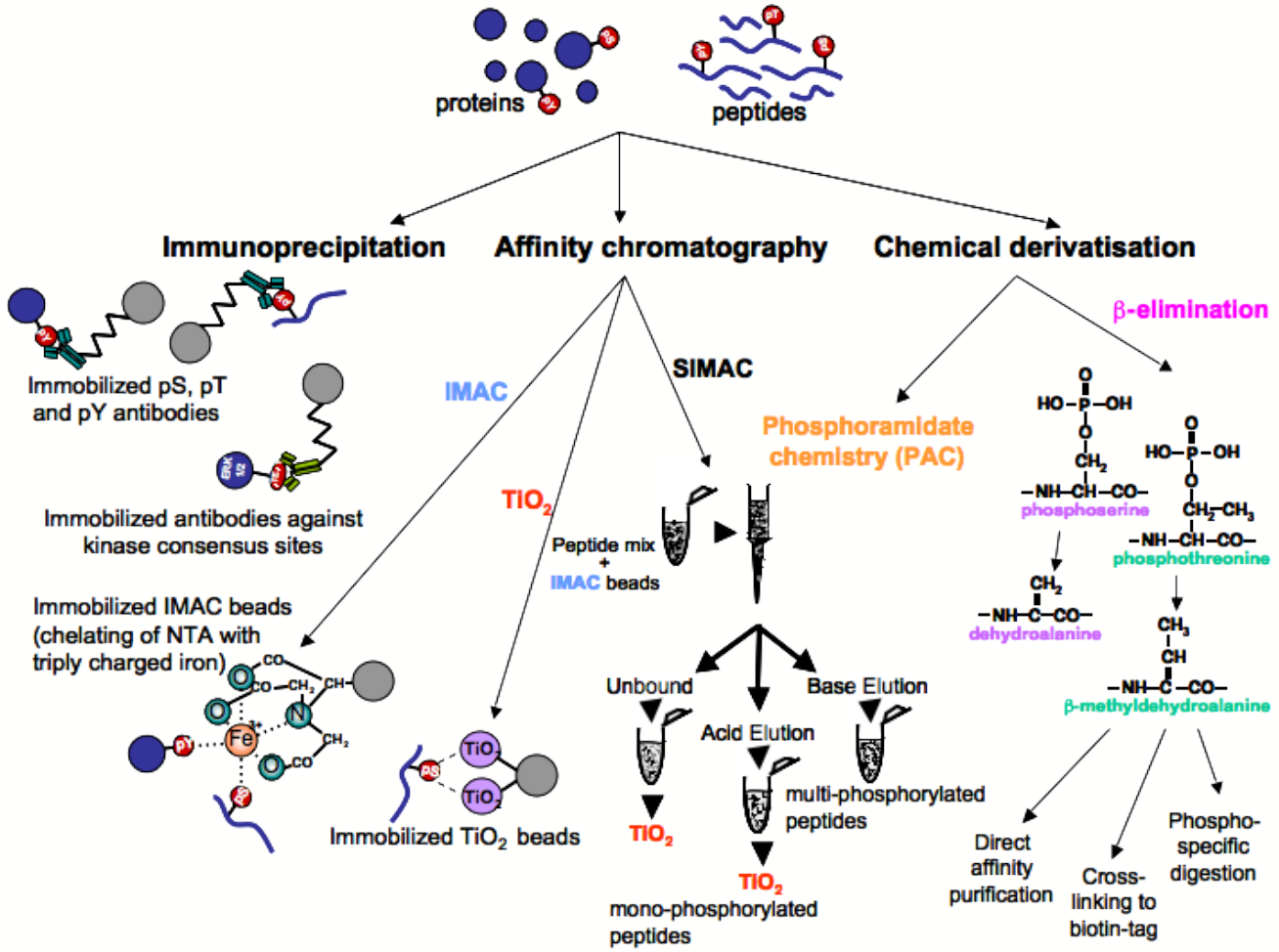

Figure 1.1: **Overview of important phospho-specific enrichment strategies.** The most common enrichment methods for phosphorylated peptides are illustrated. The picture is taken from [Thingholm et al., 2009]

and glutamate residues prior to IMAC reduces their unspecific binding and increases the phosphopeptide enrichment efficiency [Ficarro et al., 2002], [He et al., 2004]. However, *O*-methyl esterification also increases sample complexity. Another possibility is to increase the specificity of IMAC by pH adjustment, as the pKa of carboxyl groups is slightly higher than that of phosphate groups. For sample loading, the pH should be adjusted to around 2.7, since the carboxyl groups of the acidic amino acid residues are already protonated, whereas the phosphate groups still carry a negative charge and can interact with the IMAC stationary phase [Kokubu et al., 2005].

Titanium dioxide chromatography - TiO_2

Titanium dioxide chromatography is another common method for the enrichment of phosphopeptides. Ikeguchi and Nakamura (1997) showed that organic phosphates effectively bind titanium spheres in acidic conditions and can be subsequently eluted under basic conditions. However, under the acidic conditions during loading, peptides with several aspartic and glutamic acids are retained on the TiO_2 material resulting in the same problems associated with IMAC. To overcome this problem, Larsen *et al.* (2005) added dihydroxy benzoic acid (DHB) to the loading solution. DHB is a competitive binder which suppresses the interaction of the acidic peptides with the TiO_2 material without inhibiting binding of the phosphopeptides. However, DHB excessively binds to reversed phase (RP) material which results in problems for LC-MS/MS applications using RP columns. A later study showed that other organic acids, like phthalic acid or glycolic acid, have the same suppression effects for the acidic peptides as DHB, but do not interfere with LC-MS/MS [Jensen and Larsen, 2007].

TiO_2 is extremely tolerant to buffers and salts which makes the method convenient and easy to implement in the laboratory.

Sequential elution from IMAC - SIMAC

For the enrichment of phosphopepties, IMAC and TiO_2 chromatography were considered the best methods available. With TiO_2 mainly mono-phosphorylated peptides are identified, whereas IMAC has a preference for multiply phosphorylated ones. In 2008, Thingholm *et al.* suggested a strategy called SIMAC (sequential elution from IMAC) which overcomes the drawbacks of IMAC and TiO_2 chromatography. With this strategy, mono- and multi-phosphorylated peptides from complex samples are enriched in separate fractions. For SIMAC, the crude peptide mixture is first loaded onto the IMAC resin. The

mono-phosphorylated peptides are subsequently eluted from the IMAC material under acidic conditions and the multi-phosphorylated peptides eluted with basic conditions. The IMAC flow-through and the mono-phosphorylated fraction are collected separately and further enriched with TiO_2 (Figure 1.1). The three fractions are subsequently analysed by LC-MS/MS.

1.2.2 Shotgun proteomics

Shotgun proteomics identifies proteins in complex mixtures from tandem mass spectra of their proteolytic peptides [Marcotte, 2007]. In a typical workflow, the peptides are fractionated by LC-MS/MS to reduce sample complexity and peptides are introduced into a tandem mass spectrometer for analysis. The analysis can yield information on both peptide sequence and the existence of posttranslational modifications. From the peptide sequences, the proteins originally present in the sample can be identified.

Analysing peptides with a mass spectrometer consists of three different essential steps. The first is the ionization of the peptides in the ionization source which converts them into gas-phase ions. At the second stage, the ions are separated by their individual m/z (mass-to-charge ratio) values in the mass analyser. The last step is the detection of the ions by the ion detector [Yates, 2000]. For the identification of the peptide, the determined mass of the unknown molecule is searched against a database which contains the theoretical masses of the peptides from the relevant species ([McCormack et al., 1997]).

Two peptide ionization methods for proteome applications are available, matrix-assisted laser desorption ionization (MALDI) [Karas and Hillenkamp, 1988] and electrospray ionization (ESI) [Fenn et al., 1989]. Both ionization methods are capable of generating intact gas-phase ions from non-volatile and thermally labile molecules, like proteins and peptides [Chapman, 1996]. MALDI generates gas-phase ions from peptides embedded in a crystalline matrix with laser pulses and is preferentially used for samples with low complexity. ESI, on the other hand, generates the ions from liquid samples and is therefore easy to combine with liquid chromatography [Wilm et al., 1996]. In addition, it allows a cleaning of the sample, if required, prior to ionization. During ionization, mainly multiply charged proteins or peptides are generated in ESI.

Common mass analysers used in phosphoproteomics research are ion traps and quadrupoles. The quadrupoles consist of four rods, and the different ions are separated by varying the electric field applied to the rods. The ion traps, on the other hand, capture all ions and scan them out from low to high m/z by changing the applied radio frequency

(rf) potential. Since 2005, the Orbitrap mass analyser has been available. Orbitraps have a high resolving power (up to 100.000) and very high mass accuracy (<5 parts per million (ppm). The combination of the Orbitrap with a linear ion trap for peptide fragmentation has been highly suitable for the identification of phosphorylated peptides. In the present study, the tandem mass spectra were obtained using an LTQ-Orbitrap. The masses of the intact peptides are obtained in the Orbitrap and the subsequent fragmentation of the individual peptides is performed in the LTQ (linear ion trap).

Fragmentation of peptides

To retrieve structural information on the peptide level using MS, the peptide needs to be isolated and fragmented based on the amino acid. The resulting m/z ratios of these fragments are determined by the mass spectrometer and can then be compared to the theoretical fragment spectra of peptides in the peptide database. The acquired fragmentation spectrum is known as a MS^2 (MS/MS) spectrum. If the sequence of the protein is not known, the obtained sequence information can be searched against homologous protein sequences in a database using BLAST.

For the fragmentation of peptides, a MS scan of the sample is first performed. In the next step, in order of decreasing intensity, peptides are isolated in the mass spectrometer based on their m/z ratios and fragmented through the transfer of extra energy to the peptides. There are several ways to supply the additional energy for fragmentation. The most common method is termed collision-induced dissociation (CID), where the peptide of interest is isolated in a collision cell and mixed with an inert gas (Ar, He, N). Collision of the peptide with the gas converts some of the kinetic energy of the peptide into vibrational energy [Biemann, 1988]. As a result, the peptide mainly breaks at the peptide backbone between the carboxy carbon and the amide nitrogen. The fragment ions are termed daughter ions, the peptide ion is called precursor or parent ion. The daughter ions are then separated in a second mass analyser and measured by a detector.

The nomenclature of the generated fragment ions depends on the position of the backbone cleavage and whether the charge is retained at the N-terminus or C-terminus of the peptide [Roepstorff and Fohlman, 1984]. In general, the cleavage of the peptide backbone can occur at three different positions. The break of the Cα-C bond generates a and x ions, fragmentation of the C-N bond b and y ions and of the N-Cα bond c and z ions. Fragments will only be detected if they carry at least one positive charge. If the positive charge occurs on the N-terminus after fragmentation, the fragment ions are termed a_n, b_n or c_n, where

n indicates the position of the fragment amino acid counted from the N-terminus. If the charge is retained on the C-terminal fragment, the ions are called x_n, y_n or z_n.

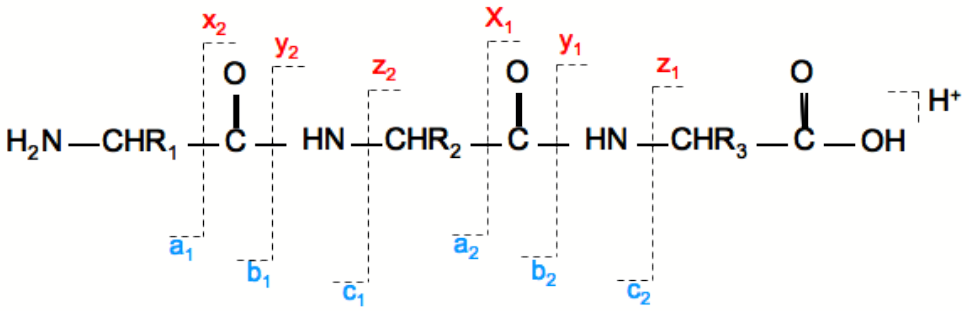

Figure 1.2: **Common nomenclature for peptide fragmentation.** Shown is the common nomenclature for the fragment peptide ions generated by MS/MS. The nomenclature was originally proposed by Roepstorff and Fohlman [1984] and modified four years later by Biemann [1988].

An overview of the fragmentation nomenclature is shown in Figure 1.2. For CID fragmentation, primarily y and b ions are obtained. A detailed illustration of this fragmentation is shown in Figure 1.3.

For the identification of phosphopeptides, conventional CID is not sufficient. Phosphorylations on serine and threonine residues are highly labile, and with CID fragmentation, the MS/MS spectra predominantly show the precursor ion at a lower m/z corresponding to a loss of the phosphoric acid group (neutral loss of 98 Da). A sufficient fragmentation of this phosphorylated peptide can be obtained through selecting the fragment ion originating from the loss of the phosphoric acid group for a second round of fragmentation, which is termed phosphorylation-directed MS^3 [Beausoleil et al., 2004]. This method yields more detailed sequence infomation and can indicate the specific phosphorylation site on the serine or threonine residue. Recently, a new variation of the MS^3 method was developed, termed multi-stage activation (MSA) [Schroeder et al., 2004]. For MSA, the MS^2 and the MS^3 scan are combined in a hybrid MS/MS spectrum with the sequence information derived from fragmentation of the precursor after neutral loss and original fragmentation. This technique is faster than the MS^3, but MSA is limited to ion traps. For the present study, MSA type fragmentation was used.

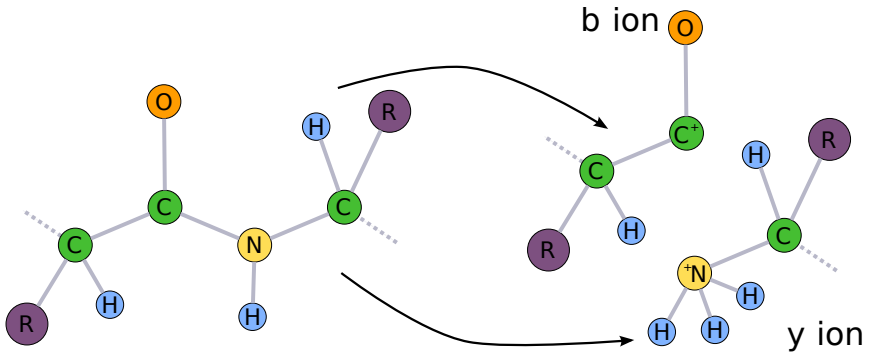

Figure 1.3: **Schematic representation of the CID fragmentation.**

1.2.3 Quantitative phosphoproteomics

Quantitative phosphoproteomics is the relative quantitation of the phosphoproteins or phosphopeptides from two or more samples, such as cultured cells treated with a test agent and untreated cells. This quantitative approach can be differentiated into three different types: metabolic labelling, chemical labelling and label-free approach [Palmisano and Thingholm, 2010]. For metabolic and chemical labelling, a stable isotope is used to tag the protein or peptide, but the point in the workflow where the isotope is incorporated differs, depending on the particular method chosen. For metabolic labelling, the labels are introduced into live cells through the culture medium. For chemical labelling, the label is introduced at some downstream stage during sample processing. For both methods, the same proteins or peptides from the control cells can be distinguished from those treated during MS analysis because of the different masses of the isotopes. For the label-free approach, no label is introduced into the samples. Here, the quantitation is based on the liquid chromatography, MS or the MS/MS data. For the present study, a metabolic labelling approach, the stable isotope labelling with amino acids in cell culture (SILAC), was used.

SILAC was introduced in 2002 by two different groups and is based on the incorporation of isotopically labelled amino acids into growing cells in culture [Zhu et al., 2002], [Ong et al., 2002]. The labelled amino acids will be incorporated into the proteins, and after several cell cycles, certain amino acids will be nearly completely exchanged by the labelled ones. As a result, the labelled peptides are heavier than the peptides containing the natural amino acid. The cells are then lysed and combined with the cells grown in normal medium. During MS analysis, the labelled and unlabelled peptides appear together and can be quantified by comparing their relative signal intensities. The most common

amino acids for the SILAC approach are lysine and arginine, where the carbon atom is exchanged with ^{13}C and/or the nitrogen atom with ^{15}N. Both isotopes have no influence on the chemical behaviour of the peptides during the subsequent phosphopeptide enrichment step and the liquid chromatography step prior to MS analysis.

SILAC is a straightforward method and has already successfully been used for the study of phosphorylation changes under different conditions [Gruhler et al., 2005], [Olsen et al., 2006], [Malik et al., 2009]. The early introduction of the label into the samples reduces the risk of variations in sample handling during sample processing and, thus, the generation of erroneous quantitative results.

1.3 The aim of the present study

Whereas the genomic response to TCDD has been analysed in several large-scale studies at the level of the transcriptome and the proteome both *in vitro* and *in vivo*, a systematic study of the proteins involved in the early nongenomic action of TCDD has not been performed previously. Therefore, the present study was conducted with the aim to identify TCDD-induced alterations in protein phosphorylation occurring early after the onset of TCDD exposure in order to shed light on the alterations in signal transduction potentially involved in the early, nongenomic effects of TCDD.

In the present study, the rat hepatoma cell line 5L was used as a model system. This cell line is a descendant of the H-4-II-E cell line established by [Pitot et al., 1964] from the Reuber H35 rat hepatoma [Reuber, 1961]. 5L cells are epithelial-like cells which express both the AhR and the ARNT protein and which are highly responsive to TCDD-induced gene activation. They have been previously used in a variety of studies dealing with the role of AhR in cell cycle regulation and TCDD toxicity [Göttlicher et al., 1990], [Göttlicher and Wiebel, 1991], [Wiebel et al., 1991], [Weiss et al., 1996], [Ge and Elferink, 1998], [Reiners et al., 1999], [Elferink et al., 2001], [Levine-Fridman et al., 2004]. With respect to nongenomic actions of TCDD in this cell line, Weiss et al. (2005) observed that TCDD exposure of the cells is associated with the rapid phosphorylation of the p38 mitogen-activated protein kinase (MAPK) in an AhR-dependent, but, importantly, transcription-independent manner. p38 activation was observed as early as 1 h after addition of TCDD and resulted in subsequent transcriptional induction of the proto-oncogene *c-jun*. Phosphorylation of p38 was not effected by any of the kinases known to phosphorylate p38, suggesting a novel cross-talk

between AhR and MAPK signalling. The signalling pathway resulting in p38 phosphorylation and the kinase involved remained unclear.

In the present quantitative phosphoproteomic analysis of the effects of TCDD in 5L cells, short exposure periods of 0.5, 1 and 2 hours were used, i.e. treatments that were unlikely to result in significant alterations in the abundance of proteins with TCDD-regulated expression which requires some time due to its dependence on *de novo* transcription and translation. The study was performed with the expectation to uncover proteins previously unknown to exhibit rapid alterations in phosphorylation as a consequence of TCDD exposure and which might give clues to pathways involved in nongenomic signalling preceding alterations in gene expression. Moreover, it was anticipated to identify proteins with altered phosphorylation as a consequence of their involvement in the regulation of transcription induced by the DRE-bound liganded AhR/ARNT heterodimer. And, finally, the study was expected to provide novel information on the global phosphoproteome of rat cells with respect to the identification of novel phosphorylation sites of phosphoproteins and the discovery of proteins previously not known to be phosphorylated.

Chapter 2

Material and methods

2.1 Materials

RPMI 1640 without arginine and lysine, PBS and dialysed fetal calf serum were from Gibco-Invitrogen (Carlsbad, CA). U-$^{13}C_6$-L-lysine hydrochloride and U-$^{13}C_6$ $^{15}N_4$-L-arginine hydrochloride were from Invitrogen (Carlsbad, CA, USA). U-$^{15}N_4$-L-arginine hydrochloride was from Cambridge Isotope Laboratories (Andover, MA, USA) and TCDD (purity > 99%) in dimethyl sulfoxide was from Ökometric (Bayreuth, Germany). Benzonase, KN-92, KN-93 and W-7 were from Merck (Darmstadt, Germany). Arginine, lysine, Tris, $MgCl_2$, NaCl, phosphatase inhibitor cocktails 1 and 2, acetonitrile, formic acid, ethanol, acetone, PHOS-Select^{TM} Iron Affinity Gel, 2-APB, BAPTA-AM, besylate, Diltiazem hydrochloride, Nifedipine, sodium orthovanadate and Triton X-100 were from Sigma-Aldrich (Taufkirchen, Germany). "Complete" protease inhibitor cocktail tablets were from Roche (Mannheim, Germany). Sequencing grade modified trypsin was from Promega (Madison, WI, USA). Lys-C was from Wako (Richmond, VA, USA). Hydrogen peroxide was purchased from J.T. Baker (Deventer, Netherlands). TSKGel Amide-80 5 μm HILIC 2 mm column was from Tosoh Bioscience (Stuttgart, Germany). Poros Oligo R3 RP material was from PerSeptive Biosystems (Framingham, MA, USA). GELoader tips were from Eppendorff (Hamburg, Germany). Glycolic acid and trifluoroacetic acid were from Fluka (St. Louis, MO, USA). 3M Empore C8 disks were from 3M Bioanalytical Technologies (St. Paul, MN, USA). Syringe for HPLC loading was from SGE (Victoria, Australia). The water was from an Elga Purelab Ultra (Bucks, UK). Titanium dioxide beads were from GL Sciences Inc. (Tokyo, Japan). ReproSil-Pur C18 AQ, 5 μm was from D. Maisch

(Ammerbuch-Entringen, Germany). PicoTip^{TM}emitter needles were from New Objective, DNU - Nowak Umweltanalysen (Berlin, Germany).

2.1.1 Software

The mass spectrometry raw files generated by the LTQ Orbitrap XL mass spectrometer were inspected with the software Xcalibur 2.1 (Thermo Fisher Scientific, Bremen, Germany). MALDI spectra were analysed using the program flexAnalysis (Bruker Daltonics, Bremen, Germany). MSQuant (University of Southern Denmark, Odense, Denmark) was used for the quantitation and phosphosite localization scoring of the identified phosphopeptides. The program "R" (Version 2.9.1), a statistical data analysis software freely available under: http://cran.r-project.org, was used for the statistical analysis. For this work, the following R-Packages were dowloaded and used: limma, q-value, BioIDmapper and biomaRt.

Protein Center (http://www.proxeon.com; Proxeon, Odense, Denmark) is a consolidated protein database. The software was used for the annotation of proteins to databases like Pfam or Gene Ontology to support the interpretation of the experimental data.

2.2 Methods

2.2.1 Cell culture

5L Rat hepatoma cells

5L cells were cultured as monolayers in RPMI 1640 medium supplemented with 10% fetal bovine serum, 100 μg/ml streptomycin and 100 U/ml penicillin at 37 °C in a humidified atmosphere containing 5% CO_2.

SILAC labelling

For stable isotope labelling of the 5L cells, normal lysine (Lys0), $^{13}C_6$-lysine (Lys6), $^{15}N_4$-arginine (Arg4) and $^{13}C_6{}^{15}N_4$-arginine (Arg10) were used. The amino acids were dissolved in RPMI medium without arginine and lysine supplemented with 10% dialysed fetal bovine serum, 100 μg/ml streptomycin and 100 U/ml penicillin. For the "light" condition, the medium was supplemented with Lys0 and Arg4 and for the "heavy" condition with Lys6

and Arg10 according to the labelling scheme of van Hoof et al. [Van Hoof et al., 2007]. The concentrations of arginine and lysine were 75 mg/L.

Arginine and lysine are the most common amino acids for labelling. This is due to the use of the protease trypsin in the majority of proteomic experiments. Trypsin cleaves at the carboxy termini of arginine and lysine residues. Thus, when these amino acids are used for labelling, every tryptic peptide is labelled except for the C-terminal one.

The cells were grown for at least seven cell cycles (about seven days) with periodical splitting when they reached a density of around $1 * 10^7$ cells/10-cm dish.

TCDD treatment

During the final 16 hours before the start of the TCDD exposure, the cells were starved in labelling medium without serum. The "heavy" cells were treated with 1 nM TCDD dissolved in Me_2SO and the "light" cells with Me_2SO alone as a control for 0.5, 1 or 2 hours.

Preparation of sodium pervanadate

To produce the protein tyrosine phosphatase inhibitor pervanadate, 100 mM sodium orthovanadate solution was prepared and the pH adjusted to 10 with 1 M HCl. Due to the basic pH the solution became yellow. After another boiling step, the solution became clear again. The pH was again adjusted to 10 when the sodium orthovanadate solution reached room temperature. The boiling and cooling steps were repeated until the pH was stable at pH 10.0 and the solution remained clear. Directly before use, the prepared 100 mM sodium orthovanadate solution was mixed 1:1 (vol/vol) with a 0.36% hydrogen peroxide solution to generate a 50 mM sodium pervanadate solution.

Cell lysis

Following cellular exposure, the medium was removed and cells were washed twice with 10 ml ice cold PBS. Then 1.5 ml of lysis buffer containing 1 μl/ml Benzonase, 1 mM $MgCl_2$, 25 mM Tris-HCl, pH 7.4, 120 mM NaCl, 1% Triton X-100, protease inhibitors (one "complete" protease inhibitor cocktail tablet per 50 ml), phosphatase inhibitor cocktails 1 and 2 (0.5 ml each per 50 ml) and 1 mM sodium pervanadate was added to each 10 -cm dish. The lysates were transferred to Eppendorf tubes, shaken for 30 min at 4 °C and centrifuged at 15.000 g for 10 min at 4 °C. The protein concentrations of the supernatants from the "light"

and the "heavy" cells were determined with the Bradford assay and mixed 1:1. The pellets were discarded.

2.2.2 Sample preparation

Acetone/ethanol precipitation

The proteins were precipitated by adding four volumes of ice cold ethanol. After 15 min incubation, four volumes of ice cold acetone were added and the mixture was incubated at -20 °C overnight. The precipitated proteins were centrifuged at 15.000 g for 20 min at 4 °C. The pellet was washed three times with 2:2:1 ethanol/acetone/water.

Proteolysis

The precipitated proteins were dissolved in 6 M urea, 2 M thiourea and 50 mM NH_4HCO_3. The proteins were reduced for 2 h at 30 °C with 20 mM DTT and then alkylated with 40 mM iodoacetamide for 45 min in the dark at room temperature. Then they were digested with endoproteinase Lys-C (1:100 enzyme to protein ratio) for 3 hours. For digestion with trypsin (1:50 enzyme to protein ratio), the proteins were diluted in 50 mM NH_4HCO_3 to a urea concentration of 1 M and incubated with trypsin at 30 °C for 16 h. The digestion was quenched by adding trifluoroacetic acid (TFA) to reach a pH of <3.

Sequential elution from IMAC - SIMAC

PHOS-Select™ Iron Affinity Gel beads were washed twice with 0.1% TFA and once with 50% ACN, 0,1% TFA (loading buffer) to remove the glycerol. Finally, the beads were resuspended in loading buffer and the sample was added. For 200 μg of peptides, approximately 50 μl PHOS-Select™ Iron Affinity Gel beads were used. After incubation by end-over-end rotation for 1 h, the peptide-bead mixture was transferred to a constricted gel loader tip. The flow-through and the first wash with loading buffer (100 μl) were collected. The mono-phosphorylated peptides were eluted with 20% ACN, 1% TFA (100 μl) and again collected. Both fractions were combined and dried down in a vacuum centrifuge. The multi-phosphorylated peptides were eluted with 1% NH_4OH (70 μl) and acidified with formic acid (FA) to obtain a final FA concentration of 1%. The multi-phosphorylated peptides were desalted using Poros R3 P10 micro columns and analysed by LC MS/MS.

Hydrophilic interaction chromatography - HILIC

The mono-phosphorylated peptides from the SIMAC enrichment were fractionated by hydrophilic interaction chromatography (HILIC). The dried SIMAC fraction was resuspended in B-solvent (80% ACN, 0.1% TFA) and loaded onto a 2 mm TSKGel Amide-80 HILIC column connected to an Äkta Basic FPLC system.

Loading was performed in B-solvent at a flow rate of 200 μl/min for 12 min. The peptides were separated by an inverse gradient (100% - 70% B-solvent within 28 min and 70% - 0% B-solvent within 5 min) with an increasing amount of A-solvent (0.1% TFA) at a flow rate of 200 μl/min. A total of 16 fractions were collected, as shown in Table 2.1. The fractions were dried down in a vacuum centrifuge.

HILIC fraction	Part of the gradient	Fraction time
1	Sample loading	15 min
2	Gradient 1 - 5 min	5 min
3	Gradient 6 - 9 min	4 min
4	Gradient 10 - 12 min	3 min
5	Gradient 13 min	1 min
6	Gradient 14 min	1 min
7	Gradient 15 min	1 min
8	Gradient 16 min	1 min
9	Gradient 17 min	1 min
10	Gradient 18 min	1 min
11	Gradient 19 min	1 min
12	Gradient 20 min	1 min
13	Gradient 21 - 22 min	2 min
14	Gradient 23 - 24 min	2 min
15	Gradient 25 - 28 min	4 min
16	End	10 min

Table 2.1: Overview of the collected HILIC fractions

Titanium dioxide chromatography - (TiO_2)

To enrich the mainly mono-phosphophorylated peptides, the TiO_2 method was used essentially as described by Thinghol et al. (2006). TiO_2 beads were washed with water, then ACN and finally loading buffer (1 M glycolic acid in 80% ACN, 5% TFA). For every 200 μg of peptides around 0.6 mg TiO_2 particles were used. Each HILIC fraction was dissolved

in 5 μl 1% SDS, 200 μl loading buffer, and the appropriate amount of TiO_2 added. The peptides and TiO_2 resin were incubated for 15 min under vigorous shaking before the beads were spun down by centrifugation at 2000 g for 30 s. The supernatant was collected in a fresh tube and the TiO_2 beads were washed with loading buffer, followed by 80% ACN/ 5% TFA, then 30% ACN/ 0,1% TFA and by distilled water. Phosphopeptides were eluted from the beads with 50 μl 1% NH_4OH using an incubation time of 10 min under vigorous shaking. The supernatant was acidified with 5 μl FA. The phosphopeptides were desalted using Poros R3 P10 micro columns and analysed by LC-MS/MS. The collected supernatant from the first TiO_2 incubation with loading buffer was again treated with TiO_2 as described above.

Comparison of the SIMAC and TiO_2 method

In order to compare the performance of the SIMAC and TiO_2 method when used alone, they were tested with a tryptically digested 12-protein-mixture (Protein Research Group, University of Southern Denmark, Odense, DK). Each protein was dissolved in 50 mM NH_4HCO_3 and reduced and alkylated in 10 mM DTT and 20 mM iodoacetamide. The proteins were digested with trypsin (1/50 w/w) overnight and the reaction quenched with TFA. The phosphorylated peptides were then enriched using the SIMAC or TiO_2 method as described above.

StageTip purification

Peptides were purified using StageTips. StageTips were prepared by stamping out a small plug of a 3M Empore C8 disk and depositing at the end of a P10 tip. Poros R3 material in ACN was packed in the pipette tip on top of the C8 disk. The microcolumn was washed with ACN and equilibrated with 0.1% TFA. Phosphopeptide samples were loaded onto the columns using a 1 ml disposable syringe. The columns were washed once with 0.1% TFA and the peptides eluted with 50% ACN and 0.1% TFA. Samples were nearly dried down in a vacuum centrifuge and redissolved in 0.5 μl 100% FA and an additional 4.5 μl 0.1% FA for analysis by LC MS/MS.

2.2.3 Mass spectrometric methods

MALDI MS

To evaluate the success of the phosphopeptide enrichment methods SIMAC and TiO_2, the samples obtained from the tryptic digestion of the 12-protein-mixture and the subsequent enrichment were analysed on a Bruker Ultraflex mass spectrometer (Bruker Daltonics, Bremen, Germany). All spectra were acquired in positive reflector ion mode. The samples were spotted on a MALDI target together with DHB (20 mg/ml) in 70% ACN/ 0.1% TFA/ 1% phosphoric acid. The spectra were processed using the flexAnalysis software (Bruker Daltonics, Bremen, Germany).

LC MS/MS

The enriched and purified phosphopeptides were analysed on an LTQ Orbitrap XL Mass Spectrometer (Thermo Fischer Scientific, Bremen, Germany). The samples were applied onto an EASY nano-HPLC system (Proxeon Biosystems, Odense, Denmark) comprising a self-packed 16 -cm analytical column (100 μm I.D., 360 μm O.D., ReproSil-Pur C18 AQ 3 μm). The peptides were loaded with a flow rate of 550 nl/min in 0.1% FA (solvent A) and eluted at a flow rate of 250 nl/min with a gradient from 100% solvent A to 34% solvent B (95% ACN/ 0.1% FA). The length of the gradient depended on the complexity of the sample. Three different gradients were used: 100 min, 50 min and 30 min. The nano-HPLC system was connected online to the mass spectrometer with a nano ES ion source and PicoTip^{TM} emitter needles. The mass spectrometer was operated in positive ion mode and a data-dependent acquisition method that automatically switched between MS and MS/MS was employed. Each MS scan was followed by up to 5 MS/MS scans. The full scan was acquired in the Orbitrap with an automatic gain control (AGC) target value of 1 * 10^6 ions and a maximum fill time of 500 ms. The ion resolution was set to R = 60000 at 400 m/z. The top five most intense ions were selected for fragmentation in the LTQ. Fragmentation was induced by collision-induced dissociation. For the LTQ, the AGC target value was set to 30000 ions and a maximum fill time of 300 ms. For an improved fragmentation of phosphopeptides, the MSA algorithm was employed if a MS/MS spectrum showed a loss of phosphoric acid from the parent ion (neutral loss of 97.97, 48.99, or 32.66 Thomson (Da)). Ions selected for MS/MS were dynamically excluded from further fragmentation for a duration of 45 s.

2.2.4 Bioinformatics and biostatistics analysis

Database searching

The acquired MS^n spectra were converted into Mascot generic format (mgf) using the software DTASuperCharge, version 1.37 (http://msquant.sourceforge.net/). De-isotoping was performed using the default settings from DTASuperCharge. The processed spectra were searched against the rat IPI protein database version 3.60 which contains 39863 protein sequences. The search was performed using an in-house Mascot database search program (version 2.2) with carbamidomethyl (C) as a fixed modification and acetylation (protein N-terminal), oxidation (M), phoshphorylation (ST and Y) and the SILAC labelling (K-6, R-4, R-10) as variable modifications. Trypsin was chosen as the enzyme and up to two miss-cleavages were allowed. For the parent ion, a mass accuracy of 10 ppm was used and for the fragment ions a mass accuracy of 0.8 Da was specified. A concatenated decoy database search was performed derived from the IPI rat database. Proteins with a false discovery rate (FDR) of $\leq 1\%$ and peptides with an ion score of ≥ 20 (MudPIT) multidimensional protein identification technology) scoring) were accepted.

Quantitation and phosphosite localization

In general, for a reliable protein identification and subsequent quantitation at least two different peptides must be identified. However, the different phosphorylation sites on a given protein can be differentially regulated [Olsen et al., 2006], and therefore every identified phosphorylated peptide must be quantitated individually [de la Fuente van Bentem et al., 2008]. Quantitation of phosphopeptides and non-phosphorylated peptides was performed using the software MSQuant version 1.0a70. MSQuant quantifies the peptides based on the first isotopic peak of the isotopically labelled peptides by summing up the ion intensities in a specified interval around the centroid of the peak [Mortensen et al., 2009]. As a measure of the reliability of the phosphorylation site assignment, a PTM score for every phosphosite was calculated using MSQuant. The PTM score is a probability-based scoring system for phosphorylation site assignment [Olsen and Mann, 2004]. Briefly, to calculate the PTM score, the four most intense fragment ions per 100 Da in a MS^2 or MS^3 spectrum are taken and the matches k with all possible combinations of b- and y- ions and their phosphorylation sites in a given peptide sequence are counted. The PTM score is calculated as $-10 \cdot \log_{10}(p)$, where p is calculated

as:

$$\begin{aligned} p &= (k!/(n!(n-k)!) \cdot p^k \cdot (1-p)^{(n-k)} \\ &= (k!/(n!(n-k)!) \cdot 0.04^k \cdot 0.96^{(n-k)} \end{aligned}$$

With n as the total number of possible b- and y-ions.

After calculating the PTM score and the regulation factors with MSQuant, every MS and MS/MS spectrum was manually validated. Peptides with a low signal to noise ratio, ion score under 20, low number of MS scans and overlapping peaks were removed. The retained peptide lists from MSQuant were then further processed with the statistical program R to identify the statistically significantly regulated peptides.

Removal of duplicate peptides and normalisation

Before the statistical test was performed, redundant peptides were removed,where the peptide with the highest ion score was kept. Furthermore, the occurrence of duplicate peptide sequences with different IPI accessions was inspected. If one peptide was detected with different accessions, only the peptide belonging to the IPI identifier with the highest number of different peptides observed was retained.

Next, a normalisation of the calculated peptide ratios was performed to correct inaccuracies caused by the sample preparation, i.e. the 1:1 mixing of proteins from the "light" and the "heavy" state. A global normalisation method was used, where the log median of the peptide ratios was adjusted to zero. The normalisation was performed with the open source program R. To visualize the normalisation effect, MA plots were generated using R.

Statistical analysis

In the present study, three different, independent biological replicates were analysed for the datasets obtained for the 30 min and 1 hour exposures to TCDD and two biological replicates were analysed for the 2 hours dataset.

To assess the conformance of the individual data sets of a time point, Pearson correlation coefficients "r" were calculated by R for the peptide ratios from the biological replicates against the mean of the ratios of the biological replicates. The coefficient r indicates the degree of linear dependence between two variables and is between -1 and 1. A positive value stands for a positive association, whereas a negative value implies a negative or inverse association [Sachs and Hedderich, 2009].

The ratios of the biological replicates were merged together based on the peptide sequence. Only peptides that were found at least twice for a given time point were used for the following statistical test. The normalised and merged ratios were than fitted to a linear model and a moderated t-test conducted. The linear modelling and the moderated t-test were performed using the R-package "limma". The resulting p-values were used to calculate q-values with the R-package "q-value". The p-value is a measure for significance in statistics [Käll et al., 2008] and is a measure of probability of rejecting or accepting the null hypothesis. A low p-value means a low probability that the null hypothesis is true. The null hypothesis in this analysis is that no peptides are regulated. The q-value is a method for the correction of multiple testing, meaning the value is a threshold for the false discovery rate (FDR, i.e. the null hypothesis was wrongly rejected).

Peptides with a q-value lower than 0.05 were accepted as significantly regulated and Volcano plots were generated with the limma package.

Annotation

Following the statistical analysis, the data for every time point were mapped to different identifiers from different protein databases such as Uniprot, Gene Ontology (GO) or KEGG using the IPI accession number. The mapping was done using the software R in combination with the packages BioIDMapper and biomaRt.

Phosphoset analysis

For the global analysis of the enriched phosphorylated peptides, all identified peptides from the different time points and biological replicates were merged together. The redundant peptides were removed and saved as an Excel file. Counting of the phosphorylated peptides, sites and proteins was performed in Microsoft Excel. The identification of known and hitherto unknown phosphorylation sites was done with an in-house written Perl script. For this analysis, the Swiss-Prot accession numbers were used and searched against the UniProt database.

2.2.5 Western blot analysis

For Western blot analysis of the effects of TCDD on the abundance of CYP1A1 and Rdbp protein, cells were treated and lysed as described above and equal amounts of total protein (20 μg) were resolved on 12% polyacrylamide gels (XCell SureLock, Invitrogen, Darmstadt,

Germany). Proteins were transferred on nitrocellulose membranes using the iBlot dry blotting system (Invitrogen). Membranes were blocked with 3% bovine serum albumin in TBS/Tween, and CYP1A1 and Rdbp were detected using an anti-CYP1A1 antibody (G-18, Santa Cruz Biotechnology, Santa Cruz, USA) and an anti-RDBP antibody (AVIVA Systems Biology, San Diego, USA), respectively, horseradish peroxidase-labelled secondary antibodies and ECL detection kit (LumiGLO, Cell Signaling Technology, Beverly, USA). Bands were quantitated by densitometry using the ImageMaster 1D Elite software, v4.00 (Pharmacia Biotech, Uppsala, Sweden). The actin band, which served to normalize for the amount of protein loaded, was detected using an anti-actin antibody (clone AC-40, Sigma).

2.2.6 Ethoxyresorufin *O*-deethylase (EROD) assay

As a measure of the enzymatic activity of cytochrome P4501A1 (CYP1A1) in 5L cells, the 7-ethoxyresorufin *O*-deethylase (EROD) activity was determined in whole cell lysates. The assay determines the conversion of the substrate 7-ethoxyresorufin into the strongly fluorescent dealkylation product resorufin. The assay was performed according to the method of Pohl and Fouts (1980) using modifications described by Schwirzer et al. (1998). Following incubation of the cells with DMSO or TCDD for up to 24 h. They were washed twice with PBS, pelleted by centrifugation and stored frozen (-20 °C) until use. The frozen pellets were re-suspended in 50 mM Tris-HCl (pH 7.6) to obtain a protein concentration between 1-2 mg/ml, and 20 μl of the cell suspension was added to 230 μl of a solution containing 2 μM 7-ethoxyresorufin, 400 μM NADPH, 10 μM dicumarol, and 5 μM $MgSO_4$. Dicumarol was included to inhibit the enzyme DT-diaphorase which converts resorufin into a non-fluorescent product. The mixture was incubated in a water bath at 37 °C for 30 min in the dark. The reaction was stopped by placement of the mixture in ice water and addition of 500 μl of ice-cold methanol. Following centrifugation in a desktop centrifuge, 300 μl of the supernatant were transferred into black 96-well microtiter plates (Nunclon Delta, Thermo Scientific Nunc, Roskilde, Denmark). The fluorescence of the dealkylation product resorufin was read in a microplate reader (Synergy 2, BioTek, Vermont, USA) using an excitation wavelength of 540 nm and an emission wavelength of 620 nm. Each sample was analyzed in duplicate. The amounts of resorufin formed were calculated using a calibration curve generated with resorufin standards.

Chapter 3

Results

To detect changes in protein phosphorylation resulting from the treatment of 5L cells with TCDD, we employed stable isotope labelling in cell culture (SILAC) as a quantitation method. The SILAC approach is based on the differential metabolic labelling of proteins from treated and untreated cells at the cell culture level.

The cells designated for the use as control cells were labelled with normal lysine and $^{15}N_4$-arginine (Arg4), while those designated for TCDD treatment were labelled with $^{13}C_6$-lysine (Lys6) and $^{13}C_6{}^{15}N_4$-arginine (Arg10). After complete substitution of the normal amino acids by the heavy analogues, the cells were serum-starved for 16 hours followed by treatment of the "light" and "heavy" cells with DMSO and TCDD, respectively, for 30 minutes, 1 hour and 2 hours. Following cell lysis and determination of the protein concentrations, treated and control cells were mixed in a one-to-one ratio. The proteins were then precipitated and proteolysed with trypsin. The resulting peptides were separated by hydrophilic interaction chromatography (HILIC) and the fractions enriched for phosphorylated peptides using SIMAC and TiO_2. Phosphopeptides were analysed by high-resolution mass spectrometry on a linear ion trap instrument coupled to an Orbitrap (LTQ-Orbitrap). All data were searched using an in-house MASCOT server. A peptide was accepted for quantitation when it had a MASCOT ion score of at least 20. The relative quantitation of the peptides was performed using MSQuant software [Mortensen et al., 2009] (http://msquant.sourceforge.net). All peptide spectra were manually validated and peptides with low number of MS scans, low signal/noise ratio or overlapping peaks were removed and not used for quantitation. As a guide, Figure 3.1 shows the workflow of cell culture, sample preparation and phosphopeptide analysis.

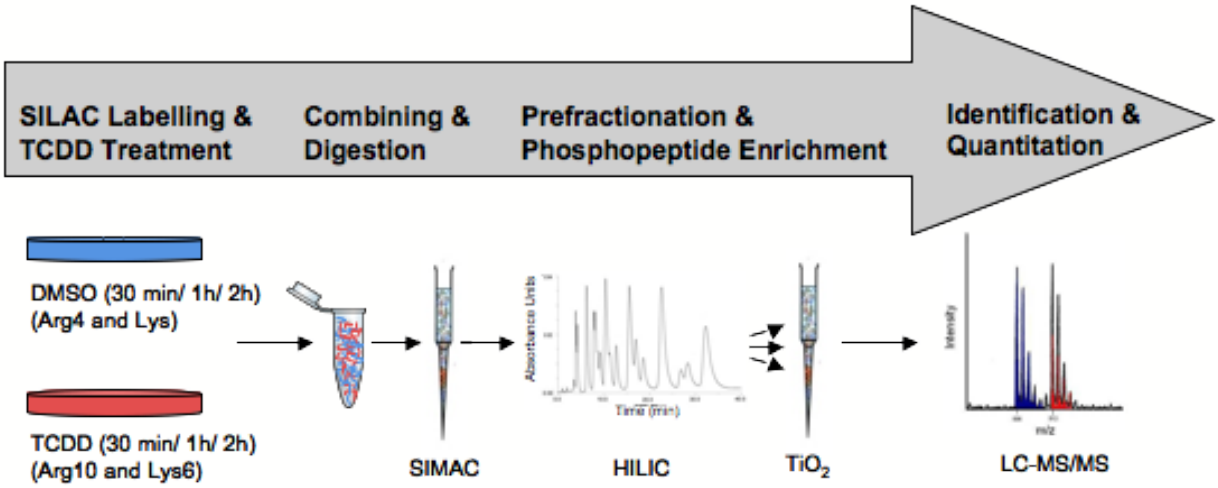

Figure 3.1: **Workflow illustrating the principal steps of sample preparation and processing**

3.1 SILAC labelling

SILAC is a method for relative quantitation, based on the relative peak intensities of labelled and unlabelled peptides measured by mass spectrometric analysis. An accurate protein quantitation requires a near complete substitution of the normal amino acid by the isotopically labelled ("heavy") amino acid. Therefore, essential amino acids, i.e. amino acids that cannot be synthesised by the cell, are generally used for labelling. Lysine is an essential amino acid and needs to be added to the medium. Arginine, on the other hand, is a non-essential amino acid in adult vertebrates. However, Scott et al. (2002) showed that arginine is an essential amino acid for several cell lines. In this study, Scott and co-workers tested 26 different cell lines and observed that the majority were very sensitive to arginine deprivation which caused a loss of viability. Since no information was available on the dependence of the 5L cells on lysine, the non-essential amino acid arginine and the efficiency of the isotopic labelling, cell proliferation in medium with and without lysine and arginine was monitored.

A total of $5 * 10^5$ cells each were seeded in 5-cm dishes in arginine- and lysine- deficient medium supplemented with 10% dialysed fetal calf serum and arginine and lysine (100 mg/L each), only arginine (100 mg/L) or only lysine (100 mg/L). Microscopic pictures were taken after 24 h, 48 h and 72 h. The photographs in Figure 3.2 demonstrate a dramatic change of cell growth and cell morphology in arginine- or lysine-deficient media compared to those in complete medium. Already after 24 h, cells with arginine or lysine deprivation

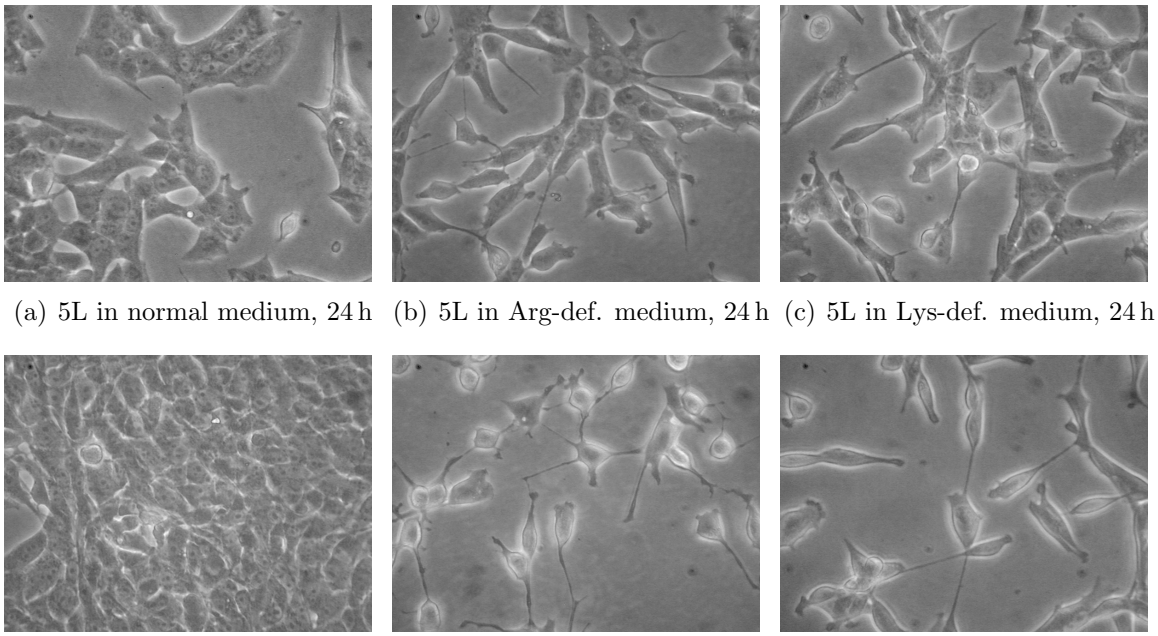

(a) 5L in normal medium, 24 h (b) 5L in Arg-def. medium, 24 h (c) 5L in Lys-def. medium, 24 h

(d) 5L in normal medium, 48 h (e) 5L in Arg-def. medium, 48 h (f) 5L in Lys-def. medium, 48 h

Figure 3.2: **Growth of 5L cells cultured in different media for 24 h and 48 h.** Pictures were taken with an inverted optical microscope at a magnification of 32x. The cells were grown in normal medium (a, d), arginine-deficient medium (b, e) and lysine-deficient medium (c, f) for 24 h (a, b, c) and 48 h (d, e, f).

were more slender and less firmly attached to the culture dishes suggesting that they were stressed. After 48 h, a significant decrease in cell number was observed for these cells, whereas cells cultured in normal medium were already confluent. After 72 h, nearly all cells in arginine- or lysine-deficient media were detached from the dishes and undergoing apoptosis (not shown).

These data show that 5L cells require the provision of the essential amino acid lysine as well as arginine for cell proliferation and survival. It appears that 5L cells, like various other cell lines, cannot synthesize arginine in sufficient quantities and both arginine and lysine must be regarded as essential amino acids for these cells. Arginine and lysine are therefore suitable amino acids for the stable isotope labelling of proteins of 5L cells.

In order to determine the time required for a complete incorporation of the labelled amino acids (Arg4, Arg10, Lys6) into the cellular proteins, a time course experiment was performed. One population of cells was grown in Lys/Arg4 medium and another population in Lys6/Arg10 medium (100 mg/L concentration for the heavy amino acids). After 1 day, 3, 5 and 7 days samples were lysed, proteins separated using a SDS-PAGE gel, protein bands were cut out, proteolysed with trypsin and analysed by MALDI MS. As shown in Figure 3.3, an incorporation of the labelled amino acids of about 50% was observed already after 24 hours. This finding was consistent with the doubling time of 5L cells of around 24 h observed in our laboratory. An incorporation of around 98% was obtained after five cell doublings and almost total incorporation after seven doublings.

The similar experiment was used to establish concentrations of the labelled amino acids optimal for cell growth and sufficient label incorporation. Concentrations of 50 mg/L, 75 mg/L and 100 mg/L medium were tested for Lys6 and Arg10-supplemented media. The incorporation of the isotope-labelled amino acids was quantified for five different peptides with C-terminal arginine and lysine residues, respectively. Figure 3.4 clearly shows that after seven days almost complete incorporation was reached with all three concentrations. However, whereas for 75 mg/L and 100 mg/L a nearly complete substitution was already reached after five days, the rate of incorporation was slightly lower for 50 mg/L, suggesting that this concentration was insufficient to fully support the growth of the cells. Thus, 75 mg/L was chosen as the optimal concentration of arginine and lysine for experiments involving the quantitation of phosphopeptides from 5L cells.

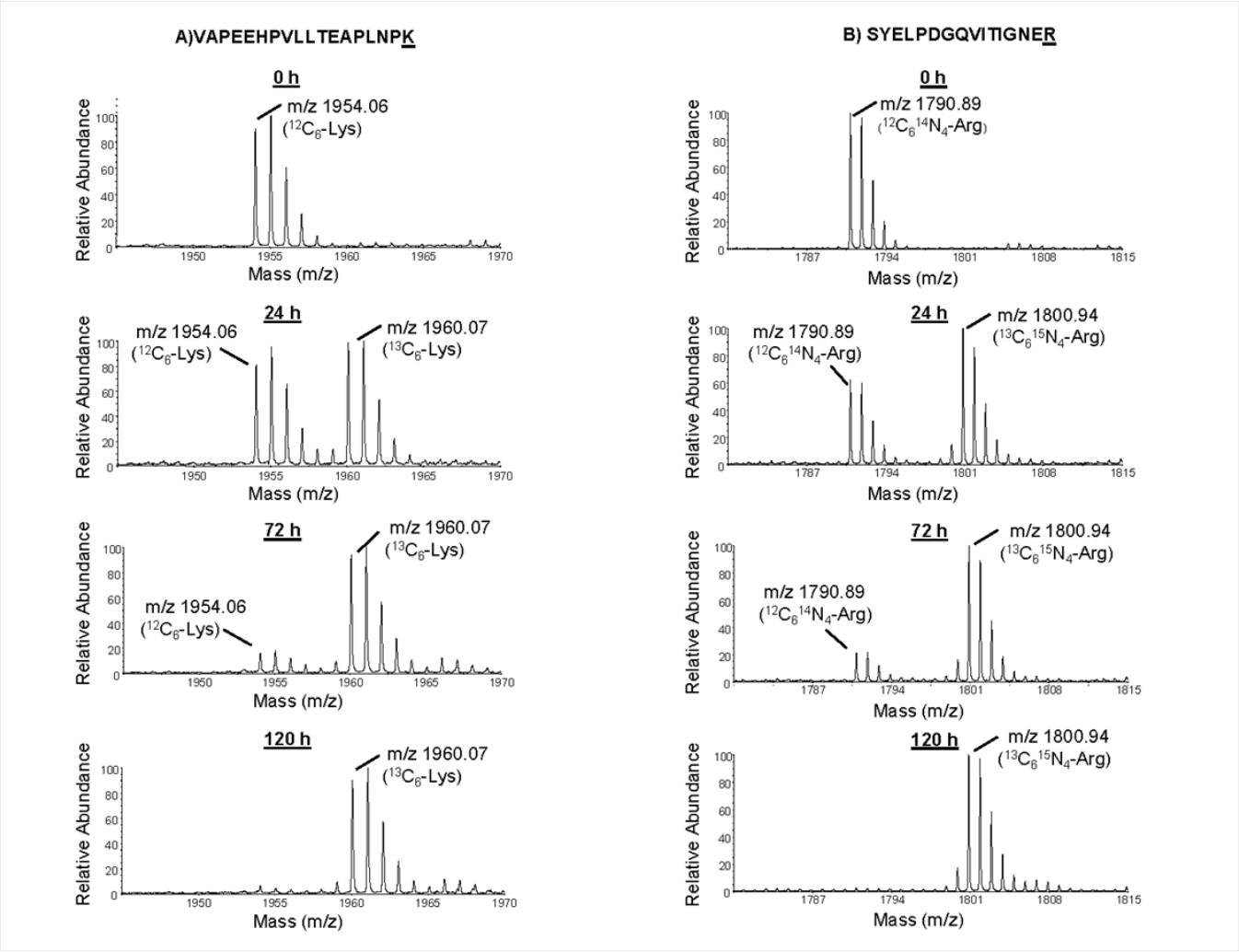

Figure 3.3: **Incorporation of Lys6- and Arg10-labelled amino acids over time.** MALDI MS spectra for two different peptides after 0 h, 24 h, 72 h and 120 h are shown. a) SILAC incorporation of $^{13}C_6$-lysine (Lys6) for the peptide VAPEEHPVLLTEAPLNPK. b) SILAC incorporation of $^{13}C_6{}^{15}N_4$-arginine (Arg10) for the peptide SYELPDGQVITIGNER.

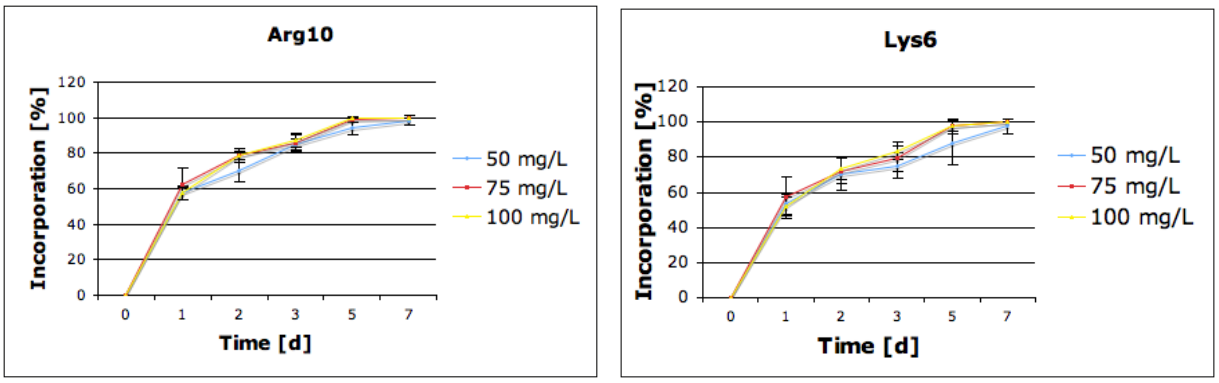

(a) 5L cells in Arg10 medium

(b) 5L cells in Lys6 medium

Figure 3.4: **Time and concentration dependence of the incorporation of isotopically labelled lysine and arginine into 5L cells.** The labelled amino acids were (a) $^{13}C_6{}^{15}N_4$-arginine and (b) $^{13}C_6$-lysine. The incorporation was determined 1 day, 2, 3, 5 and 7 days after addition of the labelled amino acid.

3.2 SIMAC for phosphopeptide enrichment

3.2.1 Applying SIMAC to standard peptides

In the present study, a combination of two different affinity-based methods, immobilized metal affinity chromatography (IMAC) and TiO_2 affinity chromatography, was used for the enrichment of phosphopeptides.

To evaluate the performance of the SIMAC and the TiO_2 approach alone, a comparison of both methods using a peptide mixture originating from 12 different standard proteins which included three phosphoproteins (α-casein, β-casein and ovalbumin) was performed. For the comparison, the proteins were proteolysed with trypsin and mixed in equal amounts. One pmol of the standard mixture was used for this comparison. Figure 3.5 shows a MALDI spectrum of the peptide mixture prior to enrichment. In this spectrum no phosphopeptides were detected which clearly indicates the need for a phosphospecific enrichment step prior to MS analysis.

Applying the SIMAC approach to the standard peptide mixture resulted in three different peptide fractions. The first fraction was the flow-through from the IMAC material which was further enriched with TiO_2. The second fraction was generated by washing the IMAC beads with 1% TFA which mainly eluted mono-phosphorylated peptides. This fraction was again further enriched with TiO_2. The third fraction was obtained by eluting the IMAC column with a basic solvent (NH_4OH) and this fraction was not enriched with TiO_2.

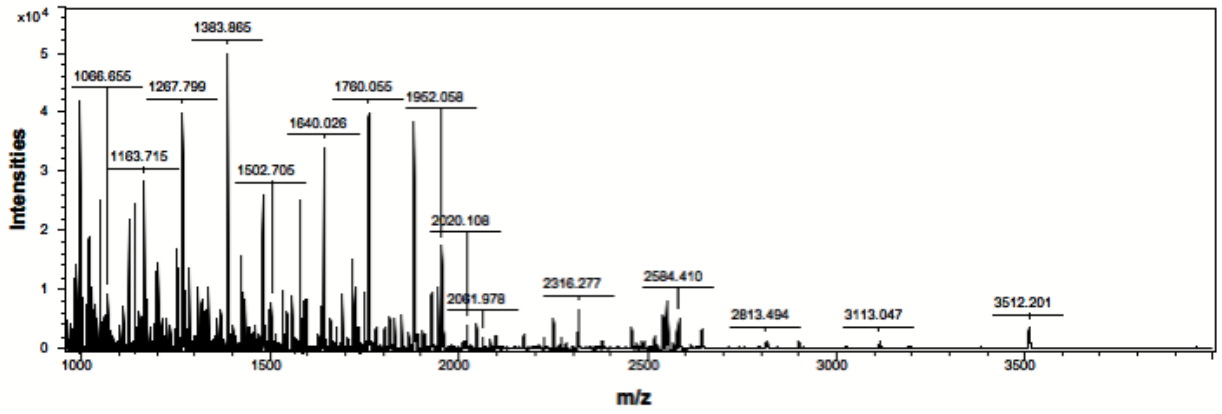

Figure 3.5: **MALDI MS analysis of a peptide mixture containing peptides derived from 12 standard proteins by trypsin digestion.** A MALDI MS spectrum of the peptides without any prior phosphopeptide enrichment is shown. The proteins included the phosphoproteins α-casein, β-casein and ovalbumin. No phosphorylated peptide could be observed in the spectrum.

The MALDI spectra of these fractions are shown in Figure 3.6. For all three fractions, a clear separation of phosphorylated from non-phosphorylated peptides was obtained. Furthermore, a separation of the mono- from the multi-phosphorylated peptides was achieved. The first two SIMAC fractions predominately contained peptides carrying one phosphate group, whereas the basic eluate comprised almost no mono-phosphorylated peptides but a higher number of multi-phosphorylated peptides. An overview of all phosphorylated peptides identified after using SIMAC in combination with TiO_2 is shown in Table 3.1.

The finding that already in the first fraction a substantial number of mono-phosphorylated peptides was detected indicates their weak binding to the IMAC resin. Furthermore, it should be noticed that the first two SIMAC fractions contain the same phosphorylated peptides. Due to the similarity of the phosphorylated peptides identified in these two fractions, they were pooled for the following quantitative analysis. This pooling step increases the abundance of the individual phosphorylated peptides in subsequent LC-MS/MS-based approaches.

In Figure 3.7 the MALDI spectrum for the enrichment of phosphopeptides from the standard peptide mixture using TiO_2 is shown. The spectrum indicates that the enrichment with TiO_2 results in the same mono-phosphorylated peptides as the SIMAC approach, but only a small fraction of the multi-phosphorylated peptides could be identified using TiO_2 in comparison to SIMAC. This clearly shows the benefit of the SIMAC approach for phosphopeptide enrichment as compared to the TiO_2 approach.

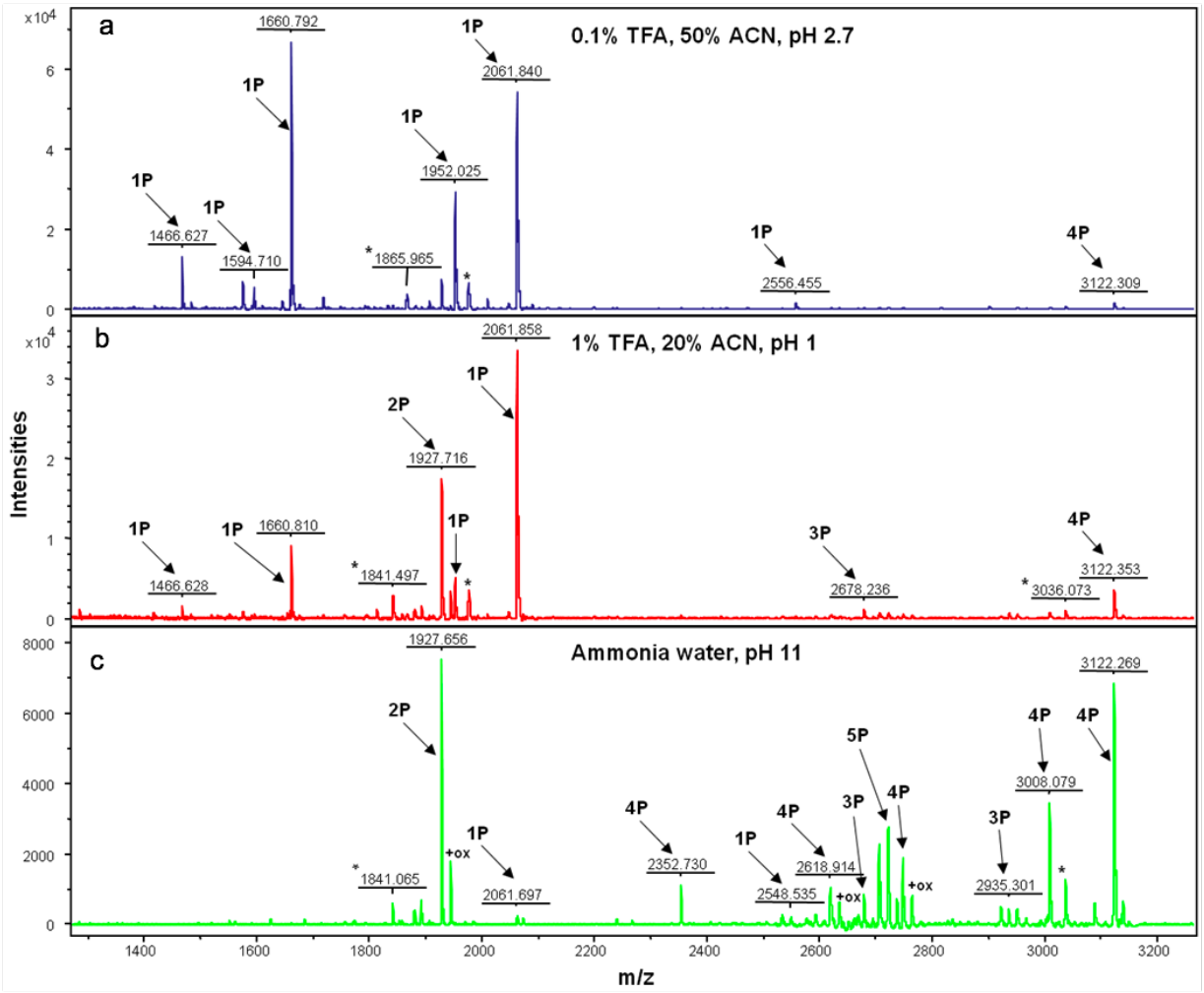

Figure 3.6: **Phosphopeptide enrichment by SIMAC.** MALDI MS spectra of 1 pmol of the tryptic peptides derived from a mixture of 12 standard proteins after phosphopeptide enrichment using SIMAC and TiO_2. MALDI MS spectra from a) the IMAC flow-through and first wash subsequently enriched by TiO_2 b) the acidic (1% TFA) IMAC eluate subsequently enriched by TiO_2 c) the basic IMAC eluate. An asterisk indicates the loss of phosphoric acid and P denotes the number of phosphorylation sites per identified peptide.

Peptide sequence	**Protein**	**Mass [Da] MH^+**	**No. of phosphosites**
TVDME*STEVFTK	α-casein S2	1466.63	1
TVDME*STEVFTKK	α-casein S2	1594.71	1
VPQLEIVPN*SAEER	α-casein S1	1660.79	1
DIG*SE*STEDQAMEDIK	α-casein S1	1927.72	2
YKVPQLEIVPN*SAEER	α-casein S1	1952.03	1
FQ*SEEQQQTEDELQDK	β-casein	2061.84	1
EVVG*SAEAGVDAASVSEEFR	Ovalbumin	2088.93	1
NVPGEIVE*SL*S*S*SEESITR	β-casein	2352.73	4
YKVPQLEIVPN*SAEERLHSMK	α-casein S1	2548.53	1
NTMEHV*S*S*SEE*SIISQETYK	α-casein S2	2618.91	4
VNEL*SKDIG*SE*STEDQAMEDIK	α-casein S1	2678.24	3
QMEAE*SI*S*S*SEEIVPN*SVEQK	α-casein S1	2703.15	5
QMEAE*SI*S*S*SEEIVPN*SVEQK	α-casein S1	2720.98	5
NTMEHV*S*S*SEE*SIISQETYKQ	α-casein S2	2748.29	4
EKVNEL*SKDIG*SE*STEDQAMEDIK	α-casein S1	2935.30	3
NANEEEYSIG*S*S*SEE*SAEVATEEVK	α-casein S2	3008.08	4
RELEELNVPGEIVE*SL*S*S*SEESITR	β-casein	3122.01	4

Table 3.1: **Phosphorylated peptides in the peptide mixture from the digested standard proteins identified using SIMAC and TiO_2.** The phosphorylation sites are marked with an asterisk. The peptides were analysed by MALDI MS.

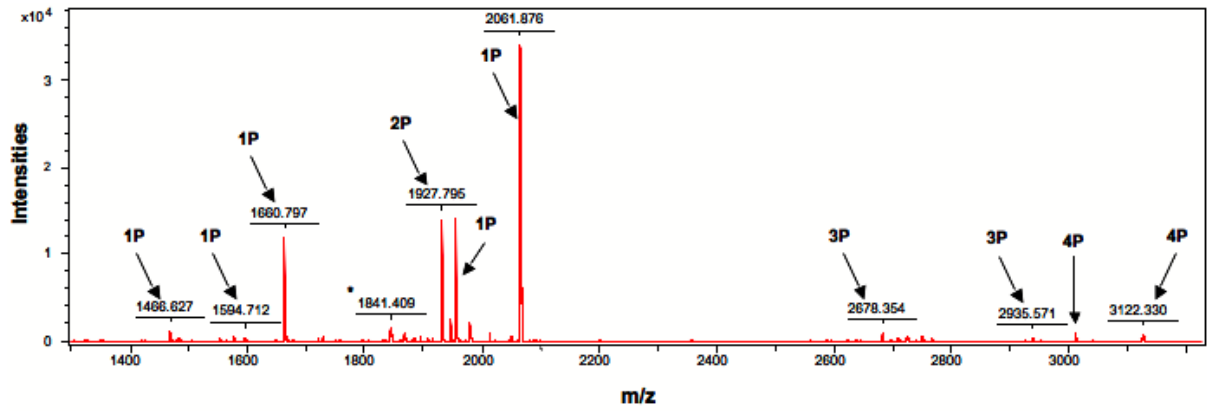

Figure 3.7: **Phosphopeptide enrichment by TiO_2.** MALDI MS spectra of 1 pmol of the standard peptide mixture after phosphopeptide enrichment by TiO_2. The P indicates the number of phosphorylation sites per identified peptide.

3.2.2 Applying SIMAC to complex samples

Having demonstrated the performance of the SIMAC strategy when applied to a standard peptide mixture, its suitability for the enrichment of phosphopeptides from a cellular phosphoproteome was assessed by comparing the enrichment efficiency against the TiO_2 approach alone that is commonly used for this purpose. Approximately 200 μg of protein from a 5L cell lysate were used with each strategy and the enriched phosphopeptides were analysed by LC-MS/MS. A summary of the results obtained is presented in Figure 3.8.

For the SIMAC approach, a total of 863 unique phosphorylated peptides was identified in the three fractions. These consisted of 469 unique mono-phosphorylated and 394 unique multi-phosphorylated peptides being observed. Thus, nearly half of all identified peptides contained two or more phosphosites per peptide. About 84% of these multi-phosphorylated peptides were identified in the basic fraction. The enrichment efficiency, i.e. the proportion of phosphorylated peptides among all identified enriched peptides, of the SIMAC approach was ~82%. For the TiO_2 approach, a total of 345 unique phosphorylated peptides was identified, the majority (~85%) being mono-phosphorylated. The enrichment efficiency was ~72%. The overlap of the identified phosphorylated peptides between the two methods amounted to 238 peptides. This low number is probably largely due to the undersampling of the MS instrument (only the 5 most intense ions are selected for MS/MS per one MS survey scan).

Collectively, these data show that the SIMAC strategy is in fact suitable for the enrichment of phosphorylated peptides in highly complex samples. Importantly, the number

of identified multi-phosphorylated peptides was much higher for the SIMAC method as compared to the TiO_2 method indicating that SIMAC provides a more comprehensive phosphopeptide pattern than the TiO_2 approach alone.

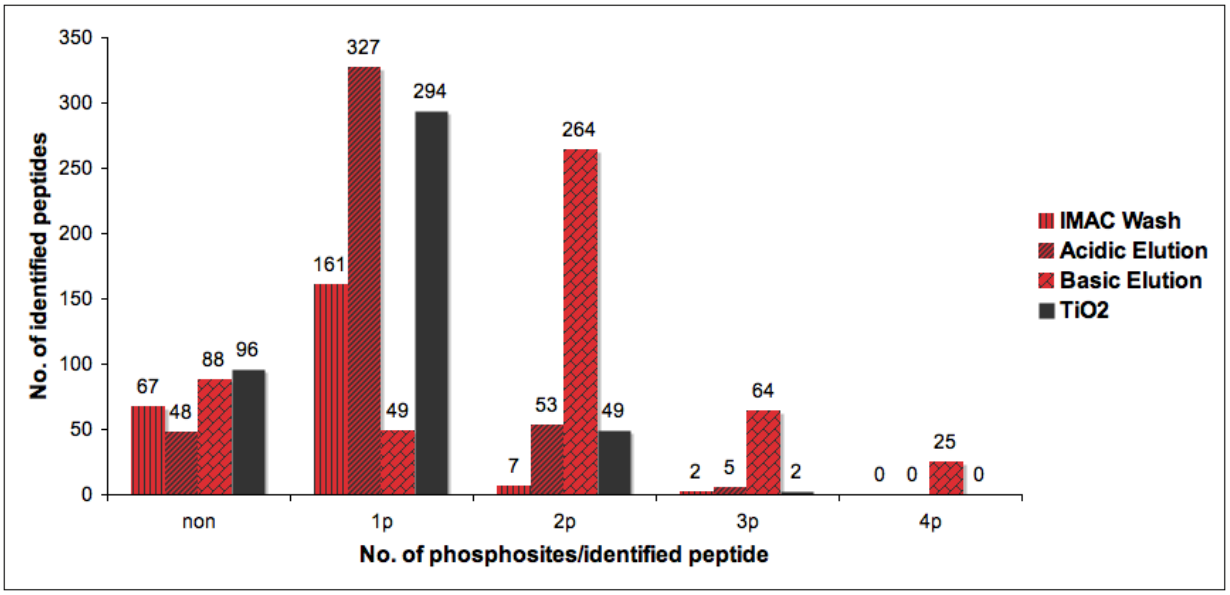

Figure 3.8: **Analysis of phosphorylated peptides from 5L cell lysate enriched by SIMAC or TiO_2.** The bar chart shows the number of non-, mono- and multi-phosphorylated peptides identified by the SIMAC approach resulting in three different fractions and the TiO_2 approach with one fraction.

3.3 HILIC as a prefractionation method

The analysis of phosphorylated peptides from a complex sample usually results in the identification of the phosphopeptides from the most abundant proteins. A prefractionation prior to LC-MS/MS reduces the sample complexity and improves the identification of phosphopeptides from low abundant proteins. For a phosphoproteomic approach, several prefractionation strategies have been described previously including isoelectric focusing (IEF), strong cation exchange (SCX) or hydrophilic interaction liquid chromatography (HILIC) [Essader et al., 2005], [Beausoleil et al., 2004], [McNulty and Annan, 2009].

For the present study, HILIC was chosen for prefractionation. For phosphoproteomic approaches, HILIC is an ideal method as it takes advantage of the hydrophilic character of the phosphopeptides. HILIC separation was performed after the SIMAC separation and prior to TiO_2 enrichment. Only the combination of flow-through and acidic eluate was

loaded onto the HILIC column. Previous studies had suggested that HILIC is not suitable for multi-phosphorylated peptides as they bind to the HILIC material very tightly and cannot be efficiently eluted using a gradient of organic solvent.

The proteins of a 5L cell lysate were proteolysed with trypsin and the peptides were subjected to an IMAC phosphopeptide enrichment. The flow-through and acidic eluate from IMAC were combined and used for HILIC prefractionation. The number and the size of the collected fractions were optimized in order to achieve a good distribution of phosphorylated peptides, as well as a manageable number of fractions. The elution profiles obtained were very similar for all the test samples. A typical example is displayed in Figure 3.9.

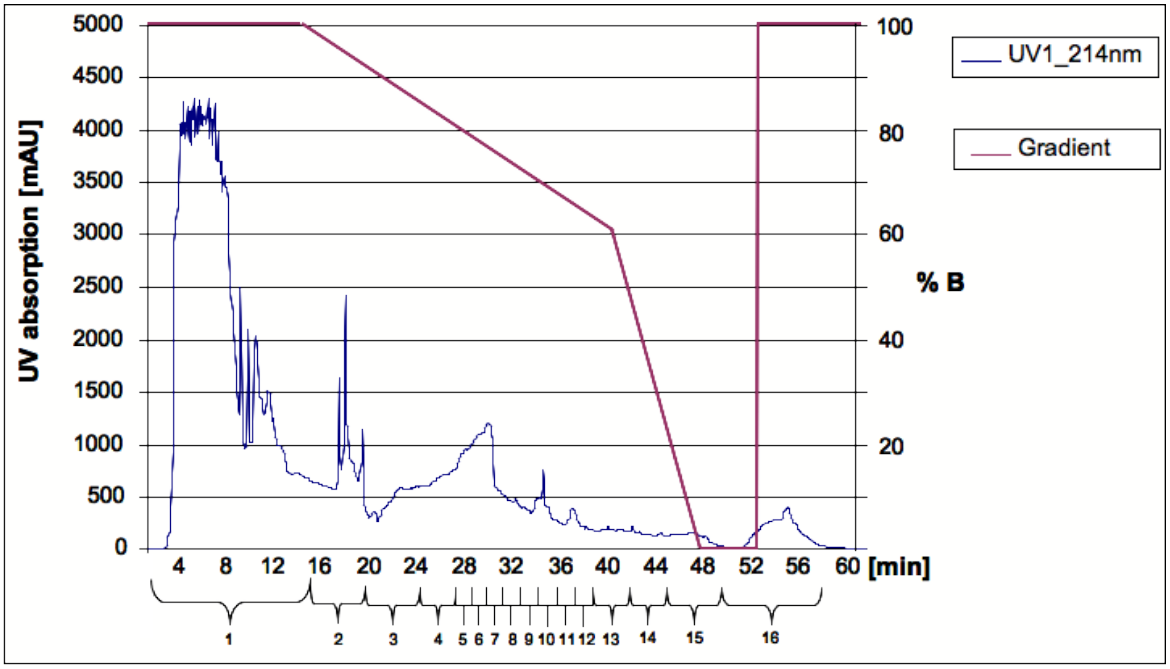

Figure 3.9: **HILIC elution profile.** Elution of tryptic peptides in the flow through and the acidic eluate from IMAC from the TSKgel Amide 80 column with an increasingly aqueous solvent. The blue curve displays the UV absorbancy at 214 nm and the pink curve the gradient of the eluent. Below the x-axis the fraction numbers are displayed.

The resulting fractions were enriched for phosphorylated peptides using the TiO_2 approach and the phosphopeptides were identified and quantified using LC-MS/MS. Figure 3.10 shows an overview of the number of identified phosphorylated peptides and non-phosphorylated peptides in the different HILIC fractions. The largest fraction, which comprised the flow-through from the HILIC column loading, contained only few phosphorylated peptides. This was probably due to the elution of mainly hydrophobic peptides which do

not bind to the column in 80% ACN. The majority of the phosphopeptides eluted after a lag period of ∼14 min corresponding to an ACN concentration of 65%. HILIC prefractionation in combination with the TiO_2 approach for phosphopeptide enrichment resulted in a good enrichment efficiency. Overall, 70% of the subsequently identified peptides were found to be phosphorylated. Interestingly, in the fractions 8 to 16, an efficiency of around 95% was obtained. More than 85% of the overall identified phosphorylated peptides were contained in these fractions.

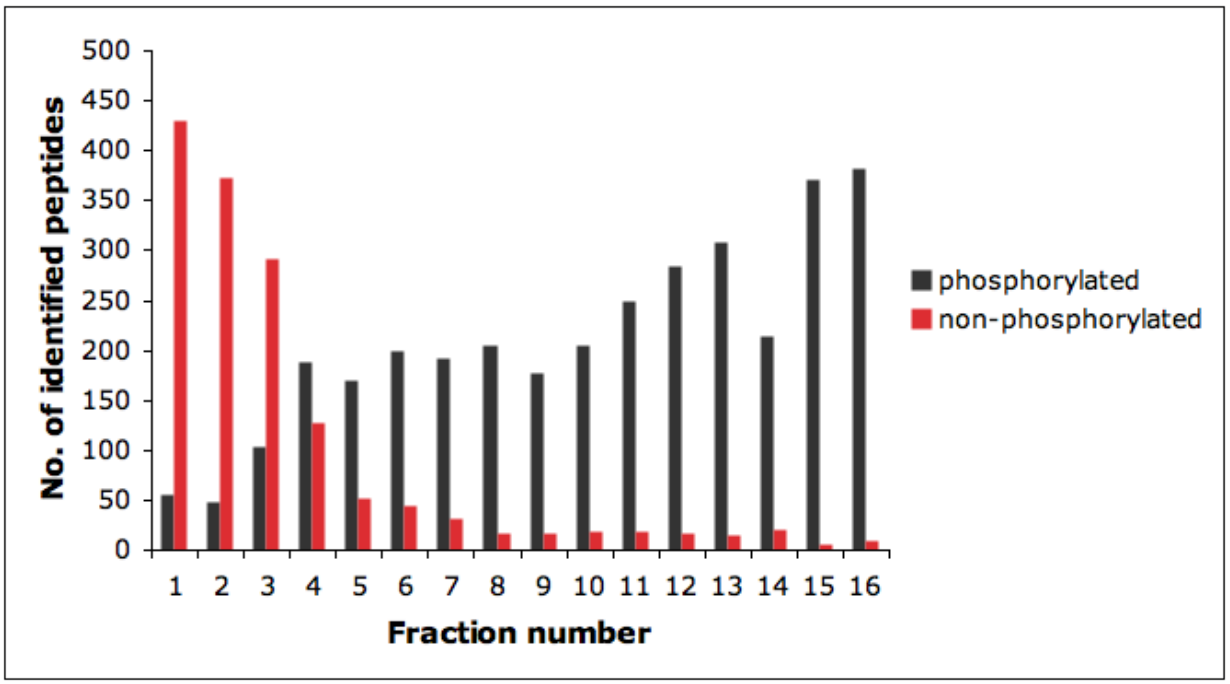

Figure 3.10: **Distribution of phosphorylated and non-phosphorylated peptides in the HILIC fractions.** Elution of tryptic peptides in the flow through and the acidic eluate from IMAC from the TSKgel Amide 80 column with an increasingly aqueous solvent. The black bars display the number of identified phosphorylated peptides per fraction. The red bars display the number of identified non-phosphorylated peptides per fraction.

The overall redundancy of the identified phosphorylated peptides was ∼20%, meaning ∼80% of the individual peptides were found in only one fraction.

Taken together, HILIC prefractionation prior to TiO_2 enrichment is a very efficient method to reduce sample complexity and improve the overall identification of phosphopeptides. Sample prefractionation resulted in a higher number of identified phosphorylated peptides than using SIMAC and TiO_2 alone. Without prefractionation, ∼900 unique phosphorylated peptides were identified, whereas using HILIC the number of identified phos-

phorylated peptides increased to ∼3000. Furthermore, HILIC by itself already enriches phosphopeptides as indicated by the increase in the numbers of phosphorylated peptides per fraction during the course of the elution shown in Figure 3.10.

3.4 The phosphoproteome of 5L cells

3.4.1 Identified phosphorylation sites

Eight individual experiments involving SILAC labelling and exposure of the cells to DMSO/TCDD (1 nM) for 0.5 - 2 hours, proteolysis, HILIC prefractionation and phosphopeptide enrichment with subsequent analysis using LC-MS/MS were performed. In these experiments, 800 μg of protein were used as starting material for each analysis. In total, 5648 different phosphorylated peptides comprising distinct 6573 phosphosites were identified. For these peptides, 2156 corresponding phosphoproteins were identified. The major part, ∼84% of the identified peptides, was phosphorylated at serine residues, while ∼14% were phosphorylated at threonines and only ∼2% were phosphorylated at tyrosines (Figure 3.11(a)). This distribution is consistent with the frequencies observed in other large-scale studies [Olsen et al., 2006] [Van Hoof et al., 2009]. The majority of the peptides was mono-phosphorylated (∼86%), but a substantial number of peptides (∼12%) was doubly phosphorylated. Only ∼2% of all identified peptides contained three or more phosphorylation sites (Figure 3.11(b)). The number of multi-phosphorylated peptides was only slightly higher than that reported in other publications ([Hou et al., 2010]).

All MS files of the phosphopeptides were searched against the rat sequence library in the International Protein Index (IPI) protein sequence database using an inhouse Mascot server. The acquired IPI accession numbers of the identified phosphorylated proteins were mapped against the Uniprot database to achieve more detailed information on the proteins. The Uniprot database consists of two different subdatabases, the Swiss-Prot and the TrEMBL database. Of the 2156 phosphoproteins identified with IPI, only 688 could be mapped to a Swiss-Prot accession number and 452 phosphoproteins could be mapped to a TrEMBL accession number. In the Swiss-Prot database, all proteins are manually annotated and reviewed and multifaceted information like known phosphosites and protein functions is available. In contrast, in the TrEMBL database, the proteins are automatically annotated and not reviewed. Like IPI, TrEMBL does not supply information on known protein modifications, for example phosphorylation. For this reason, only the 688 phosphoproteins mapped to Swiss-Prot were selected for the analysis of whether their phos-

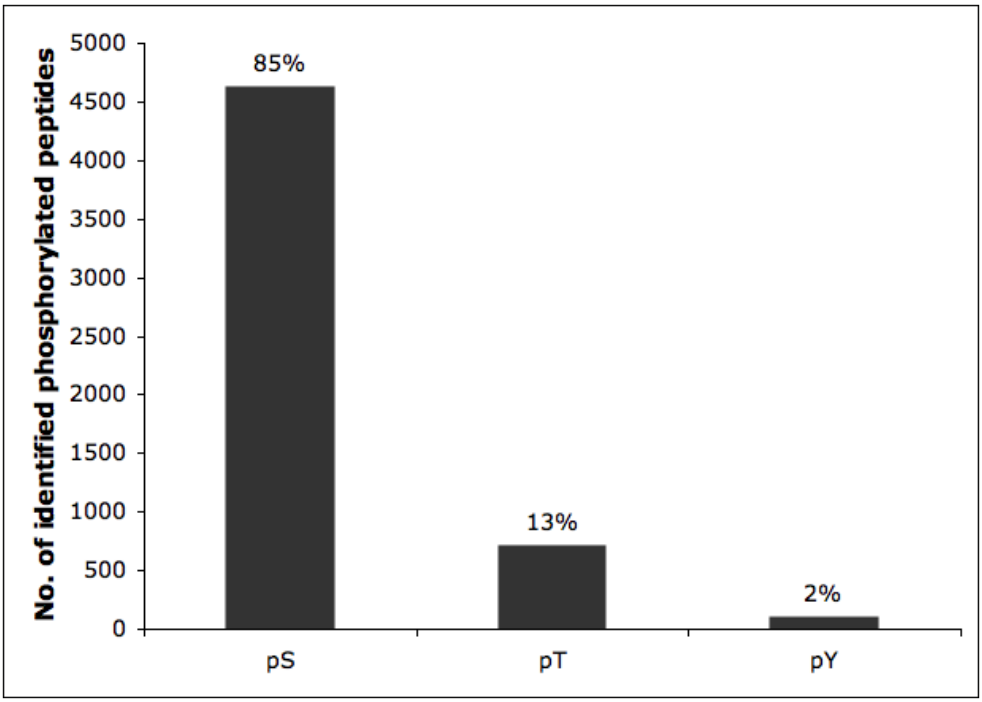

(a) Overview of the distribution of pSer, pThr and pTyr.

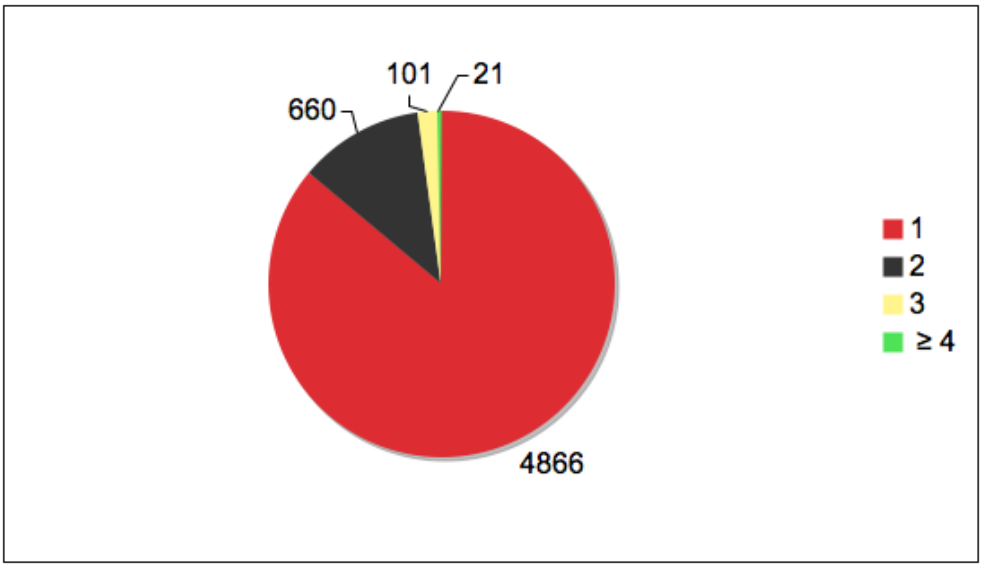

(b) Overview of mono- and multi-phosphorylated peptides

Figure 3.11: **Analysing the phosphoproteome of 5L cells.**

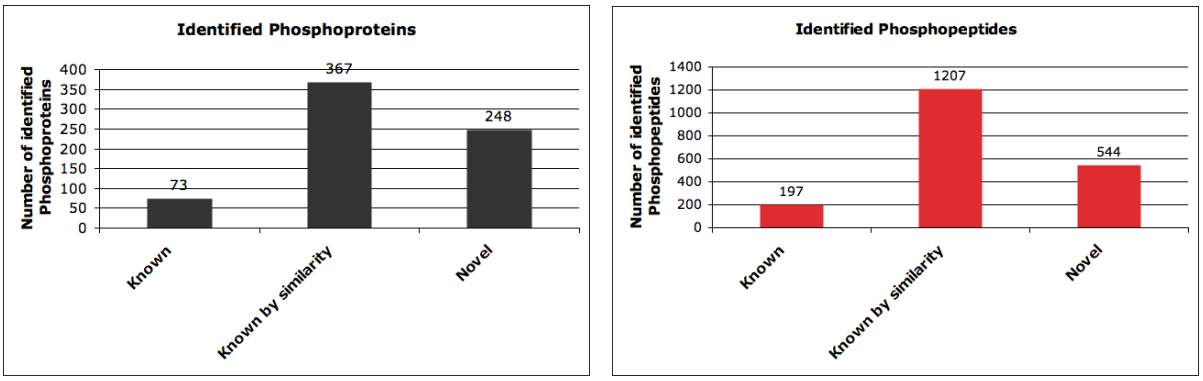

(a) Phosphoproteins (b) Phosphopeptides

Figure 3.12: **Overview of known, "known by similarity" or novel phosphoproteins and -peptides identified in the present study.** Only 688 phosphoproteins (with 1948 phosphorylated peptides) identified with IPI could be mapped to a Swiss-Prot accession number.

phorylation sites had been identified before. Among these 688 rat phosphoproteins, only 73 proteins were previously known to be phosphorylated and 367 proteins were known to be phosphorylated "by similarity", which means that they were known to be phosphorylated in other species such as mouse or human, but not in rat. A large portion of the 248 proteins had not been known to be phosphorylated until now. With respect to the identified phosphopeptides, the actual phosphosite had already been described for 197 of them. The main part of the phosphosites (1207) had been known "by similarity" and 544 phosphosites were novel. These results clearly show that the present study provides substantial new information on the rat phosphoproteome. The "known", "known by similarity" and "novel" phosphoproteins and phosphorylation sites are listed in the Table 9 in the Appendix.

3.5 Multiple testing for finding statistically significantly "regulated" phosphopeptides

3.5.1 Normalisation

Before the p-values for the individual ratios of the phosphopeptides from DMSO- and TCDD-treated cells were calculated, a normalisation of the ratios was performed in order to remove biases introduced by sample preparation, i.e. differences in the amount of protein from the "light" and the "heavy" state in the sample. The ratios were calculated by MSQuant based on the intensity of the first isotopic peak of the particular SILAC pairs in the MS spectra. The intensity value of the "heavy" state (TCDD-treated) is divided by the intensity value of the "light" state (DMSO-treated) (Regulation factor H/L). In order to find the right normalisation method for the data sets, ratios-vs-average MA plots were drawn for all biological replicates of the individual time points. For MA plots, the peptide ratios were plotted against the average of the peptide intensities. MA plots are very common visualization tools originally developed for the micro-array area and give a quick overview of the data. Figure 3.13 shows the MA plots for the biological replicates of the 30-min exposure period before normalisation. The plots showed no definite trend with respect to intensity and ratio indicating that peptides with low intensity had ratios similar to those of peptides with high intensity. Nearly all peptides of the three plots were distributed around one value showing that a global normalisation method was appropriate. Therefore, the "median normalisation" at the peptide level was applied. The ratios calculated by the MSQuant program were normalised by subtracting the ratios with a fixed value selected such that the median of the logarithmized ratios became zero [Do and Choi, 2006].

In Figure 3.13, a lowess trend line (blue) is shown for the unnormalised plots which is fitted through the data points. Lowess is a local regression using a sliding window across a range of intensity levels and reflects the trend of the data points [Smyth and Speed, 2003]. A second, horizontal line (red) is displayed in the unnormalised plots. This line intersects the y axis at y=0 and displays the median of 0. In all three unnormalised plots both lines were very similar, indicating that the correction factors for the normalisation of the data were very small and that the biases introduced by the sample preparation were minimal. In Figure 3.14, the MA plots for the replicates for 30 min after normalisation are shown. For the 1 hour and 2 hours data, the MA plots looked very similar and are shown in the

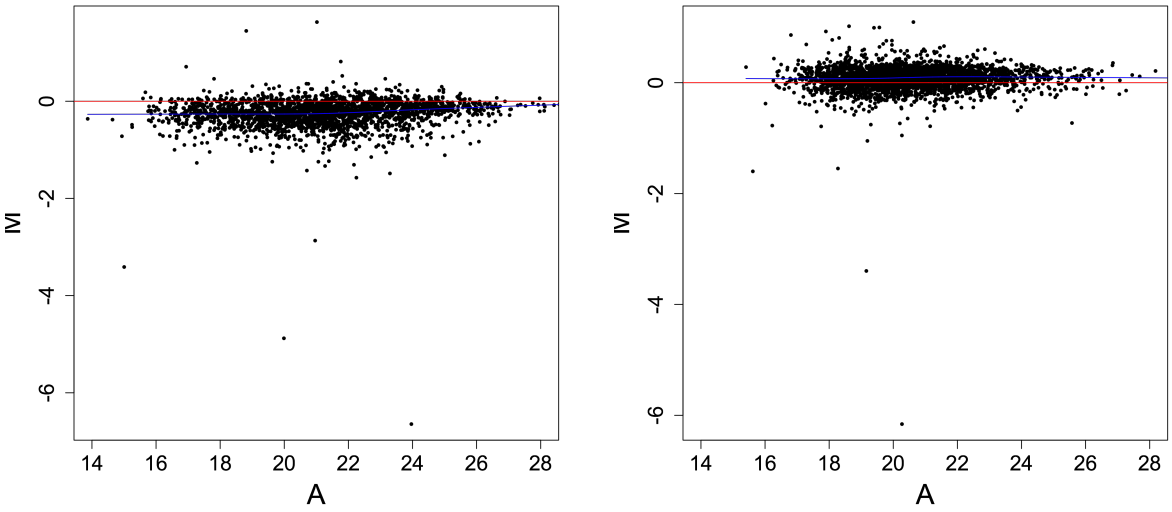

(a) 30 min DMSO/TCDD; Biological Replicate 1 (b) 30 min DMSO/TCDD; Biological Replicate 2

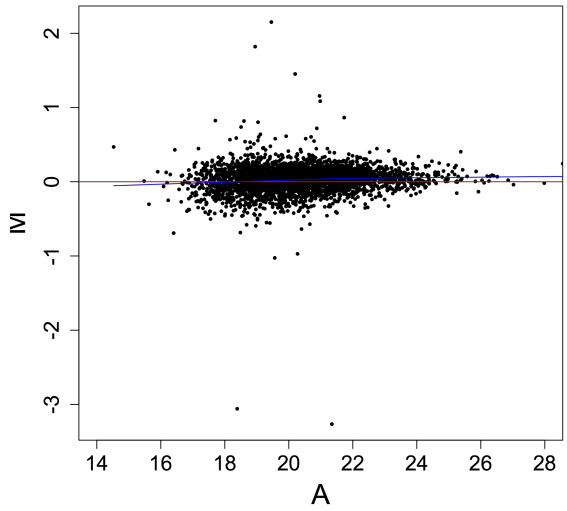

(c) 30 min DMSO/TCDD; Biological Replicate 3

Figure 3.13: **MA plots of peptides before normalisation.** Unnormalised peptide ratios were plotted as ratios-vs-average (MA) plots. The log2 ratios H/L (y-axis) are plotted against the log2 average of the peptide intensities H (heavy = TCDD treated) and L (light = control). The blue line is a lowess line, the red line indicates y = 0. a), b) and c) show the data from the three different biological replicates obtained after treatment of the cells with DMSO/TCDD for 30 min.

Exposure Period	Pearson correlation coefficient		
	Biological Replicate 1	Biological Replicate 2	Biological Replicate 3
30 min	0.79	0.80	0.63
1 h	0.75	0.68	0.73
2 h	0.84	0.74	-

Table 3.2: **Calculated Pearson correlation factors for the biological replicates of the different time points.** The correlation coefficients were calculated for the peptide ratios of the biological replicate in question against the mean of the ratios of the biological replicates of the time point.

Appendix (see Figures 1, 2, 3, 4). These data sets were also normalised using the "median normalisation" approach.

3.5.2 Correlation

To assess the conformity of the biological replicates of the individual exposure periods, the Pearson correlation coefficients were calculated. The coefficients of the correlation between the different biological replicates are shown in Table 3.2.

Pearson correlation coefficients can vary between -1 and 1, where 1 indicates a perfect correlation between the biological replicates. From all replicates of all time points positive correlation coefficients were obtained. In two cases the coefficient was below 0.7 (0.68 and 0.63). For these two data sets, the correlation with the other replicates of the same time point was "weakly positive" (range of +0.3 to +0.7), but close to a "strongly positive" correlation (+0.7 to +1.0) [Sachs and Hedderich, 2009]. These data sets were therefore included in the statistical tests.

3.5.3 Statistical analysis

To identify the statistically significantly regulated phosphopeptides for the particular time points, an empirical Bayes moderated t-test was applied to the data sets using the R/Bioconductor package limma. For the statistical tests, the biological replicates of each time point were merged together and peptides found in only one replicate were removed. Thus, the tests were only performed on peptides found at least twice. A well established significance threshold for accepting peptides as regulated is $p \leq 0.05$. All peptides with a calculated p-value below this threshold were considered as differentially regulated. A

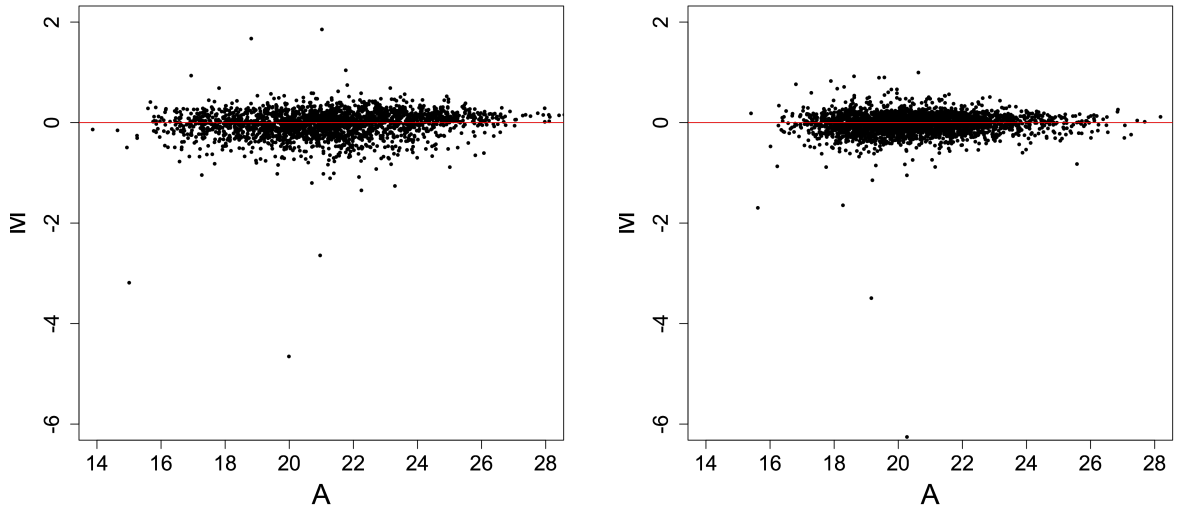

(a) 30 min DMSO/TCDD; Biological Replicate 1

(b) 30 min DMSO/TCDD; Biological Replicate 2

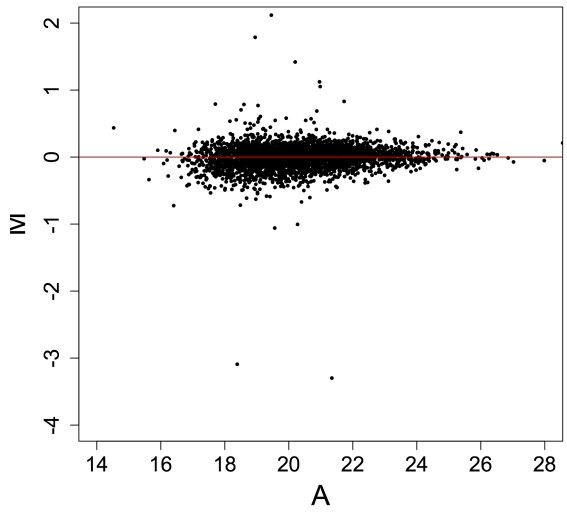

(c) 30 min DMSO/TCDD; Biological Replicate 3

Figure 3.14: **MA plots of peptides after normalisation.** Normalised peptide ratios were plotted as ratios-vs-average (MA) plots. The log2 ratios H/L (y-axis) are plotted against the log2 average of the peptide intensities H (heavy = TCDD treated) and L (light = control). The red line indicates y = 0. a), b) and c) show the data from the three different biological replicates obtained after treatment of the cells with DMSO/TCDD for 30 min.

total of 126, 140 and 84 peptides with $p \leq 0.05$ were identified for the exposure periods 30 min, 1 hour and 2 hours, respectively. It appeared possible, however, that the moderated t-tests had resulted in many false positives, i.e. peptides erroneously accepted as regulated (type 1 error). To control for the number of false positives, the false discovery rate (FDR) based on the p-value was estimated. Various methods for controlling FDR are available, and for the present study the q-value method [Storey and Tibshirani, 2003] was chosen as it had been shown [Qian and Huang, 2005] to give the highest apparent power in comparison to various other FDR controlling methods, such as the approach of Benjamini and Hochberg [Benjamini and Hochberg, 1995]. Peptides with a q-value equal or below 0.05 were accepted as statistically significantly regulated, i.e. with a value of $p \leq 0.05$ an error rate of 5% was accepted. For the 30 min data sets, no peptides were identified with a q-value equal or below 0.05. For the 1 hour data sets, 4 peptides had a q-value below this threshold and for the 2 hours datasets, 6 peptides had a q-value below 0.05 (see below).

Figure 3.15 shows two different volcano plots for each time point. The volcano plot is a scatter plot which displays the fold-changes (FC) versus a measure of the statistical significance of the change [Cui and Churchill, 2003]. For the left-sided panel for each time point, the log FC values of the normalised peptide ratios were plotted against the log p-values, i.e. against the measure of statistical significance. For the panel on the right side for each time point, the log FC values were plotted against the log q-values, i.e. against the measure of statistical significance after correction for false positives. The horizontal dashed line in all plots displays the significance threshold of 0.05 for the p- and the q-values. The two vertical dashed lines in all plots are set at an FC value of 1.5 for up- and down-regulation.

The volcano plots where the log FC values were plotted versus the log p-values (left panels) exhibit many peptides with a p-value $p \leq 0.05$ (above the horizontal dashed line). However, no peptides for the 30 min plot and only few for the 1 hour and 2 hours plots occur outside the region edged by the two vertical lines indicating an FC >1.5. This observation indicated a marked discrepancy between the FC method and the statistical test. In contrast, the volcano plots where the log FC was plotted versus the log q-values (right panels) exhibit a very homogeneous picture, as nearly all peptides with an FC of >1.5 are also identified as significantly regulated ($p \leq 0.05$) after correction for false positives. An exception was one peptide from the 1 hour dataset which exhibited a q-value below the threshold of 0.05 whereas the FC was inside the 1.5 FC range. The variance of this data set was very low, which was taken into account by the statistical test but not by the

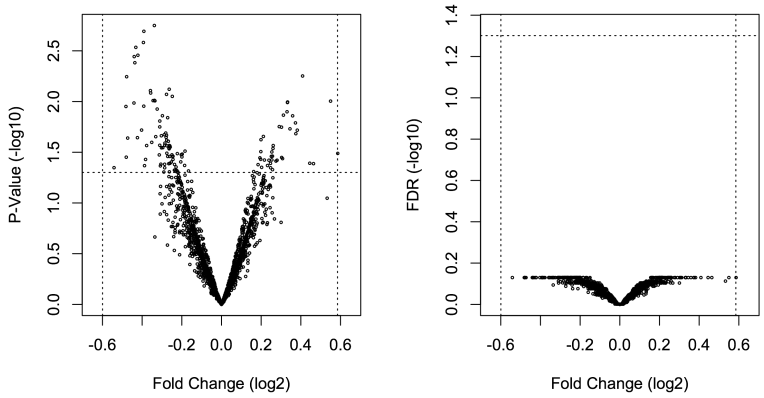

(a) 30 min DMSO/TCDD exposure

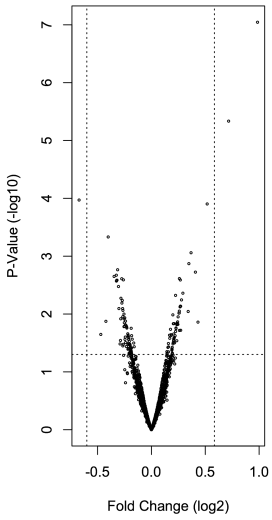

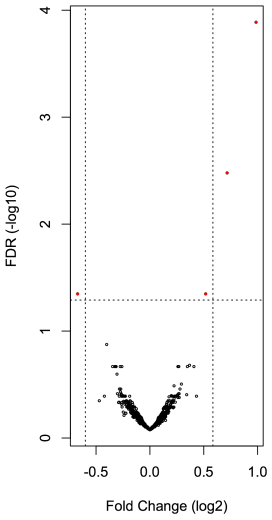

(b) 1h DMSO/TCDD exposure

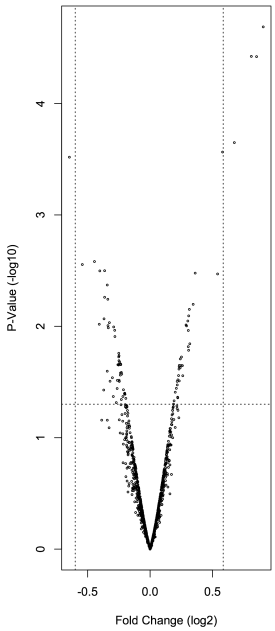

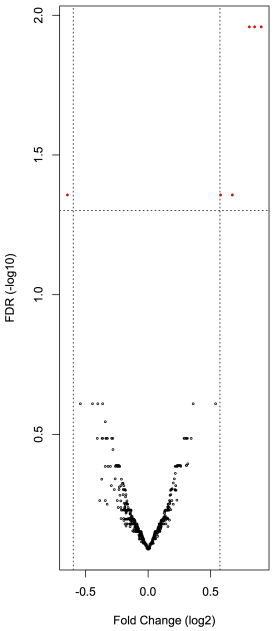

(c) 2h DMSO/TCDD exposure

Figure 3.15: **Volcano plots for each time point.**The plots display the relationship between statistical significance and FC for all peptides subjected to the statistical tests. The log2 FC (x-axis) was plotted against the -log10 p-value (y-axis) (left) and against the -log10 q-value (y-axis) (right). The horizontal dashed line indicates the p- and q-value threshold of 0.05. The two vertical dashed lines indicate the 1.5 FC threshold.

FC threshold. Thus, the present study essentially yielded the same results with respect to the identification of regulated peptides when the classification relied on a statistical test in combination with the calculation of the q-value and when the classification was based on the FC of 1.5. In contrast, the Bayes moderated t-test alone yielded many false positive results. These observations showed that both a biological threshold of 1.5 FC and a statistical threshold of $q \leq 0.05$ are appropriate for this data set. Peptides which were found in only one of the biological replicates were removed before applying the moderated t-test to the datasets. These peptides were analysed separately to identify regulated ones. A cut off value of 1.5 FC was used based on the results of the volcano plots. The results will be discussed separately from the results of the statistical tests in the next chapter.

3.6 Peptides with altered phosphorylation after treatment of the 5L cells with TCDD

3.6.1 Time course of the induction of CYP1A1

In the present study, the 5L cells were treated with 1 nM TCDD for 0.5, 1 and 2 hour(s). These relatively short exposures were not expected to result in significant alterations in protein levels as a consequence of TCDD-altered gene expression which would complicate the comparison of phosphopeptide abundances in control cells and TCDD-treated cells. To obtain information on the time course of the stimulation of gene expression by TCDD in 5L cells at the protein level, the induction of cytochrome P4501A1 (CYP1A1) was analyzed with respect to the protein level and the enzymatic activity in the cells.

Figure 3.16 shows the results obtained from Western Blotting experiments. They indicate that no alteration in protein abundance could be detected after TCDD exposures of 1 hour. A significant up-regulation was observed after 1.5 hours and longer exposure periods. The measurement of the 7-ethoxyreorufin deethylase (EROD) activity, an enzymatic activity associated with CYP1A1, did not show any detectable alteration at 0.5 to 2 hours and was thus a less sensitive approach for the detection of alterations in CYP1A1 protein level (Figure 3.17).

Thus, since CYP1A1 is the most rapidly and most potently induced target gene of TCDD in essentially every cell type, it appeared highly unlikely that the exposure of the cells to TCDD for 0.5 and 1 h would result in changes in the abundance of proteins even if

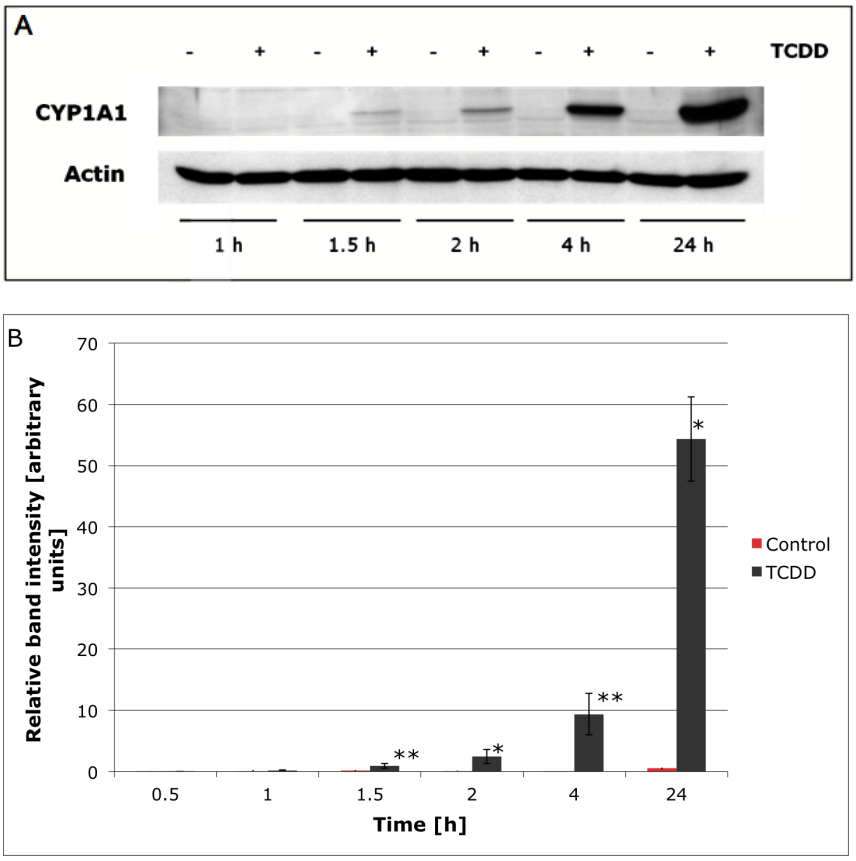

Figure 3.16: **Time course of the induction of CYP1A1 protein by TCDD in 5L cells.** Cells were exposed to 1 nM TCDD for the times indicated. Total cell lysates were prepared and analysed on 12% PAGE gels. Proteins were electroblotted, and CYP1A1 and actin (loading control) were visualised using specific antibodies and ECL detection. Bands were quantitated by densitometry. A), Sections of the respective blots from one experiment out of three which yielded very similar results. B), Means ±SD from three independent experiments. * $p < 0.01$, ** $p < 0.001$

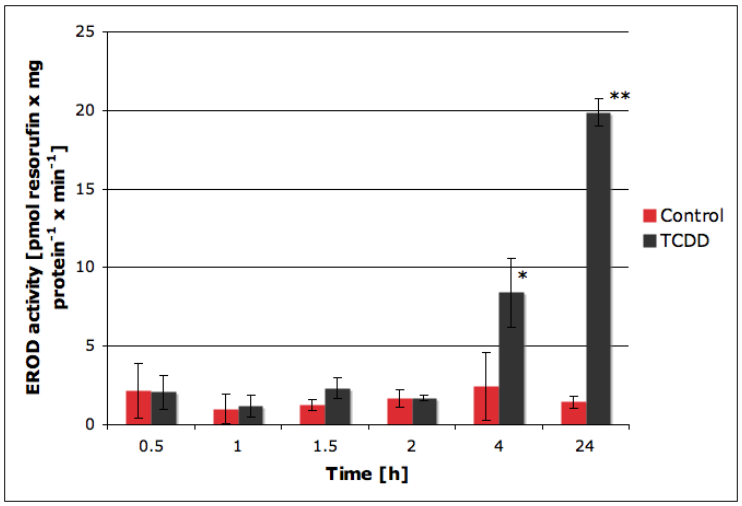

Figure 3.17: **Time course of the induction of EROD activity by TCDD in 5L cells.** Cells were exposed to 1 nM TCDD for the times indicated, and EROD activity was determined in whole cell lysates. Results are the means ±SD from three independent experiments. *, $p < 0.05$; **, $p < 0.00001$.

they were transcriptionally induced by the dioxin. For the 2 h exposure period, however, alterations of the cellular levels of such proteins would appear possible.

3.6.2 Peptides with altered phosphorylation after 30 min TCDD treatment

For the protein samples from 5L cells treated with TCDD for 30 min, 1368 phosphorylated peptides were found in at least two of the biological replicates and used for the statistical test to calculate the p-value and q-value of the individual peptides. With the set significance threshold of $q = 0.05$, no significantly regulated phosphorylated peptides were found.

3942 peptides were found in only one of the three biological replicates. This number is surprisingly high and indicates a low overlap between the biological replicates. The analysis of these peptides applying an FC threshold of 1.5 identified 4 peptides as regulated (Table 3.3). For two of the four proteins from which the regulated peptides were derived (Transcription intermediary factor 1-beta and RCG52671, isoform CRA_a), other phosphorylated peptides were identified. These, however, showed regulation factors close to 1 (see Table 8 in the Appendix). This suggests that for these two proteins the phosphorylation of the specific phosphosite was affected by TCDD but not their overall protein level.

Accession number	Gene name, protein name	Sequence	Phosphosite localization in protein	Validated	Ion score	PTM score	Regulation factor H/L
IPI00765369	*LOC686261*, similar to forkhead box K1 isoform alpha	SAPA*SP*THPGLMSPR	496/ 498	novel	30	45	0.62
IPI00194567	*Trim28*, Transcription intermediary factor 1-beta (TIF1β)	*SGEGEVSGLMR	474	by similarity	40	142	1.58
IPI00190390	*Cdc2*, Cell division control protein 2 homolog	IGEGT*YGVVYK	15	by similarity	48	142	1.64
IPI00362117	*Ubxn7*, RCG52671, isoform CRA$_a$	SESLIDASED*SQLEAAIR	267 or 289	novel	76	96	1.86
IPI00364957	*Ahr*, Isoform 1 of Aryl hydrocarbon receptor	ATGEAVL*YEI*SSPFSP	412/ 415	novel	25	18	0.68**

Table 3.3: **Phosphopeptides identified as regulated after treatment of the cells with TCDD for 30 min.** The displayed peptides were found in only one biological replicate and were accepted as regulated with an FC factor of >1.5. The asterisks (*) in the peptide sequences indicate the position of the phosphorylation site and the (**) indicates that this protein is not regulated according to the criteria of the present study.

For the Isoform 1 of Aryl hydrocarbon receptor, one phosphorylated peptide was observed. It exhibited a regulation factor of 0.68 just below the threshold of 1.5 used as a cut-off value for the classification of a peptide as "regulated".

3.6.3 Peptides with altered phosphorylation after 1 hour TCDD treatment

For the protein samples from cells treated with TCDD for 1 hour, 1075 phosphorylated peptides occurred in at least two of the three replicates. Four peptides with a q-value <0.05 were found (Table 3.4). Three of these peptides were up-regulated and one was down-regulated.

For the protein "similar to AHNAK", 26 different phosphorylated peptides were identified, but only one of them was significantly regulated (shown in Table 8, Appendix). The others exhibited regulation factors between 0.9 and 1.2. Interestingly, for the regulated phosphorylated peptide LPSGpSGAASPTTGSAVDIR another phosphosite (LPSGSGAApSPTTGSAVDIR) was identified which was not regulated. The regulated phosphorylation occurred on y15/b5 and the non-regulated on y11/b9. Inspection of the MS/MS spectra of both forms of the peptide verified the results obtained from MSQuant indicating that the peptide was phosphorylated at different sites. The extracted ion chromatograms (XIC)[1] as well as the MS- and the MS/MS spectra of both forms of the peptide are shown in Figures 3.18, 3.19, 3.20. Whereas for both peptides the y10 fragment ion had the same mass, the y11 fragment showed a loss of a phosphate group for the peptide LPSGSGAApSPTTGSAVDIR but not for the peptide LPSGpSGAASPTTGSAVDIR. Both forms of the peptide were identified side-by-side due to their different retention times on the C18 column. Phosphate groups close to the N-terminus of the peptide can form a salt bridge with the free amide group. This reaction results in an increased hydrophobicity of the peptide and, therefore, a different retention behaviour on the RP-column. This could explain the different retention times of the two phospho-species.

For the Rdbp protein two different phosphorylated peptides were identified. Both exhibited similar regulation factors of 1.64 and 1.79 (Table 3.4 and 3.5). Whereas the peptide SMpSADEDLQEPSR was identifed in more than one biological replicate (Table 3.4), the peptide SLpSEQPVVDTATATEQA was found in only one sample (Table 3.5).

[1]The extracted ion chromatogram (XIC) is the chromatographic profile of an ion with a particular m/z. An XIC provides information about the elution time and length of the particular ion [Lottspeich and Engels, 2006].

Accession number	Gene name, protein name	Sequence	Phosphosite localization in protein	Validated	Maximal ion score	PTM score	Mean regulation factor H/L	q-Value
IPI00769072	*Ahnak*, similar to AHNAK nucleoprotein isoform 1 isoform 2	LPSG*SGAASPTTGSAVDIR	212	novel	60	64	1.98	$1.3*10^{-4}$
IPI00422013	*Rdbp*, Rdbp protein	SM*SADEDLQEPSR	115	by similarity	70	144	1.64	$3.3*10^{-3}$
IPI00358819	*Pragmin*, Pragmin	EAVQPEPI*YAESAK	391	by similarity	43	98	0.63	0.04
IPI00187767	*Prkra*, Interferon-inducible double stranded RNA-dependent protein kinase activator A	ED*SGTFSLGK	18	known	46	59	1.43	0.04

Table 3.4: **Phosphopeptides identified as regulated after treatment of the cells with TCDD for 1 hour and found at least twice.** The displayed peptides were found in at least two biological replicates. Peptides were accepted as regulated with a q-value $p \leq 0.05$. The asterisks in the peptide sequences indicate the position of the phosphorylation site.

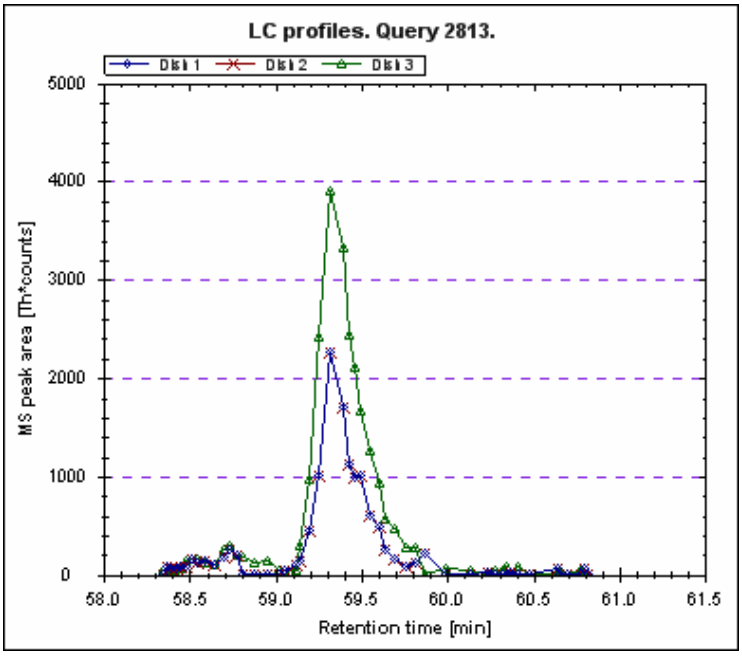

(a) Extracted Ion Chromatogram; y15/b5

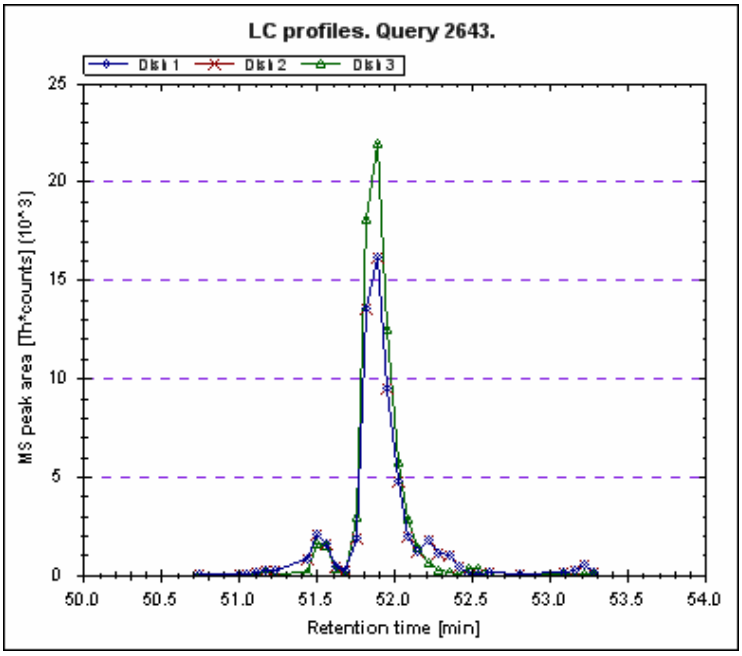

(b) Extracted Ion Chromatogram; y11/b9

Figure 3.18: **Phosphosite-specific quantitation of an AHNAK peptide carrying different phosphorylations - Extracted ion chromatograms.** The extracted ion chromatograms for the peptides LPSGpSGAASPTTGSAVDIR (a) and LPSGSGAApSPTTGSAVDIR (b) are shown. The blue peak indicated the XIC derived from the "light" peptide from the DMSO-treated cells, the green peak the XIC derived from the "heavy" peptide from the TCDD-treated cells.

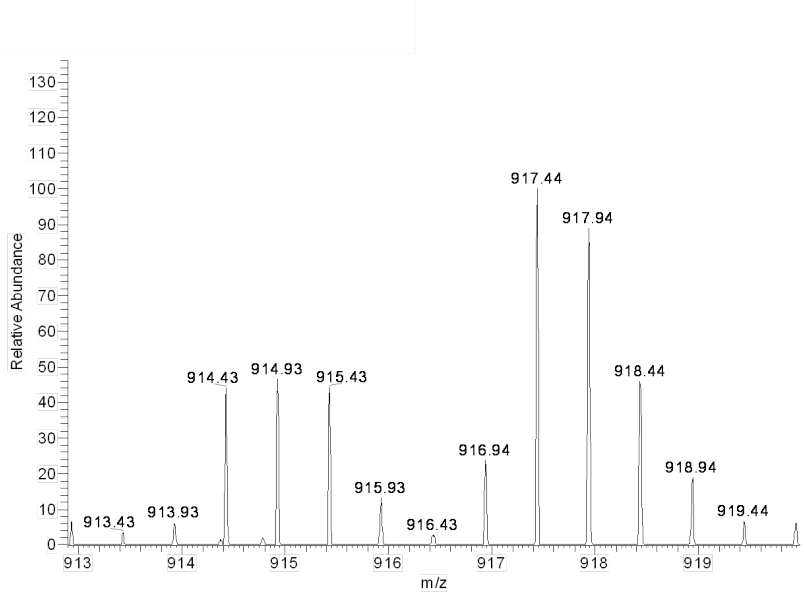

(a) MS spectrum; y15/b5

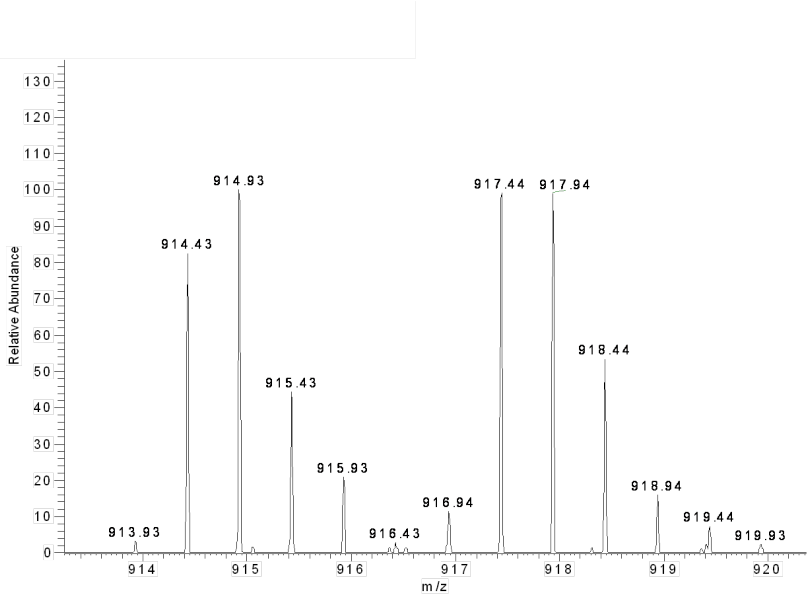

(b) MS spectrum; y11/b9

Figure 3.19: **Phosphosite-specific quantitation of an AHNAK peptide carrying different phosphorylations - MS spectra.** The MS-spectra for the peptides LPSGpS-GAASPTTGSAVDIR (a) and LPSGSGAApSPTTGSAVDIR (b) are shown. The monoisotopic mass at m/z 914.43 (z +2) was derived from the "light" peptide (DMSO-treated cells) and that at m/z 917.44 (z +2) from the "heavy" peptide (TCDD-treated cells). The unnormalised ratios between the monoisotopic peak intensities of the "heavy" and the "light" labelled forms were 2.008 (a) and 1.176 (b), respectively.

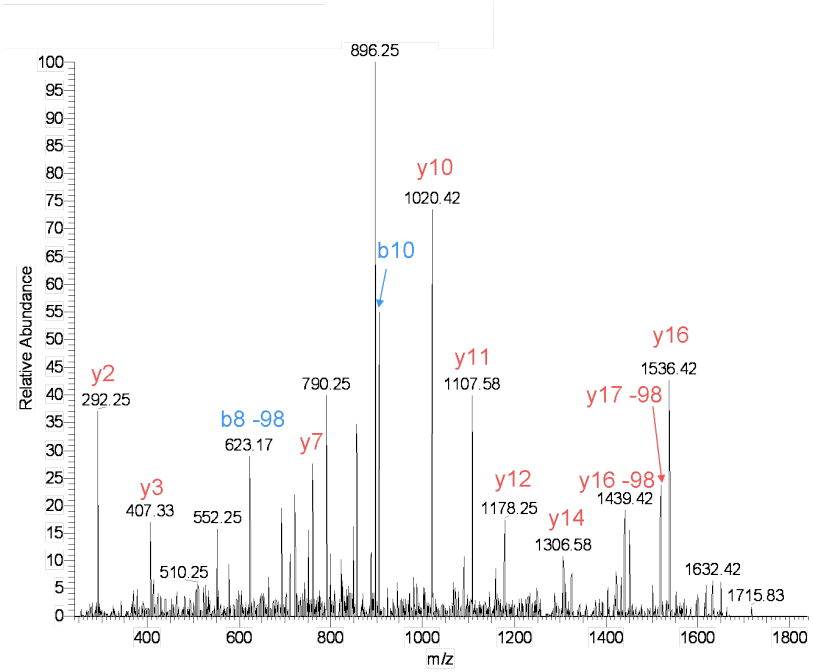

(a) MS/MS spectrum; y15/b5

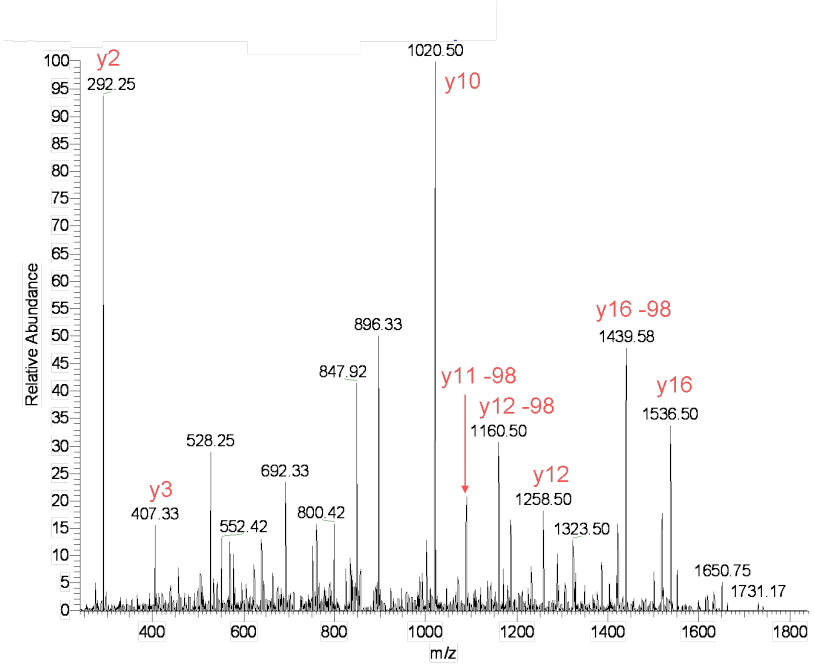

(b) MS/MS spectrum; y11/b9

Figure 3.20: **Phosphosite-specific quantitation of an AHNAK peptide carrying different phosphorylations - MS/MS spectra.** The MS/MS spectra annotations for the two different phosphopeptides (LPSGpSGAASPTTGSAVDIR (a) and LPSGSGAAp-SPTTGSAVDIR (b)) are shown. A comparison of both fragmention spectra indicates two different phosphorylation sites for the same peptide, on serine y15 and serine y11, respectively.

As a consequence of the similar regulation factors it was not possible to decide whether their upregulation reflected a higher phosphorylation level of these peptides or a higher expression level of the Rdbp protein. This question has been addressed in the following chapter 3.6.4.

For the protein Pragmin two other phosphorylated peptides were found in addition to the regulated one shown in Table 3.4. These peptides were not regulated suggesting that the upregulation of the peptide EAVQPEPIpYAESAK reflected an elevated phosphorylation (Table 8).

For the protein Interferon-inducible double stranded RNA-dependent protein kinase activator A no other peptides were found.

2774 phosphorylated peptides where observed in only one of the biological replicates. Seven of them were up-regulated and one was down-regulated (Table 3.5). For 5 of the corresponding proteins, namely zinc and double PHD fingers family 2, UBX domain-containing protein 4, DENN/MADD domain containing 5A, similar to Chromosome-associated kinesin KIF4A and Isoform 1 of Protein LYRIC, other phosphorylated peptides were found which were all not regulated (Table 8) suggesting that the upregulation of their phosphopeptides shown in Table 3.5 reflected specifically increased phosphorylation events. In addition, for UBX domain-containing protein 4 the regulated phosphorylated peptide was also present in its unphosphorylated state, and this peptide was neither regulated (Table 8). The spectra of both forms of this peptide are shown in the Appendix (14, 15).

3.6.4 Peptides with altered phosphorylation after 2 hours TCDD treatment

For this treatment period, two biological replicates were analysed. As a consequence of the lower number of samples, a lower number of phosphorylated peptides was observed. 883 peptides occurred in both replicates and were taken to calculate the p- and q-values. 83 peptides with a p-value <0.05 were identified. After FDR correction, 6 peptides remained significantly regulated (q-value <0.05) of which 5 were up-regulated and 1 was down-regulated (Table 3.6).

For (TIF1β), Isoform 1 of Protein LYRIC and "similar to AHNAK", further phosphopeptides were identified which were not regulated (Table 8). For the Rdbp protein two peptides were found and, as had been observed for the 1 hour data set, both peptides were up-regulated. Again, the peptide SMpSADEDLQEPSR was found in two biological

Accession number	Gene name, protein name	Sequence	Phosphosite localization in protein	Validated	Ion score	PTM score	Regulation factor H/L
IPI00366160	*Dpf2*, Dpf2 protein protein 2	VDDD*SLGEFPVTNSR	141	novel	57	88	0.56
IPI00188182	*Zfp36l1*, Butyrate response factor 1	RH*SVTLPSSK	54	known	47	97	1.50
IPI00371952	*Ubxn4*, UBX domain-containing protein 4	NTELCE*TPTTSDPK	156	novel	86	28	1.63
IPI00359669	*Dennd5a*, DENN/MADD domain containing 5A 4	FN*SYDISR	193	novel	39	74	1.65
IPI00563843	*Kif4*, similar to Chromosome-associated kinesin KIF4A	TF*SRDEVHGQDSGAEDSISK	802	novel	52	73	1.73
IPI00422013	*Rdbp*, Rdbp protein	SL*SEQPVVDTATATEQAK	51	by similarity	80	184	2.79
IPI00209277	*Mtdh*, Isoform 1 of Protein LYRIC	LSSQL*SAGEEK	297	by similarity	55	73	1.99
IPI00195864	*Arnt*, Aryl hydrocarbon receptor nuclear translocator	FAR*SDDEQSSADK	77	by similarity	41	70	2.44

Table 3.5: **Phosphopeptides identified as regulated after treatment of the cells with TCDD for 1 hour and found only once.** The displayed regulated peptides were found in only one biological replicate and were accepted as regulated with an FC factor of ≥ 1.5. The asterisk in the sequence symbolizes the position of the phosphorylation site.

Accession number	Gene name, protein name	Sequence	Phosphosite localization in protein	Validated	maximal ion score	PTM Score	Mean regulation factor H/L	q-Value
IPI00194567	*Trim28*, Transcription intermediary factor 1-beta (TIF1β)	*SGEGEVSGLMR	474	by similarity	48	131	1.87	0.01
IPI00209277	*Mtdh*, Isoform 1 of Protein LYRIC	LSSQL*SAGEEK	297	by similarity	52	94	1.81	0.01
IPI00422013	*Rdbp*, Rdbp protein	SM*SADEDLQEPSR	115	by similarity	57	112	1.75	0.01
IPI00370361	*Hn1*, Hematological and neurological expressed 1 protein	SN*SSEASSGDFLDLK	82	by similarity	87	164	1.49	0.04
IPI00367996	*Sgef*, similar to Src homology 3 domain-containing guanine nucleotide exchange factor	ALDID*SDEEPEPK	390	novel	49	133	0.64	0.04
IPI00769072	*Ahnak*, similar to AHNAK nucleoprotein isoform 1 isoform 2	LPSG*SGAASPTTGSAVDIR	212	novel	82	79	1.60	0.04

Table 3.6: **Phosphopeptides identified as regulated after treatment of the cells with TCDD for 2 hours and found at least twice.** The displayed peptides were found in at least two biological replicates. Peptides were accepted as regulated with a q-value ≤ 0.05. The asterisks in the peptide sequences indicate the position of the phosphorylation site.

replicates and the peptide SLpSEQPVVDTATATEQAK in only one replicate. Thus, the regulated phosphosites were the same for the two time points.

1997 phosphorylated peptides were observed in only one of the two biological replicates. 10 of them were up-regulated and 6 were down-regulated (Tables 3.7 and 3.7). For the following proteins more phosphopeptides than just the regulated one were identified, but none of these was regulated suggesting that the level of these proteins in the cells was not affected by TCDD: Cdc42 effector protein 1, RNA binding motif, single stranded interacting protein 2, ataxin 2, PTPRF interacting protein, binding protein 1, p38alpha, similar to zinc finger, ZZ type with EF hand domain 1, 106 kDa protein and MARCKS-related protein (Table 8; Appendix).

Since for the Rdbp protein two upregulated phosphorylated peptides, but no others, were observed both for the 1 hour and the 2 hours exposure period, the possibility remained the up-regulation reflected an increase in the level of Rdbp protein by TCDD rather than increased phosphorylations. To address this problem, the level of the Rdbp protein at the different time points was examined by Western blotting. Figure 3.21 shows that treatment of the 5L cells with TCDD for 0.5 – 4 hours did not cause any detectable alteration in the amount of Rdbp protein, supporting the conjecture that the observed up-regulation actually reflected specifically increased phosphorylations of Rdbp.

3.6.5 Summary of the identified peptides with altered phosphorylation after TCDD treatment

For the three periods of TCDD exposure, 7 proteins carrying specific phosphorylation sites significantly regulated by TCDD as analysed by the moderated t-test and the q-value calculation were found. In addition, 23 proteins with TCDD-regulated phosphorylation sites were observed in only one biological replicate but with an FC of ≥ 1.5. For all regulated phosphorylated peptides the MS/MS spectra where manually validated and are shown in the Appendix. For the majority of the proteins with altered phosphorylation at specific sites further phosphopeptides were observed that were not regulated indicating that specific phosphorylations, but not the level of the protein, were affected by TCDD.

A short overview of all proteins with TCDD-regulated phosphorylation and the affected phosphorylation sites for all exposure periods is shown in Tables 3.8 and 3.8. An extended version of this table, providing more detailed information, can be found in the Appendix (Table 7).

Accession number	Gene name, protein name	Sequence	Phosphosite localization in protein	Validated	Ion score	PTM score	Regulation factor H/L
IPI00372282	*Rabgap1*, RAB GTPase activating protein 1	QGDETPS*TNNGSDDEK	38	novel	51	58	0.51
IPI00196865	*Cdc42ep1*, Cdc42 effector protein 1	EQS*SSPSEPNPNPELR	193	novel	44	45	0.59
IPI00371268	*Rbms2*, RNA binding motif, single stranded interacting protein 2	LYVAQQMAPP*SPR	33	nove	30	50	0.61
IPI00371094	*Atxn2*, ataxin 2	TN*SPSA*SPSVLSNAEHK	511/515	novel	36	53	0.62
IPI00203281	*Cby1*, Protein chibby homolog 1	SA*SLSNLHSLDR	20	novel	49	57	0.65
IPI00655262	*Senp3*, SUMO/sentrin specific peptidase 3	G*SPPVPSGPPMEEDGLR	205	novel	34	84	0.67
IPI00371952	*Ubxn4*, UBX domain-containing protein 4	NTELCE*TPTTSDPK	156	novel	83	23	1.51
IPI00366315	*Ppfibp1*, PTPRF interacting protein, binding protein 1	LATKPE*TSFEEGDGR	413	novel	39	59	1.54

Table 3.7: **(Part 1) Phosphopeptides identified as regulated after treatment of the cells with TCDD for 2 hours and found only once.** The displayed regulated peptides were found in only one biological replicate and were accepted as regulated with an FC factor of ≥ 1.5. The asterisk in the sequence symbolizes the position of the phosphorylation site.

Accession number	Gene name, protein name	Sequence	Phosphosite localization in protein	Validated	Ion score	PTM score	Regulation factor H/L
IPI00190530	*Mapk14*, Isoform 1 of Mitogen-activated protein kinase 14 (p38alpha)	HTDDEMTG*YVATR	182	by similarity	57	64	1.57
IPI00364123	*Zzef1*, similar to zinc finger, ZZ type with EF hand domain 1	SMEE*TRPVPTVK	1541	novel	34	28	1.73
IPI00203720	*Med24*, 106 kDa protein	LL*SSNEDDASILSSPTDR	879	novel	74	131	1.75
IPI00563843	*Kif4*, similar to Chromosome associated kinesin KIF4A	TF*SRDEVHGQDSGAEDSISK	802	novel	52	73	1.83
IPI00189061	*Marcksl1*, MARCKS-related protein	GDV*TAEEAAGASPAK	14	by similarity	42	104	1.94
IPI00422013	*Rdbp*, Rdbp protein	SL*SEQPVVDTATATEQAK	51	by similarity	83	152	1.95
IPI00364994	*Ncbp1*, Nuclear cap-binding protein subunit 1	RH*SYENDGGQPHK	7	by similarity	37	24	1.96
IPI00195864	*Arnt*, Aryl hydrocarbon receptor nuclear translocator	FAR*SDDEQSSADK	77	by similarity	40	114	3.67

Table 3.7: **(Part 2) Phosphopeptides identified as regulated after treatment of the cells with TCDD for 2 hours and found only once.** The displayed regulated peptides were found in only one biological replicate and were accepted as regulated with an FC factor of ≥ 1.5. The asterisk in the sequence symbolizes the position of the phosphorylation site.

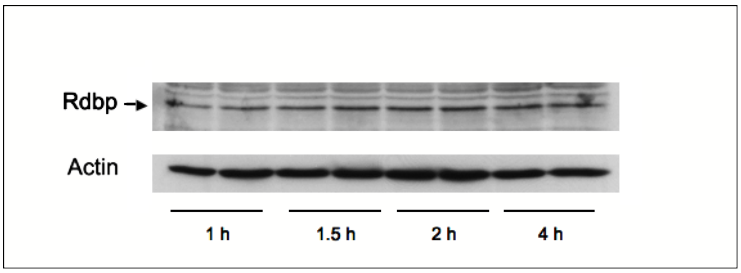

(a)

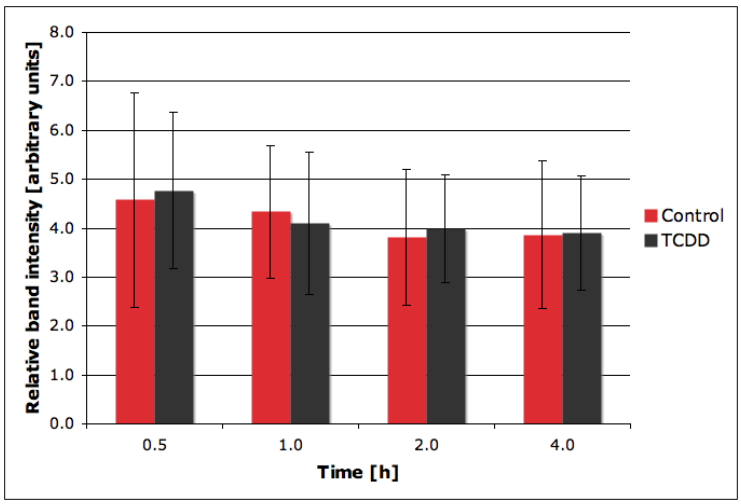

(b)

Figure 3.21: **Western blot analysis of the effects of TCDD on Rdbp protein abundance in 5L cells.** Cells were exposed to DMSO or 1 nM TCDD for the times indicated. Total cell lysates were prepared and analysed on 12% PAGE gels. Proteins were electroblotted, and Rdbp and actin (loading control) were visualized using specific antibodies and ECL detection. Bands were quantitated by densitometry. (a), Sections of the respective blots from one experiment out of three which yielded very similar results. (b), Means ±SD from three independent experiments.

No.	IPI Accession	Gene Name	PTM Sequence	ave. Regulation factor H/L 30 min	ave. Regulation factor H/L 1 hour	ave. Regulation factor H/L 2 hours
1	IPI00190530	*Mapk14*	HTDDEMTG*YVATR	0.83	1.41	1.57
2	IPI00364957	*Ahr*	GEAVL*YEI*SSPFSP	0.68	-	-
3	IPI00195864	*Arnt*	FAR*SDDEQSSADK	-	2.44	3.67
4	IPI00194567	*Trim28*	*SGEGEVSGLMR	1.58	1.36	1.87
5	IPI00190390	*Cdc2*	IGEGT*YGVVYK	1.64	-	1.10
6	IPI00371268	*Rbms2*	LYVAQQMAPP*SPR	-	-	0.61
7a	IPI00422013	*Rdbp*	SM*SADEDLQEPSR	1.12	1.65	1.76
7b	IPI00422013	*Rdbp*	SL*SEQPVVDTATATEQAK	-	1.79	1.95
8	IPI00188182	*Zfp36l1*	RH*SVTLPSSK	-	1.50	-
9	IPI00364994	*Ncbp1*	RH*SDDEQSSADK	-	-	1.96
10	IPI00203720	*Med24*	LL*SSNEDDASILSSPTDR	-	-	1.75
11	IPI00371094	*Atxn2*	TN*SPSA*SPSVLSNAEHK	-	-	0.62
12	IPI00358819	*Pragmin*	EAVQPEPI*YAESAK	0.89	0.69	0.99
13	IPI00367996	*Sgef*	ALDID*SDEEPEPK	1.15	0.95	0.64
14	IPI00196865	*Cdc42ep1*	EQS*SSPSEPNPNPELR	1.06	-	0.59
15	IPI00370361	*Hn1*	SN*SSEASSGDFLDLK	1.03	1.21	1.50
16	IPI00359669	*Dennd5a*	FN*SYDISR	-	1.65	-
17	IPI00372282	*Rabgap1*	QGDETPS*TNNGSDDEK	-	-	0.51
18	IPI00371952	*Ubxn4*	NTELCE*TPTTSDPK	0.86	1.63	1.51
19	IPI00362117	*Ubxn7*	SESLIDASED*SQLEAAIR	1.86	-	1.18

Table 3.8: **(Part 1) Overview of the phosphopeptides identified as regulated after TCDD treatment.** The table includes all phosphorylated peptides identified as regulated for the three different time points treatment with TCDD. The asterisk in the sequence symbolizes the position of the phosphorylation site.

No.	IPI Accession	Gene Name	PTM Sequence	ave. Regulation factor H/L 30 min	ave. Regulation factor H/L 1 hour	ave. Regulation factor H/L 2 hours
20	IPI00203281	*Cby1*	SA*SLSNLHSLDR	0.82	0.94	0.65
21	IPI00769072	*Ahnak*	LP*SGSGAASPTTGSAVDIR	1.30	1.99	1.60
22	IPI00187767	*Prkra*	ED*SGTFSLGK	1.02	1.44	-
23	IPI00209277	*Mtdh*	LSSQL*SAGEEK	1.19	1.99	1.81
24	IPI00366160	*Dpf2* D4	VDDD*SLGEFPVTNSR	1.10	0.56	1.20
25	IPI00563843	*Kif4*	TF*SRDEVHGQDSGAEDSISK	-	1.73	1.83
26	IPI00655262	*Senp3*	G*SPPVPSGPPMEEDGLR	-	0.93	0.67
27	IPI00366315	*Ppfibp1*	LATKPE*TSFEEGDGR	0.92	1.03	1.54
28	IPI00364123	*Zzef1*	SMEE*TRPVPTVK	-	-	1.73
29	IPI00189061	*Marcksl1*	GDV*TAEEAAGASPAK	0.96	0.96	1.94
30	IPI00765369	*LOC686261*	SAPA*SP*THPGLMSPR	0.62	-	-

Table 3.8: **(Part 2) Overview of the phosphopeptides identified as regulated after TCDD treatment.** The table includes all phosphorylated peptides identified as regulated for the three different time points treatment with TCDD. The asterisk in the sequence symbolizes the position of the phosphorylation site.

3.7 Mechanism of the calcium dependence of TCDD-induced gene activation in 5L cells

For the protein AHNAK, highly significant increases in the phosphorylation of a specific residue, Ser212, were observed in four of the experiments with 1 hour and 2 hours exposures to TCDD. Since one of the known functions of AHNAK is the regulation of L-type voltage-gated Ca^{2+} channels in the plasma membrane [Haase et al., 1999], [Hohaus et al., 2002], [Alvarez et al., 2004] and since an increased Ca^{2+} influx is required for the AhR/ARNT-dependent transcriptional activation of target genes of TCDD like CYP1A1 [Monteiro et al., 2008], the potential role of L-type voltage-gated Ca^{2+} channels in the regulation of CYP1A1 expression was assessed by determining the effect of inhibitors of these channels on the inducibility of CYP1A1 protein in 5L cells by TCDD using Western blotting. In addition, the effects of certain experimental conditions and other inhibitors and agents interfering with different aspects of Ca^{2+} homeostasis were investigated. The results of these experiments are shown in Figure 3.22. The incubation of the cells with TCDD for 4 h or 8 h strongly increased CYP1A1 protein level. The concurrent presence of the L-type voltage-gated Ca^{2+} channel inhibitors amlodipine, diltiazem or nifedipine had no significant effect on CYP1A1 induction indicating that these Ca^{2+} channels are unlikely to be involved in the regulation of TCDD-induced gene activation. By contrast, induction of CYP1A1 was completely abrogated in the absence of Ca^{2+} from the culture medium or in the presence of the cell-permeable Ca^{2+} chelator BAPTA-AM indicating a requirement for extra- and intracellular Ca^{2+} ions in this process. The presence of 2-APB, an inhibitor of store-operated Ca^{2+} entry and, inconsistently, inositol 1,4,5-trisphosphate receptor-mediated Ca^{2+} release from the endoplasmic reticulum [Bootman et al., 2002], also blocked the action of TCDD completely. Supplementation of the medium with the specific Ca^{2+}/calmodulin kinase I (CAMKI) inhibitor KN-93 also fully prevented CYP1A1 induction by TCDD. In contrast, the KN-93 analogue KN-92, which does not inhibit CAMKI, was without any effect at 4 h and only slightly reduced CYP1A1 protein level after 8 h. The calmodulin antagonist W-7, which binds to the calmodulin binding site of the enzyme, slightly inhibited CYP1A1 induction after 4 h but completely abolished the strong induction by TCDD observed after 8 h. The latter observations are fully consistent with those reported by Monteiro et al. [Monteiro et al., 2008] for human mammary MCF-7 cells and primary macrophages.

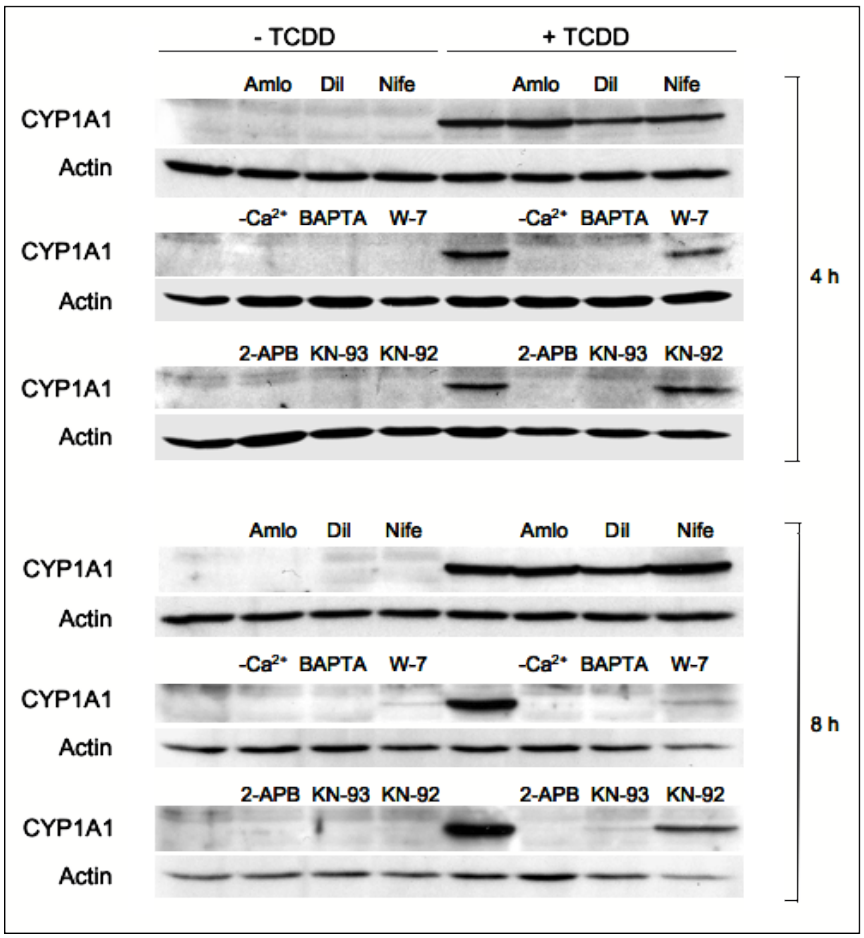

Figure 3.22: **Western blot analysis of the effects of inhibitors and agents interfering with Ca^{2+} homeostasis on the inducibility of CYP1A1 protein by TCDD in 5L cells.** Following pre-incubation of the cells with amlodipine ("Amlo", 10 μM), diltiazem ("Dil", 50 μM), nifedipine ("Nife", 50 μM), BAPTA-AM ("BAPTA", 50 μM), W-7 (50 μM), KN-93 (50 μM), KN-92 (50 μM) or Ca^{2+}-free medium for 15 min, DMSO or TCDD (1 nM) was added and the incubation continued for 4 and 8 h. Total cell lysates were prepared and analysed on 12% PAGE gels. Proteins were electroblotted, and CYP1A1 and actin (loading control) were visualized using specific antibodies and ECL detection. Sections of the respective blots from one experiment out of three which yielded very similar results are shown.

Thus, the present data support the notion that AhR/ARNT-dependent induction of CYP1A1, and probably other AhR/ARNT target genes, in 5L cells is dependent on the availability of extra- and intracellular Ca^{2+}, that store-operated Ca^{2+} channels, but not L-type voltage-gated Ca^{2+} channels, mediate Ca^{2+} entry into the cells and that active CAMKI is required. With respect to AHNAK, the data indicate that the observed up-regulation of Ser212 phosphorylation of AHNAK by TCDD is unlikely to be functionally important for the regulation of Ca^{2+} entry into cells by TCDD.

Chapter 4

Discussion

The present phosphoproteomic study was performed with the aim to identify hitherto unknown changes in protein phosphorylation caused by TCDD in 5L cells independent of TCDD-induced gene expression. In order to detect these alterations, a quantitative "global" comparison of the relative abundances of phosphorylated peptides using a shotgun phosphoproteomics approach was taken. Cells were differentially SILAC-labelled with amino acids containing stable heavy isotopes to enable the discrimination of peptides in control cells and TCDD-treated cells and then treated for short periods (0.5, 1 and 2 hours) with DMSO or TCDD. Following combination of control cells and treated cells in a single sample, proteins were proteolysed and phosphopeptides were enriched using the SIMAC approach, fractionated by HILIC and analyzed by LC-MS/MS. This strategy yielded information on the relative amounts of the phosphopeptides in control and TCDD-treated cells and identified both the phosphorylation sites and the corresponding phosphoproteins.

4.1 Methodological aspects

In the following, several methodological aspects of the present quantitative phosphoproteomics study will be discussed briefly.

4.1.1 SILAC labelling

In order to detect and quantitate the changes of protein phosphorylation between control cells and TCDD-treated cells, the SILAC approach was taken. SILAC is a very precise

method for the relative quantitation of peptides and proteins and allows the detection of relatively small differences between different cell states [Park et al., 2006].

The pooling of control and TCDD-exposed cells directly after cell lysis was expected to allow a very accurate quantitation of the phosphorylated peptides. This expectation was fulfilled as the MA plots for the data sets before normalisation shown in Section 3.5.1, clearly indicated that the error introduced by sample handling was minimal.

In addition to the advantage that every tryptic peptide except for the C-terminal one becomes isotopically labelled when heavy arginine and lysine are used for SILAC labelling, the use of these amino acids in their ^{15}N- and ^{13}C-labelled form provides the benefit that the heavy isotopes do not affect the chemical behaviour of the peptides. This is in contrast to the use of deuterated amino acids which result in an altered LC retention of the peptides [Zhang et al., 2001]. Deuterated peptides elute from the reversed phase material earlier than peptides containing the light hydrogen due to a different transient dipole of the ^{2}H-C bond [Ong et al., 2003a] which complicates the following quantitation by MS. A potential problem associated with the use of isotopically labelled arginine for SILAC labelling is the fact that fast growing cells can metabolically convert an excess of arginine into proline [Ong et al., 2003b]. This results in the formation of isotopically labelled proline from labelled arginine and, thus, the appearance of multiple peaks for proline-containing peptides which will complicate their quantitation. The 5L cells exhibit this interconversion (not shown), and therefore a solution to this problem was employed that had recently been described by van Hoof et al. [Van Hoof et al., 2007]. It involves the use of $^{15}N_4$-arginine as "light" arginine label for the control cells and $^{13}C_6{}^{15}N_4$-arginine as "heavy" arginine label for the TCDD-treated cells. The method is based on the assumption that for both forms of heavy arginine, the arginine-to-proline conversion is quantitatively equal. In the MS spectra, light and heavy arginine-containing peptides can then be quantitated accurately when the analysis is based on the first monoisotopic peak of the two types of peptides. This strategy is very easy to adapt to the cells and allows a precise relative peptide quantitation in any proliferating cell. However, this choice of isotopes complicated the data analysis in the present study as both open-source software packages available for the analysis of SILAC quantitation data, MSQuant and MaxQuant, cannot handle this labelling type. Only after changes in the source code of MSQuant this program was able to quantify this type of labelling. An unavoidable drawback of the SILAC method as well as any other isotopic labelling strategy is the increased sample complexity as every single peptide results in two different peaks in the MS spectrum [Ytterberg and Jensen, 2010]. For both mass

peaks a MS/MS spectrum will be acquired which will not deliver additional information but reduce the number of peptide identifications.

4.1.2 A comprehensive phosphoproteomic analysis?

In the course of establishing the experimental protocols for this project, it was seeked to keep the amount of starting material low in order to be able to use the same phosphopeptide enrichment set-up for future experiments on tissue samples which may provide only limited amounts of protein. In the present study, 5648 unique phosphorylated peptides were identified from a relatively low amount of protein, 800 μg, which compares favourably with results from other large-scale phosphoproteomics studies which identified roughly similar numbers of phosphorylated peptides but started with a higher amount of protein. Thus, Rinschen et al. identified 3869 unique phosphopeptides from an initial 4 mg of protein [Rinschen et al., 2010] and Hou et al. identified 2230 unique phosphopeptides starting with 4.5 mg [Hou et al., 2010].

Only few of the identified phosphopeptides were found to be differentially "regulated" following treatment of the cells with TCDD in the present study. There are two possible explanations for this outcome. First, it appears likely that the action of TCDD mainly takes place on the genomic level by altering gene expression and only few signalling pathways are directly affected by TCDD at early time points. A second reason for the low number could be the enrichment and identification of phosphorylated peptides mainly from highly abundant proteins which are unaffected by TCDD. The latter problem could be attenuated by a further reduction of sample complexity. As a result, a higher number of peptide identifications and a higher number of differentially regulated phosphopeptides detected would be expected. In this study, the implementation of HILIC as a method for phosphopeptide prefractionation in the experimental protocol already increased the number of identified peptides by more than three times as shown in Chapter 3.3. However, several other strategies for sample preparation or changes of the MS set-up may improve the number of identifications, particularly for less abundant phosphoproteins. In the following, a few options will be shortly discussed.

Cell fractionation before or after cell lysis will result in reduced sample complexity on the protein level. Moreover, it would be expected to provide a detailed overview of the alterations of the phosphoproteome in the different cell compartments. Another possibility to increase the number of identifications would be the implementation of a gas-phase fractionation (GPF) at the MS level [Spahr et al., 2001]. Instead of acquiring a sample over

one wide mass-to-charge range, the MS spectrum is split into several smaller mass ranges to select ions for fragmentation. GPF has been demonstrated to result in higher proteome coverage than the LC-MS/MS approach without fractionation [Kennedy and Yi, 2008]. In the present study, the five most intense peptide ions from the survey scan (MS) were selected for fragmentation to reveal the peptide sequence. The fragmentation method employed was CID, where the peptides collide with an inert gas resulting in backbone fragmentation of the peptides. This type of fragmentation is currently the most commonly used method in mass spectrometry-based proteomics. Recently, a new fragmentation technique, electron transfer dissociation (ETD), was introduced [Syka et al., 2004]. ETD has been shown to be highly suitable for the identification of labile post-translational modifications which remain intact on the peptide during fragmentation. The fragmentation of phosphorylated peptides using ETD results in a higher number of identified peptides [Swaney et al., 2009]. The overlap between the phosphopeptides identified with ETD or CID is fairly low which demonstrates the complementary character of the two methods. CID fragmentation is more efficient for peptides with a charge state of 2 or 3 and a mass range of 400 - 600 m/z. ETD, on the other hand, results in better fragmentation spectra for peptides with a higher charge state and higher m/z range. The group of Coon used these observations to develop a special algorithm, the so-called "decision tree" (DT) [Swaney et al., 2008], where the fragmentation method is chosen automatically based on the mass and charge state of the peptide in question. Using the DT approach, the number of identified peptides, particularly that of phosphorylated ones, could be increased considerably. Thus, there are various options to increase the number of peptide identifications and, therefore, to analyse proteins of low abundance. However, all of these methods require a certain amount of starting material and a lot of measurement time on the mass spec instruments. For this study, the amount of starting material was not a critical issue, but the measurement time was the limiting factor. In total, 259 individual LC-MS/MS runs were performed in the course of this project. It resulted in a non-comprehensive data set which yielded several clues with respect to early actions of TCDD. Based on this information, more targeted (hypothesis-driven) studies can now be conducted.

4.1.3 Enrichment of phosphopeptides

The calculation of the enrichment efficiency of phosphorylated peptides is a common way to evaluate the success of the approach. The efficiency is calculated by dividing the number of identified phosphopeptides by the total number of identified peptides. Based on

this calculation, the enrichment strategy with SIMAC, HILIC and TiO_2 yielded an average enrichment efficiency of about 70%. A benefit of the enrichment approaches used was the separation of mono- from multiphosphorylated peptides by the SIMAC method. However, for the 5L cell lysate, the method was not as efficient as had been expected. Only 14% of all identified phosphorylated peptides were multiphosphorylated. This number was just slightly higher than the numbers obtained in other studies that did not attempt to specifically enrich multiphosphorylated peptides [Tweedie-Cullen et al., 2009]. For further experiments, therefore, SIMAC needs to be optimized for use with 5L cells in order to enrich more multiphosphorylated peptides. Following SIMAC, the sample was pre-fractionated on a TSK-HILIC column. This technique proved highly suitable for the pre-fractionation of the phosphopeptides, the overlap of individual peptides between different fractions being only ∼20%. Moreover, sample loading and elution occur under salt-free conditions which obviates the need for additional desalting steps prior the following sample processing steps. The phosphopeptide enrichment efficiency of HILIC in combination with IMAC has been shown superior to that of SCX in combination with IMAC [McNulty and Annan, 2008]. However, since HILIC as a standalone enrichment method is not efficient enough, an additional specific enrichment step is necessary. Therefore, a further enrichment with TiO_2 was performed. TiO_2 is easy to apply and has turned out to be very efficient.

4.1.4 Statistics

In the field of proteomics, various strategies are available to define differentially regulated peptides or proteins. The most common method is based on the determination of the "fold-change". The fold-change parameter displays the ratio between the treated and the control samples [Andersen et al., 2009]. A 1.5- or 2-fold change is a typical threshold for the definition of regulated peptides. A drawback of the fold-change cut-off is that the variability between biological replicates is not taken into account and reproducibility is not guaranteed [McCarthy and Smyth, 2009]. During the last few years which saw the publication of numerous proteomic studies reporting the identification of continuously increasing numbers of proteins and peptides it became more and more obvious that it is important to apply statistical tests in order to obtain more confident results. For this study, an empirical Bayes moderated t-test together with the q-value for the FDR calculation was used. The moderated t-test can be used for studies with only few replicates [Smyth, 2005] and for this reason was ideal for the analysis of the data sets presented here. The q-value, which is getting more and more important in the proteomics area, was calculated to narrow the frac-

tion of false positive hypotheses (adjustment of the p-values) [Sachs and Hedderich, 2009]. This method is less conservative than the very common Bonferroni method. The q-value adjustment avoids a rejection of true differential phosphorylation events. The combination of the empirical Bayes moderated t-test with the q-value approach was a good strategy to achieve reliable results. However, for the p- and q-value calculation several replicates are required and with increasing numbers of replicates the statistical power increases. In contrast, the FC method can be applied to single runs, which is particularly interesting for e.g. clinical samples where only a limited amount of sample material is available and running replicates is impossible. Another problem associated with the statistical tests is the lack of good software. The major part of the available software covers only very few statistical functions. One exception is the statistics platform R [Gentleman et al., 2004a] in combination with Bioconductor [Gentleman et al., 2004b] which offers a great variety of options to the user. Due to a missing graphical user interface it is, however, not very user-friendly.

4.1.5 Reproducibility

Only peptides found in at least two biological replicates where taken for the p-value calculation. The overlaps between the biological replicates were relatively low. In Figure 4.1 the Venn Diagrams for the 30-min and the 2-h exposures to DMSO/TCDD are shown.

A substantial number of the identified phosphorylated proteins were observed in one replicate only. This observation was not surprising. Variations of identified proteins/peptides between datasets are a common problem in large-scale proteomics studies and a much-debated topic [Aittokallio, 2010]. Durr et al. found that only 66% of the proteins identified in one LC-MS/MS run were confirmed when the same sample was injected a second time into the mass spectrometer [Durr et al., 2004]. After ten measurements, only 5 newly identified proteins were not confirmed by the nine other measurements. This clearly shows a great technical variance.

Incomplete datasets due to missing values can be caused by biological differences and technical bias. To increase reproducibility, different biological replicates can be pooled together during sample preparation and the sample can be measured several times.

Before data analysis, the missing values have to be removed or predicted as accurately as possible. A non-optimal solution is to fill up the missing values with zeros or the average values [Albrecht et al., 2010]. However, this method does not take into account the biases from the data sets. Different mathematical models were developed to overcome the problem

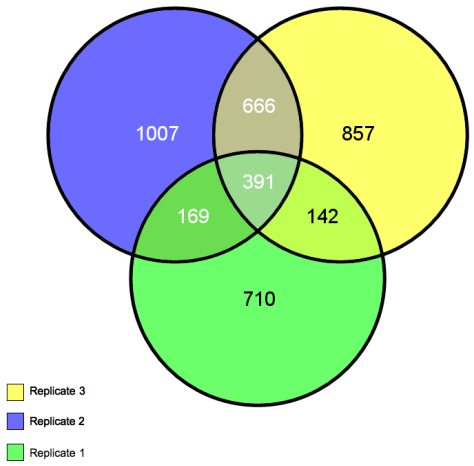

(a) Venn Diagram Biological Replicates 30 min

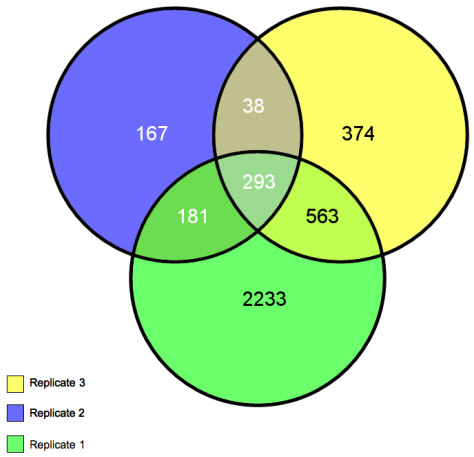

(b) Venn Diagram Biological Replicates 1 hours

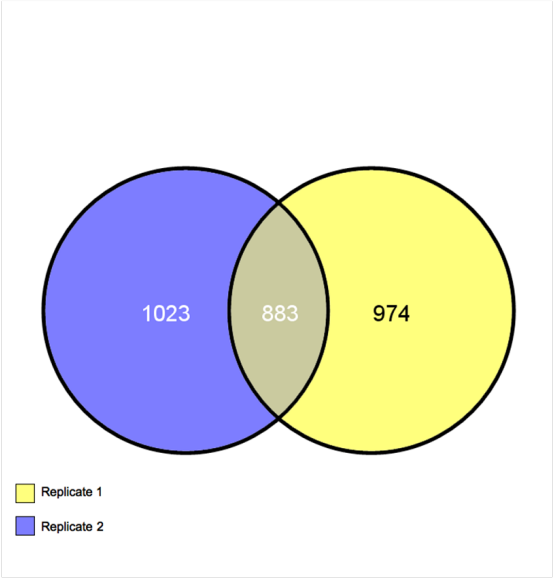

(c) Venn Diagram Biological Replicates 2 hours

Figure 4.1: **Venn diagrams for 30 min, 1 and 2 hours samples.** Diagrams show the overlap of the identified phosphorylated peptides between the biological replicates. (a) (b) (c) The diagrams were created with program Venny (http://bioinfogp.cnb.csic.es/tools/venny/index.html)

of the missing values. The k-nearest-neighbour imputing (KNN) was introduced in 2001 and originally used for the analysis of microarray data [Troyanskaya et al., 2001]. This approach has been also applied to LC-MS-based proteomics data [Roxas and Li, 2008]. The missing value from one data set is imputed by the weighted mean of available values of the k most related proteins/peptides in this set [Albrecht et al., 2010]. However, to apply this approach, a certain minimal number of biological experiments have to be performed. For the present project, mainly three biological replicates were analysed. This number of replicates is not sufficient for missing value calculations. Therefore, the peptides identified only once within the replicates were not subjected to a statistical test.

4.2 The identified TCDD-induced alterations in protein phosphorylation

Changes in protein phosphorylation by TCDD which occur before the alteration of protein expression may occur as the consequence of different mechanisms. These include i) the activation of signalling pathways preceding and required for the binding of the liganded AhR/ARNT heteromer to the DRE [Monteiro et al., 2008], [Lin et al., 2008], ii) activation or inactivation of transcriptional regulators accompanying or following the binding of the liganded AhR/ARNT heteromer to the DRE and the activation of transcription [Beischlag et al., 2008] as well as iii) the activation of other signalling pathways not required for the transcriptional activation of target genes of TCDD [Matsumura, 2009]. The first (i) and the third (iii) group of events are generally regarded as nongenomic responses. In the Discussion, the identified alterations in protein phosphorylation will be discussed with respect to the nature of the affected proteins and, whenever possible, the potential functional consequences of the phosphorylation change. In many cases, a meaningful interpretation of the obtained findings appeared difficult or was virtually impossible as the majority of the identified phosphorylation sites affected by TCDD were novel, i.e. had not been known for the particular protein in any species. In other cases, they had been reported already, but were not associated with any information of their function thus precluding an assessment of the functional consequences of the alteration. Moreover, several of the peptides exhibiting TCDD-induced phosphorylation changes were observed in only one of the experiments performed, probably as a consequence of the undersampling problem associated with the limited MS/MS scan speed in the LC-MS/MS analysis of highly complex peptide mixtures. Clearly, these phosphorylation changes will require independent

experimental confirmation, e.g. by Selected Reaction Monitoring which would allow the targeted quantitative analysis of specified phosphopeptides. However, in view of the high precision of the SILAC approach which allows the side-by-side quantitation of peptides derived from different samples it is considered that the phosphorylation changes of the majority of these "one hit peptides" which exhibited a regulation factor of ≥ 1.5 actually indicate a true effect of TCDD that will be reproduced in further in-depth studies. They will, therefore, also be discussed herein whenever it appears useful for the understanding of certain activities of TCDD in the cells.

4.2.1 Proteins previously associated with nongenomic actions of TCDD

Mitogen-activated protein kinase 14 (p38alpha/ *Mapk14*)

Previous to the present work, the transcription-independent increased phosphorylation of the Mitogen-activated protein kinase 14 by TCDD observed by Weiss et al. (2005) was the only phosphorylation change reported to occur in 5L cells during short exposures (1-2 hours) to TCDD [Weiss et al., 2005]. This finding has been confirmed here by the observation of a significant up-regulation of the Tyr182 phosphorylated form of p38alpha, also known as Mitogen-activated protein kinase 14 (MAPK 14), by a factor of ∼1.6 in one of the two experiments with 2 h TCDD exposure (Table 3.8, No. 1). Activation of MAPK 14 occurs by simultaneous phosphorylation of Tyr182 and Thr180 by upstream kinases. After 1 h exposure to TCDD, both phosphorylations were found up-regulated by a factor of 1.41 in one of the experiments (Table 3.8, No. 1). Although this factor was below the threshold of 1.5 regarded as significant in the present study, the fact that the increases were identical for both phosphorylation sites strongly suggests that they actually reflected an early activation of MAPK 14 in the presence of TCDD. In two of the 1 h experiments, a peptide containing the phosphorylated Ser residue of MAPK 14 (pSQERPTFYR) was observed without any indication of a TCDD-dependent regulation (Table 8, Appendix). An observation in accord with the finding of Weiss et al. [Weiss et al., 2005] that the protein level of p38 in 5L cells is not affected by TCDD treatment.

Other proteins previously associated with nongenomic actions of TCDD

Remarkably, no TCDD-induced phosphorylation changes associated with nongenomic actions of TCDD reported for certain other cell systems, such as activation of phospholipase

A2 and c-Src [Matsumura, 2009], were observed. This may be due to the limited resolving power of the mass spectrometric method used for the analysis of the highly complex protein samples. It could, however, also reflect certain specific features discriminating the 5L cells from other cells used in earlier studies on nongenomic effects of TCDD. Thus, preliminary studies aiming at the detection of increases in Tyr419 phosphorylation or decreases in Tyr530 phosphorylation as indicators of c-Src activation [Thomas and Brugge, 1997] did not provide any evidence for an alteration of c-Src activity by TCDD in 5L cells, and cyclooxygenase 2 induction, which has been associated with c-Src activation, does not occur in these cells (U. Andrae, personal communication). It appears possible that the absence of these nongenomic effects of TCDD is a consequence of the recently discovered fact that a functional EGF receptor, which has been implicated in these nongenomic actions of TCDD [Dong and Matsumura, 2008], is lacking in 5L cells (U. Andrae, personal communication).

4.2.2 AhR (*Ahr*) and ARNT (*Arnt*)

In the present study, evidence was obtained for TCDD-induced phosphorylation changes of both partners of the AhR/ARNT heterodimer, although at different levels of certainty. For the AhR, in one of the 30-min experiments a peptide phosphorylated at two closely spaced sites (Tyr412/Ser415) was identified that was down-regulated by a factor of 0.68 (Table 3.8, No. 2), a value just above the FC threshold of 1.5. It appears that this phosphorylation of the AhR has not been described before. The phosphorylation site is located C-terminal of the PAC (PAS-associated C-terminal) domain of the AhR (residues 346-384) and might thus affect the contribution of PAC to the PER-ARNT-SIM 2 (PAS 2) domain [Hefti et al., 2004] of the receptor. It remains to be confirmed that the Tyr412/Ser415 phosphorylation is actually down-regulated by TCDD and, if this turns out to be the case, to be determined whether it is involved in the activation of the AhR by TCDD.

A clear result was obtained for the AhR heterodimerization partner ARNT, for which 2.4 and 3.7-fold increases in the phosphorylation of its Ser77 residue in TCDD-exposed cells were observed in two experiments for the 1 h and the 2 h time points, respectively(Table 3.8, No. 3). Ser77 phosphorylation of ARNT has been tentatively associated with the targeting of ARNT dimers to different enhancers [Kewley and Whitelaw, 2005]. In addition to forming active heterodimeric complexes with AhR which bind to DREs within dioxin-responsive enhancers and thereby mediate transcriptional activation of genes of the AhR gene battery, the homodimers of ARNT have been shown to bind to a palindromic enhancer sequence 5' CACGTG-3' termed "E-box element" [Sogawa et al., 1995], [Huffman et al., 2001], a se-

quence not recognized by the AhR/ARNT heterodimer [Whitelaw et al., 1993]. Interestingly, *in vitro* phosphorylation of Ser77 of ARNT by casein kinase II (CKII) was shown to result in decreased binding by ARNT homodimers to an E-box element probe and decreased the activation of an E-box reporter gene in 293T cells whereas binding of the ARNT/AhR heterodimer to the DRE was not affected [Kewley and Whitelaw, 2005]. These observations indicated that Ser77 phosphorylation regulates ARNT DNA binding and gene activation, but it remained open to question whether Ser77 phosphorylation also occurs *in vivo* and how phosphorylation might be controlled. The present results for the first time show that phosphorylation of Ser77 of ARNT indeed occurs *in vivo* and that TCDD up-regulates this phosphorylation. It thus appears likely that TCDD inhibits binding of ARNT homodimers to the E-box element, and this inhibition may increase the availability of ARNT for dimerization with the Ah receptor, binding to DREs and activation of dioxin-responsive genes. In accordance with the observations of Kewley and Whitelaw (2005), an *in silico* search using the Group-based Prediction System (GPS) v2.1.1 software, a tool for predicting protein phosphorylation sites and their cognate kinases [Xue et al., 2008], suggested CKIIa/b, but no other kinase, to be involved in the Ser77 phosphorylation of ARNT (not shown). These data suggest that CKII is involved in TCDD-induced nongenomic phosphorylation events upstream of DNA binding of the AhR/ARNT heterodimer and that it promotes AhR/ARNT binding to the DRE.

4.2.3 Regulators of the transcriptional machinery involved in AhR/ARNT-mediated gene activation

Transcriptional activation of dioxin-responsive genes by the liganded AhR/ARNT heterodimer can be differentiated into the assembly of a pre-initiation complex at the promoters of TCDD-responsive genes, chromatin remodelling over the promoter, initiation of transcription and transcript elongation. It had been expected that the present study would identify TCDD-induced alterations of proteins involved in these processes, and it turned out that this was actually the case.

Transcription intermediary factor 1-beta (TIF1β/ *Trim28*)

Transcription intermediary factor 1-beta (TIF1β), also known as KRAB-associated protein 1 or Nuclear corepressor KAP-1, is an epigenetic regulator of transcription involved in the control of chromatin remodelling. TIF1β showed an up-regulation of its Ser474 phos-

phorylation by a factor of 1.58 in one of the 30-min experiments and a highly significant up-regulation in two of the experiments with 2 h exposure to TCDD (Table 3.8, No. 4). Phosphorylation of Ser474 has not yet been described for the rat protein but has been observed in numerous studies for the corresponding Ser473 residue of the human ortholog, i.e. [Beausoleil et al., 2004], [Kim et al., 2005], [Olsen et al., 2006]. TIF1β functions as the universal corepressor for the Krüppel-associated box (KRAB) domain-containing zinc finger protein superfamily of transcriptional repressors [Abrink et al., 2001]. Physical interaction between TIF1-beta and these zinc finger proteins occurs through a conserved interaction between variants of the KRAB domain and TIF1β. The KRAB-TIF1β complex recruits members of the heterochromatin protein 1 (HP1) family as well as other chromatin modification factors to specific loci and thereby causes the formation of heterochromatin-like complexes and gene silencing. Chang et al. (2008) recently reported that the formation of the TIF1β-HP1beta complex is regulated by the phosphorylation of TIF1β at Ser473, a residue conserved between man and mouse and corresponding to Ser474 of the rat ortholog [Chang et al., 2008]. These residues are located closely to the HP1-box (amino acids 477-514 for the rat protein). This phosphorylation is dynamically associated with cell cycle progression and functionally linked to transcriptional regulation. Chang et al. showed that target genes of TIF1β are cyclin A2, the cell cycle regulators cyclin-dependent kinase 1 (*Cdc2*/CDK1) and *Cdc25a*. Expression of these genes should therefore potentially be enhanced by TCDD. Interestingly , TCDD actually increases cyclin A protein level in the rat liver oval cell line WB-F344 [Dietrich et al., 2002], [Weiss et al., 2008] and the dog kidney epithelial cell line MDCK [Weiss et al., 2008]. In WB-F344 cells the increase in cyclin A protein was associated with a release from contact inhibition. The stimulation of cyclin A expression was attributed to an AhR-dependent, but probably ARNT-independent, induction of the AP-1 transcription factor jun-D which resulted in transcriptional up-regulation of cyclin A expression and thereby deregulation of cell cycle control. In 5L cells, TCDD inhibits proliferation, even though Ser474 phosphorylation of TIF1β is up-regulated, and cyclin A is not induced, probably as a consequence of a lack of jun-D induction in these cells [Weiss et al., 2008].

In one of the 30-min experiments, the TIF1β target gene and binding partner of cyclin A, *Cdc2*/CDK1, exhibited an increased phosphorylation of its Tyr15 residue (3.8, No. 5), a phosphorylation that has been associated with the inactivation of the enzyme and inhibition of cell cycle progression [Ferrari, 2006]. This observation appears consistent with the induction of the G1/S cell cycle block consistently observed in TCDD-exposed 5L cells

although this block, which has been attributed to the induction of the cyclin-dependent kinase inhibitor p27/Kip1 [Kolluri et al., 1999], does not become manifest until a few hours later [Göttlicher et al., 1990], [Sarioglu et al., 2006].

Moreover, in one of the 2-h experiments, a down-regulation of Ser33 phosphorylation of the RNA binding protein "RNA-binding motif, single-stranded-interacting protein 2" (*Rbms2*)was observed (Table 3.8, No. 6). Almost no information is available on the rat protein, but for the human ortholog, which is also known as "Suppressor of CDC2 with RNA-binding motif 3" (SCR3), evidence has been obtained that it may be involved in the regulation of *Cdc2*/CDK1 translation [Kanaoka and Nojima, 1994]. The potential implications of these phosphorylation changes of *Cdc2*/CDK1 and RNA-binding motif, single-stranded-interacting protein 2, which clearly require experimental confirmation, for the function of *Cdc2*/CDK1 in TCDD-exposed cells remain to be determined.

RD RNA binding protein (Rdbp protein/ *Rdbp*)

A further interaction partner of TIF1β with TCDD-altered phosphorylation detected in the present study was the protein "RD RNA binding protein", the ortholog of the human protein "Negative elongation factor E" (NELF-E) or "RD RNA binding protein". The protein exhibited a regulation factor of its Ser115 phosphorylation of 1.12 in one of the experiments with 30 min TCDD exposure and highly significant increases at both 1 and 2 hours (Table 3.8, No. 7a). In addition, Ser51 phosphorylation was increased in one experiment each at the latter time points (Table 3.8, No. 7b). Western blotting experiments showed that these up-regulations were not due to TCDD-induced increases in total protein levels.

The phosphorylation of these serine residues had not been described before for the rat but observed in several large scale phosphoproteomics studies for the human ortholog NELF-E for both Ser115 and Ser51 [Beausoleil et al., 2004], [Olsen et al., 2006], [Wang et al., 2008], [Gauci et al., 2009], [Oppermann et al., 2009]) and Ser51 [Imami et al., 2008], [Mayya et al., 2009]. NELF-E is an essential component of a complex known as "negative elongation factor" (NELF) which is involved in the regulation of transcript elongation by RNA polymerase II during transcription, an important target of mechanisms regulating gene expression in response to exogenous stimuli [Peterlin and Price, 2006]. Shortly after initiation, NELF acts in concert with another negative transcription elongation factor, the "DRB (5,6-dichloro-1-beta-D-ribofuranosylbenzimidazole)-sensitivity inducing factor" (DSIF), to repress transcript elon-

gation by trapping the elongation complex near the promoter, a process referred to as "promoter-proximal pausing". This NELF-induced transcription suppression has been proposed to provide a window of time for proper coordination of transcript processing [Fujinaga et al., 2004]. Knockdown of NELF-E resulted in a 3- to 4-fold increase of AhR mRNA expression indicating a role of the NELF complex in the negative regulation of the expression of a basic component of the AhR signalling pathway [Narita et al., 2007]. Phosphorylation of DSIF and NELF-E by the "positive transcription elongation factor b" (P-TEFb) kinase complex transforms DSIF into a positive elongation factor and releases NELF from the RNA thereby reversing the NELF/DSIF-induced transcriptional pausing and initiating transcript elongation. Serine residues 181, 185, 187, and 191 of NELF-E, which are located N-terminal to its RNA recognition motif domain (positions 247 to 342), have been identified as targets for phosphorylation by P-TEFb [Fujinaga et al., 2004]. Interestingly, P-TEFb has been shown to physically interact with the TCDD-liganded AhR which binds to the cyclinT subunit of P-TEFb and recruits P-TEFb to the *cyp1A1* promoter [Tian et al., 2003] resulting in the phosphorylation of the C-terminal domain of RNA polymerase II to enable transcript elongation.

The present results now show that Ser51 and Ser115 phosphorylation of the rat homologue of NELF-E can be modulated by exogenous factors. They further suggest that increases in the phosphorylation of these sites by an unknown kinase may contribute to the positive regulation of transcription elongation of AhR target genes by the TCDD-liganded AhR. At present, there are only few mammalian genes for which a regulation by a NELF-mediated transcriptional pausing mechanism has been clearly established. These include the early immediate genes *c-fos*, *tis-11* and *junB* suggesting an important role of NELF in the regulation of a subset of inducible genes [Aida et al., 2006]. That TCDD positively affects the expression of early immediate genes expression has been shown, among others, for Hepa-1 mouse hepatoma cells, where TCDD increased the mRNA levels for *c-fos* and *junB* as well as for *c-jun* and *junD* [Puga et al., 1992], [Hoffer et al., 1996]. In 5L cells, TCDD stimulated the expression of *c-jun* mRNA and protein [Weiss et al., 2005]. In the present study, the NELF-E- regulated immediate early gene product "Butyrate response factor 1" (also known as Zinc finger protein 36, C3H1 type-like 1, *Zfp36l1*), a further nucleic acid binding protein, was one of the proteins with elevated phosphorylation at 60 min in one experiment (Table 3.8, No. 8). Since no further phosphorylated or non-phosphorylated peptide was identified it remained open to question whether this up-regulation was caused

by an increased expression of this early immediate gene or by a specific stimulation of its Ser54 phosphorylation which had been observed before [Moser and White, 2006].

It also appears possible that the increase in NELF-E phosphorylation by TCDD contributes to an enhanced mRNA processing of TCDD-regulated genes as NELF is also involved in 3' end transcript processing [Narita et al., 2007]. Intriguingly, NELF-E, but none of the other NELF subunits, has been reported to bind to CBP80, a subunit of the nuclear cap binding complex (CBC), another RNA binding protein complex [Narita et al., 2007]. CBP80 is the human ortholog of "Nuclear cap-binding protein subunit 1" (*Ncbp1*), a protein identified in one of the 2 h experiments to exhibit a doubling of phosphorylation at Ser7 following TCCD exposure of the cells (Table 3.8, No. 9). The Ser7 residue is located within the bipartite nuclear localization signal of CBP80 and its phosphorylation may thus promote its translocation to the nucleus. It has been shown that NELF and CBC function together in the 3' end processing of histone mRNAs and, probably, other types of RNA. Knockdown of CBP80 resulted in a decrease of ARNT mRNA expression by ∼50%, implicating both the functional NELF holocomplex and its interaction partner CBC in the regulation of the expression of basic components of the AHR signalling pathway [Narita et al., 2007]. The observation of the simultaneous up-regulation of specific phosphorylations of the two directly interacting proteins NELF-E and CBP80 by TCDD supports the assumption that TCDD modulates RNA synthesis and transcript processing by interfering with the phosphorylation of specific components of the NELF and the CBC complexes.

Mediator of RNA polymerase II transcription subunit 24 (Thyroid hormone receptor associated protein 4, isoform CRA_a/ *Med24*)

A further novel observation on the interaction of TCDD with the transcription machinery is the increased phosphorylation at Ser879 of the protein "Mediator of RNA polymerase II transcription subunit 24" (*Med24*) or "Thyroid hormone receptor associated protein 4, isoform CRA_a" (Table 3.8, No. 10). This protein is a component of the so-called "Mediator of RNA polymerase II complex" ("Mediator"). Mediator is a multisubunit coactivator complex involved in the regulation of gene expression of nearly all RNA polymerase II-dependent genes. It also conveys information from sequence-specific bound transcriptional activators and repressors to the RNA polymerase II (PolII) pre-initiation complex in the regulated transcription of specific genes [Conaway et al., 2005]. Intriguingly, Wang et al. (2004) showed that the Mediator complex physically associates with the ligand-bound AhR

and MED220 (a subunit of the Mediator complex). The complex is recruited to the enhancer of the CYP1A1 gen, but not to the promoter [Wang et al., 2004]. Our present results suggest that the TCDD-induced interaction between the Mediator complex and the AhR is accompanied by the phosphorylation of "Thyroid hormone receptor associated protein 4" at Ser879, but the relation between "Thyroid hormone receptor associated protein 4" phosphorylation and Mediator recruitment is still currently unclear. It appears likely, however, that this phosphorylation is involved in the stimulation of AhR/ARNT-mediated gene expression by TCDD.

Ataxin-2 (ATXN2/*Atxn2*)

A further transcriptional regulator exhibiting a TCDD-induced phosphorylation change was Ataxin-2 for which the down-regulation of a peptide doubly phosphorylated at two closely spaced serine residues, Ser511 and 515, by a factor of ∼0.6 was observed in one of the experiments with 2 hours TCDD exposure (Table 3.8, No. 11). Recently, it has been shown that Ataxin-2 acts as a co-regulator of a KRAB-containing zinc-finger transcriptional regulator known as "BRCA1-interacting protein with a KRAB domain 1" and that the interaction of the two proteins results in the activation of the transcription of the *sca2* gene [Hallen et al., 2011]. In addition to its function as a transcriptional co-regulator, the gene product of *Atxn2* appears to function in RNA metabolism and endocytosis. The functional relevance of the Ser511/515 phosphorylation, which had not been described so far, is still unclear.

4.2.4 Regulators of small GTPases of the Ras superfamily

An unexpected outcome of the present study was the presence of six proteins functionally involved in signalling events mediated by small GTPases of the Ras superfamily within the group of proteins with TCDD-altered phosphorylation. These GTPases can occur in an active GTP-bound form and an inactive GDP-bound form and their activity is controlled by a variety of activating guanine nucleotide exchange factors (GEFs) which exchange GDP by GTP, and GTPase-activating proteins (GAPs) which promote the inactivation of the protein by GTP hydrolysis [Geyer and Wittinghofer, 1997]. In their active states, small GTPases bind to a plethora of downstream effector proteins to regulate cellular responses.

Regulators of Rho GTPases

The identified proteins include three effectors of GTPases of the Rho family (Pragmin, Src homology 3 domain-containing guanine nucleotide exchange factor (*Sgef*) and Cdc42 effector protein 1 (*Cdc42ep1*)). Rho GTPases play key roles in cytoskeletal dynamics and regulate a wide range of morphogenetic events, such as cell adhesion, cell migration, cell spreading, vesicle trafficking, cytokinesis and endocytosis [Etienne-Manneville and Hall, 2002]. They can also control many other functions, such as cell-cycle progression and gene expression.

Pragmin (*Pragmin*)

Pragmin ("pragma of Rho family GTPase 2") exhibited a statistically significant down-regulation of its phosphorylation at Tyr391 after 1 h of TCDD exposure (Table 3.8, No. 12). The protein is a specific effector protein of Rho family GTPase 2, a member of the Rnd subfamily of Rho GTPases which has been implicated in the reorganisation of the actin cytoskeleton and subsequent morphological changes in various cells. The human ortholog of Pragmin is termed Tyrosine-protein kinase SgK223. SgK223 was identified as a Src substrate in metastatic human SW620 colorectal carcinoma cells [Leroy et al., 2009] and furthermore it has been reported, Pragmin was phosphorylated by Src at Tyr391, the observed phosphorylation site affected by TCDD in the present study. Expression of Pragmin Y391F, in which the tyrosine was replaced by phenylalanine, had a reduced rescuing effect on invasiveness in cells with reduced SgK223 implicating phosphorylation of Tyr391 in invasive signalling [Leroy et al., 2009]. This function of the gene product of *Pragmin* is consistent with the reorganisation of the actin cytoskeleton for which strong evidence had been obtained in previous quantitative proteomic studies on 5L cells exposed to TCCD [Sarioglu et al., 2006], [Sarioglu et al., 2008]. Preliminary studies on 5L cells did not provide evidence for an alteration of Src activity by TCDD (see below) suggesting that the observed down-regulation of Tyr391 phosphorylation of Pragmin is mediated by another mechanism.

Similar to Src homology 3 domain-containing guanine nucleotide exchange factor (*Sgef*)

The protein "Similar to Src homology 3 domain-containing guanine nucleotide exchange factor" (*Sgef*) exhibited significantly decreased phosphorylation of its serine residue 390

by a factor of ∼0.6 in the 2-h experiments (Table 3.8, No. 13). This phosphorylation site corresponds to Ser392, one of two known phosphorylation sites identified for the human ortholog known as Rho guanine nucleotide exchange factor 26 [Mayya et al., 2009]. This protein has been shown to be a GEF involved in the regulation of Rho protein signal transduction [Qi et al., 2003]. It specifically activates RhoG GTPase [Ellerbroek et al., 2004], an upstream regulator of other Rho GTPases. Rho guanine nucleotide exchange factor 26 is known to be required for actin remodelling and the formation of membrane ruffles during macropinocytosis [Ellerbroek et al., 2004], which in most cells is transient and occurs downstream of growth factor receptor activation.

At present there is no information on the functional role of the Ser390 phosphorylation. This phosphorylation site is located relatively close to the N-terminal end of the Dbl-homologous (DH) domain (residues 438-619, NCBI Reference Sequence XP_227201.4), the conserved catalytic core of most Rho GEF proteins, and the conservation of this phosphorylation site in the rat and human sequences suggests that it is important for the activity of the protein.

Cdc42 effector protein 1 (*Cdc42ep1*)

Cdc42 effector protein 1 (*Cdc42ep1*), also known as Binder of Rho GTPases 5, exhibited a down-regulation of its Ser193 phosphorylation by a factor of ∼0.6 at 2 h in one experiment (Table 3.8, No. 14). Whereas nothing is known about the rat protein, the human ortholog has been shown to be an effector protein of the product of the CDC42 gene, Cell division control protein 42 homolog, a plasma membrane-associated small GTPase [Joberty et al., 1999], [Burbelo et al., 1999]. Cdc42 effector protein 1 was suggested to function as a negative regulator of Rho GTPase signalling and to affect the organization of the actin cytoskeleton at the plasma membrane resulting in an inhibition of cell spreading [Joberty et al., 1999]. At present, nothing is known about the functional consequences of Ser193 phosphorylation of Cdc42 effector protein 1 of the rat.

Regulators of Rab GTPases

The altered phosphorylation-containing regulators of the activity of small GTPases also included three proteins involved in the regulation of Rab GTPase family members, namely Hematological and neurological expressed 1 protein, DENN/MADD domain containing 5A, and Rab GTPase activating protein 1. Rab familiy GTPases are recognized as premier

organizers of intracellular transport and membrane trafficking pathways in eukaryotic cells [Zerial and McBride, 2001].

Hematological and neurological expressed 1 protein (*Hn1*)

The protein "Hematological and neurological expressed 1 protein" (*Hn1*) was found to show a significantly increased phosphorylation of its Ser82 residue by a factor of ∼1.5 after 2 h of TCDD exposure (Table 3.8, No. 15). This phosphorylation of the rat protein has not yet been reported, but that of the corresponding site in the human ortholog, Ser87, has been observed in several studies [Imami et al., 2008], [Zahedi et al., 2008], [Dephoure et al., 2008], [Zougman and Wiśniewski, 2006], [Mayya et al., 2009]. The gene product of (*Hn1*) is highly conserved among species and widely expressed in numerous tissues during embryonic development [Zhou et al., 2004] and tissue regeneration [Zujovic et al., 2005]. Laughlin et al. (2009) observed an increased association of the small GTPase Ras-related protein Rab-27A with actin as a consequence of the knockdown of Hematological and neurological expressed 1 protein indicating an effect of this protein on cytoskeleton-associated functions [Laughlin et al., 2009]. In comparative microarray analyses of human normal ovarian surface epithelial tissue and ovarian carcinoma, it was identified as one of four genes whose expression perfectly distinguished tumor samples from normal ones [Lu et al., 2004]. Laughlin et al. (2009) also reported that in mouse melanoma cells, knock down of the expression of the protein resulted in a suppression of cell proliferation as evidenced by a G1/S cell cycle arrest. Although the precise function of the protein is unknown, these observations collectively point to a role in promoting growth and maintaining an undifferentiated or dedifferentiated state for cell development and repair. The functional importance of the Ser82 phosphorylation is still unknown, but it may be related to TCDD-induced alterations in cell cycle regulation or cytoskeleton remodelling.

DENN/MADD domain containing 5A (Dennd5a protein/ *Dennd5a*)

The protein "DENN/MADD domain containing 5A" (Dennd5a protein/ *Dennd5a*) was identified to exhibit an up-regulated Ser193 phosphorylation in one of the experiments with 1 h exposure to TCDD (Table 3.8, No. 16). Studies on the mouse homolog identified this protein as a binding partner of the GTP-bound small GTPase Rab-6 [Janoueix-Lerosey et al., 1995] on Golgi membranes [Miserey-Lenkei et al., 2007]. By recruiting various effectors, Rab-6 GTPase regulates vesicle trafficking at the level of the Golgi apparatus. DENN/MADD domain containing 5A also binds to active Rab11 sug-

gesting that it coordinates the functions of Rab-6 and Rab-11 in retrograde transport events between the Golgi complex and recycling endosomes and possibly at mitosis and during cytokinesis.

The phosphorylation of Ser193 had not yet been reported for the rat protein but for the human ortholog which is also known as rab6-interacting protein 1. It constitutes the only posttranslational modification of this protein described so far [Dephoure et al., 2008]. The functional importance of this phosphorylation is unknown and it remains to be determined whether TCDD affects Rab-6/Rab-11 interaction.

Rab GTPase activating protein 1 (*Rabgap1*)

RAB GTPase activating protein 1 (*Rabgap1*) was a further direct interactor of Rab-6 with a phosphorylation change in TCDD-exposed cells. It exhibited a down-regulation of its Thr38 phosphorylation by a factor of ∼0.5 in one of the experiments with 2 h exposure (Table 3.8, No. 17). For the human orthologue of this protein, evidence has been obtained that it acts as a GTPase-activating protein (GAP) of the two known Rab-6 isoforms Rab-6A and Rab-6A' which differ by only three amino acids [Echard et al., 2000] and that it plays a role in microtubule nucleation by the centrosome [Cuif et al., 1999]. Rab GTPase activating protein 1 has been also suggested to specifically act as an effector of Rab-6A' and thereby to participate in a Rab-6A'-mediated pathway required for metaphase-anaphase transition during mitosis [Miserey-Lenkei et al., 2006]. The Thr38 phosphorylation observed as down-regulated by TCDD represents a novel phosphorylation site Rab GTPase activating protein 1 with currently no clues with respect to its function.

Taken together, the present observations on the phosphorylation changes of six proteins involved in the regulation of the activity of small GTPases of the Rho and Rab families provide novel evidence that the pronounced effects of TCDD on the actin cytoskeleton and actin-associated proteins previously observed in 5L cells [Sarioglu et al., 2006], [Sarioglu et al., 2008] may be initiated by early alterations of signalling cascades resulting in altered Rho GTPase signalling rather than by TCDD-elicited alterations in gene expression. However, since e.g. the Rho family of GTPases also mediates changes in gene expression and cell division that are independent of the actin cytoskeleton it appears possible that other, still unknown actions of TCDD may be initiated by an early interference of TCDD with these GTPases. The upstream events triggered by TCDD and resulting in the altered phosphorylations of the small GTPase regulators are still unknown.

4.2.5 UBX domain-containing proteins

The proteins with phosphorylations up-regulated by TCDD also included two members of the family of ubiquitin regulatory X (UBX) domain-containing proteins, namely UBX domain-containing protein 4 and an uncharacterised protein predicted to be the product of the *ubxn7* gene, i.e. UBX domain-containing protein 7. UBX proteins, the functions of which are largely unknown, are characterized by the presence of a UBX domain that has recently been identified to mediate the binding to the molecular chaperone p97/valosin-containing protein (VCP), also known as Cell division control protein 48 in yeast [Alexandru et al., 2008]. p97 is a highly conserved ATPase performing a variety of functions in all types of cells. It is assumed that it provides the main driving force for the extraction of misfolded or unassembled proteins in the endoplasmic reticulum (ER) to the cytoplasm for degradation by the proteasome by the ER-associated protein degradation (ERAD) pathway [Ye, 2006].

UBX domain-containing protein 4 (*Ubxn4*)

UBX domain-containing protein 4, also known as erasin, exhibited an up-regulation of a hitherto unknown Thr156 phosphorylation that was observed for both the 1-h and the 2-h exposure period (Table 3.8, No. 18). It is a UBX-only protein lacking the ubiquitin-associated (UBA) domain contained in many other UBX domain-containing proteins and, thus, the ability to bind ubiquitinated proteins directly [Alexandru et al., 2008]. The ER membrane-associated UBX domain-containing protein 4 plays a central role in the ERAD pathway [Lim et al., 2009]. It has been suggested to act as a scaffold ensuring the ordered transfer of the protein destined for degradation from the ER lumen to the proteasome. The potential role of the Thr156 phosphorylation which is located in the large N-terminal cytoplasmic portion of the protein in this process is unknown, but the observed phosphorylation change suggests that TCDD might somehow affect ERAD. In this context it is noteworthy that the ER is also a TCDD target as there is evidence that TCDD activates inositol 1,4,5-trisphosphate (IP3) receptors in the ER resulting in the release of Ca^{2+} from the ER into the cytoplasm and facilitating the downstream activation of AhR receptor target genes [Monteiro et al., 2008]. Recent studies have shown that the IP3 receptors, which function as Ca^{2+} release channels in the ER, are immediately destroyed via the ERAD pathway following activation in order to reduce the sensitivity of ER Ca^{2+} stores to IP3 and, probably, to protect the cells against deleterious effects of over-activation of Ca^{2+} signalling pathways [Wojcikiewicz et al., 2009]. Although it is presently pure speculation, it appears

conceivable that the increase in Thr156 phosphorylation of UBX domain-containing protein 4 by TCDD may be functionally associated with the stimulation of the ERAD-dependent degradation of IP3 receptors following their activation by TCDD.

UBX domain-containing protein 7 (*Ubxn7*)

For UBX domain-containing protein 7, the other UBX protein with altered phosphorylation identified after TCDD treatment, two splice isoforms had been observed at the mRNA level for the rat, and the affected phosphorylation which was up-regulated by a factor of ∼1.9 in one of the 30-min experiments corresponds to Ser267 and Ser289 of the two forms (Table 3.8, No. 19). For the human ortholog of the protein, this site corresponds to Ser288 the phosphorylation of which has been identified in several large-scale studies, see e.g., [Kim et al., 2005]. UBX domain-containing protein 7, like UBX domain-containing protein 4, has been reported to interact with p97 [Alexandru et al., 2008]. It can directly associate with ubiquitin conjugates via its UBA domain as well as with the E3 CUL2/VHL ubiquitin ligase complex and recruit them to p97 for delivery of the ubiquitin conjugate to the proteasome for degradation [Alexandru et al., 2008] in an ERAD-independent way. A specific p97/UBX domain-containing protein 7 substrate is hypoxia-inducible factor 1α (HIF1α), the transcriptional key regulator of cellular responses to hypoxia. Under hypoxic conditions, HIF1α forms a heterodimer with ARNT which binds to an enhancer termed hypoxia response element (HRE) which mediates the induction of HIF1α target genes. Activation of AhR/ARNT signalling by TCDD during hypoxia has been shown to interfere with HIF1α/ARNT gene activation thereby reducing the expression of HIF1α target genes. Several studies have shown that this negative crosstalk cannot be explained by a competition of AhR and HIF1α for ARNT [Pollenz et al., 1999], [Tomita et al., 2000]. Intriguingly, TCDD has been reported to cause a AhR-dependent destabilization of HIF1α protein and proteasomal degradation [Seifert et al., 2008]. The present observation of an increased phosphorylation of UBX domain-containing protein 7 in TCDD-exposed cells therefore points to a potential hitherto unknown mechanism linking AhR activation and p97/UBX domain-containing protein 7-dependent HIF1α degradation.

4.2.6 Miscellaneous proteins

Protein chibby homolog 1 (*Cby1*)

The protein "protein chibby homolog 1", also known as "Chibby" or PIGEA-14, exhibited a down-regulation of the phosphorylation of its Ser20 residue by a factor of 0.65 in one of the 2 h experiments (Table 3.8, No. 20). The protein is highly conserved throughout evolution and has been shown to play a role in regulating the intracellular trafficking of the calcium permeable cation channel polycystin-2/PKD2 and possibly other intracellular proteins [Hidaka et al., 2004]. In addition, it acts as an inhibitor of the Wnt/β-catenin pathway by binding to the transcriptional coactivator β-catenin and inhibiting β-catenin-mediated transcriptional activation through competition with Tcf/Lef transcription factors [Takemaru et al., 2003]. In Zebrafish, TCDD has been shown to activate Wnt/β-catenin signalling by down-regulating the expression of another β-catenin binding inhibitor of Tcf/Lef activation, SOX-9 [Mathew et al., 2009]. Intriguingly, the Ser20 phosphorylation of Chibby observed as down-regulated in the present study has been recently identified to mediate the binding of 14-3-3 proteins to Chibby resulting in cytoplasmic sequestration of the tripartite 14-3-3 / Chibby / β-catenin complex and inhibition of Wnt signalling [Li et al., 2008]. Down-regulation of Ser20 phosphorylation which is catalyzed by nuclear-targeted Akt kinase would therefore be expected to result in increased nuclear localisation of β-catenin and Wnt signalling activation. It will be interesting to see whether the Chibby phosphorylation change, which clearly requires confirmation in future experiments, might be involved in a misregulation of Wnt / β-catenin signalling by TCDD in mammalian cells.

Similar to AHNAK nucleoprotein isoform 1 isoform 2 (*Ahnak*)

Highly significant increases in phosphorylation were seen after both 1 and 2 h of TCDD exposure for a serine residue of a protein designated "similar to AHNAK nucleoprotein isoform 1 isoform 2" (Table 3.8, No. 21). The hyperphosphorylated residue corresponded to Ser212 of the human ortholog whose phosphorylation at this site had been reported already [Moritz et al., 2010]. The fact that the abundance of none of the further 26 phosphorylated AHNAK peptides identified in the present study was changed by TCDD indicates that the up-regulation of Ser212 phosphorylation was not related to an increase in AHNAK total protein abundance. AHNAK1 is a giant scaffold protein that is expressed in numerous tissues and established cell lines. It is thought to play a key role in calcium signalling. It has been reported to interact with intracellular

regulatory $\beta 2$ and $\beta 1$ subunits of L-type voltage-gated calcium channels ($Ca_v 1.2$ channels) in cardiomyocytes [Haase et al., 1999], [Hohaus et al., 2002], [Alvarez et al., 2004]. Simultaneous phosphorylation of the C-terminal domain of membrane-associated AHNAK1 and the $\beta 2$ subunit by cAMP-dependent protein kinase A (PKA) in response to β-adrenoreceptor stimulation has been proposed to result in an increased Ca^{2+} influx [Alvarez et al., 2004],[Haase et al., 1999]. Recent studies have shown that AHNAK1 is also a key element regulating the Ca^{2+} influx through L-type voltage-gated calcium channels in nonexcitable cells, such as T cells [Matza et al., 2008], [Matza and Flavell, 2009] and osteoblastic cells [Shao et al., 2009]. Moreover, AHNAK has been shown to bind to intracellular Ca^{2+} binding S100B proteins and annexin 2 and thereby to regulate actin cytoskeleton organization and cell membrane cytoarchitecture [Benaud et al., 2004]. AHNAK contains a large number of phosphorylation sites, but besides PKA, only protein kinase B (PKB) has been identified to be involved in AHNAK phosphorylation [Sussman et al., 2001]. Phosphorylation of Ser5335 in the C-terminal domain of human AHNAK by PKB results in the translocation of AHNAK from the nucleus to the plasma membrane. The simultaneous interaction of the central repetitive motifs of AHNAK1 with protein kinase C-α and phospholipase C-$\gamma 1$ (PLC $\gamma 1$) has been shown to cause the activation of PKC which in turn results in the activation of cPLA2, the formation of arachidonic acid, the concerted activation of PLC-$\gamma 1$ by AHNAK and arachidonic acid and intracellular calcium mobilization [Sekiya et al., 1999], [Lee et al., 2004], [Lee et al., 2008]. The Ser212 residue that was found hyperphosphorylated in TCDD-exposed 5L cells and is located in the N-terminal structural domain. This domain has been predicted to contain a PDZ domain [Komuro et al., 2004], a specialized protein module believed to interact with C-terminal peptides of a number of channel proteins, including those involved in calcium transport [Kim and Sheng, 2004]. The precise function of this PDZ domain as well as that of the Ser212 phosphorylation is still unknown, but it appears possible that the altered phosphorylation of the N-terminal domain may result in altered recruitment of yet unknown regulators/modifiers of AHNAK activity. In view of the crucial role of AHNAK in the regulation of Ca^{2+} entry and signalling in various cell types it was tempting to speculate that the significant and reproducible increase in Ser212 phosphorylation by TCDD might be functionally associated with the increase in cytoplasmic Ca^{2+} concentration by TCDD [Le Ferrec et al., 2002], [N'Diaye et al., 2006]. However, further experiments showed that this is unlikely to be the case, since several inhibitors of L-type voltage-gated Ca^{2+} channels did not prevent the induction of CYP1A1 protein whereas 2-APB, an inhibitor of

store-operated Ca^{2+} channels, completely prevented CYP1A1 up-regulation. Thus, the functional significance of this phosphorylation and its alteration by TCDD remains to be determined.

Interferon-inducible double stranded RNA-dependent protein kinase activator A (*Prkra*)

"Interferon-inducible double stranded RNA-dependent protein kinase activator A" (*Prkra*) exhibited a significant up-regulation of its Ser18 residue in two of the 1-h experiments (Table 3.8, No. 22). The protein and its mouse and human orthologs are products of the Rax and PACT genes, respectively and are regulators of the latent protein kinase R (PKR). Activation of PRKRA can be caused by cytokines, modification of growth factor supply, disruption of intracellular Ca^{2+} homeostasis and oxidative stress, but the nature of the stress-activated protein kinase(s) involved is still not completely clear. Phosphorylation of the mouse ortholog of the protein kinase activator at Ser18, a residue conserved between human, mouse and rat, has recently been shown to be required for PKR activation and inhibition of translation initiation [Bennett et al., 2004]. In contrast, Ser18 phosphorylation was found not essential for the stress-induced activation of the human ortholog [Peters et al., 2006], and at present it is unknown whether it is essential for the activating activity of the rat protein and the inhibition of protein synthesis initiation. As Peters et al. pointed out, it remains possible that different kinds of stresses can activate the enzyme through phosphorylation of different residues, a paradigm established for the activation of various transcription factors. Interestingly, inhibition of translation due to interference with growth factor signalling does occur in TCDD-exposed 5L cells (U. Andrae, personal communication), but so far this inhibition has been only observed at later time points ($\geq$ 6 h) and it remains open to question whether it is related to the increase in Ser18 phosphorylation of Interferon-inducible double stranded RNA-dependent protein kinase activator A.

LYRIC (MTDH/ *Mtdh*)

The protein LYRIC, also known as metadherin (MTDH) or, in case of the human ortholog, "Astrocyte Elevated Gene 1 protein" (AEG-1), was a further protein which showed a significant up-regulation of a specific phosphorylation (Ser297) in both experiments with 2 h TCDD exposure (3.8, No. 23). AEG-1 functions as a transforming oncogene that is overexpressed in all cancers analyzed so far [Emdad et al., 2009] and has been strongly im-

plicated in the promotion of multiple biochemical and signalling pathways leading to cell transformation and tumor progession in diverse organs [Sarkar et al., 2009]. The protein mediates the transforming activity of oncogenic Ha-Ras and c-Myc, and its overexpression has been shown to activate PI3K/Akt, nuclear factor kappa B (NF-kappa-B), MAP kinase and Wnt/β-catenin pathways to stimulate cell survival, proliferation, invasion, metastasis, and angiogenesis. The phosphorylation at Ser297 had not yet been described for the rat but has been observed in several large-scale phosphoproteomics studies for the mouse protein [Villen et al., 2007], [Zhou et al., 2008] and the corresponding Ser298 residue of the human ortholog MTDH/AEG 1 [Olsen et al., 2006], [Dephoure et al., 2008], [Zahedi et al., 2008], [Gauci et al., 2009], [Mayya et al., 2009]. As for other posttranslational modifications of LYRIC/AEG-1, it is currently unknown how Ser297 phosphorylation influences the function of this oncogenic protein [Hu et al., 2009] and what the consequences of the TCDD-induced up-regulation for the cells might be.

Chapter 5

Conclusions

The present study has identified about 30 proteins exhibiting a statistically significantly altered phosphorylation in at least two independent experiments for a given time point or a regulation factor of at least 1.5 in a single experiment following exposure of 5L rat hepatoma cells to TCDD for 0.5 to 2 hours.

For all of the phosphorylation changes identified, the affected phosphorylation site within the protein was unambiguously identified. With the exception of the increased phosphorylation of the MAP kinase p38alpha, none of the phosphorylation changes, which appear to precede alterations in the expression of AhR/ARNT target genes at the protein level, had been described before. For a few of the observed alterations, such as the increased Ser77 phosphorylation of ARNT, the increased Ser474 phosphorylation of TIF1β or the decreased Ser20 phosphorylation of Chibby, the consequences of the changes appear to be predictable. However, for the majority of changes the functional importance with respect to the action of TCDD and the resulting consequences for the dioxin's toxicity remain to be elucidated. This is due to the facts that several of the affected phosphorylation sites have been identified for the first time and that for those phosphorylations that had already been observed in other studies the functional importance has not yet been investigated.

No TCDD-induced phosphorylation changes associated with nongenomic actions of TCDD already reported for certain other cell systems were observed. This may be a consequence of the limited resolving power of the mass spectrometric method used for the analysis of the highly complex protein samples. It could, however, also reflect certain specific features discriminating the 5L cells from other cells used in earlier studies on nongenomic effects of TCDD. On the other hand, the study identified phosphorylation changes of various other proteins, in particular proteins involved in the regulation of transcription as

well as proteins from other functional classes, such as various regulators of small GTPases or proteins involved in protein degradation pathways. These proteins or their phosphorylation changes had not been associated with the action of TCDD previously and they appear to mediate early, hitherto unknown nongenomic actions of the dioxin. The present study therefore provides a large number of novel starting points for further detailed investigations of the signalling events involved in the early actions of TCDD in mammalian cells and the consequences with respect to the mechanisms underlying the toxicity of dioxins. In future studies, the resolution capacity of the experimental approach may be enhanced by further refinement of the experimental protocol, such as the incorporation of cell fractionation steps, optimization of the phosphopeptide enrichment protocol and the implementation of ETD fragmentation and gas phase fractionation into the MS analysis step.

Bibliography

[Abrink et al., 2001] Abrink, M., Ortiz, J. A., Mark, C., Sanchez, C., Looman, C., Hellman, L., Chambon, P., and Losson, R. (2001). Conserved interaction between distinct krüppel-associated box domains and the transcriptional intermediary factor 1 beta. *Proc Natl Acad Sci U S A*, 98(4):1422–6.

[Aida et al., 2006] Aida, M., Chen, Y., Nakajima, K., Yamaguchi, Y., Wada, T., and Handa, H. (2006). Transcriptional pausing caused by nelf plays a dual role in regulating immediate-early expression of the junb gene. *Mol Cell Biol*, 26(16):6094–104.

[Aittokallio, 2010] Aittokallio, T. (2010). Dealing with missing values in large-scale studies: microarray data imputation and beyond. *Brief Bioinform*, 11(2):253–64.

[Albrecht et al., 2010] Albrecht, D., Kniemeyer, O., Brakhage, A. A., and Guthke, R. (2010). Missing values in gel-based proteomics. *Proteomics*, 10(6):1202–11.

[Alexander et al., 2006] Alexander, L. D., Ding, Y., Alagarsamy, S., Cui, X.-L., and Douglas, J. G. (2006). Arachidonic acid induces erk activation via src sh2 domain association with the epidermal growth factor receptor. *Kidney Int*, 69(10):1823–32.

[Alexandru et al., 2008] Alexandru, G., Graumann, J., Smith, G. T., Kolawa, N. J., Fang, R., and Deshaies, R. J. (2008). Ubxd7 binds multiple ubiquitin ligases and implicates p97 in hif1alpha turnover. *Cell*, 134(5):804–16.

[Alvarez et al., 2004] Alvarez, J., Hamplova, J., Hohaus, A., Morano, I., Haase, H., and Vassort, G. (2004). Calcium current in rat cardiomyocytes is modulated by the carboxyl-terminal ahnak domain. *J Biol Chem*, 279(13):12456–61.

[Andersen et al., 2009] Andersen, C. A., Gotta, S., Magnoni, L., Raggiaschi, R., Kremer, A., and Terstappen, G. C. (2009). Robust ms quantification method for phosphopeptides using 18o/16o labeling. *BMC Bioinformatics*, 10:141.

[Andersson et al., 1987] Andersson, L., Sulkowski, E., and Porath, J. (1987). Purification of commercial human albumin on immobilized ida-ni2+. *J Chromatogr*, 421(1):141–6.

[Barouki et al., 2007] Barouki, R., Coumoul, X., and Fernandez-Salguero, P. M. (2007). The aryl hydrocarbon receptor, more than a xenobiotic-interacting protein. *FEBS Lett*, 581(19):3608–15.

[Beausoleil et al., 2004] Beausoleil, S. A., Jedrychowski, M., Schwartz, D., Elias, J. E., Villén, J., Li, J., Cohn, M. A., Cantley, L. C., and Gygi, S. P. (2004). Large-scale characterization of hela cell nuclear phosphoproteins. *Proc Natl Acad Sci U S A*, 101(33):12130–5.

[Beischlag et al., 2008] Beischlag, T. V., Luis Morales, J., Hollingshead, B. D., and Perdew, G. H. (2008). The aryl hydrocarbon receptor complex and the control of gene expression. *Crit Rev Eukaryot Gene Expr*, 18(3):207–50.

[Benaud et al., 2004] Benaud, C., Gentil, B. J., Assard, N., Court, M., Garin, J., Delphin, C., and Baudier, J. (2004). Ahnak interaction with the annexin 2/s100a10 complex regulates cell membrane cytoarchitecture. *J Cell Biol*, 164(1):133–44.

[Benjamini and Hochberg, 1995] Benjamini, Y. and Hochberg, Y. (1995). Controlling the false discovery rate: a practical and powerful approach to multiple testing. *Journal of the Royal Statistical Society*, 57(1):289–300.

[Bennett et al., 2004] Bennett, R. L., Blalock, W. L., and May, W. S. (2004). Serine 18 phosphorylation of rax, the pkr activator, is required for pkr activation and consequent translation inhibition. *J Biol Chem*, 279(41):42687–93.

[Biemann, 1988] Biemann, K. (1988). Contributions of mass spectrometry to peptide and protein structure. *Biomed Environ Mass Spectrom*, 16(1-12):99–111.

[Bootman et al., 2002] Bootman, M. D., Collins, T. J., Mackenzie, L., Roderick, H. L., Berridge, M. J., and Peppiatt, C. M. (2002). 2-aminoethoxydiphenyl borate (2-apb) is a reliable blocker of store-operated ca2+ entry but an inconsistent inhibitor of insp3-induced ca2+ release. *FASEB J*, 16(10):1145–50.

[Börsch-Haubold et al., 1998] Börsch-Haubold, A. G., Bartoli, F., Asselin, J., Dudler, T., Kramer, R. M., Apitz-Castro, R., Watson, S. P., and Gelb, M. H. (1998). Identification

of the phosphorylation sites of cytosolic phospholipase a2 in agonist-stimulated human platelets and hela cells. *J Biol Chem*, 273(8):4449–58.

[Börsch-Haubold et al., 1997] Börsch-Haubold, A. G., Kramer, R. M., and Watson, S. P. (1997). Phosphorylation and activation of cytosolic phospholipase a2 by 38-kda mitogen-activated protein kinase in collagen-stimulated human platelets. *Eur J Biochem*, 245(3):751–9.

[Boutros et al., 2004] Boutros, P. C., Moffat, I. D., Franc, M. A., Tijet, N., Tuomisto, J., Pohjanvirta, R., and Okey, A. B. (2004). Dioxin-responsive ahre-ii gene battery: identification by phylogenetic footprinting. *Biochem Biophys Res Commun*, 321(3):707–15.

[Bunger et al., 2008] Bunger, M. K., Glover, E., Moran, S. M., Walisser, J. A., Lahvis, G. P., Hsu, E. L., and Bradfield, C. A. (2008). Abnormal liver development and resistance to 2,3,7,8-tetrachlorodibenzo-p-dioxin toxicity in mice carrying a mutation in the dna-binding domain of the aryl hydrocarbon receptor. *Toxicol Sci*, 106(1):83–92.

[Burbelo et al., 1999] Burbelo, P. D., Snow, D. M., Bahou, W., and Spiegel, S. (1999). Mse55, a cdc42 effector protein, induces long cellular extensions in fibroblasts. *Proc Natl Acad Sci U S A*, 96(16):9083–8.

[Canga et al., 1988] Canga, L., Levi, R., and Rifkind, A. B. (1988). Heart as a target organ in 2,3,7,8-tetrachlorodibenzo-p-dioxin toxicity: decreased beta-adrenergic responsiveness and evidence of increased intracellular calcium. *Proc Natl Acad Sci U S A*, 85(3):905–9.

[Chang et al., 2008] Chang, C.-W., Chou, H.-Y., Lin, Y.-S., Huang, K.-H., Chang, C.-J., Hsu, T.-C., and Lee, S.-C. (2008). Phosphorylation at ser473 regulates heterochromatin protein 1 binding and corepressor function of tif1beta/kap1. *BMC Mol Biol*, 9:61.

[Chapman, 1996] Chapman, J. R. (1996). Mass spectrometry. ionization methods and instrumentation. *Methods Mol Biol*, 61:9–28.

[Clark et al., 1991] Clark, J. D., Lin, L. L., Kriz, R. W., Ramesha, C. S., Sultzman, L. A., Lin, A. Y., Milona, N., and Knopf, J. L. (1991). A novel arachidonic acid-selective cytosolic pla2 contains a ca(2+)-dependent translocation domain with homology to pkc and gap. *Cell*, 65(6):1043–51.

[Coleman and Smith, 2001] Coleman, K. M. and Smith, C. L. (2001). Intracellular signaling pathways: nongenomic actions of estrogens and ligand-independent activation of estrogen receptors. *Front Biosci*, 6:D1379–91.

[Conaway et al., 2005] Conaway, J. W., Florens, L., Sato, S., Tomomori-Sato, C., Parmely, T. J., Yao, T., Swanson, S. K., Banks, C. A. S., Washburn, M. P., and Conaway, R. C. (2005). The mammalian mediator complex. *FEBS Lett*, 579(4):904–8.

[Cui and Churchill, 2003] Cui, X. and Churchill, G. A. (2003). Statistical tests for differential expression in cdna microarray experiments. *Genome Biol*, 4(4):210.

[Cuif et al., 1999] Cuif, M. H., Possmayer, F., Zander, H., Bordes, N., Jollivet, F., Couedel-Courteille, A., Janoueix-Lerosey, I., Langsley, G., Bornens, M., and Goud, B. (1999). Characterization of gapcena, a gtpase activating protein for rab6, part of which associates with the centrosome. *EMBO J*, 18(7):1772–82.

[de la Fuente van Bentem et al., 2008] de la Fuente van Bentem, S., Mentzen, W. I., de la Fuente, A., and Hirt, H. (2008). Towards functional phosphoproteomics by mapping differential phosphorylation events in signaling networks. *Proteomics*, 8(21):4453–4465.

[Dephoure et al., 2008] Dephoure, N., Zhou, C., Villén, J., Beausoleil, S. A., Bakalarski, C. E., Elledge, S. J., and Gygi, S. P. (2008). A quantitative atlas of mitotic phosphorylation. *Proc Natl Acad Sci U S A*, 105(31):10762–7.

[Dietrich et al., 2002] Dietrich, C., Faust, D., Budt, S., Moskwa, M., Kunz, A., Bock, K.-W., and Oesch, F. (2002). 2,3,7,8-tetrachlorodibenzo-p-dioxin-dependent release from contact inhibition in wb-f344 cells: involvement of cyclin a. *Toxicol Appl Pharmacol*, 183(2):117–26.

[Do and Choi, 2006] Do, J. H. and Choi, D.-K. (2006). Normalization of microarray data: single-labeled and dual-labeled arrays. *Mol Cells*, 22(3):254–61.

[Dong and Matsumura, 2008] Dong, B. and Matsumura, F. (2008). Roles of cytosolic phospholipase a2 and src kinase in the early action of 2,3,7,8-tetrachlorodibenzo-p-dioxin through a nongenomic pathway in mcf10a cells. *Mol Pharmacol*, 74(1):255–63.

[Driggers and Segars, 2002] Driggers, P. H. and Segars, J. H. (2002). Estrogen action and cytoplasmic signaling pathways. part ii: the role of growth factors and phosphorylation in estrogen signaling. *Trends Endocrinol Metab*, 13(10):422–7.

[Dunlap et al., 2002] Dunlap, D. Y., Ikeda, I., Nagashima, H., Vogel, C. F. A., and Matsumura, F. (2002). Effects of src-deficiency on the expression of in vivo toxicity of tcdd in a strain of c-src knockout mice procured through six generations of backcrossings to c57bl/6 mice. *Toxicology*, 172(2):125–41.

[Durr et al., 2004] Durr, E., Yu, J., Krasinska, K. M., Carver, L. A., Yates, J. R., Testa, J. E., Oh, P., and Schnitzer, J. E. (2004). Direct proteomic mapping of the lung microvascular endothelial cell surface in vivo and in cell culture. *Nat Biotechnol*, 22(8):985–92.

[Echard et al., 2000] Echard, A., Opdam, F. J., de Leeuw, H. J., Jollivet, F., Savelkoul, P., Hendriks, W., Voorberg, J., Goud, B., and Fransen, J. A. (2000). Alternative splicing of the human rab6a gene generates two close but functionally different isoforms. *Mol Biol Cell*, 11(11):3819–33.

[Elferink et al., 2001] Elferink, C. J., Ge, N. L., and Levine, A. (2001). Maximal aryl hydrocarbon receptor activity depends on an interaction with the retinoblastoma protein. *Mol Pharmacol*, 59(4):664–73.

[Ellerbroek et al., 2004] Ellerbroek, S. M., Wennerberg, K., Arthur, W. T., Dunty, J. M., Bowman, D. R., DeMali, K. A., Der, C., and Burridge, K. (2004). Sgef, a rhog guanine nucleotide exchange factor that stimulates macropinocytosis. *Mol Biol Cell*, 15(7):3309–19.

[Emdad et al., 2009] Emdad, L., Lee, S.-G., Su, Z. Z., Jeon, H. Y., Boukerche, H., Sarkar, D., and Fisher, P. B. (2009). Astrocyte elevated gene-1 (aeg-1) functions as an oncogene and regulates angiogenesis. *Proc Natl Acad Sci U S A*, 106(50):21300–5.

[Enan and Matsumura, 1995] Enan, E. and Matsumura, F. (1995). Evidence for a second pathway in the action mechanism of 2,3,7,8-tetrachlorodibenzo-p-dioxin (tcdd). significance of ah-receptor mediated activation of protein kinase under cell-free conditions. *Biochem Pharmacol*, 49(2):249–61.

[Essader et al., 2005] Essader, A. S., Cargile, B. J., Bundy, J. L., and Stephenson, Jr, J. L. (2005). A comparison of immobilized ph gradient isoelectric focusing and strong-cation-exchange chromatography as a first dimension in shotgun proteomics. *Proteomics*, 5(1):24–34.

[Etienne-Manneville and Hall, 2002] Etienne-Manneville, S. and Hall, A. (2002). Rho gtpases in cell biology. *Nature*, 420(6916):629–35.

[Fenn et al., 1989] Fenn, J. B., Mann, M., Meng, C. K., Wong, S. F., and Whitehouse, C. M. (1989). Electrospray ionization for mass spectrometry of large biomolecules. *Science*, 246(4926):64–71.

[Fernandez-Salguero et al., 1996] Fernandez-Salguero, P. M., Hilbert, D. M., Rudikoff, S., Ward, J. M., and Gonzalez, F. J. (1996). Aryl-hydrocarbon receptor-deficient mice are resistant to 2,3,7,8-tetrachlorodibenzo-p-dioxin-induced toxicity. *Toxicol Appl Pharmacol*, 140(1):173–9.

[Ferrari, 2006] Ferrari, S. (2006). Protein kinases controlling the onset of mitosis. *Cell Mol Life Sci*, 63(7-8):781–95.

[Ficarro et al., 2002] Ficarro, S. B., McCleland, M. L., Stukenberg, P. T., Burke, D. J., Ross, M. M., Shabanowitz, J., Hunt, D. F., and White, F. M. (2002). Phosphoproteome analysis by mass spectrometry and its application to saccharomyces cerevisiae. *Nat Biotechnol*, 20(3):301–5.

[Fujinaga et al., 2004] Fujinaga, K., Irwin, D., Huang, Y., Taube, R., Kurosu, T., and Peterlin, B. M. (2004). Dynamics of human immunodeficiency virus transcription: P-tefb phosphorylates rd and dissociates negative effectors from the transactivation response element. *Mol Cell Biol*, 24(2):787–95.

[Gauci et al., 2009] Gauci, S., Helbig, A. O., Slijper, M., Krijgsveld, J., Heck, A. J. R., and Mohammed, S. (2009). Lys-n and trypsin cover complementary parts of the phosphoproteome in a refined scx-based approach. *Anal Chem*, 81(11):4493–501.

[Ge and Elferink, 1998] Ge, N. L. and Elferink, C. J. (1998). A direct interaction between the aryl hydrocarbon receptor and retinoblastoma protein. linking dioxin signaling to the cell cycle. *J Biol Chem*, 273(35):22708–13.

[Gentleman et al., 2004a] Gentleman, R., Hornik, K., Bates, D. M., Chambers, J., Falcon, S., Iacus, S., Ihaka, R., and Leisch, F. (2004a). R: A language and environment for statistical computing. *R Foundation for Statistical Computing, Vienna, Austria.*

[Gentleman et al., 2004b] Gentleman, R. C., Carey, V. J., Bates, D. M., Bolstad, B., Dettling, M., Dudoit, S., Ellis, B., Gautier, L., Ge, Y., Gentry, J., Hornik, K., Hothorn, T., Huber, W., Iacus, S., Irizarry, R., Leisch, F., Li, C., Maechler, M., Rossini, A. J., Sawitzki, G., Smith, C., Smyth, G., Tierney, L., Yang, J. Y. H., and Zhang, J. (2004b).

Bioconductor: open software development for computational biology and bioinformatics. *Genome Biol*, 5(10):R80.

[Geyer and Wittinghofer, 1997] Geyer, M. and Wittinghofer, A. (1997). Gefs, gaps, gdis and effectors: taking a closer (3d) look at the regulation of ras-related gtp-binding proteins. *Curr Opin Struct Biol*, 7(6):786–92.

[Göttlicher et al., 1990] Göttlicher, M., Cikryt, P., and Wiebel, F. J. (1990). Inhibition of growth by 2,3,7,8-tetrachlorodibenzo-p-dioxin in 5l rat hepatoma cells is associated with the presence of ah receptor. *Carcinogenesis*, 11(12):2205–10.

[Göttlicher and Wiebel, 1991] Göttlicher, M. and Wiebel, F. J. (1991). 2,3,7,8-tetrachlorodibenzo-p-dioxin causes unbalanced growth in 5l rat hepatoma cells. *Toxicol Appl Pharmacol*, 111(3):496–503.

[Gruhler et al., 2005] Gruhler, A., Olsen, J. V., Mohammed, S., Mortensen, P., Faergeman, N. J., Mann, M., and Jensen, O. N. (2005). Quantitative phosphoproteomics applied to the yeast pheromone signaling pathway. *Mol Cell Proteomics*, 4(3):310–27.

[Haase et al., 1999] Haase, H., Podzuweit, T., Lutsch, G., Hohaus, A., Kostka, S., Lindschau, C., Kott, M., Kraft, R., and Morano, I. (1999). Signaling from beta-adrenoceptor to l-type calcium channel: identification of a novel cardiac protein kinase a target possessing similarities to ahnak. *FASEB J*, 13(15):2161–72.

[Hallen et al., 2011] Hallen, L., Klein, H., Stoschek, C., Wehrmeyer, S., Nonhoff, U., Ralser, M., Wilde, J., Röhr, C., Schweiger, M. R., Zatloukal, K., Vingron, M., Lehrach, H., Konthur, Z., and Krobitsch, S. (2011). The krab-containing zinc-finger transcriptional regulator zbrk1 activates sca2 gene transcription through direct interaction with its gene product, ataxin-2. *Hum Mol Genet*, 20(1):104–14.

[Haribabu et al., 1995] Haribabu, B., Hook, S. S., Selbert, M. A., Goldstein, E. G., Tomhave, E. D., Edelman, A. M., Snyderman, R., and Means, A. R. (1995). Human calcium-calmodulin dependent protein kinase i: cdna cloning, domain structure and activation by phosphorylation at threonine-177 by calcium-calmodulin dependent protein kinase i kinase. *EMBO J*, 14(15):3679–86.

[He et al., 2004] He, T., Alving, K., Feild, B., Norton, J., Joseloff, E. G., Patterson, S. D., and Domon, B. (2004). Quantitation of phosphopeptides using affinity chromatography and stable isotope labeling. *J Am Soc Mass Spectrom*, 15(3):363–373.

[Hefner et al., 2000] Hefner, Y., Borsch-Haubold, A. G., Murakami, M., Wilde, J. I., Pasquet, S., Schieltz, D., Ghomashchi, F., Yates, 3rd, J. R., Armstrong, C. G., Paterson, A., Cohen, P., Fukunaga, R., Hunter, T., Kudo, I., Watson, S. P., and Gelb, M. H. (2000). Serine 727 phosphorylation and activation of cytosolic phospholipase a2 by mnk1-related protein kinases. *J Biol Chem*, 275(48):37542–51.

[Hefti et al., 2004] Hefti, M. H., Françoijs, K.-J., de Vries, S. C., Dixon, R., and Vervoort, J. (2004). The pas fold. a redefinition of the pas domain based upon structural prediction. *Eur J Biochem*, 271(6):1198–208.

[Hidaka et al., 2004] Hidaka, S., Könecke, V., Osten, L., and Witzgall, R. (2004). Pigea-14, a novel coiled-coil protein affecting the intracellular distribution of polycystin-2. *J Biol Chem*, 279(33):35009–16.

[Hoffer et al., 1996] Hoffer, A., Chang, C. Y., and Puga, A. (1996). Dioxin induces transcription of fos and jun genes by ah receptor-dependent and -independent pathways. *Toxicol Appl Pharmacol*, 141(1):238–47.

[Hohaus et al., 2002] Hohaus, A., Person, V., Behlke, J., Schaper, J., Morano, I., and Haase, H. (2002). The carboxyl-terminal region of ahnak provides a link between cardiac l-type ca2+ channels and the actin-based cytoskeleton. *FASEB J*, 16(10):1205–16.

[Hohenester et al., 2010] Hohenester, U. M., Ludwig, K., Krieglstein, J., and König, S. (2010). Stepchild phosphohistidine: acid-labile phosphorylation becomes accessible by functional proteomics. *Anal Bioanal Chem*, 397(8):3209–12.

[Hou et al., 2010] Hou, J., Cui, Z., Xie, Z., Xue, P., Wu, P., Chen, X., Li, J., Cai, T., and Yang, F. (2010). Phosphoproteome analysis of rat l6 myotubes using reversed-phase c18 prefractionation and titanium dioxide enrichment. *J Proteome Res*, 9(2):777–88.

[Hu et al., 2009] Hu, G., Wei, Y., and Kang, Y. (2009). The multifaceted role of mtdh/aeg-1 in cancer progression. *Clin Cancer Res*, 15(18):5615–20.

[Huffman et al., 2001] Huffman, J. L., Mokashi, A., Bächinger, H. P., and Brennan, R. G. (2001). The basic helix-loop-helix domain of the aryl hydrocarbon receptor nuclear transporter (arnt) can oligomerize and bind e-box dna specifically. *J Biol Chem*, 276(44):40537–44.

[Hunter, 1995] Hunter, T. (1995). Protein kinases and phosphatases: the yin and yang of protein phosphorylation and signaling. *Cell*, 80(2):225–36.

[IARC, 1997] IARC (1997). Iarc working group on the evaluation of carcinogenic risks to humans: Polychlorinated dibenzo-para-dioxins and polychlorinated dibenzofurans. lyon, france, 4-11 february 1997. *IARC Monogr Eval Carcinog Risks Hum*, 69:1–631.

[Imami et al., 2008] Imami, K., Sugiyama, N., Kyono, Y., Tomita, M., and Ishihama, Y. (2008). Automated phosphoproteome analysis for cultured cancer cells by two-dimensional nanolc-ms using a calcined titania/c18 biphasic column. *Anal Sci*, 24(1):161–6.

[Janoueix-Lerosey et al., 1995] Janoueix-Lerosey, I., Jollivet, F., Camonis, J., Marche, P. N., and Goud, B. (1995). Two-hybrid system screen with the small gtp-binding protein rab6. identification of a novel mouse gdp dissociation inhibitor isoform and two other potential partners of rab6. *J Biol Chem*, 270(24):14801–8.

[Jensen and Larsen, 2007] Jensen, S. S. and Larsen, M. R. (2007). Evaluation of the impact of some experimental procedures on different phosphopeptide enrichment techniques. *Rapid Commun Mass Spectrom*, 21(22):3635–45.

[Joberty et al., 1999] Joberty, G., Perlungher, R. R., and Macara, I. G. (1999). The borgs, a new family of cdc42 and tc10 gtpase-interacting proteins. *Mol Cell Biol*, 19(10):6585–97.

[Käll et al., 2008] Käll, L., Storey, J. D., MacCoss, M. J., and Noble, W. S. (2008). Assigning significance to peptides identified by tandem mass spectrometry using decoy databases. *J Proteome Res*, 7(1):29–34.

[Kalume et al., 2003] Kalume, D. E., Molina, H., and Pandey, A. (2003). Tackling the phosphoproteome: tools and strategies. *Curr Opin Chem Biol*, 7(1):64–69.

[Kanaoka and Nojima, 1994] Kanaoka, Y. and Nojima, H. (1994). Scr: novel human suppressors of cdc2/cdc13 mutants of schizosaccharomyces pombe harbour motifs for rna binding proteins. *Nucleic Acids Res*, 22(13):2687–93.

[Karas and Hillenkamp, 1988] Karas, M. and Hillenkamp, F. (1988). Laser desorption ionization of proteins with molecular masses exceeding 10,000 daltons. *Anal Chem*, 60(20):2299–301.

[Kennedy and Yi, 2008] Kennedy, J. and Yi, E. C. (2008). Use of gas-phase fractionation to increase protein identifications : application to the peroxisome. *Methods Mol Biol*, 432:217–28.

[Kewley and Whitelaw, 2005] Kewley, R. J. and Whitelaw, M. L. (2005). Phosphorylation inhibits dna-binding of alternatively spliced aryl hydrocarbon receptor nuclear translocator. *Biochem Biophys Res Commun*, 338(1):660–7.

[Kim and Sheng, 2004] Kim, E. and Sheng, M. (2004). Pdz domain proteins of synapses. *Nat Rev Neurosci*, 5(10):771–81.

[Kim et al., 2005] Kim, J.-E., Tannenbaum, S. R., and White, F. M. (2005). Global phosphoproteome of ht-29 human colon adenocarcinoma cells. *J Proteome Res*, 4(4):1339–46.

[Klinge et al., 2000] Klinge, C. M., Kaur, K., and Swanson, H. I. (2000). The aryl hydrocarbon receptor interacts with estrogen receptor alpha and orphan receptors coup-tfi and erralpha1. *Arch Biochem Biophys*, 373(1):163–74.

[Kokubu et al., 2005] Kokubu, M., Ishihama, Y., Sato, T., Nagasu, T., and Oda, Y. (2005). Specificity of immobilized metal affinity-based imac/c18 tip enrichment of phosphopeptides for protein phosphorylation analysis. *Anal Chem*, 77(16):5144–54.

[Kolluri et al., 1999] Kolluri, S. K., Weiss, C., Koff, A., and Göttlicher, M. (1999). p27(kip1) induction and inhibition of proliferation by the intracellular ah receptor in developing thymus and hepatoma cells. *Genes Dev*, 13(13):1742–53.

[Komuro et al., 2004] Komuro, A., Masuda, Y., Kobayashi, K., Babbitt, R., Gunel, M., Flavell, R. A., and Marchesi, V. T. (2004). The ahnaks are a class of giant propeller-like proteins that associate with calcium channel proteins of cardiomyocytes and other cells. *Proc Natl Acad Sci U S A*, 101(12):4053–8.

[Kowalewska et al., 2010] Kowalewska, K., Stefanowicz, P., Ruman, T., Fraczyk, T., Rode, W., and Szewczuk, Z. (2010). Electron capture dissociation mass spectrometric analysis of lysine-phosphorylated peptides. *Biosci Rep*, 30(6):433–43.

[Kraemer et al., 1996] Kraemer, S. A., Arthur, K. A., Denison, M. S., Smith, W. L., and DeWitt, D. L. (1996). Regulation of prostaglandin endoperoxide h synthase-2 expression by 2,3,7,8,-tetrachlorodibenzo-p-dioxin. *Arch Biochem Biophys*, 330(2):319–28.

[Larsen et al., 2001] Larsen, M. R., Sørensen, G. L., Fey, S. J., Larsen, P. M., and Roepstorff, P. (2001). Phospho-proteomics: evaluation of the use of enzymatic dephosphorylation and differential mass spectrometric peptide mass mapping for site specific phosphorylation assignment in proteins separated by gel electrophoresis. *Proteomics*, 1(2):223–38.

[Laughlin et al., 2009] Laughlin, K. M., Luo, D., Liu, C., Shaw, G., Warrington, Jr, K. H., Law, B. K., and Harrison, J. K. (2009). Hematopoietic- and neurologic-expressed sequence 1 (hn1) depletion in b16.f10 melanoma cells promotes a differentiated phenotype that includes increased melanogenesis and cell cycle arrest. *Differentiation*, 78(1):35–44.

[Le Ferrec et al., 2002] Le Ferrec, E., Lagadic-Gossmann, D., Rauch, C., Bardiau, C., Maheo, K., Massiere, F., Le Vee, M., Guillouzo, A., and Morel, F. (2002). Transcriptional induction of cyp1a1 by oltipraz in human caco-2 cells is aryl hydrocarbon receptor- and calcium-dependent. *J Biol Chem*, 277(27):24780–7.

[Lee et al., 2008] Lee, I. H., Lim, H. J., Yoon, S., Seong, J. K., Bae, D. S., Rhee, S. G., and Bae, Y. S. (2008). Ahnak protein activates protein kinase c (pkc) through dissociation of the pkc-protein phosphatase 2a complex. *J Biol Chem*, 283(10):6312–20.

[Lee et al., 2004] Lee, I. H., You, J. O., Ha, K. S., Bae, D. S., Suh, P.-G., Rhee, S. G., and Bae, Y. S. (2004). Ahnak-mediated activation of phospholipase c-gamma1 through protein kinase c. *J Biol Chem*, 279(25):26645–53.

[Leroy et al., 2009] Leroy, C., Fialin, C., Sirvent, A., Simon, V., Urbach, S., Poncet, J., Robert, B., Jouin, P., and Roche, S. (2009). Quantitative phosphoproteomics reveals a cluster of tyrosine kinases that mediates src invasive activity in advanced colon carcinoma cells. *Cancer Res*, 69(6):2279–86.

[Levine-Fridman et al., 2004] Levine-Fridman, A., Chen, L., and Elferink, C. J. (2004). Cytochrome p4501a1 promotes g1 phase cell cycle progression by controlling aryl hydrocarbon receptor activity. *Mol Pharmacol*, 65(2):461–9.

[Li et al., 2008] Li, F.-Q., Mofunanya, A., Harris, K., and Takemaru, K.-I. (2008). Chibby cooperates with 14-3-3 to regulate beta-catenin subcellular distribution and signaling activity. *J Cell Biol*, 181(7):1141–54.

[Li and Matsumura, 2008] Li, W. and Matsumura, F. (2008). Significance of the nongenomic, inflammatory pathway in mediating the toxic action of tcdd to induce rapid and long-term cellular responses in 3t3-l1 adipocytes. *Biochemistry*, 47(52):13997–4008.

[Lim et al., 2009] Lim, P. J., Danner, R., Liang, J., Doong, H., Harman, C., Srinivasan, D., Rothenberg, C., Wang, H., Ye, Y., Fang, S., and Monteiro, M. J. (2009). Ubiquilin and p97/vcp bind erasin, forming a complex involved in erad. *J Cell Biol*, 187(2):201–17.

[Lin et al., 2008] Lin, C.-H., Juan, S.-H., Wang, C. Y., Sun, Y.-Y., Chou, C.-M., Chang, S.-F., Hu, S.-Y., Lee, W.-S., and Lee, Y.-H. (2008). Neuronal activity enhances aryl hydrocarbon receptor-mediated gene expression and dioxin neurotoxicity in cortical neurons. *J Neurochem*, 104(5):1415–29.

[Lottspeich and Engels, 2006] Lottspeich, F. and Engels, J. W. (2006). *Bioanalytik*. Springer Berlin Heidelberg New York, 2 edition.

[Lu et al., 2004] Lu, K. H., Patterson, A. P., Wang, L., Marquez, R. T., Atkinson, E. N., Baggerly, K. A., Ramoth, L. R., Rosen, D. G., Liu, J., Hellstrom, I., Smith, D., Hartmann, L., Fishman, D., Berchuck, A., Schmandt, R., Whitaker, R., Gershenson, D. M., Mills, G. B., and Bast, Jr, R. C. (2004). Selection of potential markers for epithelial ovarian cancer with gene expression arrays and recursive descent partition analysis. *Clin Cancer Res*, 10(10):3291–300.

[Malik et al., 2009] Malik, R., Lenobel, R., Santamaria, A., Ries, A., Nigg, E. A., and Körner, R. (2009). Quantitative analysis of the human spindle phosphoproteome at distinct mitotic stages. *J Proteome Res*, 8(10):4553–63.

[Marcotte, 2007] Marcotte, E. M. (2007). How do shotgun proteomics algorithms identify proteins? *Nat Biotechnol*, 25(7):755–7.

[Mathew et al., 2009] Mathew, L. K., Simonich, M. T., and Tanguay, R. L. (2009). Ahr-dependent misregulation of wnt signaling disrupts tissue regeneration. *Biochem Pharmacol*, 77(4):498–507.

[Matsumura, 2009] Matsumura, F. (2009). The significance of the nongenomic pathway in mediating inflammatory signaling of the dioxin-activated ah receptor to cause toxic effects. *Biochem Pharmacol*, 77(4):608–26.

[Matza et al., 2008] Matza, D., Badou, A., Kobayashi, K. S., Goldsmith-Pestana, K., Masuda, Y., Komuro, A., McMahon-Pratt, D., Marchesi, V. T., and Flavell, R. A. (2008). A scaffold protein, ahnak1, is required for calcium signaling during t cell activation. *Immunity*, 28(1):64–74.

[Matza and Flavell, 2009] Matza, D. and Flavell, R. A. (2009). Roles of ca(v) channels and ahnak1 in t cells: the beauty and the beast. *Immunol Rev*, 231(1):257–64.

[Mayya et al., 2009] Mayya, V., Lundgren, D. H., Hwang, S.-I., Rezaul, K., Wu, L., Eng, J. K., Rodionov, V., and Han, D. K. (2009). Quantitative phosphoproteomic analysis of t cell receptor signaling reveals system-wide modulation of protein-protein interactions. *Sci Signal*, 2(84):ra46.

[Mazina et al., 2004] Mazina, O., Park, S., Sano, H., Wong, P., and Matsumura, F. (2004). Studies on the mechanism of rapid activation of protein tyrosine phosphorylation activities, particularly c-src kinase, by tcdd in mcf10a. *J Biochem Mol Toxicol*, 18(6):313–21.

[McCarthy and Smyth, 2009] McCarthy, D. J. and Smyth, G. K. (2009). Testing significance relative to a fold-change threshold is a treat. *Bioinformatics*, 25(6):765–71.

[McConkey et al., 1988] McConkey, D. J., Hartzell, P., Duddy, S. K., Håkansson, H., and Orrenius, S. (1988). 2,3,7,8-tetrachlorodibenzo-p-dioxin kills immature thymocytes by ca2+-mediated endonuclease activation. *Science*, 242(4876):256–9.

[McCormack et al., 1997] McCormack, A. L., Schieltz, D. M., Goode, B., Yang, S., Barnes, G., Drubin, D., and Yates, 3rd, J. R. (1997). Direct analysis and identification of proteins in mixtures by lc/ms/ms and database searching at the low-femtomole level. *Anal Chem*, 69(4):767–76.

[McLachlin and Chait, 2003] McLachlin, D. T. and Chait, B. T. (2003). Improved beta-elimination-based affinity purification strategy for enrichment of phosphopeptides. *Anal Chem*, 75(24):6826–36.

[McNulty and Annan, 2008] McNulty, D. E. and Annan, R. S. (2008). Hydrophilic interaction chromatography reduces the complexity of the phosphoproteome and improves global phosphopeptide isolation and detection. *Mol Cell Proteomics*, 7(5):971–80.

[McNulty and Annan, 2009] McNulty, D. E. and Annan, R. S. (2009). Hydrophilic interaction chromatography for fractionation and enrichment of the phosphoproteome. *Methods Mol Biol*, 527:93–105, x.

[Miserey-Lenkei et al., 2006] Miserey-Lenkei, S., Couëdel-Courteille, A., Del Nery, E., Bardin, S., Piel, M., Racine, V., Sibarita, J.-B., Perez, F., Bornens, M., and Goud, B. (2006). A role for the rab6a' gtpase in the inactivation of the mad2-spindle checkpoint. *EMBO J*, 25(2):278–89.

[Miserey-Lenkei et al., 2007] Miserey-Lenkei, S., Waharte, F., Boulet, A., Cuif, M.-H., Tenza, D., El Marjou, A., Raposo, G., Salamero, J., Héliot, L., Goud, B., and Monier, S. (2007). Rab6-interacting protein 1 links rab6 and rab11 function. *Traffic*, 8(10):1385–403.

[Monteiro et al., 2008] Monteiro, P., Gilot, D., Le Ferrec, E., Rauch, C., Lagadic-Gossmann, D., and Fardel, O. (2008). Dioxin-mediated up-regulation of aryl hydrocarbon receptor target genes is dependent on the calcium/calmodulin/camkialpha pathway. *Mol Pharmacol*, 73(3):769–77.

[Moritz et al., 2010] Moritz, A., Li, Y., Guo, A., Villén, J., Wang, Y., MacNeill, J., Kornhauser, J., Sprott, K., Zhou, J., Possemato, A., Ren, J. M., Hornbeck, P., Cantley, L. C., Gygi, S. P., Rush, J., and Comb, M. J. (2010). Akt-rsk-s6 kinase signaling networks activated by oncogenic receptor tyrosine kinases. *Sci Signal*, 3(136):ra64.

[Mortensen et al., 2009] Mortensen, P., Gouw, J., Olsen, J., Ong, S., Rigbolt, K., Bunkenborg, J., Cox, J., Foster, L., Heck, A., Blagoev, B., Andersen, J., and Mann, M. (2009). Msquant, an open source platform for mass spectrometry-based quantitative proteomics. *J Proteome Res*.

[Moser and White, 2006] Moser, K. and White, F. M. (2006). Phosphoproteomic analysis of rat liver by high capacity imac and lc-ms/ms. *J Proteome Res*, 5(1):98–104.

[Narita et al., 2007] Narita, T., Yung, T. M. C., Yamamoto, J., Tsuboi, Y., Tanabe, H., Tanaka, K., Yamaguchi, Y., and Handa, H. (2007). Nelf interacts with cbc and participates in 3' end processing of replication-dependent histone mrnas. *Mol Cell*, 26(3):349–65.

[N'Diaye et al., 2006] N'Diaye, M., Le Ferrec, E., Lagadic-Gossmann, D., Corre, S., Gilot, D., Lecureur, V., Monteiro, P., Rauch, C., Galibert, M.-D., and Fardel, O. (2006).

Aryl hydrocarbon receptor- and calcium-dependent induction of the chemokine ccl1 by the environmental contaminant benzo[a]pyrene. *The Journal of Biological Chemistry*, 281:19906–19915.

[Neville et al., 1997] Neville, D. C., Rozanas, C. R., Price, E. M., Gruis, D. B., Verkman, A. S., and Townsend, R. R. (1997). Evidence for phosphorylation of serine 753 in cftr using a novel metal-ion affinity resin and matrix-assisted laser desorption mass spectrometry. *Protein Sci*, 6(11):2436–45.

[Olsen et al., 2006] Olsen, J. V., Blagoev, B., Gnad, F., Macek, B., Kumar, C., Mortensen, P., and Mann, M. (2006). Global, in vivo, and site-specific phosphorylation dynamics in signaling networks. *Cell*, 127(3):635–48.

[Olsen and Mann, 2004] Olsen, J. V. and Mann, M. (2004). Improved peptide identification in proteomics by two consecutive stages of mass spectrometric fragmentation. *Proc Natl Acad Sci U S A*, 101(37):13417–22.

[Ong et al., 2002] Ong, S.-E., Blagoev, B., Kratchmarova, I., Kristensen, D. B., Steen, H., Pandey, A., and Mann, M. (2002). Stable isotope labeling by amino acids in cell culture, silac, as a simple and accurate approach to expression proteomics. *Mol Cell Proteomics*, 1(5):376–386.

[Ong et al., 2003a] Ong, S.-E., Foster, L. J., and Mann, M. (2003a). Mass spectrometric-based approaches in quantitative proteomics. *Methods*, 29(2):124–30.

[Ong et al., 2003b] Ong, S.-E., Kratchmarova, I., and Mann, M. (2003b). Properties of 13c-substituted arginine in stable isotope labeling by amino acids in cell culture (silac). *J Proteome Res*, 2(2):173–181.

[Oppermann et al., 2009] Oppermann, F. S., Gnad, F., Olsen, J. V., Hornberger, R., Greff, Z., Kéri, G., Mann, M., and Daub, H. (2009). Large-scale proteomics analysis of the human kinome. *Mol Cell Proteomics*, 8(7):1751–64.

[Palmisano and Thingholm, 2010] Palmisano, G. and Thingholm, T. E. (2010). Strategies for quantitation of phosphoproteomic data. *Expert Rev Proteomics*, 7(3):439–56.

[Park et al., 2006] Park, K.-S., Mohapatra, D. P., Misonou, H., and Trimmer, J. S. (2006). Graded regulation of the kv2.1 potassium channel by variable phosphorylation. *Science*, 313(5789):976–9.

[Peterlin and Price, 2006] Peterlin, B. M. and Price, D. H. (2006). Controlling the elongation phase of transcription with p-tefb. *Mol Cell*, 23(3):297–305.

[Peters et al., 2006] Peters, G. A., Li, S., and Sen, G. C. (2006). Phosphorylation of specific serine residues in the pkr activation domain of pact is essential for its ability to mediate apoptosis. *J Biol Chem*, 281(46):35129–36.

[Pinkse et al., 2004] Pinkse, M. W. H., Uitto, P. M., Hilhorst, M. J., Ooms, B., and Heck, A. J. R. (2004). Selective isolation at the femtomole level of phosphopeptides from proteolytic digests using 2d-nanolc-esi-ms/ms and titanium oxide precolumns. *Anal Chem*, 76(14):3935–43.

[Pitot et al., 1964] Pitot, H. C., Peraino, C., Morse, Jr, P. A., and Potter, V. R. (1964). Hepatomas in tissue culture compared with adapting liver in vivo. *Natl Cancer Inst Monogr*, 13:229–45.

[Pollenz et al., 1999] Pollenz, R. S., Davarinos, N. A., and Shearer, T. P. (1999). Analysis of aryl hydrocarbon receptor-mediated signaling during physiological hypoxia reveals lack of competition for the aryl hydrocarbon nuclear translocator transcription factor. *Mol Pharmacol*, 56(6):1127–37.

[Posewitz and Tempst, 1999] Posewitz, M. C. and Tempst, P. (1999). Immobilized gallium(iii) affinity chromatography of phosphopeptides. *Anal Chem*, 71(14):2883–92.

[Puga et al., 2000] Puga, A., Barnes, S. J., Dalton, T. P., Chang, C. y., Knudsen, E. S., and Maier, M. A. (2000). Aromatic hydrocarbon receptor interaction with the retinoblastoma protein potentiates repression of e2f-dependent transcription and cell cycle arrest. *J Biol Chem*, 275(4):2943–50.

[Puga et al., 1997] Puga, A., Hoffer, A., Zhou, S., Bohm, J. M., Leikauf, G. D., and Shertzer, H. G. (1997). Sustained increase in intracellular free calcium and activation of cyclooxygenase-2 expression in mouse hepatoma cells treated with dioxin. *Biochem Pharmacol*, 54(12):1287–96.

[Puga et al., 1992] Puga, A., Nebert, D. W., and Carrier, F. (1992). Dioxin induces expression of c-fos and c-jun proto-oncogenes and a large increase in transcription factor ap-1. *DNA Cell Biol*, 11(4):269–81.

[Qi et al., 2003] Qi, H., Fournier, A., Grenier, J., Fillion, C., Labrie, Y., and Labrie, C. (2003). Isolation of the novel human guanine nucleotide exchange factor src homology 3 domain-containing guanine nucleotide exchange factor (sgef) and of c-terminal sgef, an n-terminally truncated form of sgef, the expression of which is regulated by androgen in prostate cancer cells. *Endocrinology*, 144(5):1742–52.

[Qian and Huang, 2005] Qian, H.-R. and Huang, S. (2005). Comparison of false discovery rate methods in identifying genes with differential expression. *Genomics*, 86(4):495–503.

[Reinders and Sickmann, 2005] Reinders, J. and Sickmann, A. (2005). State-of-the-art in phosphoproteomics. *Proteomics*, 5(16):4052–61.

[Reiners et al., 1999] Reiners, Jr, J. J., Clift, R., and Mathieu, P. (1999). Suppression of cell cycle progression by flavonoids: dependence on the aryl hydrocarbon receptor. *Carcinogenesis*, 20(8):1561–6.

[Reuber, 1961] Reuber, M. D. (1961). A transplantable bile-secreting hepatocellular carcinoma in the rat. *J Natl Cancer Inst*, 26:891–9.

[Rinschen et al., 2010] Rinschen, M. M., Yu, M.-J., Wang, G., Boja, E. S., Hoffert, J. D., Pisitkun, T., and Knepper, M. A. (2010). Quantitative phosphoproteomic analysis reveals vasopressin v2-receptor-dependent signaling pathways in renal collecting duct cells. *Proc Natl Acad Sci U S A*, 107(8):3882–7.

[Roepstorff and Fohlman, 1984] Roepstorff, P. and Fohlman, J. (1984). Proposal for a common nomenclature for sequence ions in mass spectra of peptides. *Biomed Mass Spectrom*, 11(11):601.

[Rogers and Foster, 2009] Rogers, L. D. and Foster, L. J. (2009). Phosphoproteomics–finally fulfilling the promise? *Mol Biosyst*, 5(10):1122–9.

[Roxas and Li, 2008] Roxas, B. A. P. and Li, Q. (2008). Significance analysis of microarray for relative quantitation of lc/ms data in proteomics. *BMC Bioinformatics*, 9:187.

[Sachs and Hedderich, 2009] Sachs, L. and Hedderich, J. (2009). *Angewandte Statistik*. Springer Berlin Heidelberg New York, Biostatistic, 13th edition.

[Safe, 2001] Safe, S. (2001). Molecular biology of the ah receptor and its role in carcinogenesis. *Toxicol. Lett.*, 120:1–7.

[Sarioglu et al., 2008] Sarioglu, H., Brandner, S., Haberger, M., Jacobsen, C., Lichtmannegger, J., Wormke, M., and Andrae, U. (2008). Analysis of 2,3,7,8-tetrachlorodibenzo-p-dioxin-induced proteome changes in 5l rat hepatoma cells reveals novel targets of dioxin action including the mitochondrial apoptosis regulator vdac2. *Mol Cell Proteomics*, 7(2):394–410.

[Sarioglu et al., 2006] Sarioglu, H., Brandner, S., Jacobsen, C., Meindl, T., Schmidt, A., Kellermann, J., Lottspeich, F., and Andrae, U. (2006). Quantitative analysis of 2,3,7,8-tetrachlorodibenzo-p-dioxin-induced proteome alterations in 5l rat hepatoma cells using isotope-coded protein labels. *Proteomics*, 6(8):2407–21.

[Sarkar et al., 2009] Sarkar, D., Emdad, L., Lee, S.-G., Yoo, B. K., Su, Z.-Z., and Fisher, P. B. (2009). Astrocyte elevated gene-1: far more than just a gene regulated in astrocytes. *Cancer Res*, 69(22):8529–35.

[Schroeder et al., 2004] Schroeder, M. J., Shabanowitz, J., Schwartz, J. C., Hunt, D. F., and Coon, J. J. (2004). A neutral loss activation method for improved phosphopeptide sequence analysis by quadrupole ion trap mass spectrometry. *Anal Chem*, 76(13):3590–8.

[Sciullo et al., 2009] Sciullo, E. M., Dong, B., Vogel, C. F. A., and Matsumura, F. (2009). Characterization of the pattern of the nongenomic signaling pathway through which tcdd-induces early inflammatory responses in u937 human macrophages. *Chemosphere*, 74(11):1531–7.

[Seifert et al., 2008] Seifert, A., Katschinski, D. M., Tonack, S., Fischer, B., and Navarrete Santos, A. (2008). Significance of prolyl hydroxylase 2 in the interference of aryl hydrocarbon receptor and hypoxia-inducible factor-1 alpha signaling. *Chem Res Toxicol*, 21(2):341–8.

[Sekiya et al., 1999] Sekiya, F., Bae, Y. S., Jhon, D. Y., Hwang, S. C., and Rhee, S. G. (1999). Ahnak, a protein that binds and activates phospholipase c-gamma1 in the presence of arachidonic acid. *J Biol Chem*, 274(20):13900–7.

[Shao et al., 2009] Shao, Y., Czymmek, K. J., Jones, P. A., Fomin, V. P., Akanbi, K., Duncan, R. L., and Farach-Carson, M. C. (2009). Dynamic interactions between l-type voltage-sensitive calcium channel cav1.2 subunits and ahnak in osteoblastic cells. *Am J Physiol Cell Physiol*, 296(5):C1067–78.

[Smyth, 2005] Smyth, G. (2005). *Bioinformatics and Computational Biology Solutions using R and Bioconductor*. Springer Berlin Heidelberg New York.

[Smyth and Speed, 2003] Smyth, G. K. and Speed, T. (2003). Normalization of cdna microarray data. *Methods*, 31(4):265–73.

[Sogawa et al., 1995] Sogawa, K., Nakano, R., Kobayashi, A., Kikuchi, Y., Ohe, N., Matsushita, N., and Fujii-Kuriyama, Y. (1995). Possible function of ah receptor nuclear translocator (arnt) homodimer in transcriptional regulation. *Proc Natl Acad Sci U S A*, 92(6):1936–40.

[Sogawa et al., 2004] Sogawa, K., Numayama-Tsuruta, K., Takahashi, T., Matsushita, N., Miura, C., Nikawa, J.-i., Gotoh, O., Kikuchi, Y., and Fujii-Kuriyama, Y. (2004). A novel induction mechanism of the rat cyp1a2 gene mediated by ah receptor-arnt heterodimer. *Biochem Biophys Res Commun*, 318(3):746–55.

[Spahr et al., 2001] Spahr, C. S., Davis, M. T., McGinley, M. D., Robinson, J. H., Bures, E. J., Beierle, J., Mort, J., Courchesne, P. L., Chen, K., Wahl, R. C., Yu, W., Luethy, R., and Patterson, S. D. (2001). Towards defining the urinary proteome using liquid chromatography-tandem mass spectrometry. i. profiling an unfractionated tryptic digest. *Proteomics*, 1(1):93–107.

[Stensballe et al., 2001] Stensballe, A., Andersen, S., and Jensen, O. N. (2001). Characterization of phosphoproteins from electrophoretic gels by nanoscale fe(iii) affinity chromatography with off-line mass spectrometry analysis. *Proteomics*, 1(2):207–22.

[Storey and Tibshirani, 2003] Storey, J. D. and Tibshirani, R. (2003). Statistical significance for genomewide studies. *Proc Natl Acad Sci U S A*, 100(16):9440–5.

[Sussman et al., 2001] Sussman, J., Stokoe, D., Ossina, N., and Shtivelman, E. (2001). Protein kinase b phosphorylates ahnak and regulates its subcellular localization. *J Cell Biol*, 154(5):1019–30.

[Swaney et al., 2008] Swaney, D. L., McAlister, G. C., and Coon, J. J. (2008). Decision tree-driven tandem mass spectrometry for shotgun proteomics. *Nat Methods*, 5(11):959–64.

[Swaney et al., 2009] Swaney, D. L., Wenger, C. D., Thomson, J. A., and Coon, J. J. (2009). Human embryonic stem cell phosphoproteome revealed by electron transfer dissociation tandem mass spectrometry. *Proc Natl Acad Sci U S A*, 106(4):995–1000.

[Syka et al., 2004] Syka, J. E. P., Coon, J. J., Schroeder, M. J., Shabanowitz, J., and Hunt, D. F. (2004). Peptide and protein sequence analysis by electron transfer dissociation mass spectrometry. *Proc Natl Acad Sci U S A*, 101(26):9528–33.

[Takemaru et al., 2003] Takemaru, K.-I., Yamaguchi, S., Lee, Y. S., Zhang, Y., Carthew, R. W., and Moon, R. T. (2003). Chibby, a nuclear beta-catenin-associated antagonist of the wnt/wingless pathway. *Nature*, 422(6934):905–9.

[Tao et al., 2005] Tao, W. A., Wollscheid, B., O'Brien, R., Eng, J. K., Li, X.-j., Bodenmiller, B., Watts, J. D., Hood, L., and Aebersold, R. (2005). Quantitative phosphoproteome analysis using a dendrimer conjugation chemistry and tandem mass spectrometry. *Nat Methods*, 2(8):591–8.

[Thingholm et al., 2009] Thingholm, T. E., Jensen, O. N., and Larsen, M. R. (2009). Analytical strategies for phosphoproteomics. *Proteomics*, 9(6):1451–68.

[Thomas and Brugge, 1997] Thomas, S. M. and Brugge, J. S. (1997). Cellular functions regulated by src family kinases. *Annu Rev Cell Dev Biol*, 13:513–609.

[Tian et al., 2003] Tian, Y., Ke, S., Chen, M., and Sheng, T. (2003). Interactions between the aryl hydrocarbon receptor and p-tefb. sequential recruitment of transcription factors and differential phosphorylation of c-terminal domain of rna polymerase ii at cyp1a1 promoter. *J Biol Chem*, 278(45):44041–8.

[Tian et al., 1999] Tian, Y., Ke, S., Denison, M. S., Rabson, A. B., and Gallo, M. A. (1999). Ah receptor and nf-kappab interactions, a potential mechanism for dioxin toxicity. *J Biol Chem*, 274(1):510–5.

[Tomita et al., 2000] Tomita, S., Sinal, C. J., Yim, S. H., and Gonzalez, F. J. (2000). Conditional disruption of the aryl hydrocarbon receptor nuclear translocator (arnt) gene leads to loss of target gene induction by the aryl hydrocarbon receptor and hypoxia-inducible factor 1alpha. *Mol Endocrinol*, 14(10):1674–81.

[Troyanskaya et al., 2001] Troyanskaya, O., Cantor, M., Sherlock, G., Brown, P., Hastie, T., Tibshirani, R., Botstein, D., and Altman, R. B. (2001). Missing value estimation methods for dna microarrays. *Bioinformatics*, 17(6):520–5.

[Tsai et al., 2008] Tsai, C.-F., Wang, Y.-T., Chen, Y.-R., Lai, C.-Y., Lin, P.-Y., Pan, K.-T., Chen, J.-Y., Khoo, K.-H., and Chen, Y.-J. (2008). Immobilized metal affinity chromatography revisited: ph/acid control toward high selectivity in phosphoproteomics. *J Proteome Res*, 7(9):4058–69.

[Tweedie-Cullen et al., 2009] Tweedie-Cullen, R. Y., Reck, J. M., and Mansuy, I. M. (2009). Comprehensive mapping of post-translational modifications on synaptic, nuclear, and histone proteins in the adult mouse brain. *J Proteome Res*, 8(11):4966–82.

[Van Hoof et al., 2009] Van Hoof, D., Munoz, J., Braam, S. R., Pinkse, M. W. H., Linding, R., Heck, A. J. R., Mummery, C. L., and Krijgsveld, J. (2009). Phosphorylation dynamics during early differentiation of human embryonic stem cells. *Cell Stem Cell*, 5(2):214–226.

[Van Hoof et al., 2007] Van Hoof, D., Pinkse, M. W. H., Oostwaard, D. W.-V., Mummery, C. L., Heck, A. J. R., and Krijgsveld, J. (2007). An experimental correction for arginine-to-proline conversion artifacts in silac-based quantitative proteomics. *Nat Methods*, 4(9):677–678.

[Villen et al., 2007] Villen, J., Beausoleil, S. A., Gerber, S. A., and Gygi, S. P. (2007). Large-scale phosphorylation analysis of mouse liver. *Proc Natl Acad Sci U S A*, 104(5):1488–1493.

[Wang et al., 2008] Wang, B., Malik, R., Nigg, E. A., and Körner, R. (2008). Evaluation of the low-specificity protease elastase for large-scale phosphoproteome analysis. *Anal Chem*, 80(24):9526–33.

[Wang et al., 2004] Wang, S., Ge, K., Roeder, R. G., and Hankinson, O. (2004). Role of mediator in transcriptional activation by the aryl hydrocarbon receptor. *J Biol Chem*, 279(14):13593–600.

[Wasinger et al., 1995] Wasinger, V. C., Cordwell, S. J., Cerpa-Poljak, A., Yan, J. X., Gooley, A. A., Wilkins, M. R., Duncan, M. W., Harris, R., Williams, K. L., and Humphery-Smith, I. (1995). Progress with gene-product mapping of the mollicutes: Mycoplasma genitalium. *Electrophoresis*, 16(7):1090–4.

[Weiss et al., 2005] Weiss, C., Faust, D., Dürk, H., Kolluri, S. K., Pelzer, A., Schneider, S., Dietrich, C., Oesch, F., and Göttlicher, M. (2005). Tcdd induces c-jun expression via a novel ah (dioxin) receptor-mediated p38-mapk-dependent pathway. *Oncogene*, 24(31):4975–83.

[Weiss et al., 2008] Weiss, C., Faust, D., Schreck, I., Ruff, A., Farwerck, T., Melenberg, A., Schneider, S., Oesch-Bartlomowicz, B., Zatloukalová, J., Vondrácek, J., Oesch, F., and Dietrich, C. (2008). Tcdd deregulates contact inhibition in rat liver oval cells via ah receptor, jund and cyclin a. *Oncogene*, 27(15):2198–207.

[Weiss et al., 1996] Weiss, C., Kolluri, S. K., Kiefer, F., and Göttlicher, M. (1996). Complementation of ah receptor deficiency in hepatoma cells: negative feedback regulation and cell cycle control by the ah receptor. *Exp Cell Res*, 226(1):154–63.

[White and Birnbaum, 2009] White, S. S. and Birnbaum, L. S. (2009). An overview of the effects of dioxins and dioxin-like compounds on vertebrates, as documented in human and ecological epidemiology. *J Environ Sci Health C Environ Carcinog Ecotoxicol Rev*, 27(4):197–211.

[Whitelaw et al., 1993] Whitelaw, M., Pongratz, I., Wilhelmsson, A., Gustafsson, J. A., and Poellinger, L. (1993). Ligand-dependent recruitment of the arnt coregulator determines dna recognition by the dioxin receptor. *Mol Cell Biol*, 13(4):2504–14.

[Wiebel et al., 1991] Wiebel, F. J., Klose, U., and Kiefer, F. (1991). Toxicity of 2,3,7,8-tetrachlorodibenzo-p-dioxin in vitro: H4iiec3-derived 5l hepatoma cells as a model system. *Toxicol Lett*, 55(2):161–9.

[Wilkins et al., 1996] Wilkins, M. R., Sanchez, J. C., Gooley, A. A., Appel, R. D., Humphery-Smith, I., Hochstrasser, D. F., and Williams, K. L. (1996). Progress with proteome projects: why all proteins expressed by a genome should be identified and how to do it. *Biotechnol Genet Eng Rev*, 13:19–50.

[Wilm et al., 1996] Wilm, M., Shevchenko, A., Houthaeve, T., Breit, S., Schweigerer, L., Fotsis, T., and Mann, M. (1996). Femtomole sequencing of proteins from polyacrylamide gels by nano-electrospray mass spectrometry. *Nature*, 379(6564):466–9.

[Wojcikiewicz et al., 2009] Wojcikiewicz, R. J. H., Pearce, M. M. P., Sliter, D. A., and Wang, Y. (2009). When worlds collide: Ip(3) receptors and the erad pathway. *Cell Calcium*, 46(3):147–53.

[Xue et al., 2008] Xue, Y., Ren, J., Gao, X., Jin, C., Wen, L., and Yao, X. (2008). Gps 2.0, a tool to predict kinase-specific phosphorylation sites in hierarchy. *Mol Cell Proteomics*, 7(9):1598–608.

[Yang and Bleich, 2004] Yang, F. and Bleich, D. (2004). Transcriptional regulation of cyclooxygenase-2 gene in pancreatic beta-cells. *J Biol Chem*, 279(34):35403–11.

[Yates, 2000] Yates, 3rd, J. R. (2000). Mass spectrometry. from genomics to proteomics. *Trends Genet*, 16(1):5–8.

[Ye, 2006] Ye, Y. (2006). Diverse functions with a common regulator: ubiquitin takes command of an aaa atpase. *J Struct Biol*, 156(1):29–40.

[Ytterberg and Jensen, 2010] Ytterberg, A. J. and Jensen, O. N. (2010). Modification-specific proteomics in plant biology. *J Proteomics*, 73(11):2249–66.

[Zahedi et al., 2008] Zahedi, R. P., Lewandrowski, U., Wiesner, J., Wortelkamp, S., Moebius, J., Schütz, C., Walter, U., Gambaryan, S., and Sickmann, A. (2008). Phosphoproteome of resting human platelets. *J Proteome Res*, 7(2):526–34.

[Zerial and McBride, 2001] Zerial, M. and McBride, H. (2001). Rab proteins as membrane organizers. *Nat Rev Mol Cell Biol*, 2(2):107–17.

[Zhang et al., 2002] Zhang, H., Zha, X., Tan, Y., Hornbeck, P. V., Mastrangelo, A. J., Alessi, D. R., Polakiewicz, R. D., and Comb, M. J. (2002). Phosphoprotein analysis using antibodies broadly reactive against phosphorylated motifs. *J Biol Chem*, 277(42):39379–87.

[Zhang et al., 2001] Zhang, R., Sioma, C. S., Wang, S., and Regnier, F. E. (2001). Fractionation of isotopically labeled peptides in quantitative proteomics. *Anal Chem*, 73(21):5142–9.

[Zhou et al., 2004] Zhou, G., Wang, J., Zhang, Y., Zhong, C., Ni, J., Wang, L., Guo, J., Zhang, K., Yu, L., and Zhao, S. (2004). Cloning, expression and subcellular localization of hn1 and hn1l genes, as well as characterization of their orthologs, defining an evolutionarily conserved gene family. *Gene*, 331:115–23.

[Zhou et al., 2008] Zhou, H., Ye, M., Dong, J., Han, G., Jiang, X., Wu, R., and Zou, H. (2008). Specific phosphopeptide enrichment with immobilized titanium ion affinity

chromatography adsorbent for phosphoproteome analysis. *J Proteome Res*, 7(9):3957–67.

[Zhu et al., 2002] Zhu, H., Pan, S., Gu, S., Bradbury, E. M., and Chen, X. (2002). Amino acid residue specific stable isotope labeling for quantitative proteomics. *Rapid Commun Mass Spectrom*, 16(22):2115–23.

[Zougman and Wiśniewski, 2006] Zougman, A. and Wiśniewski, J. R. (2006). Beyond linker histones and high mobility group proteins: global profiling of perchloric acid soluble proteins. *J Proteome Res*, 5(4):925–34.

[Zujovic et al., 2005] Zujovic, V., Luo, D., Baker, H. V., Lopez, M. C., Miller, K. R., Streit, W. J., and Harrison, J. K. (2005). The facial motor nucleus transcriptional program in response to peripheral nerve injury identifies hn1 as a regeneration-associated gene. *J Neurosci Res*, 82(5):581–91.

Acknowledgments

I wish to thank PD Dr. Ulrich Andrae for excellent supervision throughout the project, both on practical issues and in the writing process. I am grateful for letting me pursue a Ph.D. under his guidance. He provided me with unique opportunities to present my work at international conferences, participate at workshops and allow me the laboratory internship at the Protein Research Group, Southern University Denmark in Odense. My sincere thanks also to Prof. Martin Göttlicher for giving me the opportunity to pursue the Ph.D. at his Institute for Toxicology, Helmholtz Zentrum München.

I am grateful to Prof. Friederike Eckardt-Schupp for representing my graduation at the Institute for Biology, Ludwig-Maximilians University Munich and being my first advisor. Furthermore I would like to thank her for the help during my Ph.D. thesis.

I would like to thank Prof. Barbara Conradt for being my second advisor.

I owe special thank to Prof. Martin R. Larsen for a fantastic stay at the Protein Research Group, Southern University Denmark in Odense and many helpful discussions. I am grateful that he gave me the opportunity to learn different methods for the enrichment of phosphorylated peptides and use the instrumentations in his laboratory.

I also wish to thank Stefanie Brander and Carola Jacobsen, who have introduced me to cell culture and western blot techniques and for the all time support.

I wish to thank Hakan Sarioglu for many helpful discussions and introducing me to different mass spectrometry techniques.

I would like to thank Giuseppe Palmisano, Kasper Engholm-Keller, Lene Jakobsen and A. Jimmy Ytterberg for supporting me in the laboratory and for many helpful discussions.

I would like to thank Peter Mortensen for helping me with MSQuant.

I also wish to thank Cliff Young for proofreading this thesis.

Thanks, to all past and present members of the Institute of Toxicology, Helmholtz Zentrum München: Mark Wormke, Ursula Stosiek, Carmen Spiller, Josef Lichtmannegger, Felix Dulich, Monika Papp, Prof. Daniel Krappmann, Michael Düwel, Bernhard Kloo and Andrea Eitelhuber.

I wish to thank the present and former members of the Protein Research Group: Ileana R. Leon, Sara E. Lendal, Tine E. Tingholm, Veit Schwämmle, Marc Sylvester, James Williamson, Richard Sprenger, Andrea Lorentzen, Helle Marquard Mortensen, Karin Hjernø, Anders Giessing, Angela Pereira da Rocha, Søren Andersen, Alistair Edwards, Benjamin Parker, Laura Lepore, Gerard Such Sanmartin, Thiago Verano Braga, Marcella Nunes de Melo Braga, Fabio C.S. Nogueira and Steffen Bak.

I would especially like to thank my family and friends for their support and believing in me.

Last, but not least, I want to thank Stefan Metzlaff, my boyfriend, for always being there for me.

Curriculum Vitae

Personal Information

Name:	Melanie Schulz
Date of birth:	26.10.1980
Place of birth:	Schwerin

Academic Qualification

2001 - 2006	Biochemistry study, University Leipzig, Germany
2006	Diploma in Biochemistry successfully completed
2006 - 2009	Ph.D. study, Institute of Toxicology, Helmholtz Zentrum München, Germany
2010 - until present	Research Assistant, Department of Biochemistry and Molecular Biology, University of Southern Denmark, Odense, Denmark

Research Experiences

02/2005 – 04/2005	Laboratory course at the Junior Research Group "Protein Engineering", BBZ (Biotechnological-Biomedical Center), Institute of Analytical Chemistry, University of Leipzig, Germany Project title: *Cloning and Expression of the Enzyme EstF1*
10/2005 – 04/2006	Graduation thesis project at the Centre for environmental research (UFZ) in Leipzig, Germany

	Project title: *Analysis of the metabolic regulation of Ps. putida (KT2440) by the change from excess to deficit substrate conditions*
05/2006 - 12/2009	Ph.D. Student at the Institute of Toxicology, Helmholtz Zentrum München, Germany Project title: *Quantitative proteomic analysis of early phosphorylation changes induced by 2,3,7,8-Tetrachlorodibenzo-p-dioxin in 5L rat hepatoma cells*
01/2010 – until present	Department of Biochemistry and Molecular Biology, University of Southern Denmark, Odense, Denmark as a research assistant

Posters at Conferences

06/2009	57th American Society for Mass Spectrometry conference (ASMS) Schulz M, Andrae U, Larsen MR *Evaluation of different fragmentation strategies for mono- and multi-phosphorylated peptides*
06/2010	Cancer Proteomics Schulz M, Andrae U, Larsen MR *Quantitative phosphoproteome analysis for the detection of early alterations of signal transduction by dioxin (TCDD)*
09/2010	9th Human Proteome Organization (HUPO) Conference Schulz M, Palmisano G, Graves Ponsaing G, Kosteljanetz M, Larsen MR, Fischer W *Quantitative Profiling of Sialylated and Phosphorylated Proteins from Brain Tumor Interstitial Fluid* Schulz M, Jakobsen L, Swistowski A, Palmisano G, Engholm-Keller K, Zeng X, Larsen MR *Comprehensive Comparison of the membrane Proteome, Phosphoproteome and Sialiome of Human Embryonic Stem Cells with Human Neuronal Stem Cells*

Appendix A Tables

The Tables 1, 3 and 5 contain the unique peptides identified in at least two biological replicates per time point including IPI and Uniprot accession, protein name (Description), ion score, PTM score, peptide sequence with phosphorylation and other modification assignment, gene name, GO ID and description, KEGG ID, REFSEQ accession, ENSEMBL ID, PFAM accession and ID, the normalized ratio for the different biological replicates and the corresponding mean as well as the p- and q-values.

The Tables 2, 4 and 6 contain the unique peptides identified in only one biological replicate per time point including IPI and Uniprot accession, protein name (Description), ion score, PTM score, peptide sequence with phosphorylation and other modification assignment, gene name, GO ID and description, KEGG ID, REFSEQ accession, ENSEMBL ID, PFAM accession and ID and the normalized ratio.

Table 1: **List of all unique peptides identified in at least two biological replicates in 5L cells after 30 min treatment with TCDD.** A total of 1918 peptides (FDR $p < 1\%$) including 1383 phosphorylated peptides were identified with an ion score of ≥ 20. (Table provided on an accompanying CD)

Table 2: **List of all unique peptides identified in only one biological replicate in 5L cells after 30 min treatment with TCDD.** A total of 3974 peptides (FDR $p < 1\%$) including 2807 phosphorylated peptides were identified with an ion score of ≥ 20. (Table provided on an accompanying CD)

Table 3: **List of all unique peptides identified in at least two biological replicates in 5L cells after 1 hour treatment with TCDD.** A total of 1717 peptides (FDR $p < 1\%$) including 1105 phosphorylated peptides were identified with an ion score of ≥ 20. (Table provided on an accompanying CD)

Table 4: **List of all unique peptides identified in only one biological replicate in 5L cells after 1 hour treatment with TCDD.** A total of 4168 peptides (FDR $p < 1\%$) including 2906 phosphorylated peptides were identified with an ion score of ≥ 20. (Table provided on an accompanying CD)

Table 5: **List of all unique peptides identified in at least two biological replicates in 5L cells after 2 hours treatment with TCDD.** A total of 1069 peptides (FDR $p < 1\%$) including 882 phosphorylated peptides were identified with an ion score of ≥ 20. (Table provided on an accompanying CD)

Table 6: **List of all unique peptides identified in only one biological replicate in 5L cells after 2 hours treatment with TCDD.** A total of 2710 peptides (FDR $p < 1\%$) including 2116 phosphorylated peptides were identified with an ion score of ≥ 20. (Table provided on an accompanying CD)

Table 7: **List of unique identified peptides found regulated at least at one time point.** In total 30 different proteins were identified, which showed alterations of at least one phosphosite after treatment with TCDD for 30 min, 1 hour or 2 hours. The table includes phosphorylated peptides identified as significantly regulated in a minimum of two biological replicates (7 different peptides) per time point as well as peptides found regulated in only one replicate per time point. For every peptide the IPI and Uniprot accession, protein name, peptide sequence with phosphorylation assignment, the phosphosite localization within the protein and the different normalized ratios are shown. (Table provided on an accompanying CD)

Table 8: **List of unique identified regulated phosphopeptides and co-analysed peptides belonging to the same protein.** The table shows the phosphopeptides identified as regulated after TCDD treatment for 30 min, 1 hour or 2 hours and all other peptides belonging to the same protein. For every peptide the IPI accession, protein name and molecular weight, peptide sequence with phosphorylation assignment and the different normalized ratios (median) are shown. (Table provided on an accompanying CD)

Table 9: **Detailed overview of known, "known by similarity" or novel phosphosites identified.** The table shows the phosphopeptides that could be mapped to a Swiss-Prot accession number with the information whether the identified phosphorylation site is known, "known by similarity" or novel. For every peptide the IPI and Swiss-Prot accession, protein name, peptide sequence with phosphorylation assignment and the phosphosite localization within the protein are shown. (Table provided on an accompanying CD)

Appendix B Figures

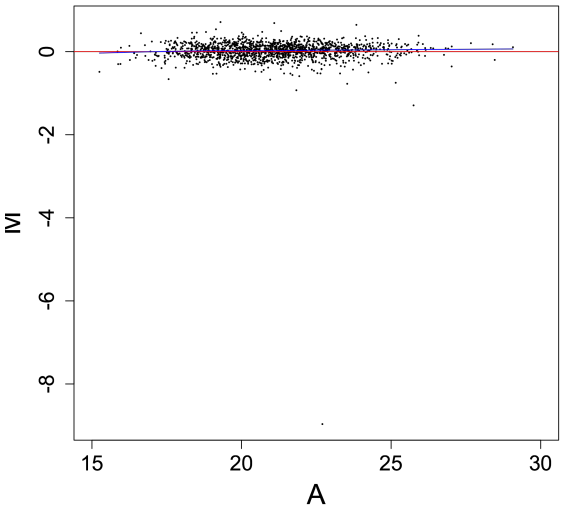

(a) 1 hour DMSO/TCDD; Biological Replicate 1

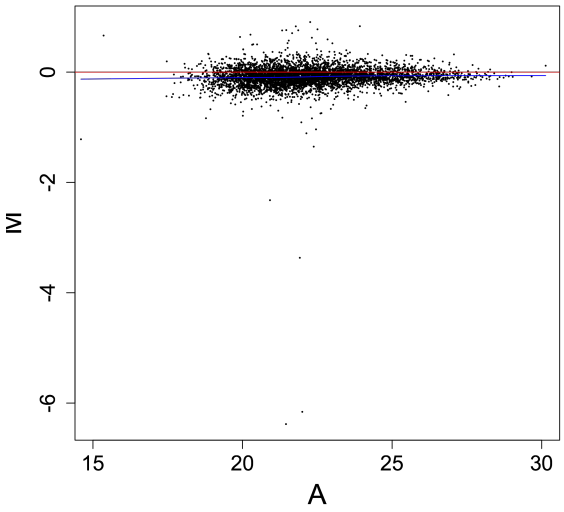

(b) 1 hour DMSO/TCDD; Biological Replicate 2

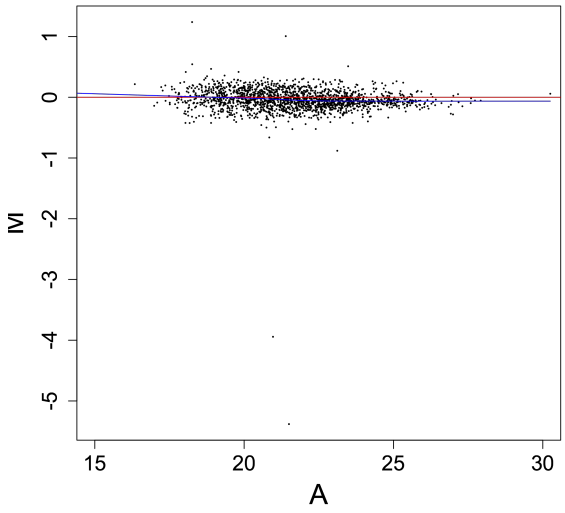

(c) 1 hour DMSO/TCDD; Biological Replicate 3

Figure 1: **MA plots of peptides before normalization from the 1 hour data set.** Unnormalized peptide ratios were plotted as ratios-vs-average (MA) plots. The log2 ratios H/L (y-axis) are plotted against the log2 average of the peptide intensities H (heavy = TCDD treated) and L (light = control). The blue line is a lowess line, the red line indicates y = 0. a), b) and c) show the data for the three different biological replicates obtained after treatment of the cells with DMSO/TCDD for 1 hour.

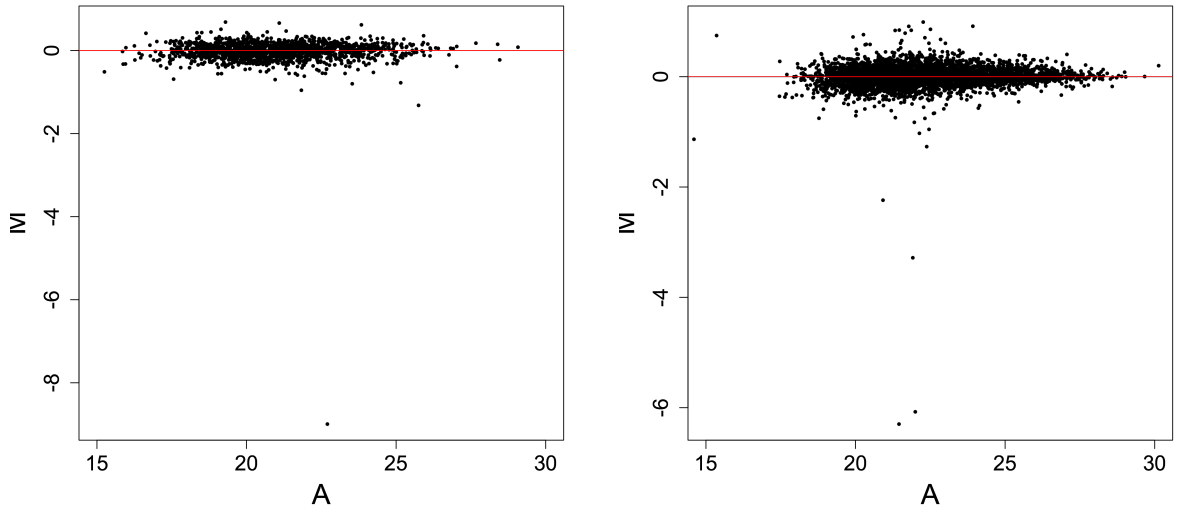

(a) 1 hour DMSO/TCDD; Biological Replicate 1

(b) 1 hour DMSO/TCDD; Biological Replicate 2

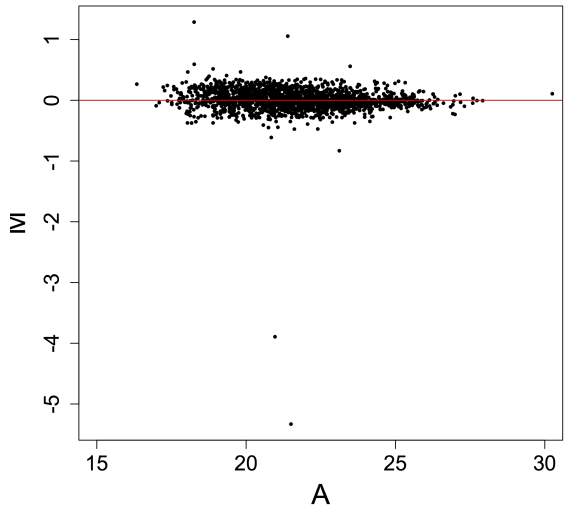

(c) 1 hour DMSO/TCDD; Biological Replicate 3

Figure 2: **MA plots of peptides after normalization from the 1 hour data set.** Normalized peptide ratios were plotted as ratios-vs-average (MA) plots. The log2 ratios H/L (y-axis) are plotted against the log2 average of the peptide intensities H (heavy = TCDD treated) and L (light = control). The red line indicates y = 0. a), b) and c) show the data for the three different biological replicates obtained after treatment of the cells with DMSO/TCDD for 1 hour.

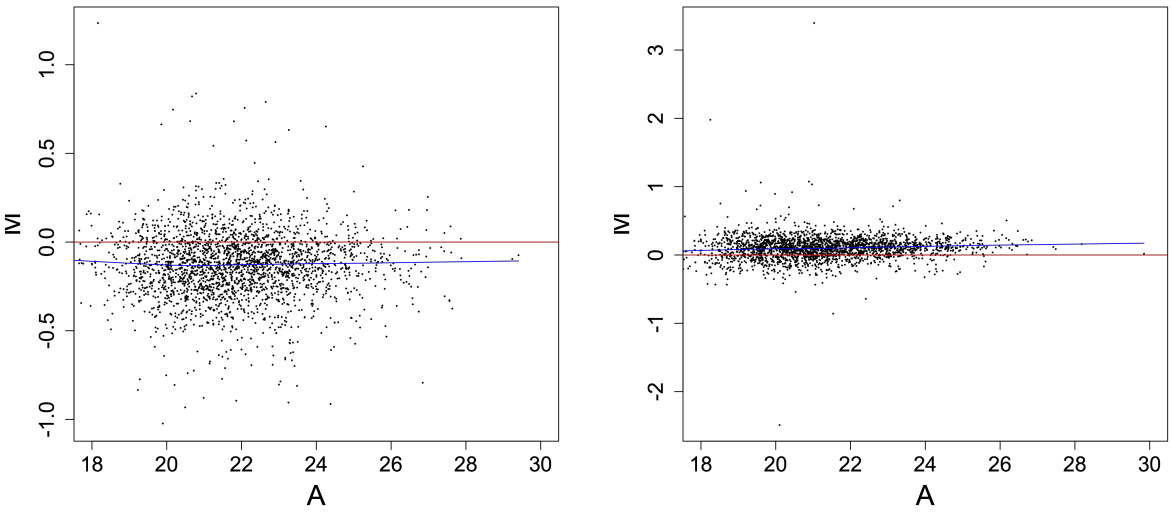

(a) 2 hours DMSO/TCDD; Biological Replicate 1 (b) 2 hours DMSO/TCDD; Biological Replicate 2

Figure 3: **MA plots of peptides before normalization from the 2 hours data set.** Unnormalized peptide ratios were plotted as ratios-vs-average (MA) plots. The log2 ratios H/L (y-axis) are plotted against the log2 average of the peptide intensities H (heavy = TCDD treated) and L (light = control). The blue line is a lowess line, the red line indicates y = 0. a) and b) show the data for the two different biological replicates obtained after treatment of the cells with DMSO/TCDD for 2 hours.

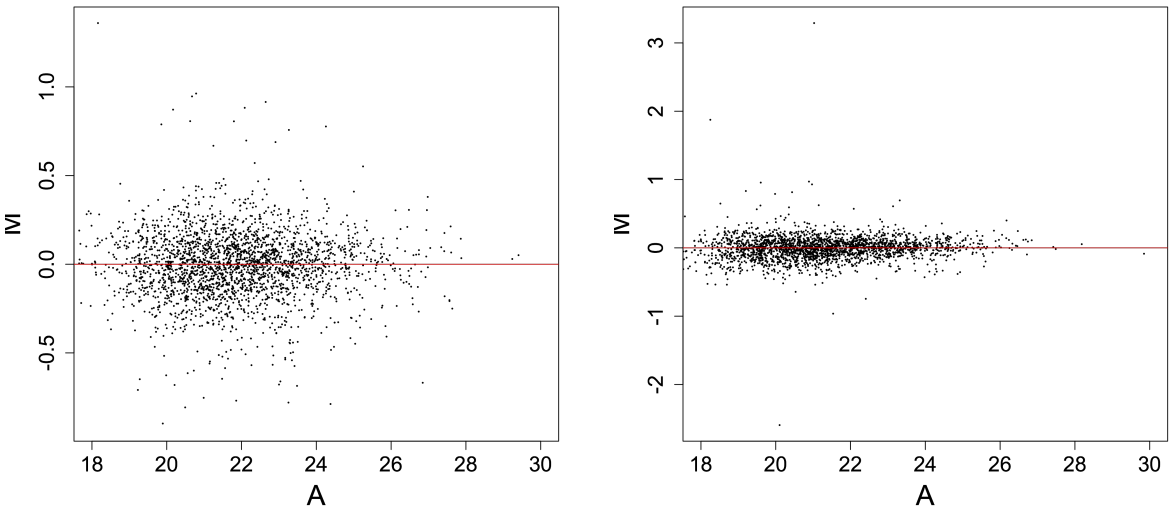

(a) 2 hours DMSO/TCDD; Biological Replicate 1 (b) 2 hours DMSO/TCDD; Biological Replicate 2

Figure 4: **MA plots of peptides after normalization from the 1 hour data set.** Normalized peptide ratios were plotted as ratios-vs-average (MA) plots. The log2 ratios H/L (y-axis) are plotted against the log2 average of the peptide intensities H (heavy = TCDD treated) and L (light = control). The red line indicates y = 0. a) and b) show the data for the two different biological replicates obtained after treatment of the cells with DMSO/TCDD for 2 hours.

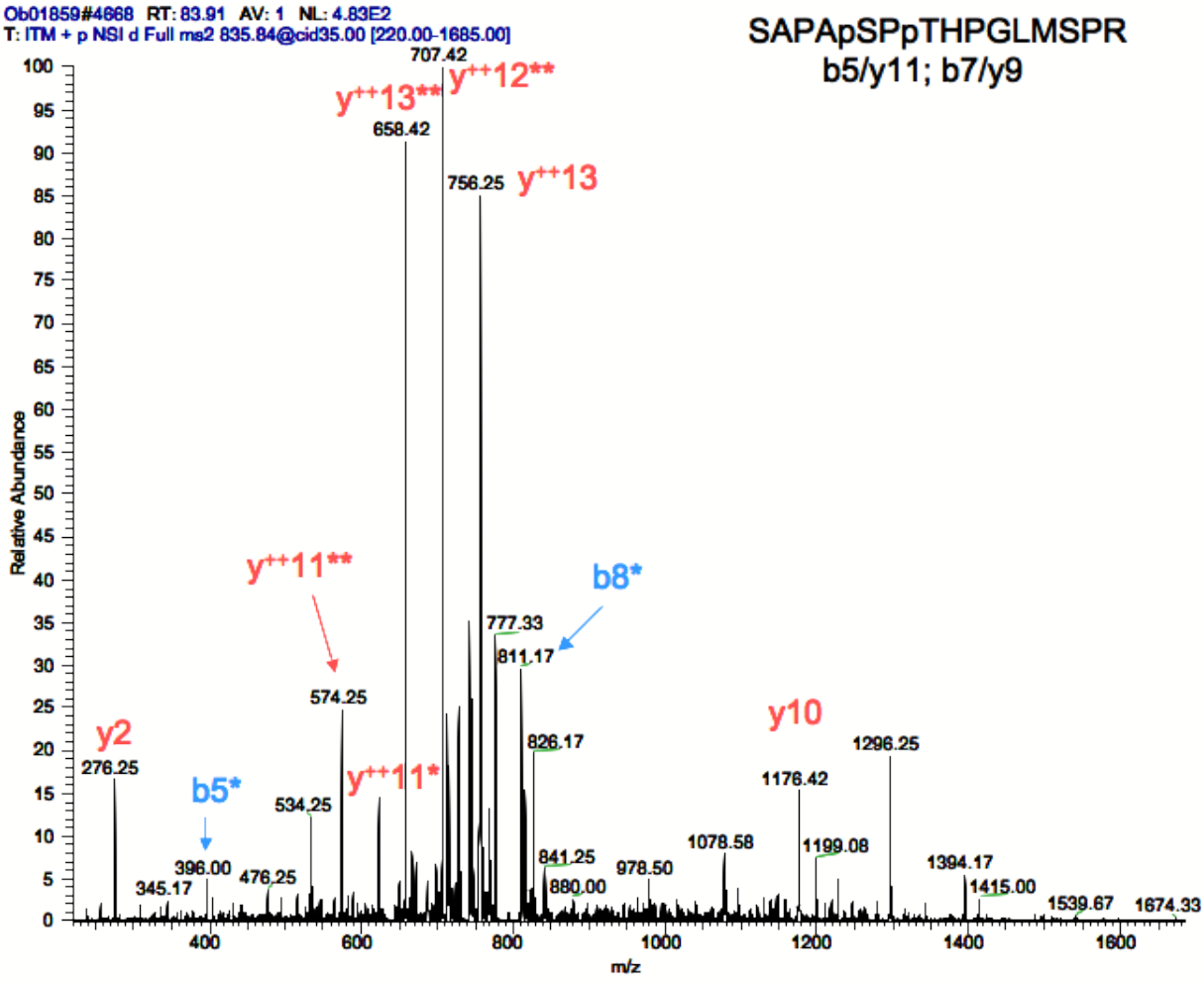

Figure 5: Annotated MS/MS spectrum of the doubly phosphorylated peptide SAPASPTHPGLMSPR. The peptide was found down-regulated (regulation factor of 0.62, TCDD treatment of 30 min) and belongs to the protein "similar to forkhead box K1 isoform alpha". * indicates a phosphoric acid loss and ++ a doubly charged peptide.

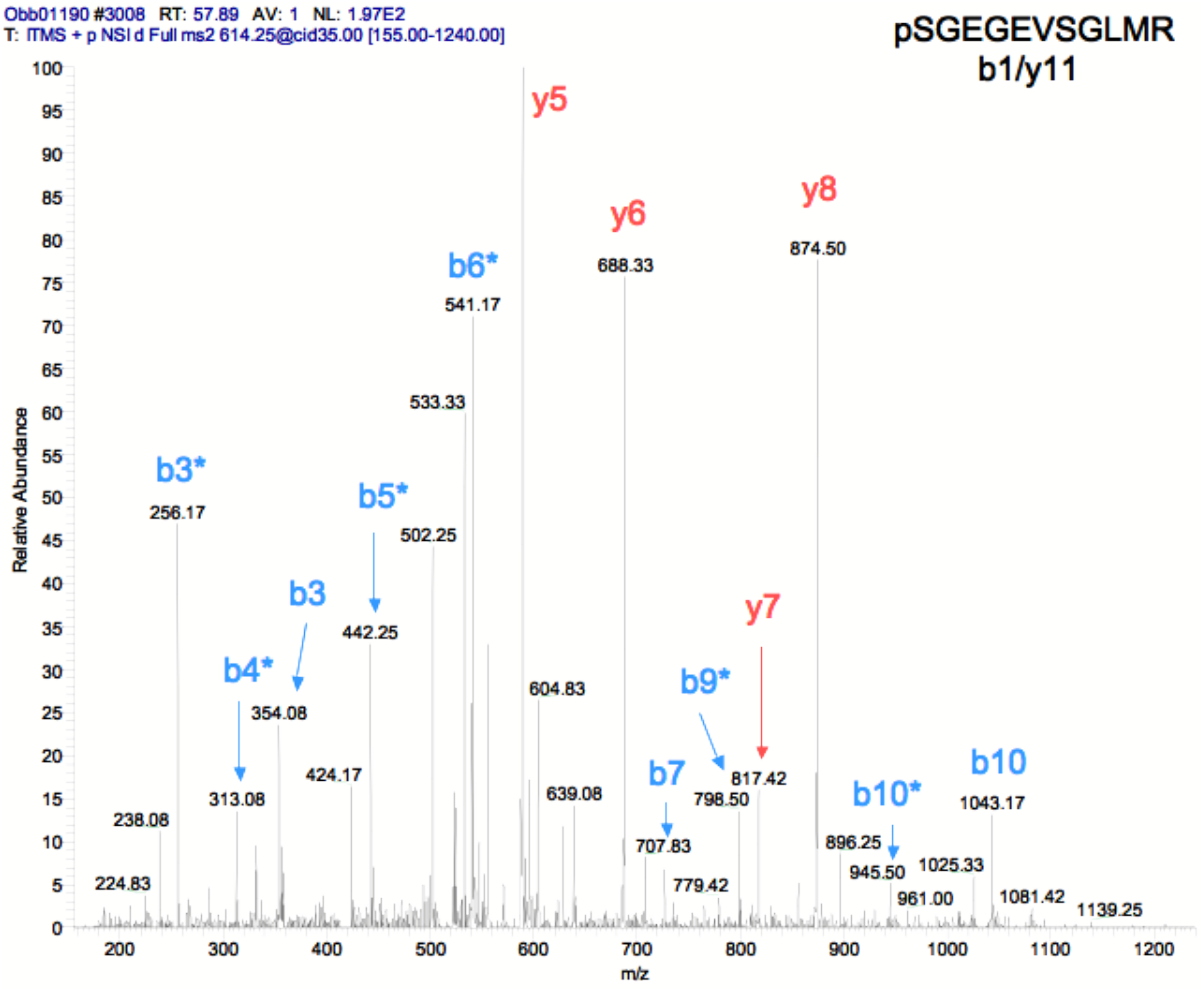

Figure 6: Annotated MS/MS spectrum of the serine-phosphorylated peptide SGEGEVSGLMR. The peptide was found up-regulated (regulation factor of 1.58, TCDD treatment of 30 min and regulation factor of 1.87, 2 hours treatment). It belongs to the protein Transcription intermediary factor 1-beta. * indicates a phosphoric acid loss.

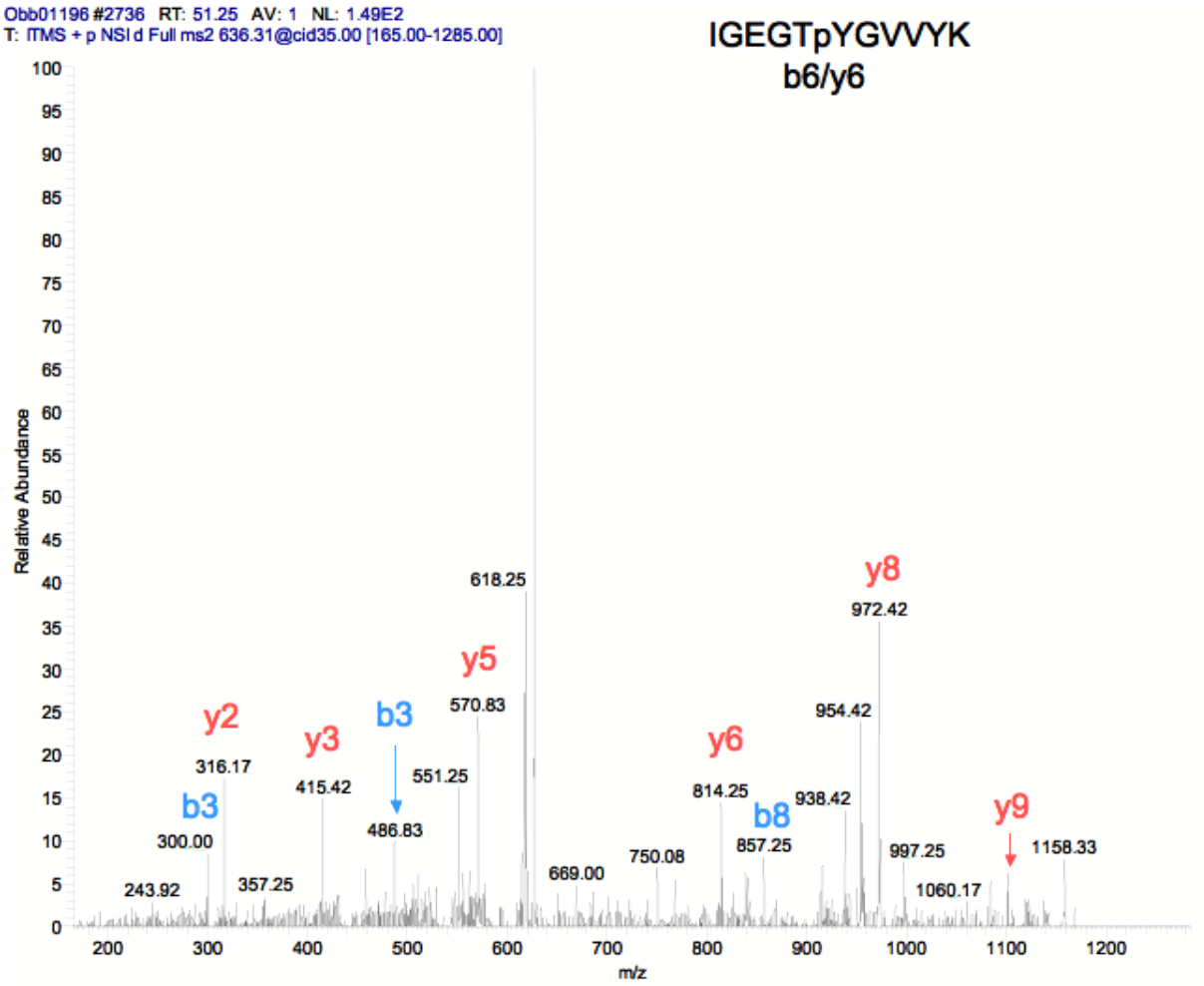

Figure 7: Annotated MS/MS spectrum of the tyrosine-phosphorylated peptide IGEGTYGVVYK. The peptide was found up-regulated (regulation factor of 1.64, TCDD treatment of 30 min) and belongs to the protein Cyclin-dependent kinase 1.

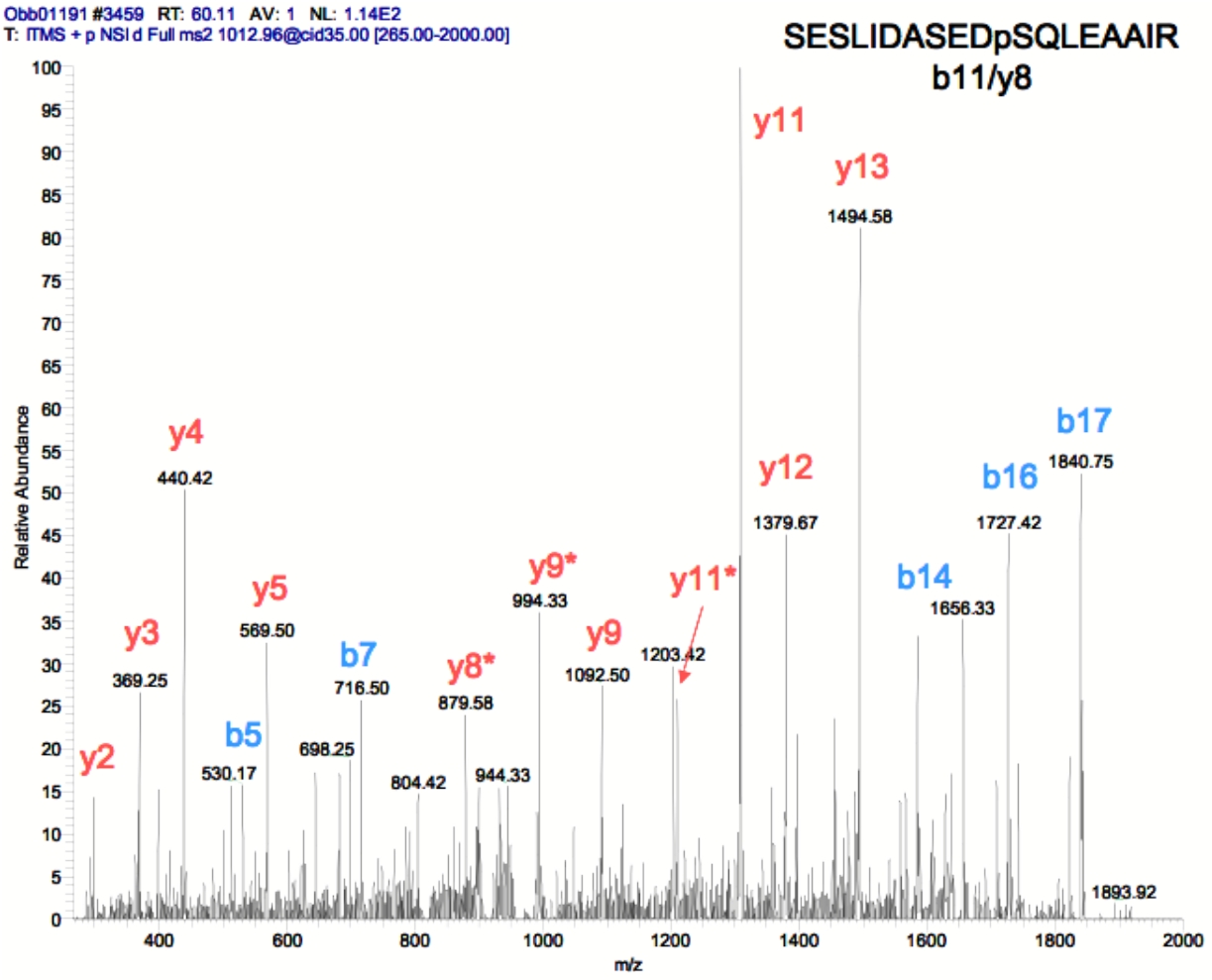

Figure 8: Annotated MS/MS spectrum of the serine-phosphorylated peptide SESLIDASEDSQLEAAIR. The peptide was found up-regulated (regulation factor of 1.86, TCDD treatment of 30 min) and belongs to the protein UBX domain-containing protein 7. * indicates a phosphoric acid loss.

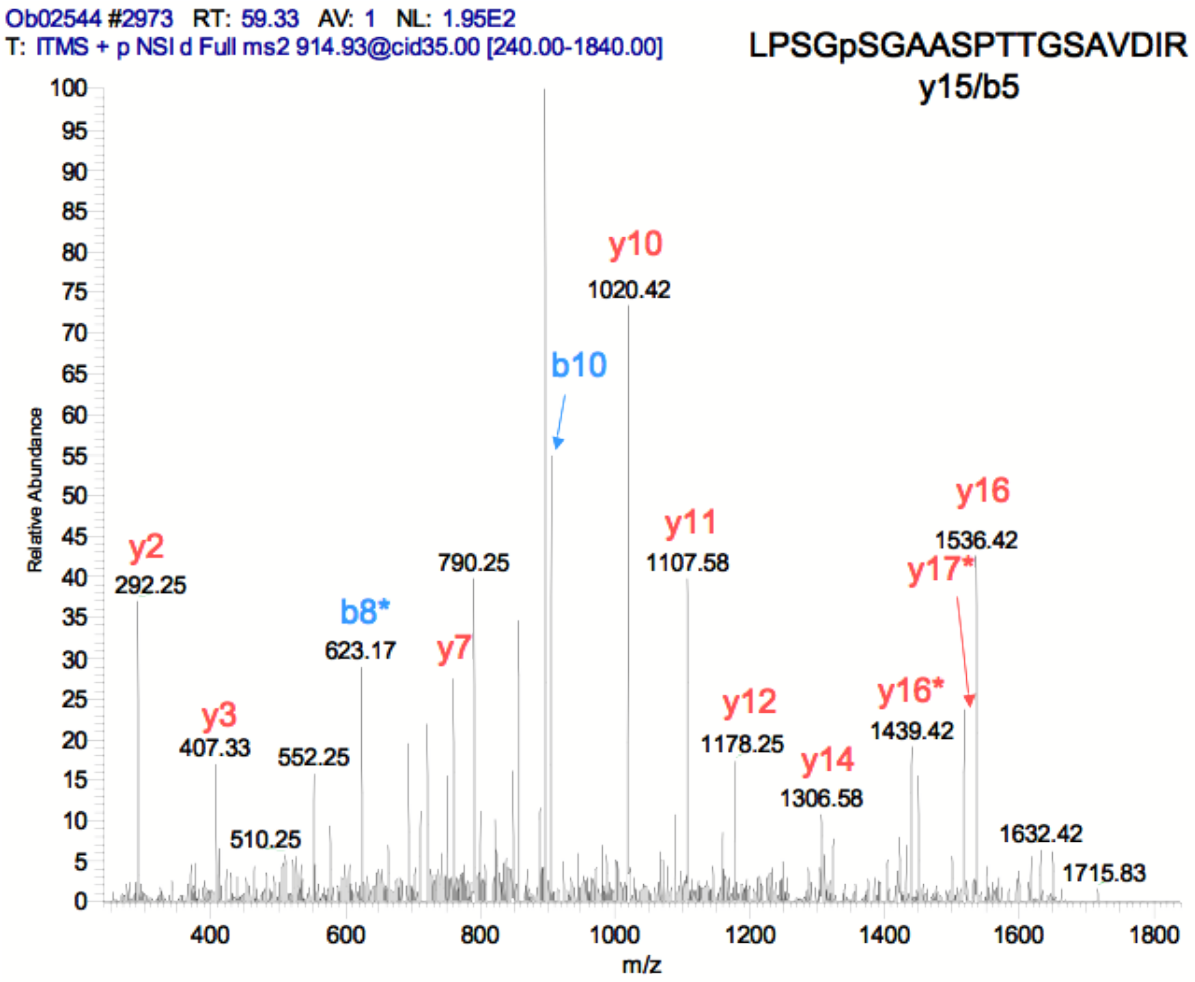

Figure 9: Annotated MS/MS spectrum of the serine-phosphorylated peptide LPSGSGAASPTTGSAVDIR. The peptide was found up-regulated (regulation factor of 1.98, TCDD treatment of 1 hour and regulation factor of 1.60, 2 hours treatment). It belongs to the protein similar to AHNAK nucleoprotein isoform 1 isoform 2. * indicates a phosphoric acid loss.

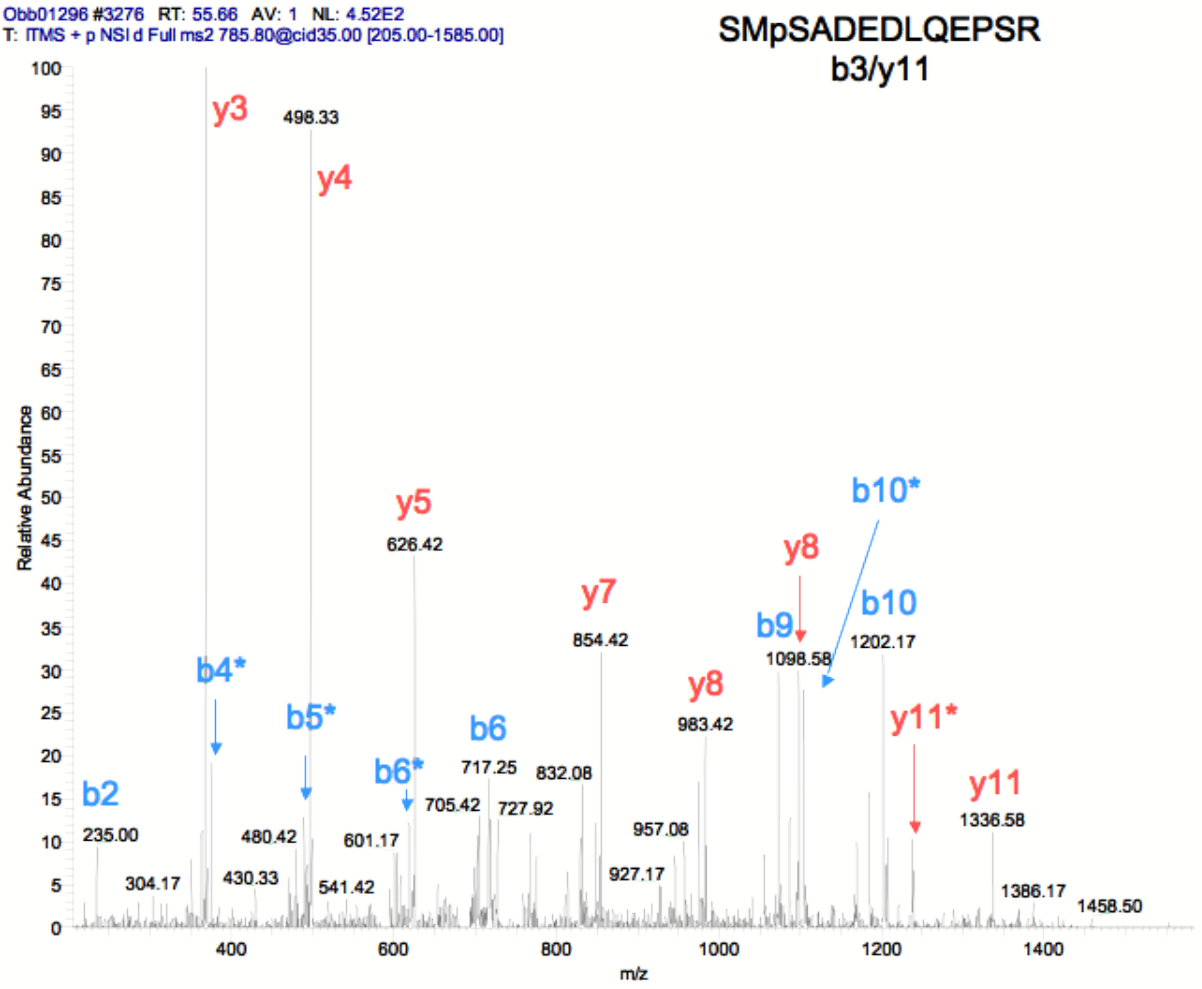

Figure 10: Annotated MS/MS spectrum of the serine-phosphorylated peptide SMSADEDLQEPSR. The peptide were found up-regulated (regulation factor of 1.64, TCDD treatment of 1 hour and regulation factor of 1.75, 2 hours treatment). It belongs to the protein RD RNA-binding protein. * indicates a phosphoric acid loss.

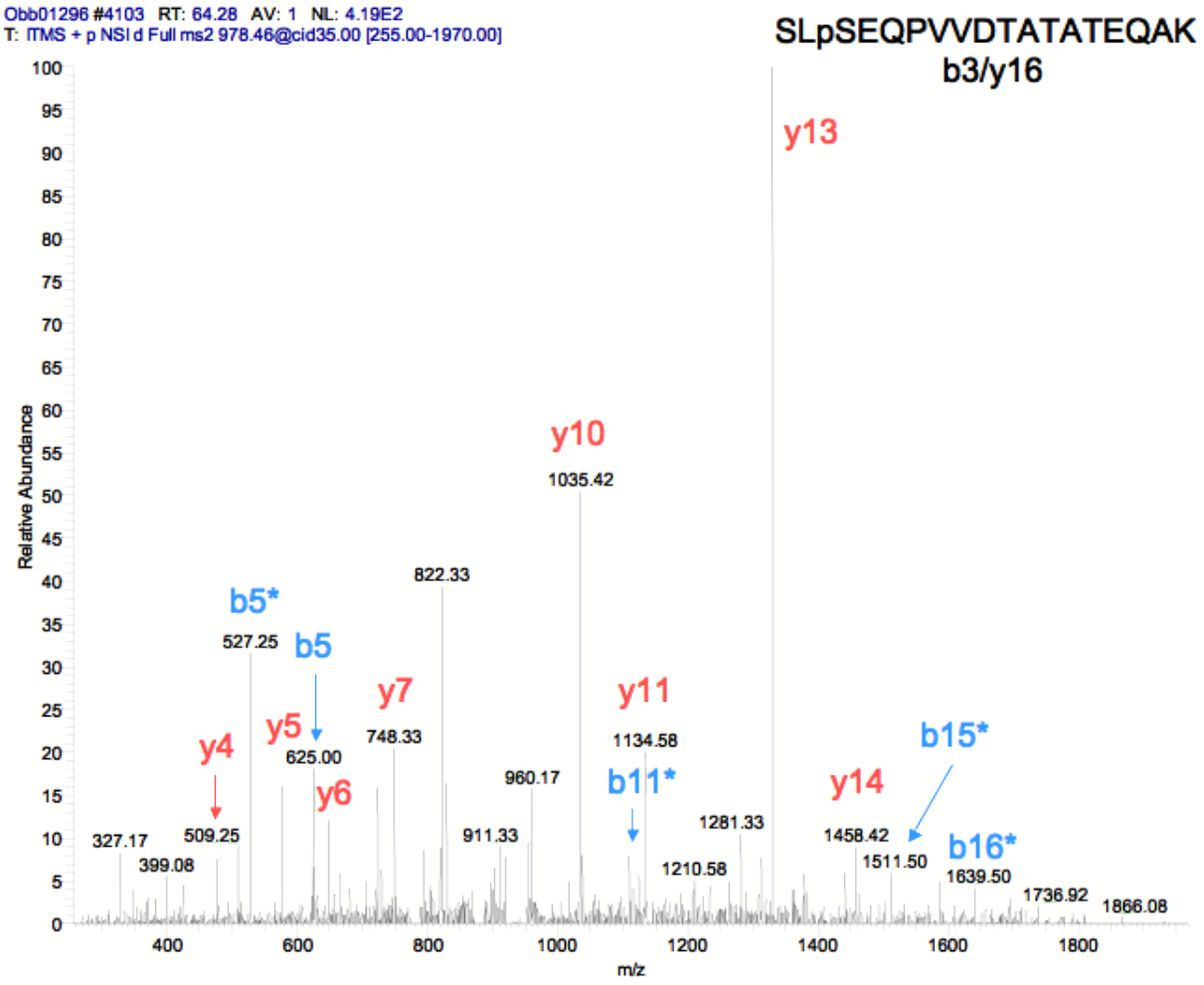

Figure 11: Annotated MS/MS spectrum of the serine-phosphorylated peptide SLSEQPVVDTATATEQAK. The peptide was found up-regulated (regulation factor of 2.79, TCDD treatment of 1 hour and belongs to the protein RD RNA-binding protein. * indicates a phosphoric acid loss.

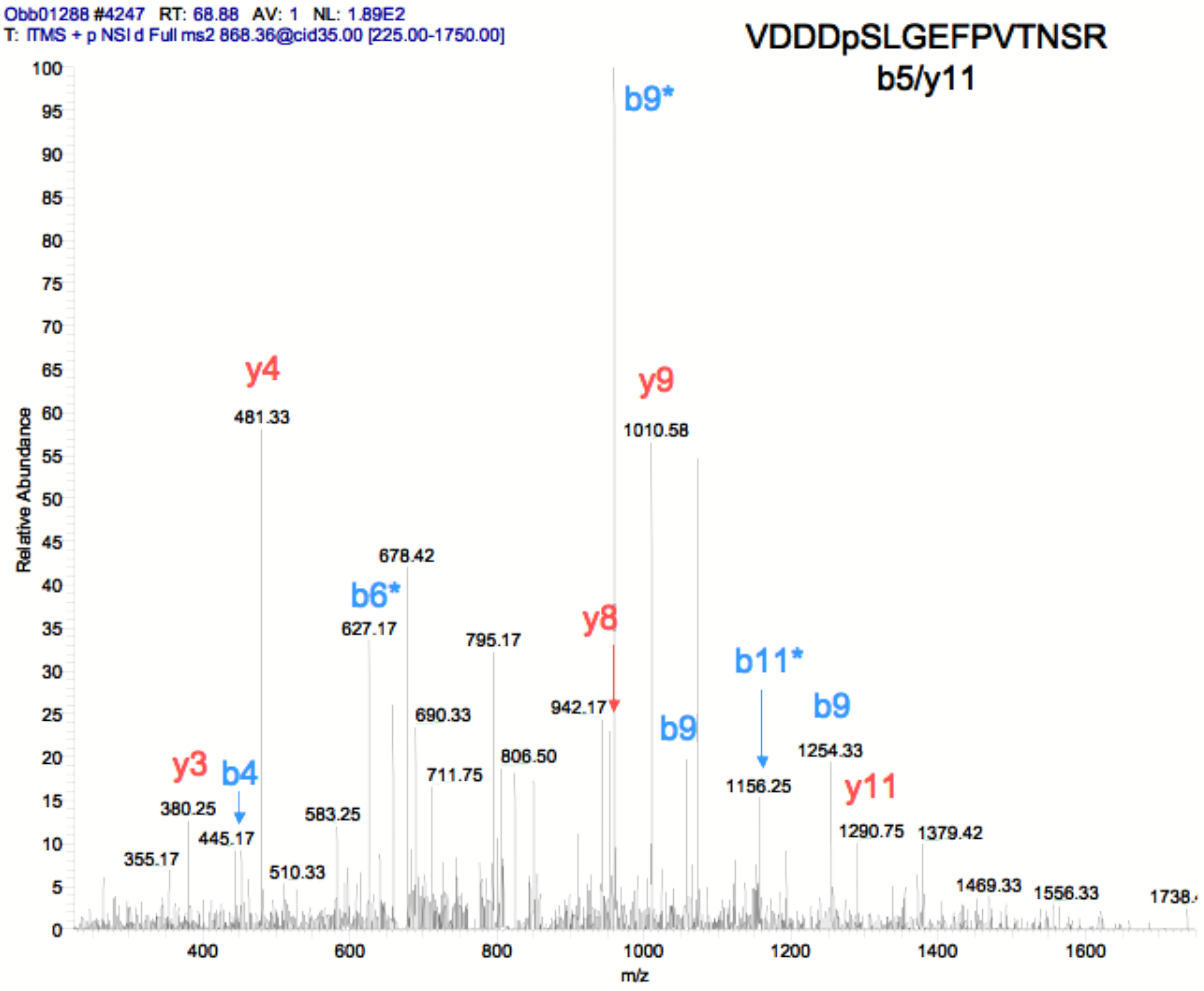

Figure 12: Annotated MS/MS spectrum of the serine-phosphorylated peptide VDDDDSLGEFPVTNSR. The peptide was found down-regulated (regulation factor of 0.56, TCDD treatment of 1 hour) and belongs to the protein Dpf2 protein. * indicates a phosphoric acid loss.

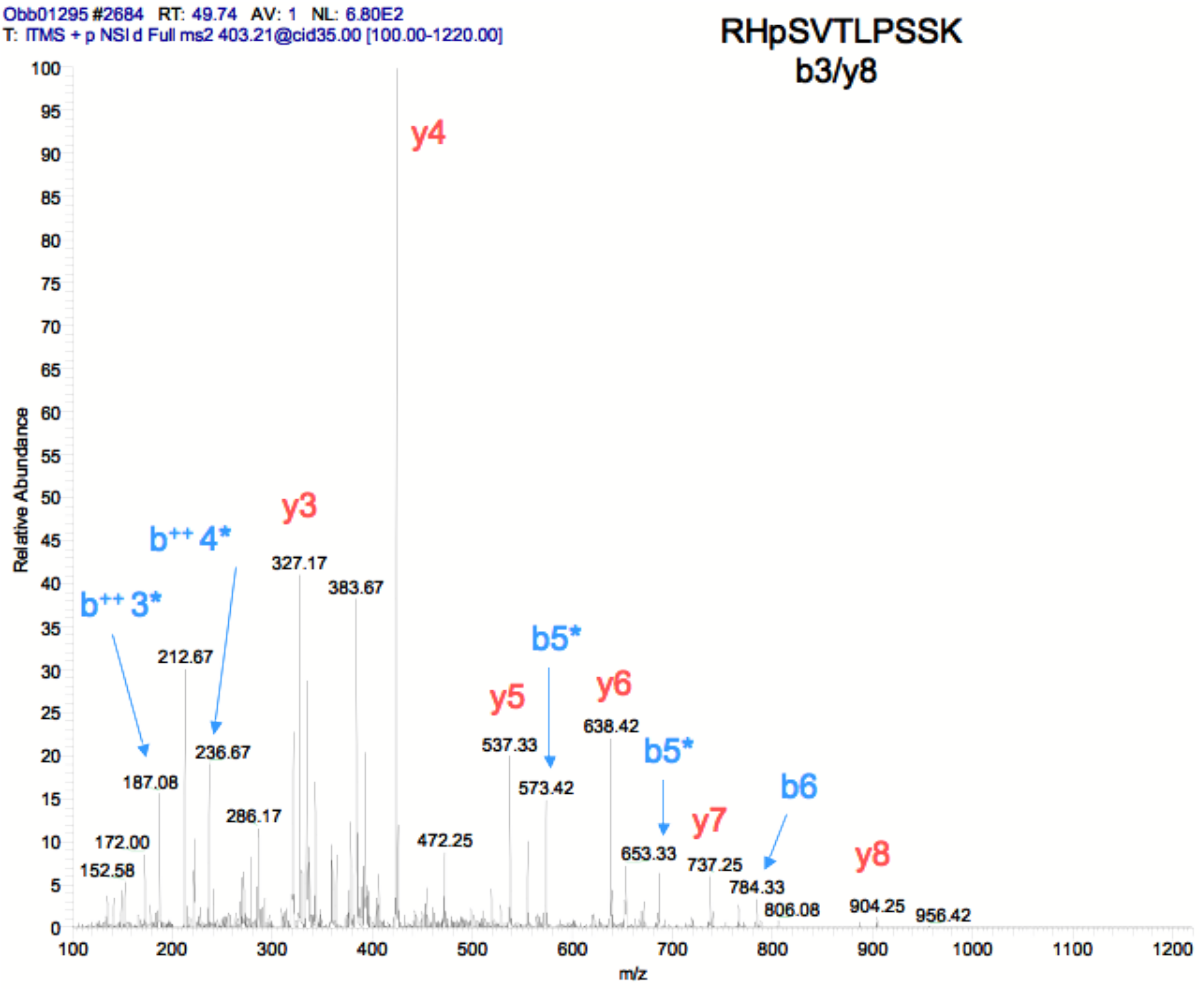

Figure 13: Annotated MS/MS spectrum of the serine-phosphorylated peptide RHSVTLPSSK. The peptide was found up-regulated (regulation factor of 1.50, TCDD treatment of 1 hour) and belongs to the protein Zfp36l1 Butyrate response factor 1. * indicates a phosphoric acid loss and ++ a doubly charged peptide.

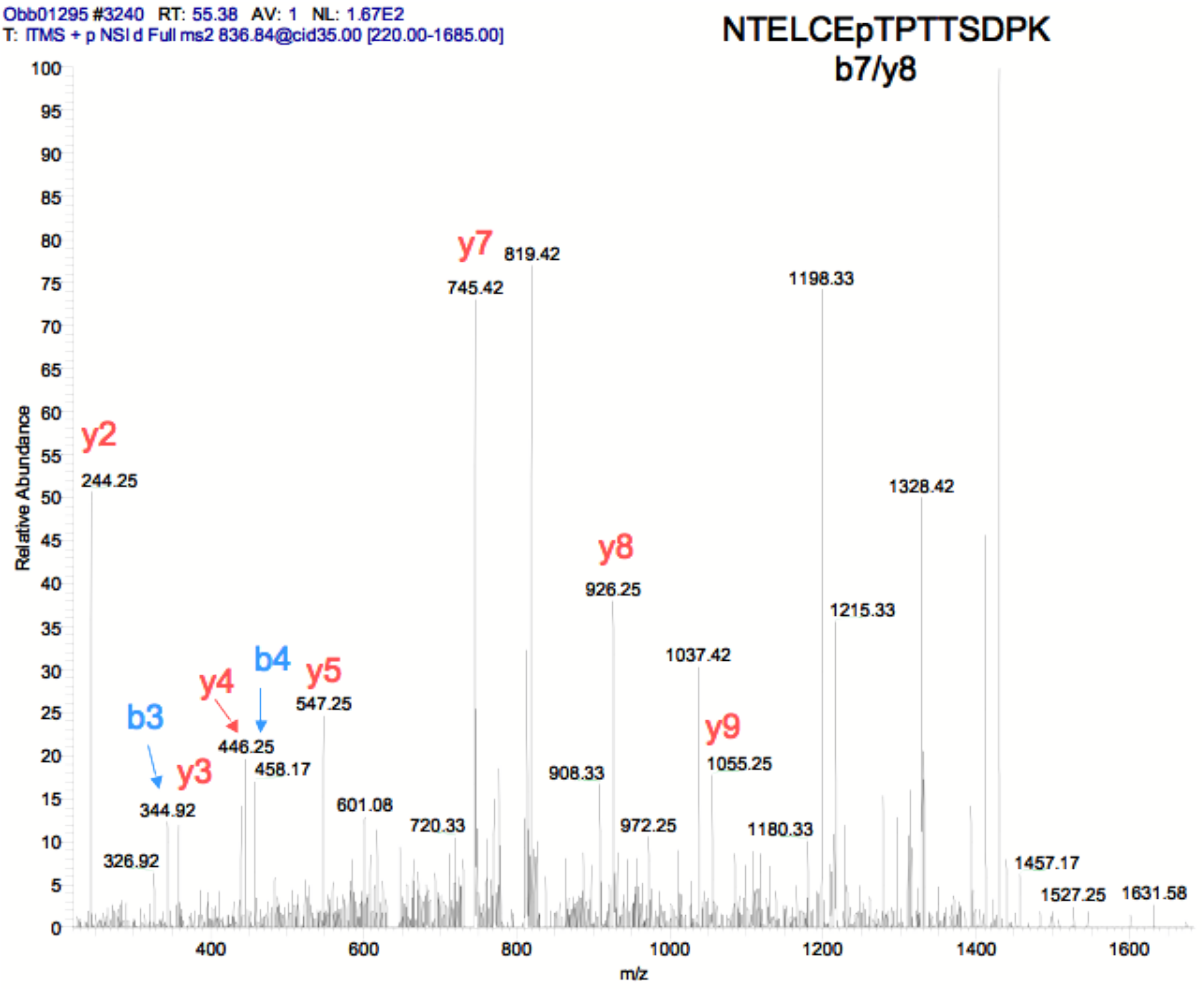

Figure 14: Annotated MS/MS spectrum of the threonine-phosphorylated peptide NTELCETPTTSDPK. The peptide was found up-regulated (regulation factor of 1.63, TCDD treatment of 1 hour and regulation factor of 1.51, 2 hours treatment). It belongs to the protein UBX domain-containing protein 4.

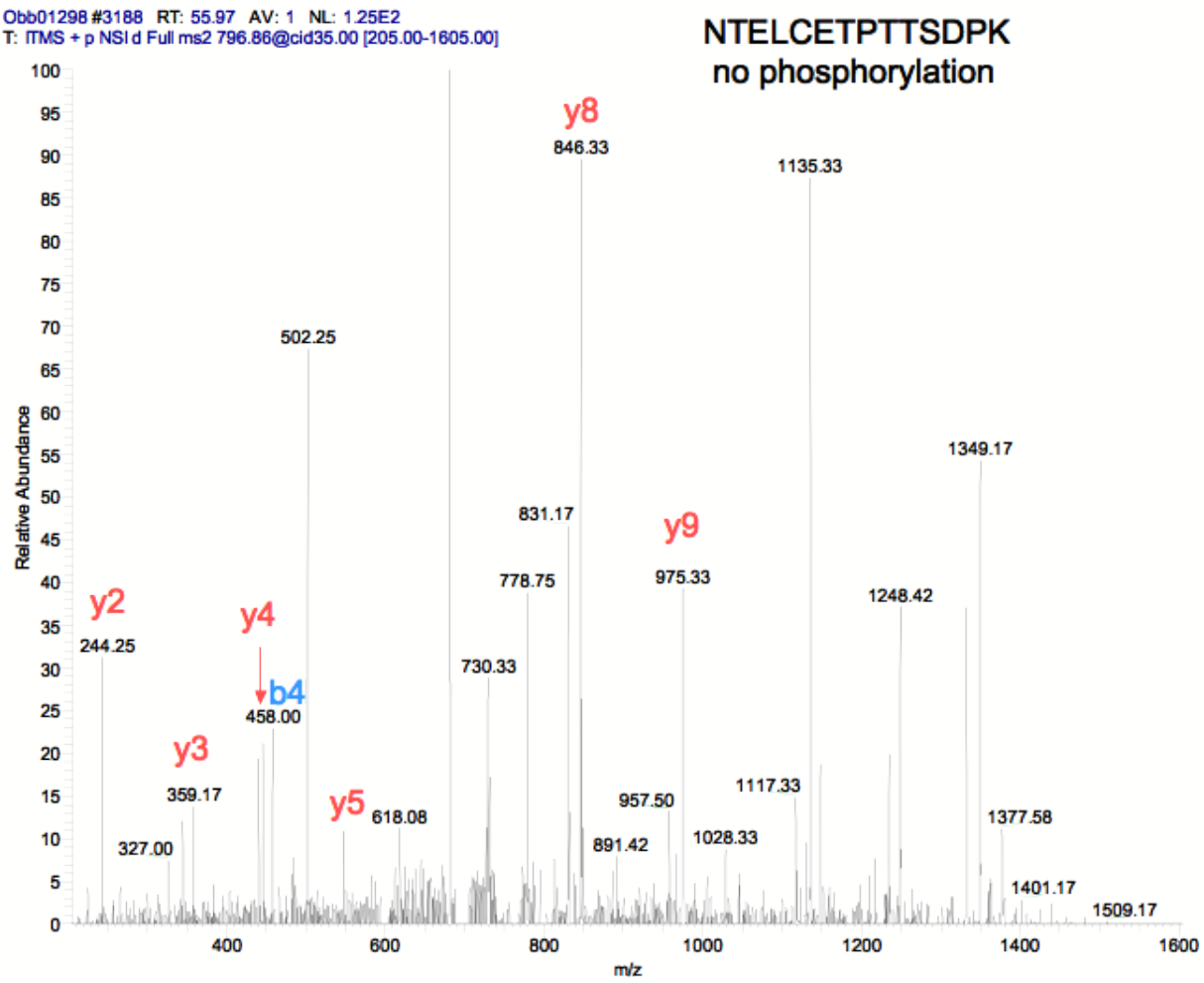

Figure 15: Annotated MS/MS spectrum of the non-phosphorylated peptide NTELCETPTTSDPK. The peptide was found not regulated (regulation factor of 0.87, TCDD treatment of 1 hour) and belongs to the protein UBX domain-containing protein 4.

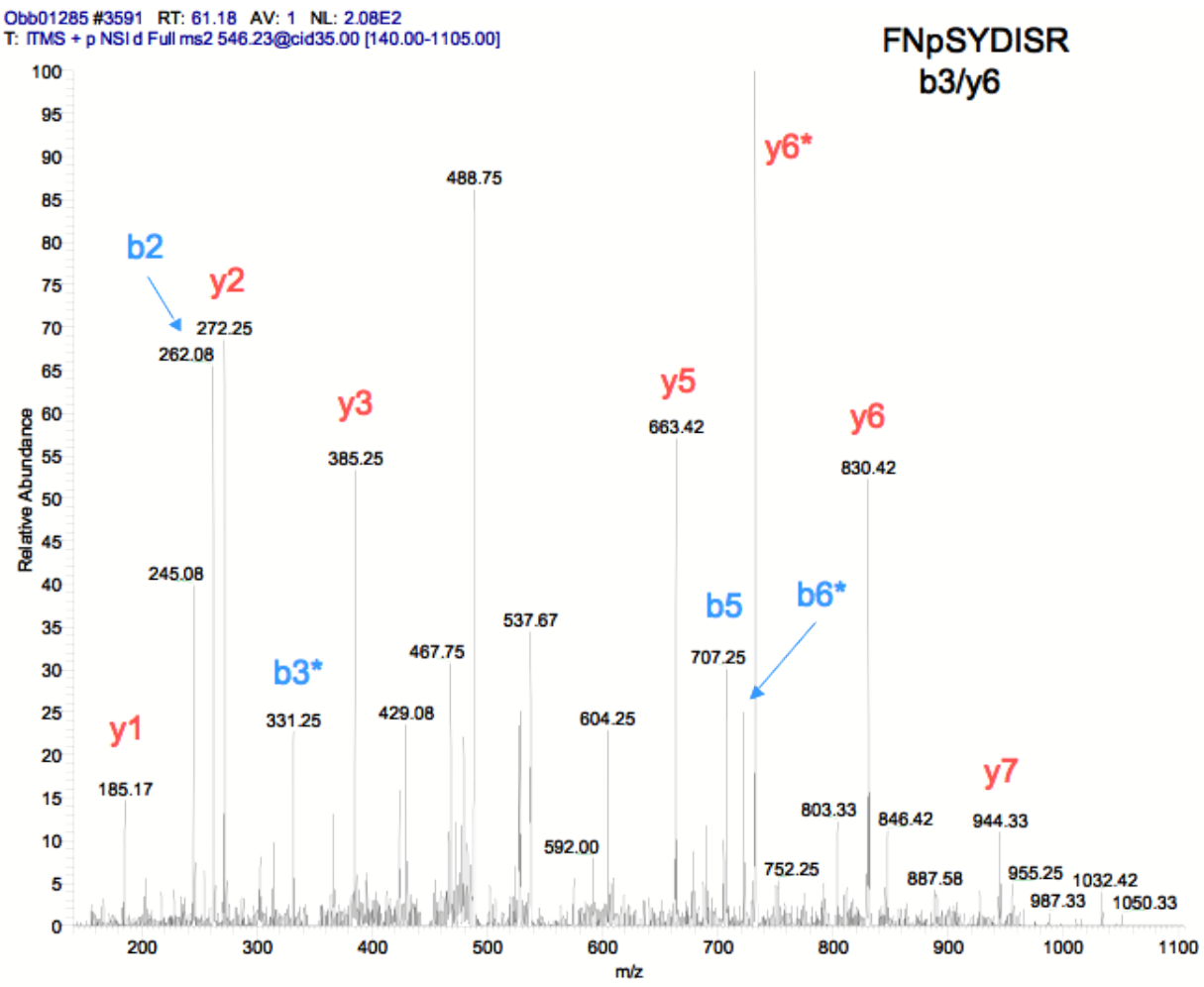

Figure 16: Annotated MS/MS spectrum of the serine-phosphorylated peptide FNSYDISR. The peptide was found up-regulated (regulation factor of 1.65, TCDD treatment of 1 hour) and belongs to the protein Dennd5a protein. * indicates a phosphoric acid loss.

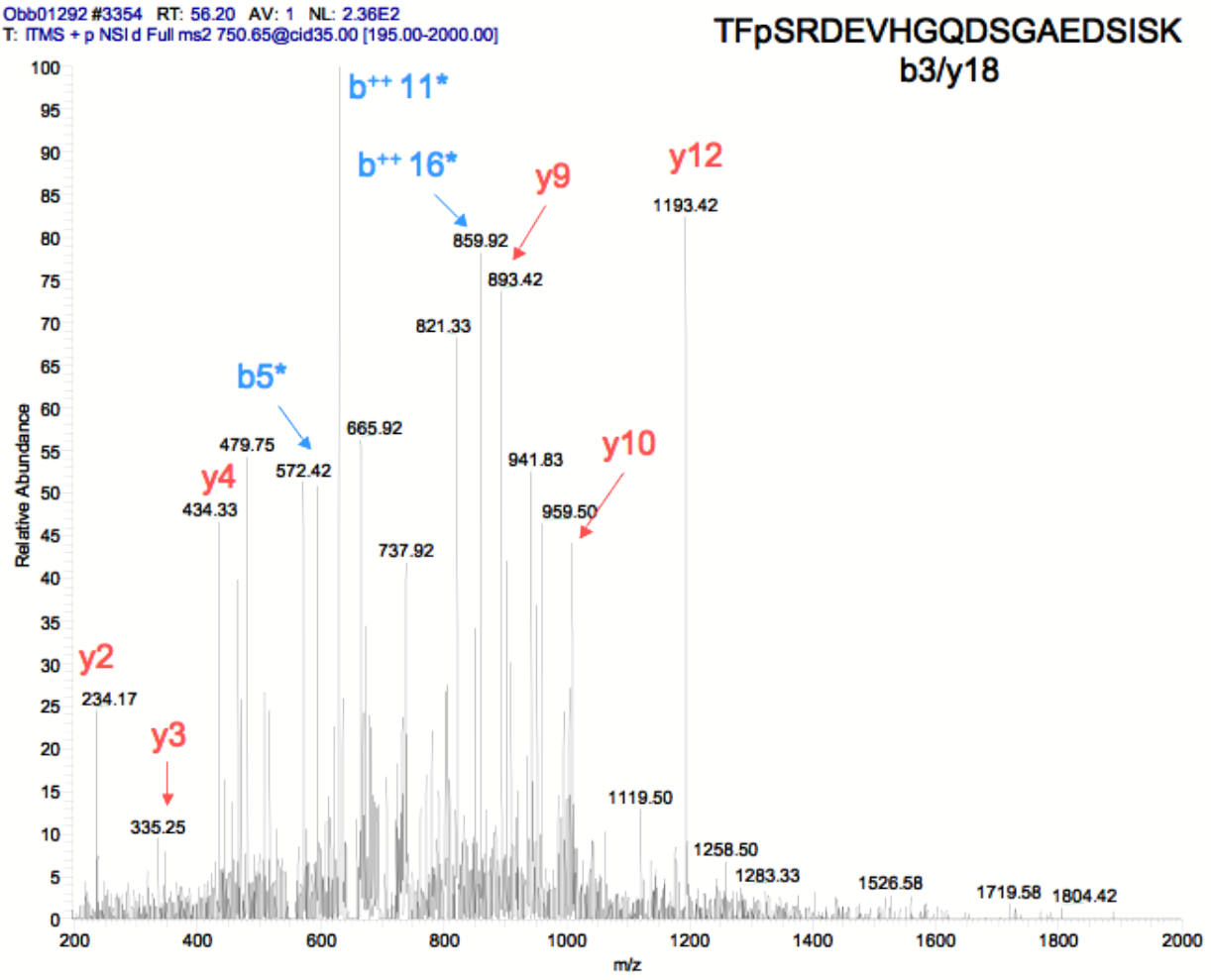

Figure 17: Annotated MS/MS spectrum of the serine-phosphorylated peptide TFSRDEVHGQDSGAEDSISK. The peptide was found up-regulated (regulation factor of 1.73, TCDD treatment of 1 hour) and belongs to the protein Kinesin-like protein KIF4. * indicates a phosphoric acid loss and ++ a doubly charged peptide.

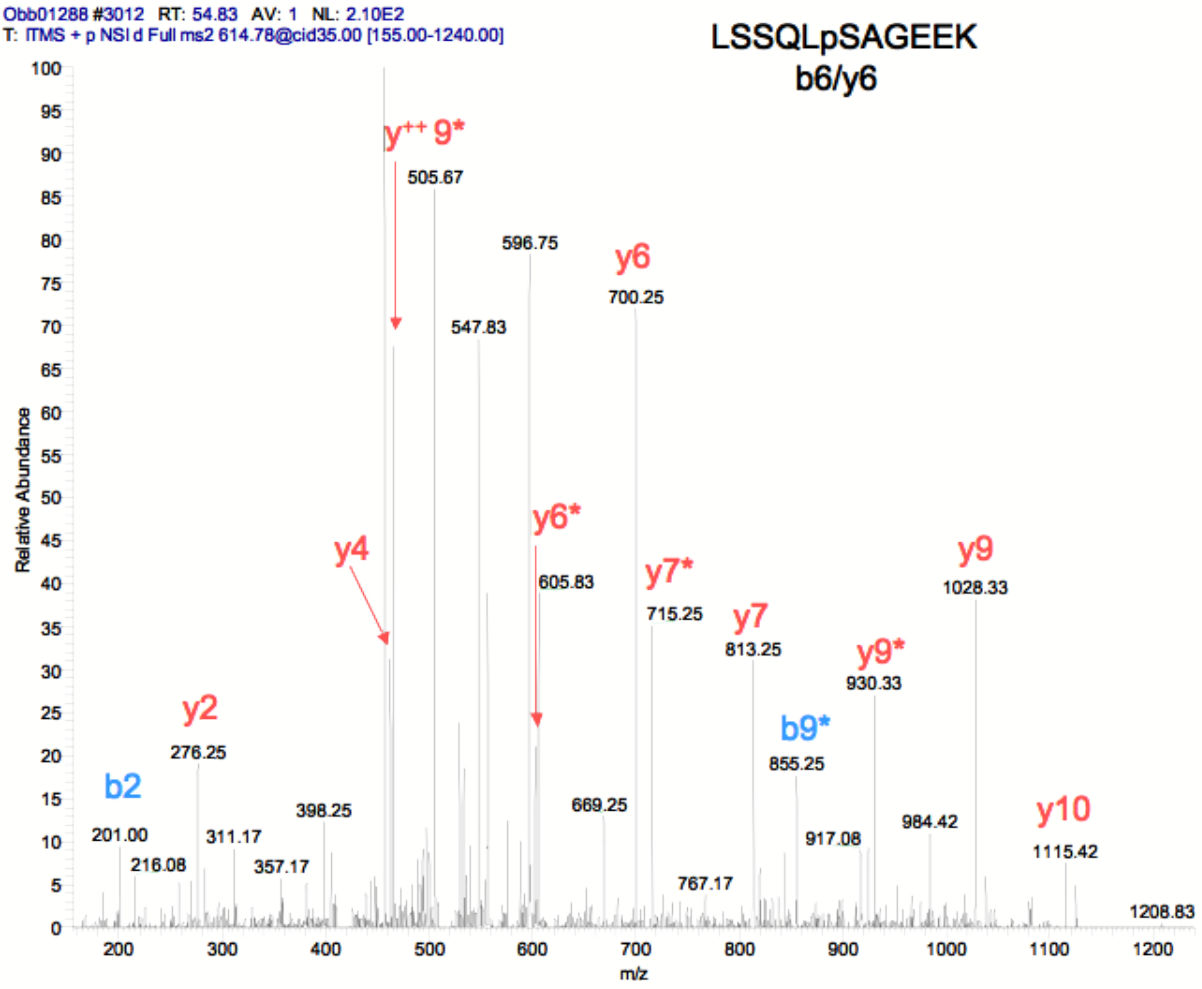

Figure 18: Annotated MS/MS spectrum of the serine-phosphorylated peptide LSSQLSAGEEK. The peptide was found up-regulated (regulation factor of 1.99, TCDD treatment of 1 hour and regulation factor of 1.81, 2 hours treatment). It belongs to the protein LYRIC. * indicates a phosphoric acid loss and ++ a doubly charged peptide.

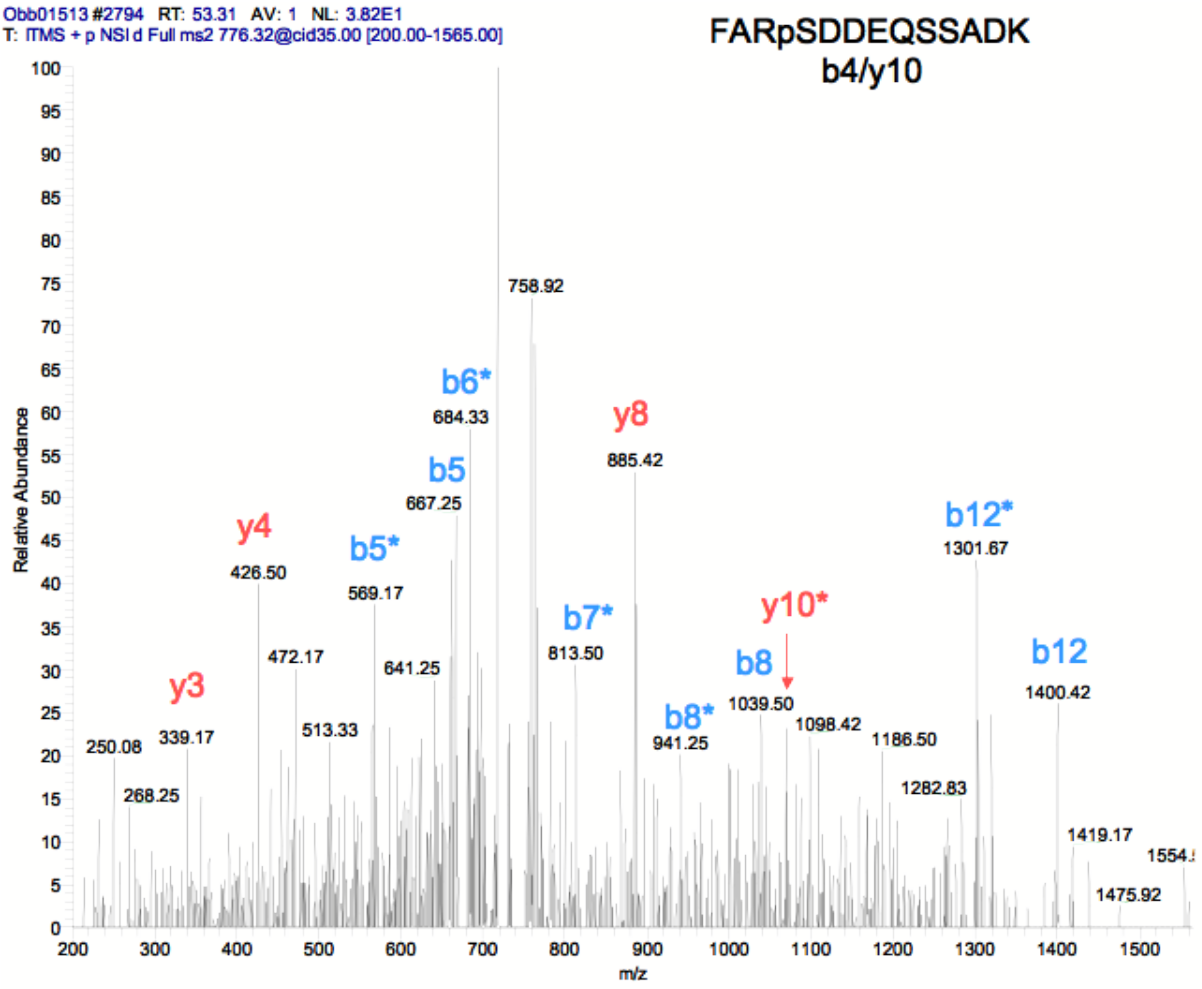

Figure 19: Annotated MS/MS spectrum of the serine-phosphorylated peptide FARSDDEQSSADK. The peptide was found up-regulated (regulation factor of 2.44, TCDD treatment of 1 hour and regulation factor of 3.67, 2 hours treatment). It belongs to the protein ARNT. * indicates a phosphoric acid loss.

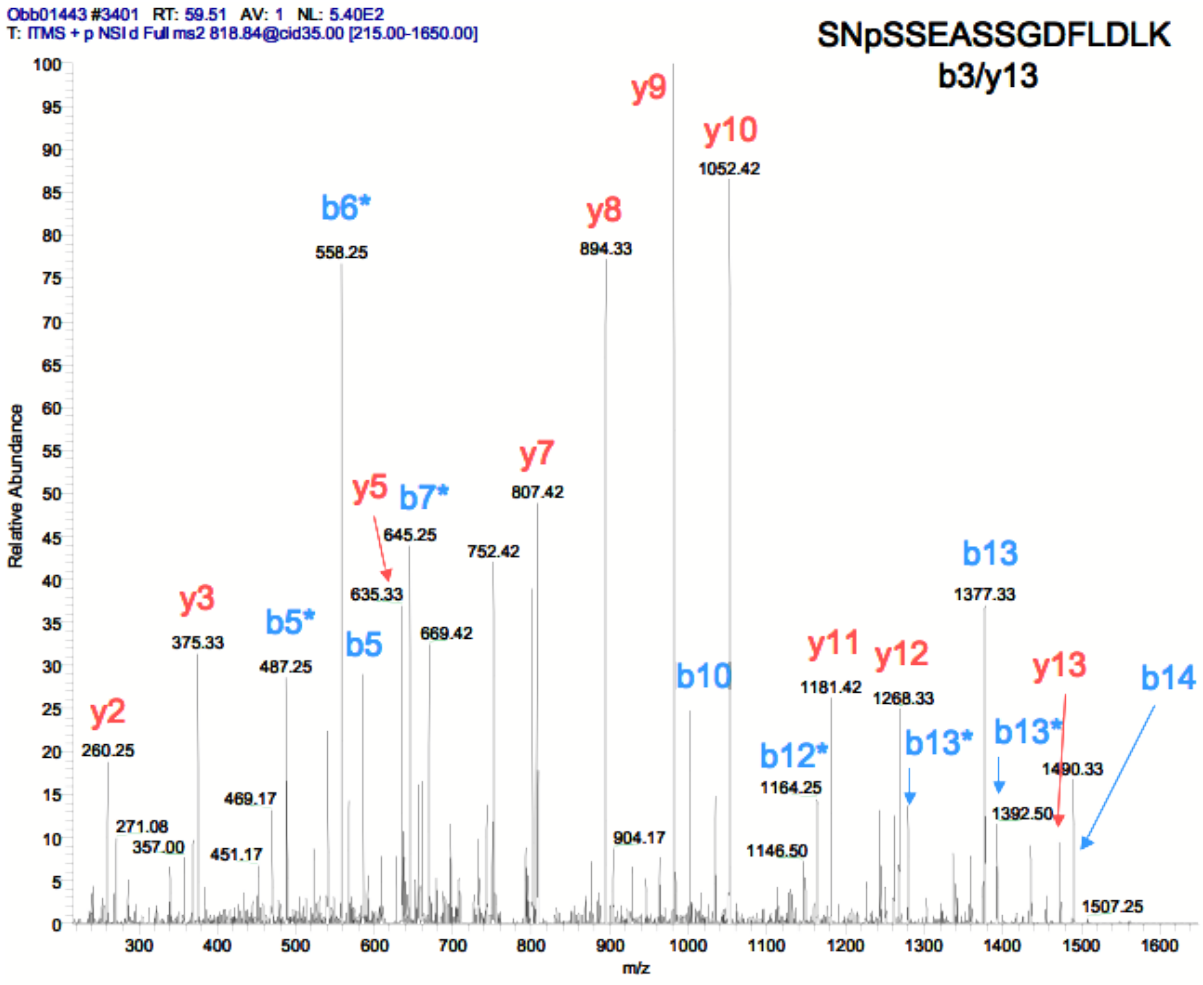

Figure 20: Annotated MS/MS spectrum of the serine-phosphorylated peptide SNSSEASSGDFLDLK. The peptide was found up-regulated (regulation factor of 1.49, TCDD treatment of 2 hours) and belongs to the protein Hematological and neurological expressed 1 protein. * indicates a phosphoric acid loss.

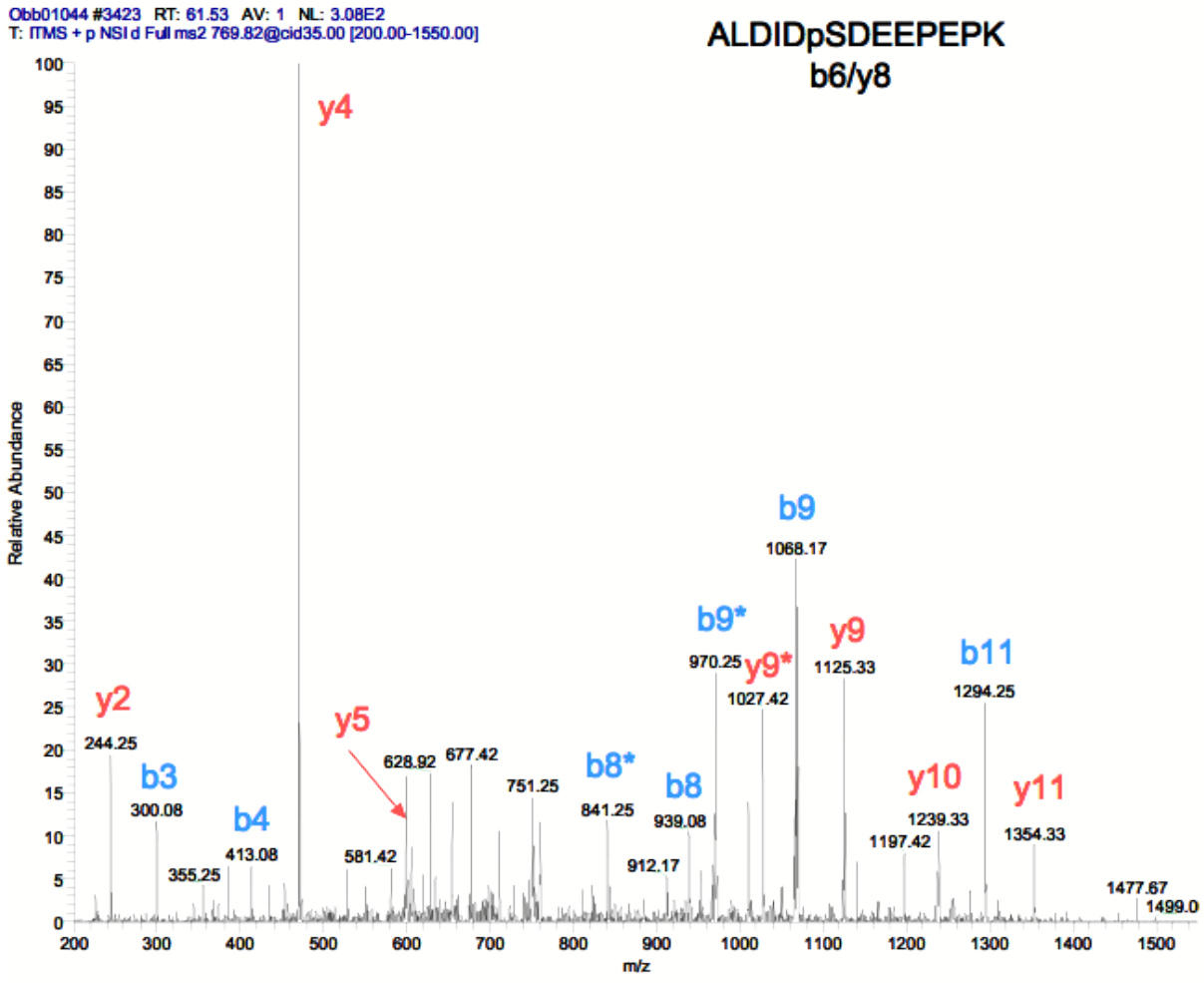

Figure 21: Annotated MS/MS spectrum of the serine-phosphorylated peptide ALDIDS-DEEPEPK. The peptide was found down-regulated (regulation factor of 0.64, TCDD treatment of 2 hours) and belongs to the protein Uncharacterized protein, Sgef. * indicates a phosphoric acid loss.

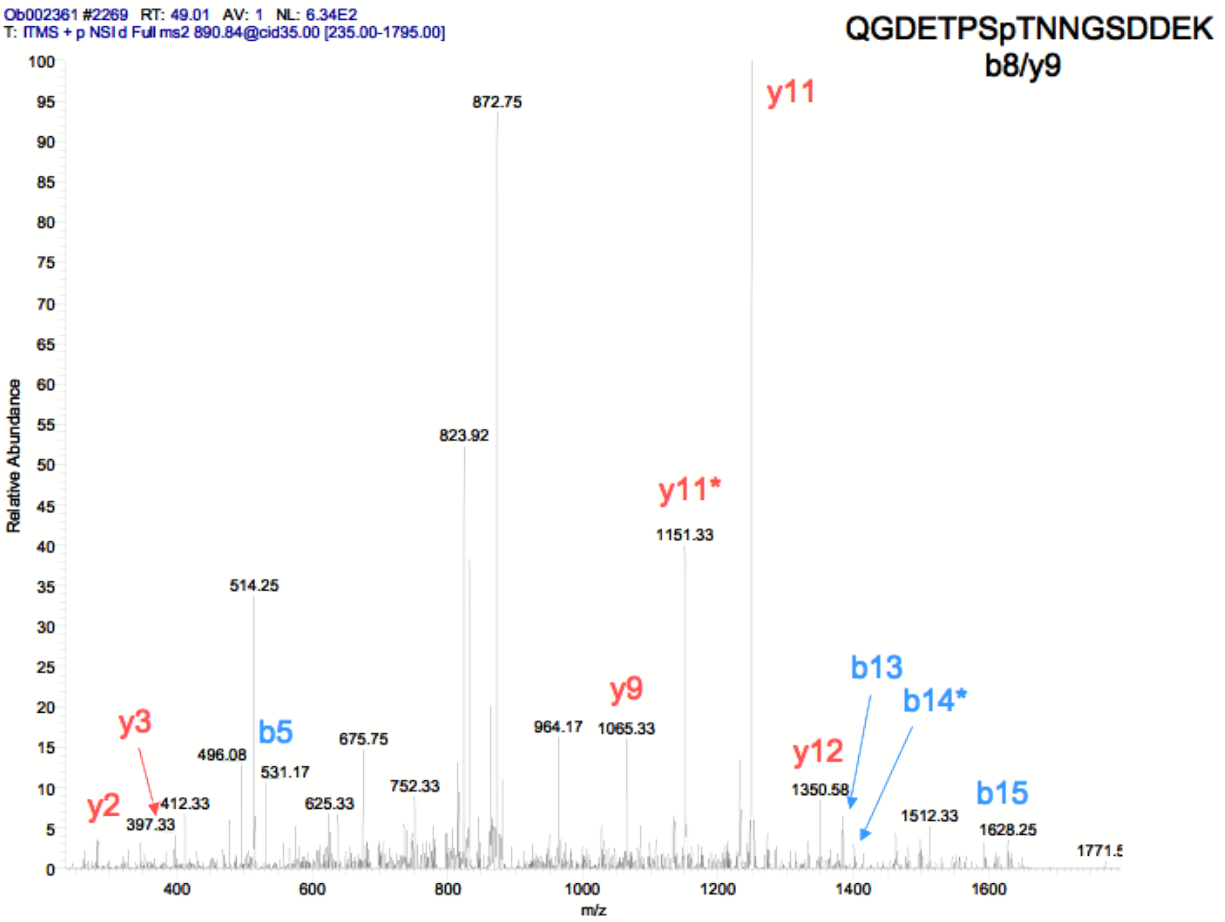

Figure 22: Annotated MS/MS spectrum of the threonine-phosphorylated peptide QGDETPSTNNGSDDEK. The peptide was found down-regulated (regulation factor of 0.51, TCDD treatment of 2 hours) and belongs to the protein Uncharacterized protein, Rabgap1. * indicates a phosphoric acid loss.

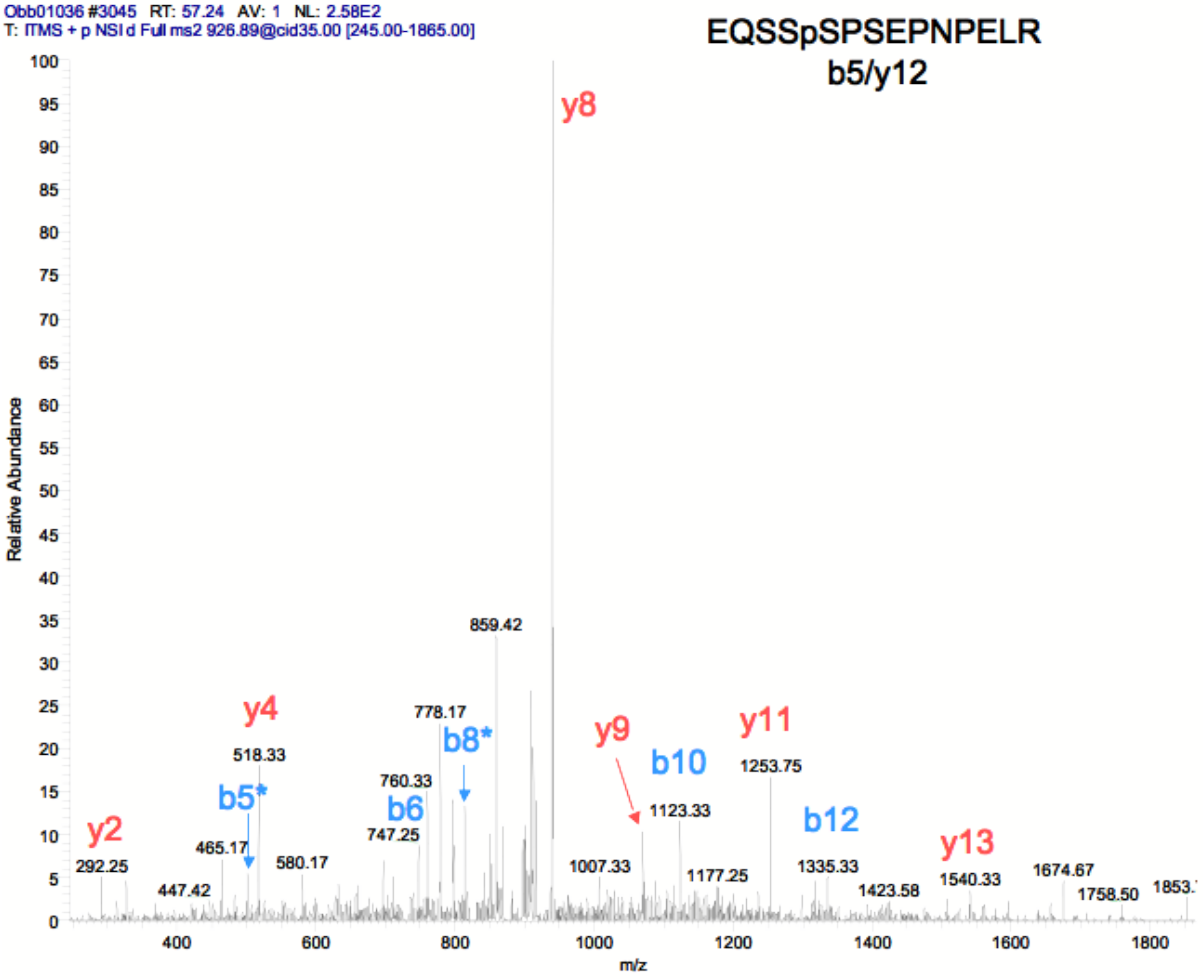

Figure 23: Annotated MS/MS spectrum of the serine-phosphorylated peptide EQSSSPSEPNPNPELR. The peptide was found down-regulated (regulation factor of 0.59, TCDD treatment of 2 hours) and belongs to the protein Cdc42 effector protein 1. * indicates a phosphoric acid loss.

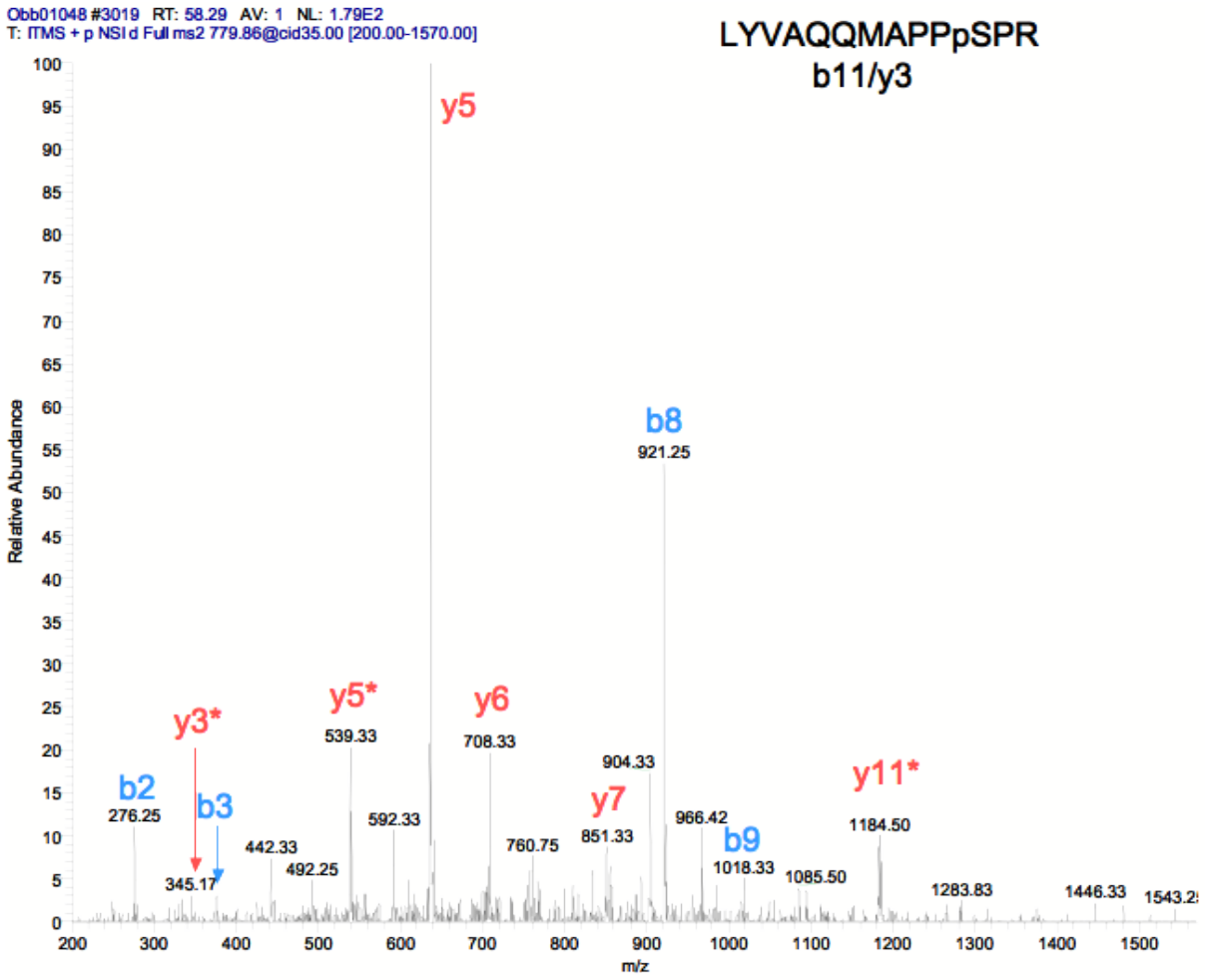

Figure 24: Annotated MS/MS spectrum of the serine-phosphorylated peptide LYVAQQMAPPSPR. The peptide was found down-regulated (regulation factor of 0.61, TCDD treatment of 2 hours) and belongs to the protein RNA binding motif, single stranded interacting protein 2. * indicates a phosphoric acid loss.

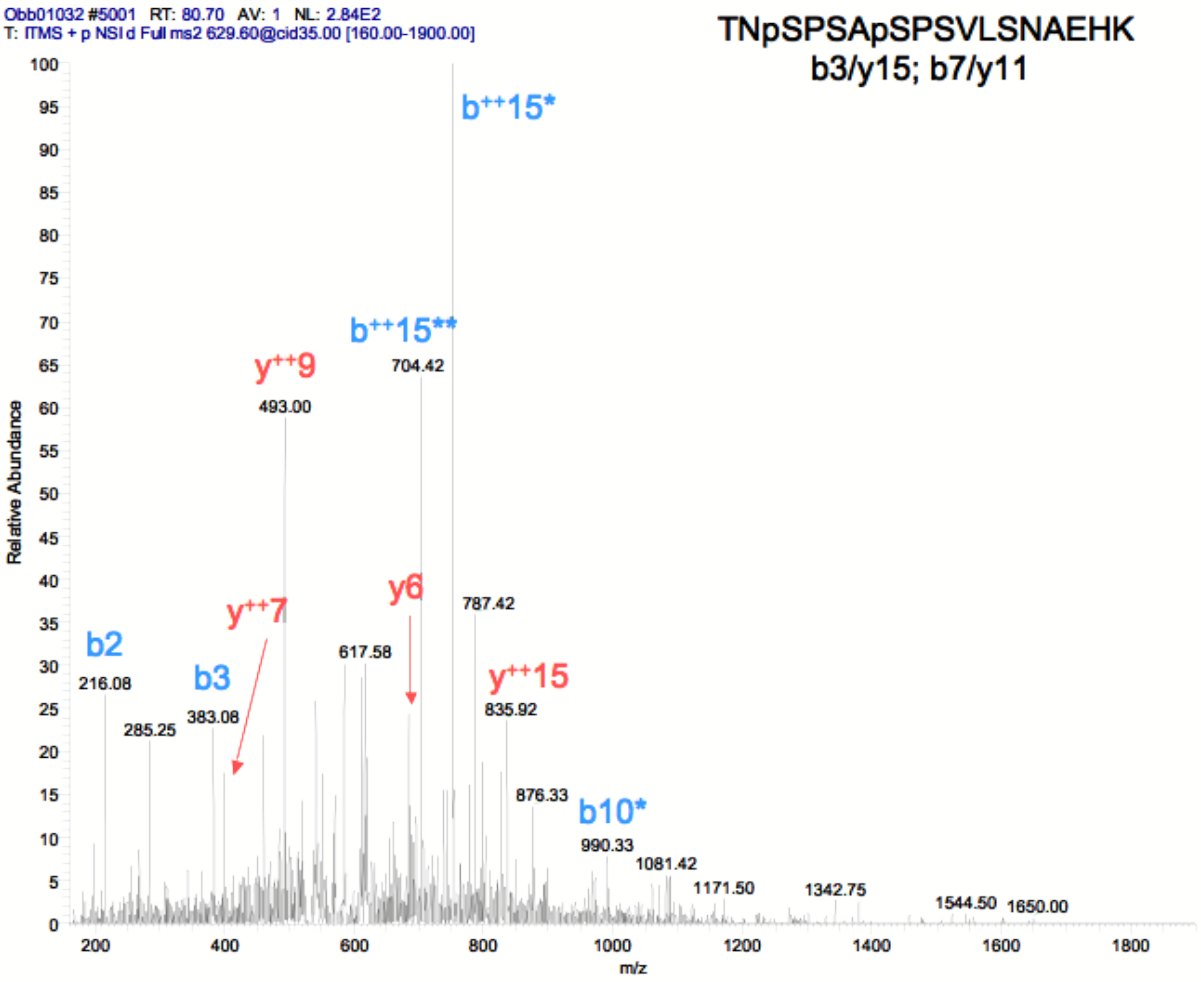

Figure 25: Annotated MS/MS spectrum of the doubly phosphorylated peptide TNSPSASPSVLSNAEHK. The peptide was found down-regulated (regulation factor of 0.62, TCDD treatment of 2 hours) and belongs to the protein Ataxin-2. * indicates a phosphoric acid loss and ++ a doubly charged peptide.

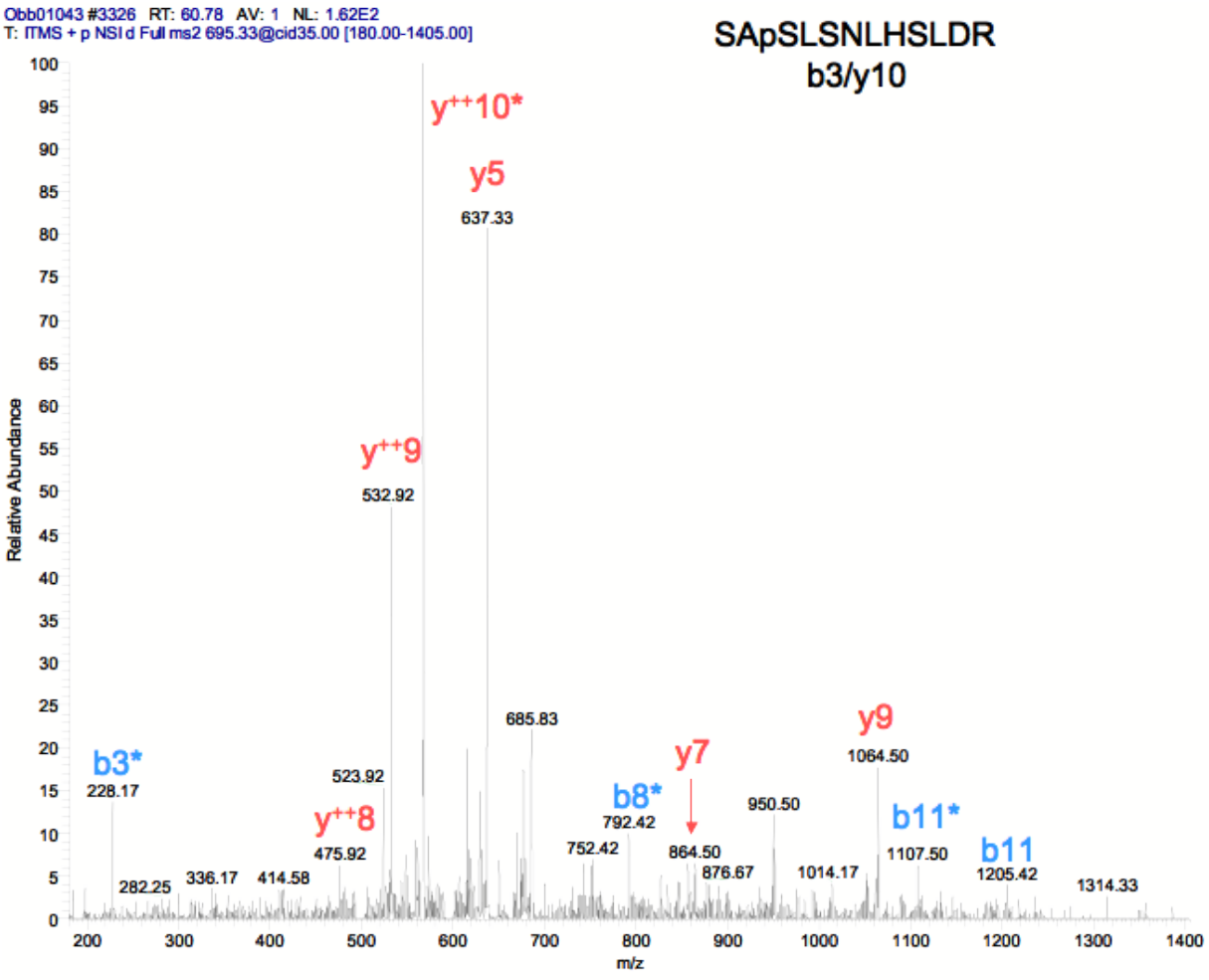

Figure 26: Annotated MS/MS spectrum of the serine-phosphorylated peptide SASLSNLH-SLDR. The peptide was found down-regulated (regulation factor of 0.65, TCDD treatment of 2 hours) and belongs to the protein Chibby homolog 1. * indicates a phosphoric acid loss and ++ a doubly charged peptide.

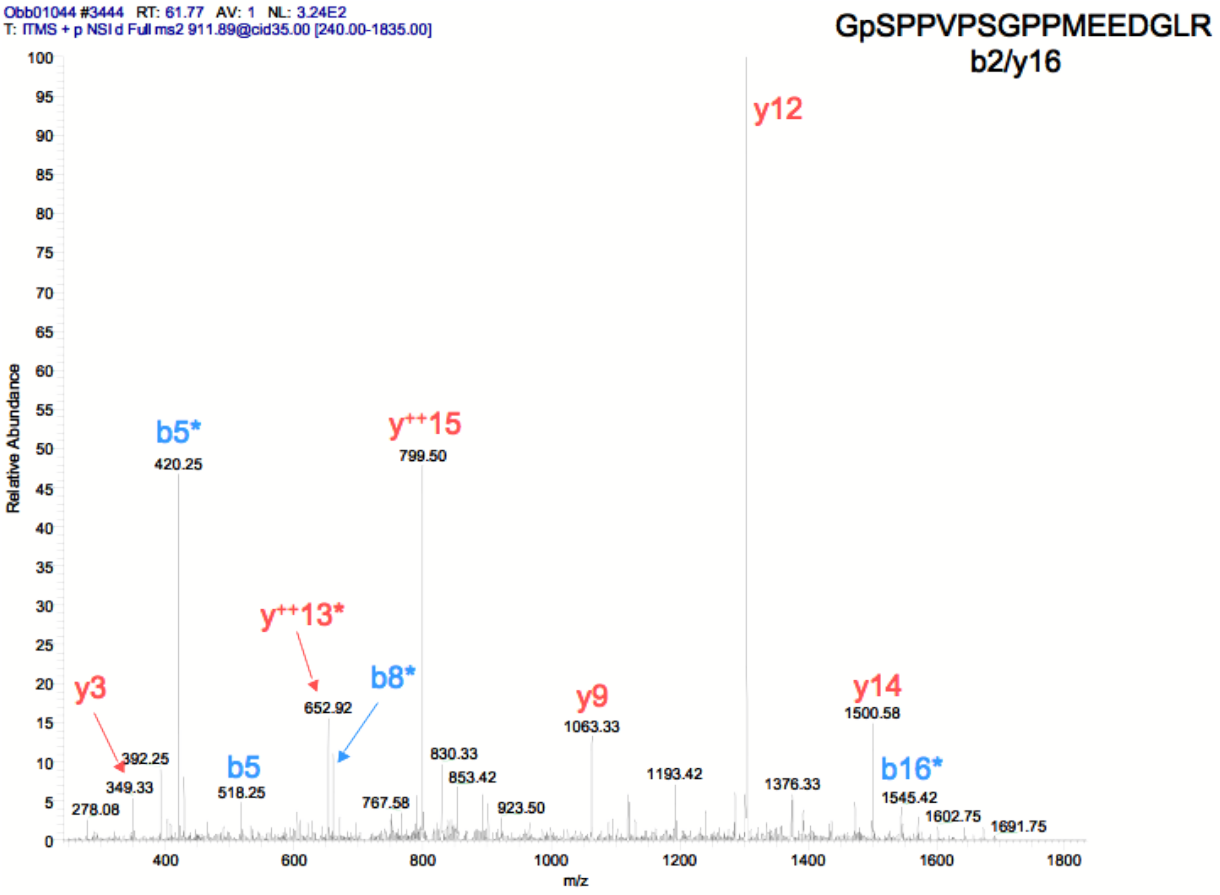

Figure 27: Annotated MS/MS spectrum of the serine-phosphorylated peptide GSPPVPSGPPMEEDGLR. The peptide was found down-regulated (regulation factor of 0.67, TCDD treatment of 2 hours) and belongs to the protein Senp3 protein. * indicates a phosphoric acid loss and ++ a doubly charged peptide.

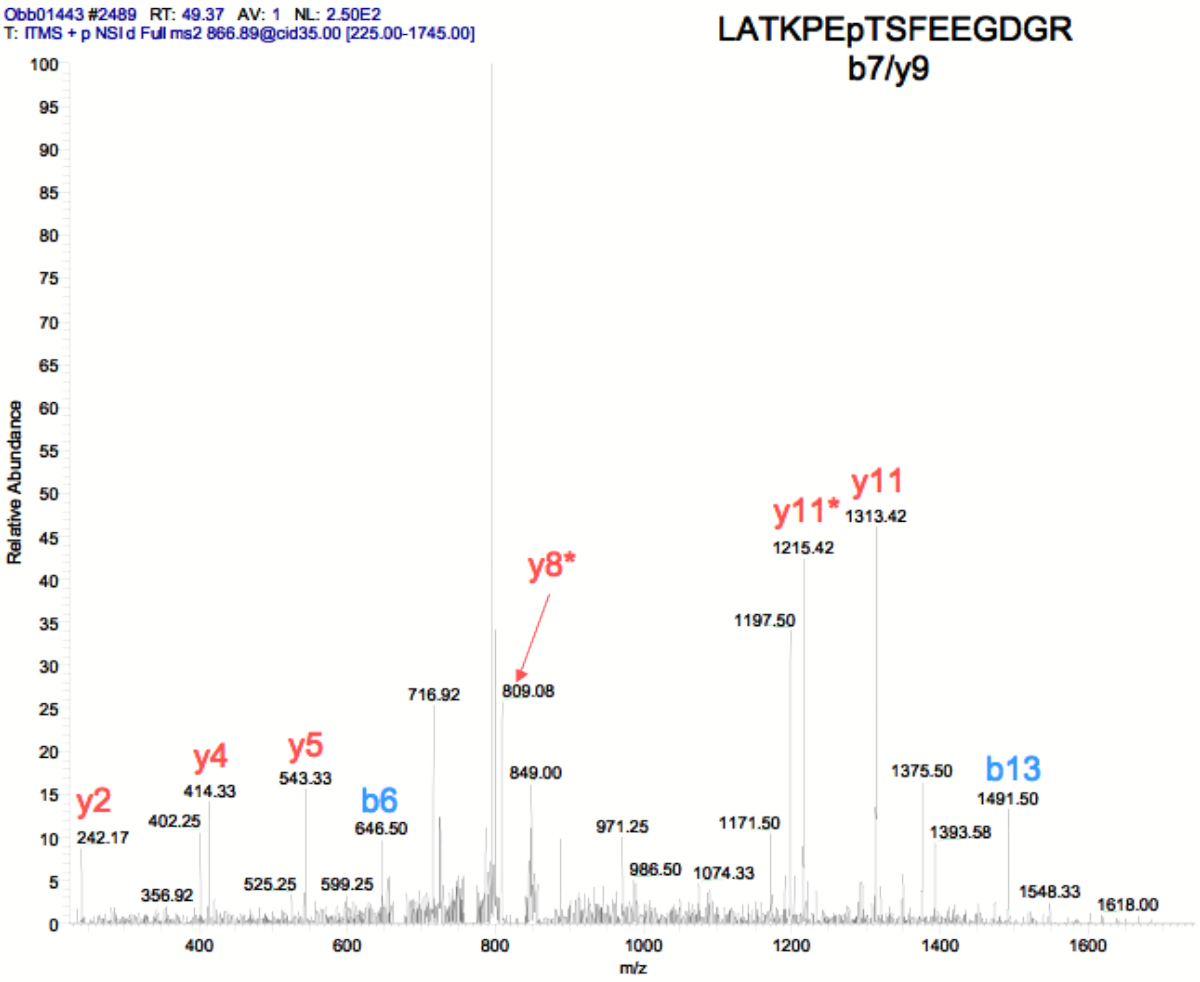

Figure 28: Annotated MS/MS spectrum of the serine-phosphorylated peptide LATKPETSFEEGDGR. The peptide was found up-regulated (regulation factor of 1.54, TCDD treatment of 2 hours) and belongs to the protein Uncharacterized protein, Ppfibp1. * indicates a phosphoric acid loss.

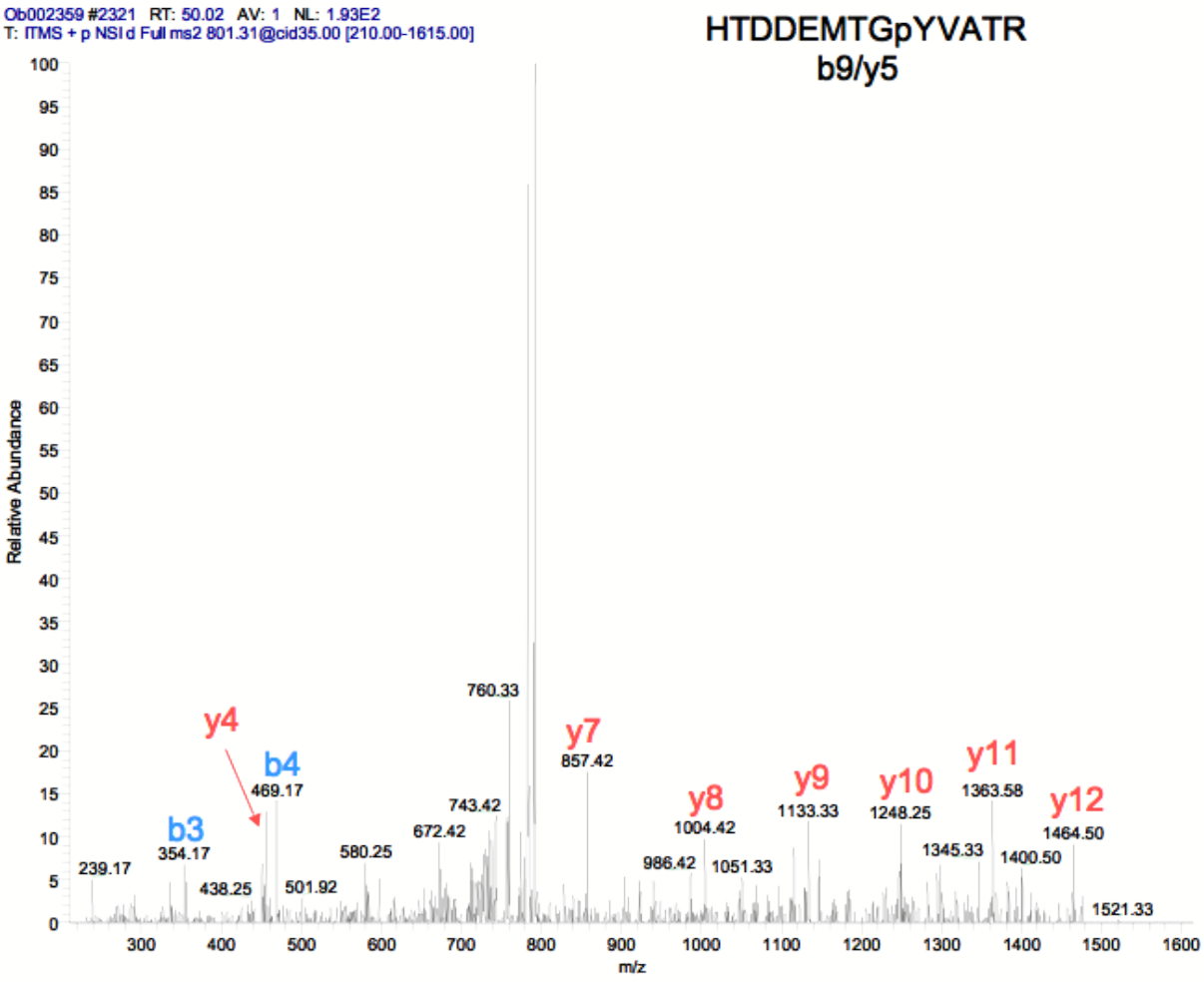

Figure 29: Annotated MS/MS spectrum of the tyrosine-phosphorylated peptide HTDDEMTGYVATR. The peptide was found up-regulated (regulation factor of 1.57, TCDD treatment of 2 hours) and belongs to the protein Mitogen-activated protein kinase 14.

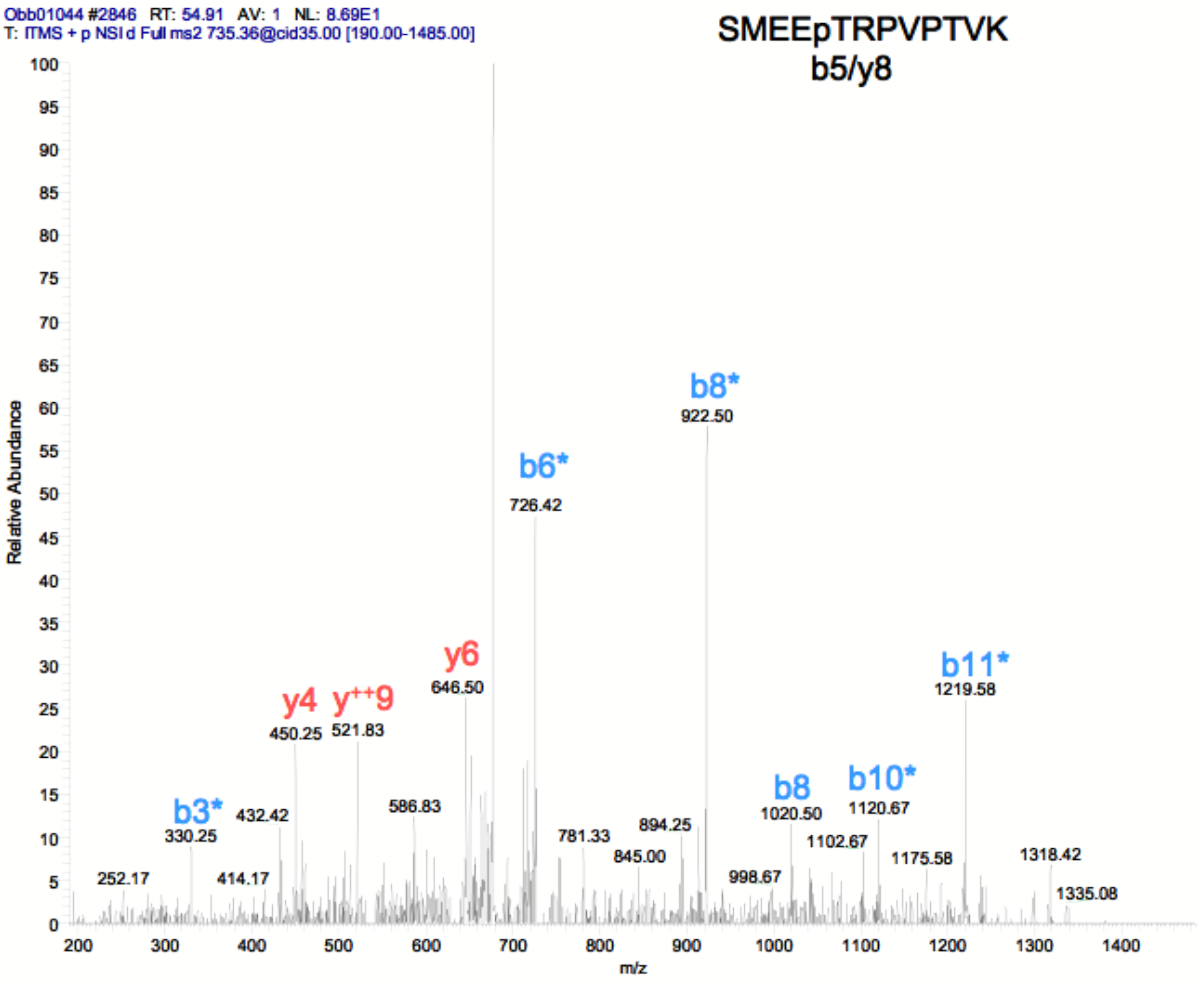

Figure 30: Annotated MS/MS spectrum of the threonine-phosphorylated peptide SMEETRPVPTVK. The peptide was found up-regulated (regulation factor of 1.73, TCDD treatment of 2 hours) and belongs to the protein ZZ-type with EF hand domain 1 isoform 1. * indicates a phosphoric acid loss and ++ a doubly charged peptide.

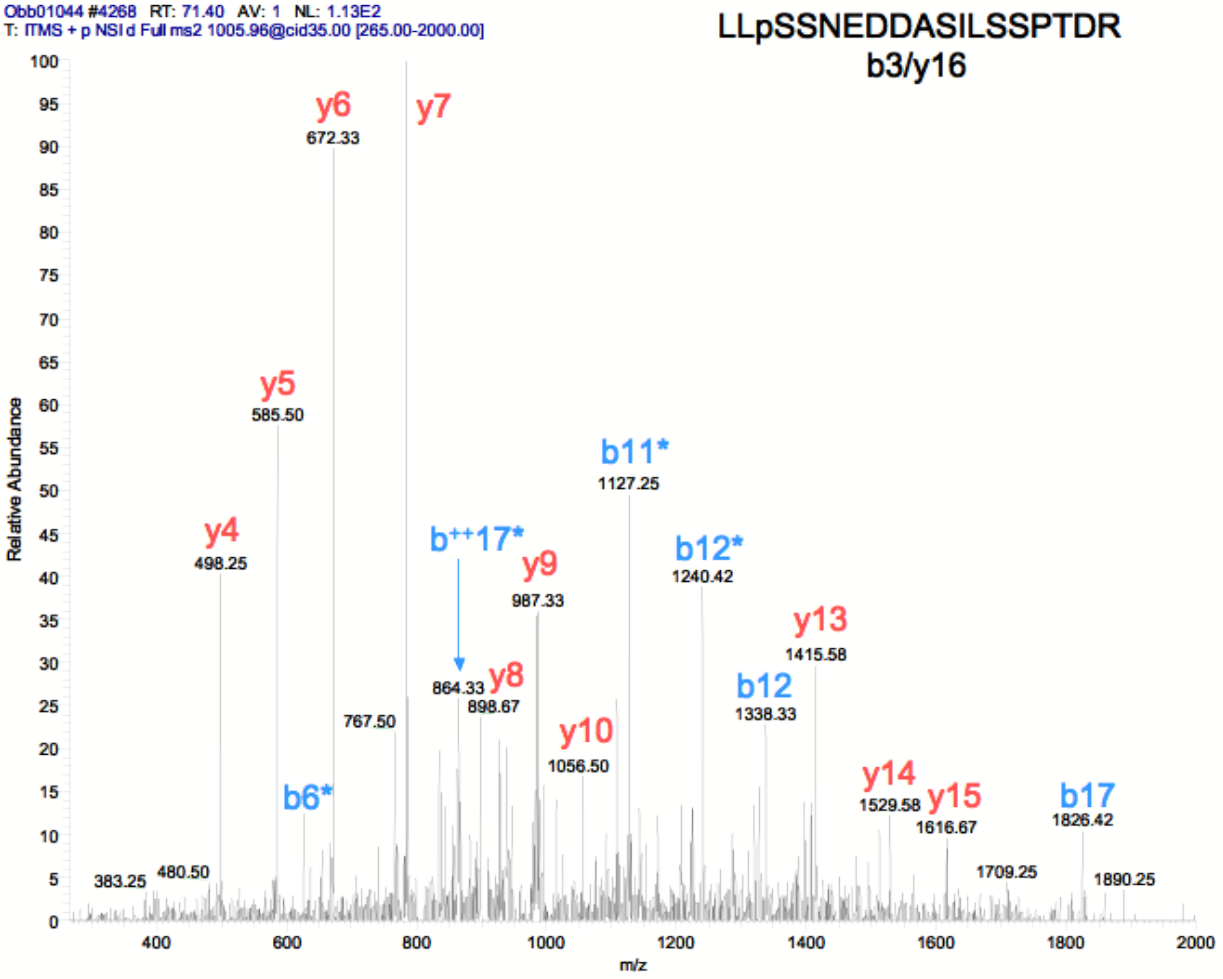

Figure 31: Annotated MS/MS spectrum of the serine-phosphorylated peptide LLSSNEDDASILSSPTDR. The peptide was found up-regulated (regulation factor of 1.75, TCDD treatment of 2 hours) and belongs to the protein Mediator of RNA polymerase II transcription subunit 2. * indicates a phosphoric acid loss and ++ a doubly charged peptide.

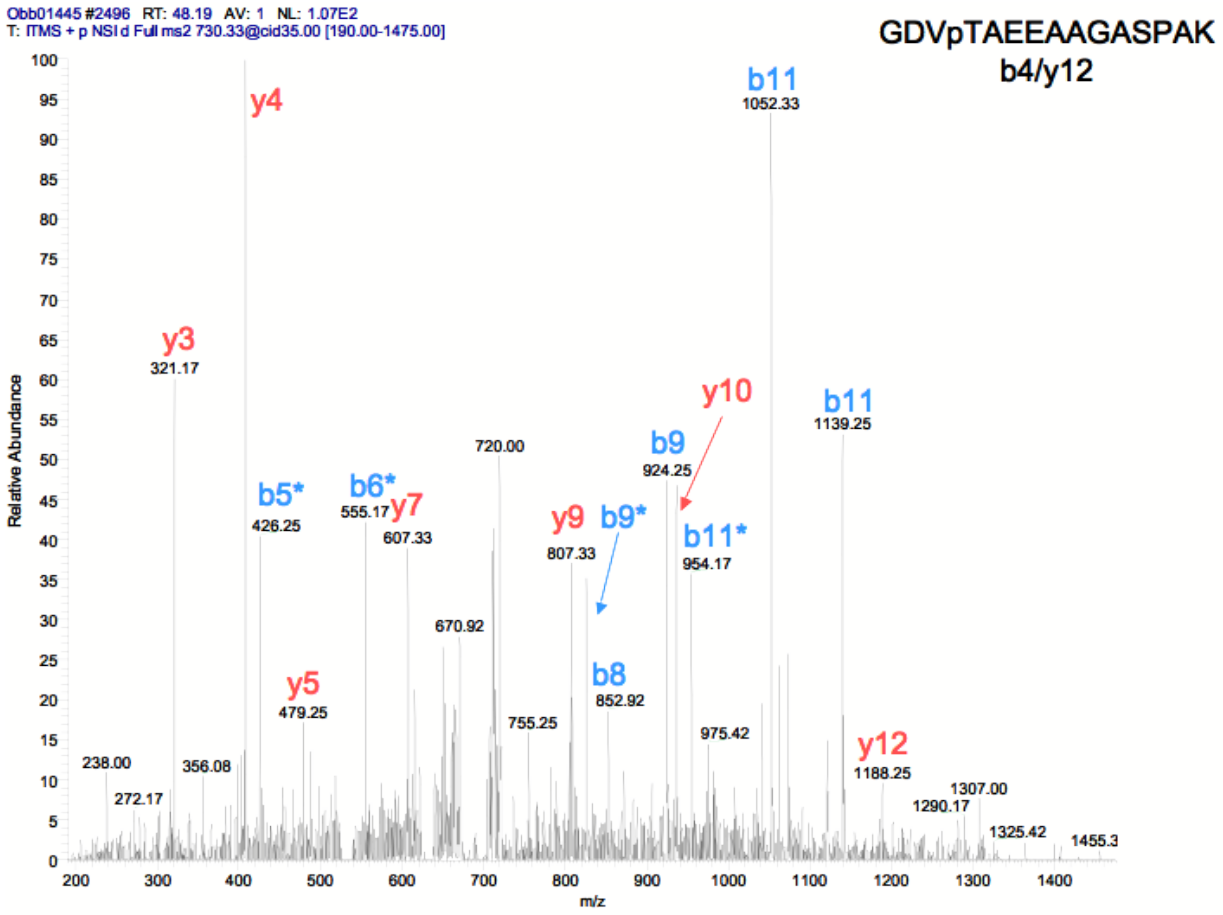

Figure 32: Annotated MS/MS spectrum of the threonine-phosphorylated peptide GDVTAEEAAGASPAK. The peptide was found up-regulated (regulation factor of 1.94, TCDD treatment of 2 hours) and belongs to the protein MARCKS-related protein. * indicates a phosphoric acid loss.

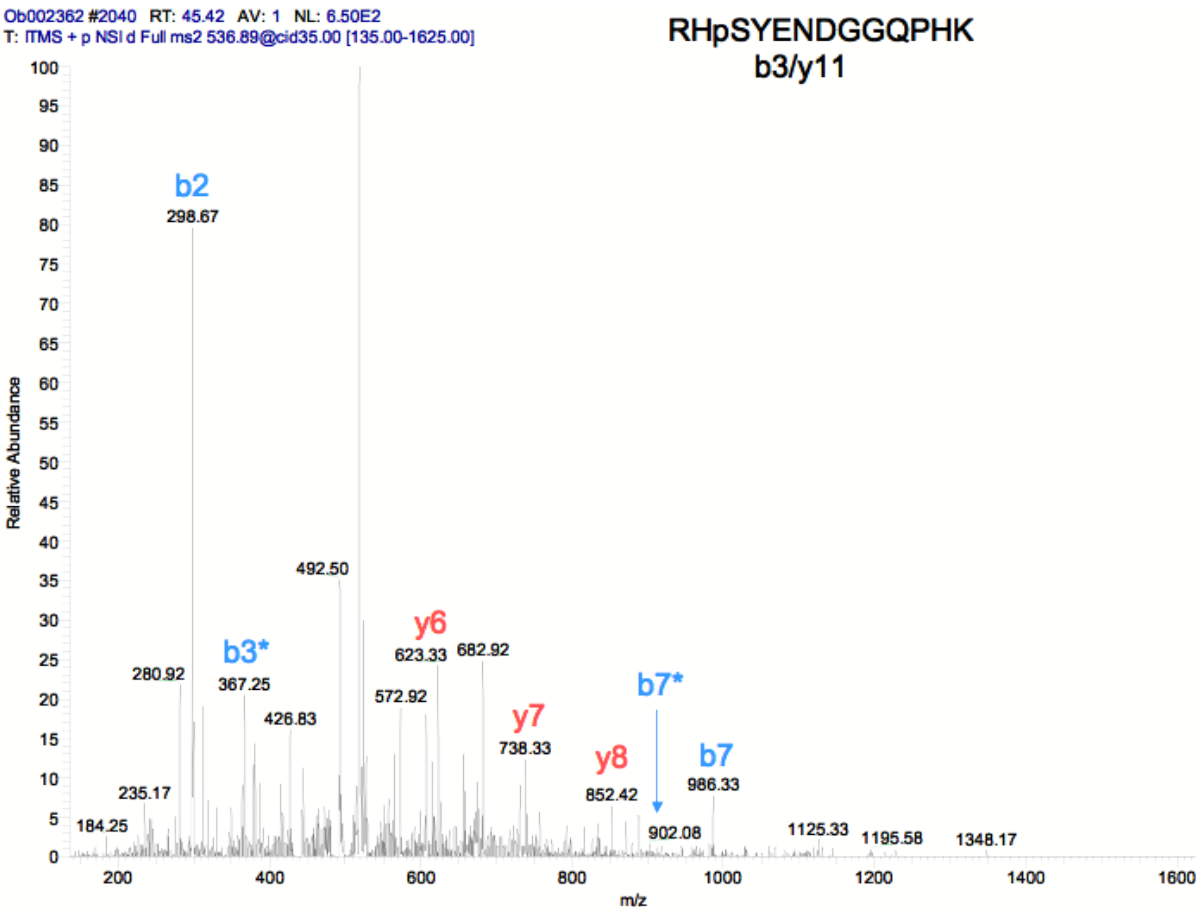

Figure 33: Annotated MS/MS spectrum of the serine-phosphorylated peptide RHSYENDGGQPHK. The peptide was found up-regulated (regulation factor of 1.96, TCDD treatment of 2 hours) and belongs to the protein Nuclear cap-binding protein subunit 1. * indicates a phosphoric acid loss.